Precise Predictions for Gravitational Binary Systems from Scattering Amplitudes

Dissertation

zur Erlangung des Doktorgrades
der Fakultät für Mathematik und Physik der

Albert-Ludwigs-Universität Freiburg

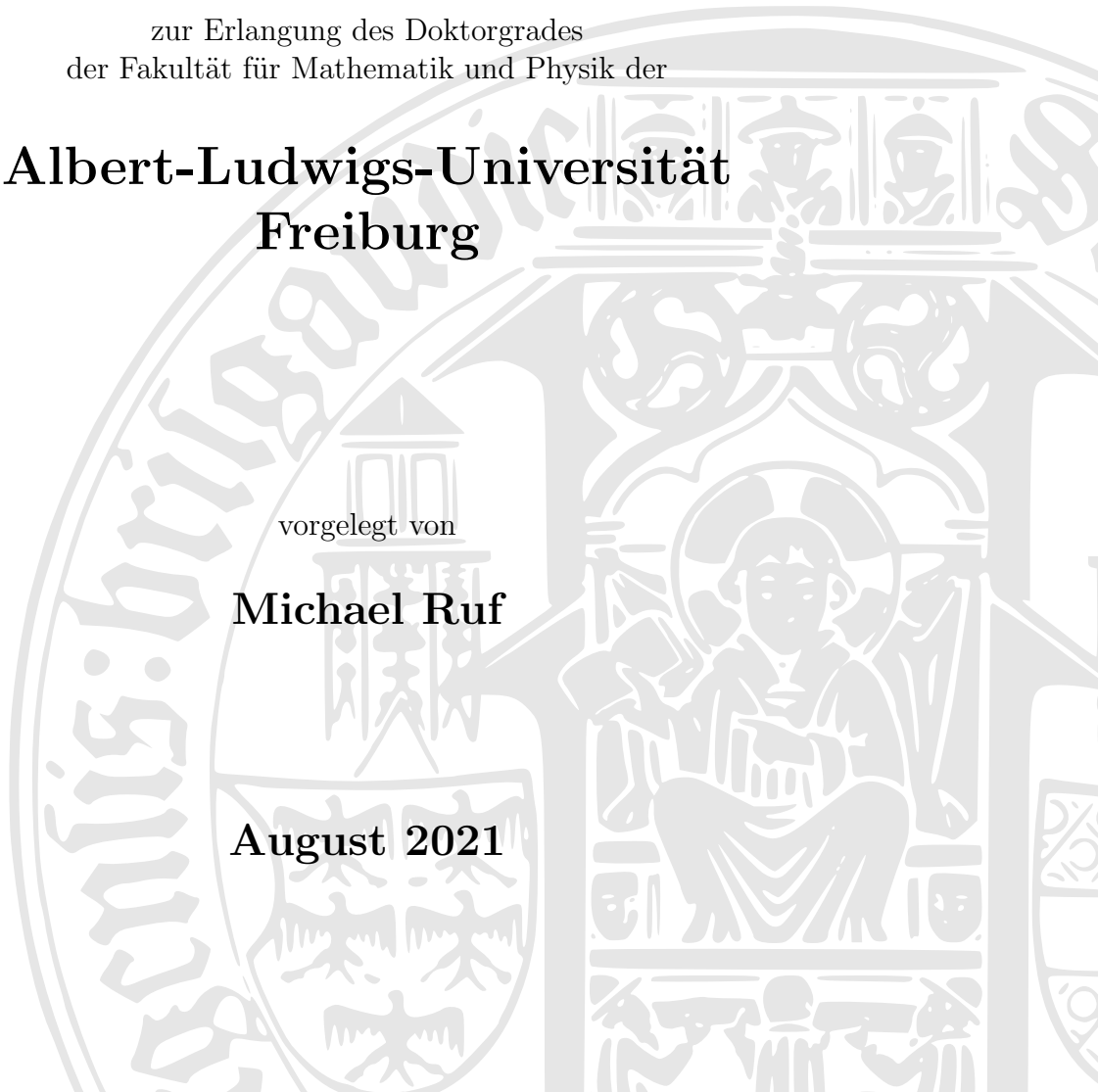

vorgelegt von

Michael Ruf

August 2021

Dekan: Prof. Dr. Michael Thoss
Referent: Prof. Dr. Harald Ita
Koreferent: JProf. Dr. Stefan Vogl
Tag der mündlichen Prüfung: 30. September 2021

Abstract

We introduce on-shell methods that originated in the context of collider physics to problems in classical and quantum gravity. The main results are precises predictions for various physical quantities that are important for the theoretical description of the gravitational two-body problem with direct applications at present and future gravitational-wave experiments.

A central result is the two-body potential to the fourth order in perturbation theory. In addition we also determine the effect of radiative corrections induced by dissipation due to gravitational waves to the scattering angle of two massive objects. Furthermore, we determine the total energy radiated during a scattering encounter as well as during an orbital period in a bound two-body system.

We establish new methods that significantly simplify these computations. A particular focus is put on complicated integrals and we describe in detail an efficient approach to their evaluation based on the method of regions and differential equations.

Another significant result is the four-graviton amplitude in general relativity, which we determine to the third order in perturbation theory including quantum effects. We use this result to compute the high-energy scattering angle in general relativity and provide an important contribution to an persisting debate about the relationship between the high-energy limit of scattering processes of massive and massless objects.

List of Publications

The contents of this thesis have been partially published in the following articles:

1. E. Herrmann, J. Parra-Martinez, M. S. Ruf and M. Zeng, *"Radiative Classical Gravitational Observables at $\mathcal{O}(G^3)$ from Scattering Amplitudes,"* arXiv:2104.03957 [hep-th] .

2. E. Herrmann, J. Parra-Martinez, M. S. Ruf and M. Zeng, *"Gravitational Bremsstrahlung from Reverse Unitarity,"* Phys. Rev. Lett. **126** 20, 201602, arXiv:2101.07255 [hep-th] .

3. Z. Bern, J. Parra-Martinez, R. Roiban, M. S. Ruf, C. H. Shen, M. P. Solon and M. Zeng, *"Scattering Amplitudes and Conservative Binary Dynamics at $\mathcal{O}(G^4)$,"* Phys. Rev. Lett. **126** (2021) 17, 171601, arXiv:2101.07254 [hep-th] .

4. S. Abreu, J. Dormans, F. Febres Cordero, H. Ita, M. Kraus, B. Page, E. Pascual, M. S. Ruf and V. Sotnikov, *"Caravel: A C++ Framework for the Computation of Multi-Loop Amplitudes with Numerical Unitarity,"* Comput. Phys. Commun. **267** (2021) 108069, arXiv:2009.11957 [hep-ph] .

5. J. Parra-Martinez, M. S. Ruf and M. Zeng, *"Extremal black hole scattering at $\mathcal{O}(G^3)$: graviton dominance, eikonal exponentiation, and differential equations,"* JHEP **11** (2020), 023, arXiv:2005.04236 [hep-th] .

6. S. Abreu, F. Febres Cordero, H. Ita, M. Jaquier, B. Page, M. S. Ruf and V. Sotnikov, *"The Two-Loop Four-Graviton Scattering Amplitudes,"* Phys. Rev. Lett. **124** (2020) 21, 211601, arXiv:2002.12374 [gr-qc] .

7. Z. Bern, H. Ita, J. Parra-Martinez and M. S. Ruf, *"Universality in the classical limit of massless gravitational scattering,"* Phys. Rev. Lett. **125** (2020) 3, 031601, arXiv:2002.02459 [hep-th] .

The following articles were published on topics unrelated to this thesis:

1. M. S. Ruf and C. F. Steinwachs, *"Quantum effective action for degenerate vector field theories,"* Phys. Rev. D **98** (2018) 8, 085014, arXiv:1809.04601 [hep-th] .

2. M. S. Ruf and C. F. Steinwachs, *"Renormalization of generalized vector field models in curved spacetime,"* Phys. Rev. D **98** (2018) 2, 025009, arXiv:1806.00485 [hep-th] .

3. M. S. Ruf and C. F. Steinwachs, *"Quantum equivalence of $f(R)$ gravity and scalar-tensor theories,"* Phys. Rev. D **97** (2018) 4, 044050, arXiv:1711.07486 [gr-qc] .

4. M. S. Ruf and C. F. Steinwachs, *"One-loop divergences for $f(R)$ gravity,"* Phys. Rev. D **97** (2018) 4, 044049, arXiv:1711.04785 [gr-qc] .

Contents

1. Introduction

Gravitational waves are a key prediction of the theory of general relativity (GR). They are relevant in practically any cosmological scenario, ranging from the early universe to supernovae explosions. At least historically the most interesting sources of gravitational waves have been ultra-compact binary systems of black holes (BH) and neutron stars (NS). The observation of the orbital decay of a binary NS system by Hulse and Taylor in 1974 [1] provided the first indirect detection of gravitational waves. This landmark result, confirming more than half a decade after their postulation that wave-like solutions in GR are realized in Nature, was subsequently awarded the 1993 Nobel prize in physics.

Gravitational waves can be detected directly as they distort space-time in a way that effectively causes the length of rulers to change on a minuscule scale. In practice such an measurement can be performed by laser-interferometric experiments. Since the relative strain of a typical gravitational-wave signal is of the order of 10^{-20}, such measurements have been out of reach of experiments until very recently. The first direct detection of gravitational wave by the LIGO and Virgo observatories [2, 3] marks a milestone in gravitational-wave science and is one of the most important discoveries in high energy physics of the past decade. Accordingly, it was recognized with the Nobel prize in physics for Weiss, Barish and Throne in 2017. Since the first detection of gravitational waves produced by a binary BH system, dozens of gravitational-wave events have been observed, including binary NS systems [3] and only very recently a BH-NS system [4].

The main prospects of gravitational-wave astronomy include: 1.) tests of GR in the dynamical strong-field regime [5, 6], 2.) the detection and cataloging of black holes, estimating their abundance in the Universe and viable parameters (mass, spin) [7, 8], 3.) probes of the merger-constituents, in particular the determination of the equation of state of neutron stars [9–11]. 4.) multi-messenger astronomy, complementary to searches in the electromagnetic spectrum [12], 5.) constraints on Lorentz invariance and the graviton mass through the observation of far-distant sources [13–15].

In the years to come the precision of the present experiments will be drastically improved [16] in conjunction with the commissioning of a new generation of ground-based detectors like the Einstein Telescope [17] and Cosmic Explorer [18]. With the Laser Interferometer Space Antenna (LISA) [19] we will see the first space-borne experiment with the potential to study systems characterized by extreme mass ratios. These next-generation experiments are expected to decrease the signal-to-noise ratio of the measurements by at least an order of magnitude [20, 21]. This requires complementary efforts for improving the theoretical predictions for the two-body problem, in particular for gravitational waveforms [22].

Theoretical predictions can be made by numerically solving Einstein's equations, together with an appropriate model describing the dynamics of the matter [23–25]. This process can be used to generate a wave-form for a given set of parameters (spin, orbital angular momenta, masses, equations of state of the constituents,...). However, Einstein's equations are a highly complicated set of non-linear coupled partial differential equations and therefore their numerical solution is computationally expensive. A problem which is amplified by the fact that templates are needed for a large parameter space. In practice, it is therefore necessary to invoke semi-analytical methods, for example in the effective one-body (EOB) framework pioneered by Buonanno and Damour [26].

A coalescence event is conveniently divided into three characteristic phases. In the initial phase the bodies circle each other in a quasi-periodic motion and adiabatically loose energy through gravitational radiation, thereby slowly approaching each other. In the second phase called the merger, the objects approach each other to the typical scale of the Schwarzschild radii of the constituents. Through a violent process they form a single excited black hole. Finally, in the ringdown phase the excited black hole transitions to its ground state by loosing energy though quasinormal modes [27]. The initial and the final stage can be addressed through perturbation theory while for the merger phase perturbation theory becomes invalid and one has to resort to numerical methods to solve the problem. The analytic predictions for the inspiral and the ringdown phase are central ingredients of the EOB framework.

The inspiral phase is characterized by weak fields and therefore the two-body problem can been addressed by perturbatively solving Einstein's equations, sourced by two point sources, for example in the framework of non-relativistic GR (NRGR) [28–30]. This computation naturally leads to an organization through diagrams that are very similar to Feynman diagrams most familiar from applications in collider physics (see e.g. Ref. [31]). Therefore, the computations in the classical field theory approach are plagued by the same problems as computations in collider physics which employ Feynman diagrams. The main challenge is the vastly increasing combinatorial complexity due to an explosion of diagrams. In particular the local covariant formulation of gauge theories in terms of unphysical off-shell degrees of freedom leads to a vast proliferation of terms in the intermediate steps of the calculation.

The equivalent problem in collider physics is successfully brought under control by the use of on-shell methods in which the computation is formulated in terms of the physical degrees of freedom alone. The iconic example is the reduction in the number of terms in gluonic scattering amplitudes in Yang-Mills theory, which can be simplified from expressions filling multiple pages down to only a few terms [32]. Furthermore, relations dictated by unitarity and factorization allow to construct a generic amplitude, including virtual degrees of freedom from tree amplitudes [33], which in turn can be constructed from three-particle amplitudes — the simplest building blocks of the theory (see e.g. Ref. [34]). The issues faced in a computation based on Feynman diagrams are even more pressing in the context of gravity, because the freedom associated with general coordinate invariance is larger than that due to gauge invariance in Yang-Mills theory. In practice this manifests in

an infinite number of Feynman rules of which even the simplest have hundreds of terms [35]. Here as well a major simplification has been achieved in the on-shell approach. It is particularly striking that gravitational on-shell amplitudes can be related in a simple manner to Yang-Mills amplitudes through double-copy relations (see Ref. [36] for a review). In practice this means on-shell computations in gravity can be performed up to very high orders in perturbation theory, while the equivalent computations using traditional methods quickly become intractable.[1] Although the usefulness of a quantum-field-theory-based approach has been appreciated at least since the seventies [38–45], the interest in the problem was only recently reinvigorated by Damour in Ref. [31].

Unfortunately to date we have not succeeded in formulating an ab initio classical approach which incorporates the benefits of the on-shell approach used in quantum field theory. If we want to make use of the on-shell paradigm we are forced to take a detour by first considering the associated quantum problem, making full use of the advanced computational techniques introduced in the context of collider physics and finally recovering classical physics by formally taking the reduced Plank constant to zero $\hbar \to 0$. In this we are confronted by a dilemma, as on the one hand we simplify the computation through the on-shell approach, but on the other hand we artificially make the problem more complicated by considering the quantum theory and introduce conceptual problems regarding the correct way to take $\hbar \to 0$ (see e.g. Ref. [46]). Balancing the complexity, the conclusion is that the simplifications greatly outweigh the additional problems. This point has been underlined in the recent years as the amplitude-based approach allowed for the first time to perform computations at the third [47, 48] and fourth order [49] in perturbation theory in the gravitational coupling.

Scattering amplitudes are naturally defined in terms of asymptotic states, and therefore they are intimately tied to the scattering problem. In contrast to mergers, scattering events are not expected to be observed with the current experimental precision [50, 51]. Fortunately, the two situations are closely related and one can translate information from scattering to the bound-state problem, for example through determination of an effective potential [52] or through analytic continuation of observables [53, 54].

For binary merger the orbits rapidly approach a circular form for which the virial theorem naturally leads to simultaneous expansion in the velocities and the gravitational coupling. The corresponding expansion is known as post-Newtonian (PN) expansion and has a long-standing tradition [55–68]. The 1PN accurate gravitational potential has been computed already in 1917 by Droste and Lorentz [69] and later by Einstein, Infeld and Hoffman Eddington and Clark [70, 71] and takes the form

$$\frac{H}{\mu} = \frac{\boldsymbol{v}^2}{2} - \frac{GM}{r} + \frac{1}{c^2}\left\{\frac{3\nu-1}{8}(\boldsymbol{v}^2)^2 - \frac{GM}{2r}\left[\nu(\boldsymbol{n}\cdot\boldsymbol{v})^2 + (\nu+3)\boldsymbol{v}^2\right] + \frac{G^2M^2}{2r^2}\right\}, \tag{1.1}$$

where G is Newton's constant, c is the speed of light, $M = m_1 + m_2$ is the total mass, $\mu = m_1 m_2/M$ the reduced mass, $\nu = \mu/M$ the symmetric mass ratio,

[1] See e.g. Ref. [37] for a computation in a gravity model at fifth order in perturbation theory

$\boldsymbol{v} = \boldsymbol{p}/\mu$ the relative velocity, $r = |\boldsymbol{r}|$ the radial separation and $\boldsymbol{n} = \boldsymbol{r}/r$. Today the state of the art for the two-body potential are fifth-order PN corrections which were first partially computed in Refs. [72–75] and completed in Ref. [76]. Partial results have been obtained recently up to the sixth PN order [77]. The additional expansion in velocity is very beneficial in simplifying the resulting expressions and in particular the integrals that have to be computed.

From the quantum field theory perspective is natural not to expand in the velocities and instead keep the discussion relativistic, while still expanding in the gravitational coupling. This setup is known as post-Minkowskian (PM) approximation [31, 78–85] or simply perturbation theory in the gravitational coupling. Given the aforementioned virialization of the system, this framework might seem like an unnecessary complication. The main advantages are that on the one hand, the expressions are much more compact in the relativistic form and expanding them will actually make things more complicated. On the other hand, we gain additional insight into the structure of the results. In particular we can probe the high-energy limit where we can make contact to massless processes. Results for scattering observables can be used to determine parameters in effective one-body models which are applicable to the bound-state problem [85]. For highly elliptic and hyperbolic motions (which might be relevant for three-body processes [86]) the velocity is not restricted by the virial theorem so that in general $v \sim c$ and there is no way around using PM perturbation theory.

In order to describe realistic systems, the analysis must be refined by including additional structure. Most important in that regard is the addition of the angular momentum of the constituents. In contrast, one needs to take into account the effects of gravitational radiation in dissipation of angular momentum and energy but also through conservative radiation. Finally, at higher orders in perturbation theory the point-particle prescription has to be modified, taking into account the finite size of the sources. Such corrections are very important for neutron stars and the determination of the corresponding operators in the effective field theory description can be used to constrain the equation of state of neutron stars [9–11]. All of this problems have been addressed successfully in the amplitudes-based framework. For example, spin has been considered in Refs. [87, 87], radiative effects in Refs. [88, 89] and finite-size effects in Refs. [90, 91].

One of the greatest obstructions in pushing the computations to higher order in perturbation theory is the explicit evaluation of complicated integrals. This is common to both approaches to the binary problem — amplitude-based or ab initio classical. Already today the integrals required are at the state of the art considered in collider physics. For example the integrals used for the fifth PN order [72, 73] are the same as the ones considered for five-loop beta functions in quantum chromodynamics (QCD) first computed in Ref. [92], while one also needs to keep track of finite contributions. The situation in the PM framework is similar as the integrals faced in state-of-the-art applications [49, 93] are of comparable complexity to three-loop problems in massless two-to-two scattering [94–96] and computation of the four-loop cusp anomalous dimension [97, 98] as well as three-loop soft functions [99]. The evaluation of integrals is therefore one of the main

problems that has to be addressed when considering high orders in perturbation theory.

In this thesis we compute state-of-the art results in the PM approximation. In particular we present the conservative two-body potential to fourth order in the gravitational coupling and the integrated energy loss per orbit as well as the scattering angle to the third order in the gravitational coupling. In a separate but closely related project we compute for the first time the complete set of four-graviton amplitudes at two-loop order. An important contribution of this work is the introduction of new methods for the computation of integrals in the PM expansion. An effort that proved crucial for the aforementioned applications and will prove even more important in an effort to push the computations to the next order in perturbation theory.

The thesis is structured as follows: In chapter 2 we state the problem and perform some computations in classical physics. In chapter 3 we explain how one can use on-shell methods to compute scattering amplitudes. Chapter 4 is dedicated to the class of Feynman integrals that occur in the PM expansion. The chapter 5 contains information about the computation of the four-graviton amplitude in GR. In chapter 6 we explain how to extract classical observables from the information contained in quantum scattering amplitudes. Finally in chapter 7 we present our main results for the observables in classical gravity. Technical details are compiled in several appendices, encompassing information about Feynman integrals, partial-wave analysis and Fourier analysis.

2. Preliminaries

In what follows we will think of the scattering of two black holes as the scattering of two point particles. The problem is naturally described in terms of the four-momenta of the particles. We will use a all-outgoing convention where particle 1 has initial momentum $-p_1$ and final momentum p_4, and particle 2 has initial momentum $-p_2$ and final momentum p_3 with physical s-channel scattering corresponding to negative energy components of p_1 and p_2. Throughout this thesis we will use natural units $c = \hbar = 1$. The process can be described in terms of Lorentz invariants, in this case by the masses m_i of the external particles

$$p_1^2 = p_4^2 = m_1^2\,, \quad p_2^2 = p_3^2 = m_2^2 \tag{2.1}$$

and by three Mandelstam invariants s, t, u

$$s = (p_1 + p_2)^2\,, \quad t = (p_1 + p_4)^2\,, \quad u = (p_1 + p_3)^2\,. \tag{2.2}$$

Due to momentum conservation, not all of the invariants are independent and we find

$$s + t + u = 2m_1^2 + 2m_2^2\,. \tag{2.3}$$

This means that massive $2 \to 2$ scattering is characterized by four scales or three dimensionless ratios. Furthermore we introduce the Lorentz-factor[1]

$$\sigma = \frac{p_1 \cdot p_2}{m_1 m_2} = \frac{s - m_1^2 - m_2^2}{2m_1 m_2}\,. \tag{2.4}$$

Sometimes it will be useful to perform the analysis in a given frame. The center-of-momentum (COM) frame is the Lorentz frame in which the total momentum of the initial states is zero

$$p_1 = -(E_1, \boldsymbol{p})\,, \quad p_2 = -(E_2, -\boldsymbol{p}) \quad p_3 = (E_2', -\boldsymbol{p}') \quad p_4 = (E_1', \boldsymbol{p}')\,, \tag{2.5}$$

with $\boldsymbol{p}, \boldsymbol{p}'$ the initial and final COM momenta and here and in the following we use boldface letters to denote three momenta. The norm of the COM momentum can be expressed in a manifestly relativistic way

$$\boldsymbol{p}^2 = \frac{\lambda(s, m_1^2, m_2^2)}{4s} = \frac{m_1^2 m_2^2(\sigma^2 - 1)}{s}\,, \tag{2.6}$$

where $\lambda(x, y, z) = x^2 + y^2 + z^2 - 2xy - 2yz - 2zx$ is the Källén triangle function. Another important quantity is the COM scattering angle χ depicted in Figure 2.1 and defined as the angle between the incoming and outgoing COM momenta

[1] In the rest-frame of particle 1 we have $\frac{p_1 \cdot p_2}{m_1 m_2} = \frac{E_2}{m_2}$ and vice-versa.

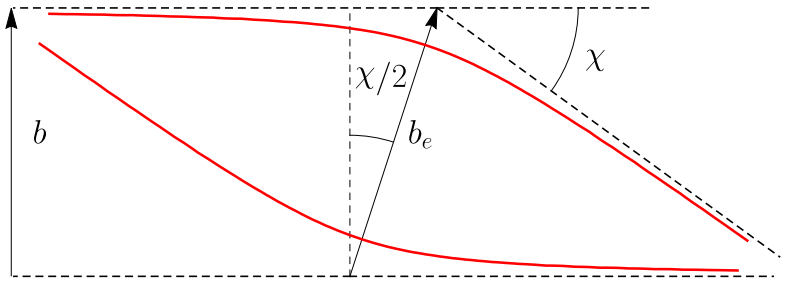

Figure 2.1.: Scattering of two massive particles.

$$\cos\chi := \frac{\boldsymbol{p}\cdot\boldsymbol{p}'}{|\boldsymbol{p}||\boldsymbol{p}'|}\,. \tag{2.7}$$

For elastic scattering we have $E_i' = E_i, |\boldsymbol{p}'| = |\boldsymbol{p}|$, so that the scattering angle also can be represented through a Lorentz-invariant quantity

$$t = (p_1 + p_4)^2 = -2\boldsymbol{p}^2(1-\cos\chi) = -4\boldsymbol{p}^2\sin^2(\chi/2)\,. \tag{2.8}$$

When working with amplitudes we will call the momentum transfer $q = p_1 + p_4$ which will typically be small, in the cases of macroscopic momentum transfer, we will denote it by Δp_i and refer to it as the *impulse*. In position space, an important quantity is the impact parameter $b = |\boldsymbol{b}|$, which represents the spatial separation of the asymptotic trajectories as depicted in Figure 2.1. An alternative definition is the symmetric or eikonal impact parameter b_e

$$b = b_\mathrm{e}\cos(\chi/2)\,. \tag{2.9}$$

In a minor abuse of notation we will also use b as a four vector. The orbital angular momentum of the system is given by

$$J = |\boldsymbol{b}\times\boldsymbol{p}| = b|\boldsymbol{p}| = b_\mathrm{e}|\boldsymbol{p}|\cos(\chi/2)\,. \tag{2.10}$$

For future reference it is also convenient to introduce the total and symmetric COM energy E and ξ as well the total and symmetric mass ratio M and ν and the reduced mass μ

$$E = E_1 + E_2, \quad \xi = \frac{E_1E_2}{(E_1+E_2)^2}\,, \tag{2.11}$$

$$M = m_1 + m_2, \quad \nu = \frac{m_1m_2}{(m_1+m_2)^2}\,, \quad \mu = \frac{m_1m_2}{(m_1+m_2)}\,. \tag{2.12}$$

We define the energy ratio as

$$h = \frac{E}{M} = \sqrt{1+2\nu(\sigma-1)}\,, \tag{2.13}$$

which entails the following useful relation

$$\frac{|\boldsymbol{p}|}{\mu} = \frac{\sqrt{\sigma^2-1}}{h(\sigma,\nu)}\,. \tag{2.14}$$

In the case of scattering the energy ratio h is always greater than one. For bound states it is smaller than one, which is equivalent to $\sigma < 1$ [100].

2.1. General Relativity

Physics on the fundamental level can be described in terms of four forces, the weak, electromagnetic, strong and gravitational forces.

Among the fundamental forces, gravity is likely the most intuitively visible in our Universe. Historically, gravity has been studied by physicists since the advent of science. The first major descriptions are due to Newton who deduced in his "Philosophiae Naturalis Principia Mathematica" 1687 that objects having a gravitational mass m_1, m_2 at distance $\boldsymbol{r} = r\boldsymbol{e}_r$ attract each other via the Newtonian force

$$\boldsymbol{F}_{\mathrm{N}} = \frac{Gm_1m_2}{r^2}\boldsymbol{e}_r\,. \tag{2.15}$$

The fundamental constant G is Newton's constant. Newtonian gravity is very successful at describing gravitational phenomena on earth and in the solar system. The Newtonian force acting on particle 2 can be derived from a potential

$$\boldsymbol{F}_{\mathrm{N}} = -\boldsymbol{\nabla}\phi_{\mathrm{N}}\,, \qquad \phi_{\mathrm{N}}(r) = -\frac{m_1G}{r}\,. \tag{2.16}$$

For a generic mass distribution, the potential can be computed from the Poisson equation

$$\Delta\phi_{\mathrm{N}} = 4\pi G\rho\,, \tag{2.17}$$

where $\Delta = \sum_{i=1}^{3}\left(\frac{\partial}{\partial x_i}\right)^2$ is the Laplacian and ρ is the matter density, for example $\rho(\vec{r}) = m_1\delta(\vec{r})$ for an isolated particle of mass m_1. A particular feature of Newtonian gravity is the superposition principle, which is evident from the Poisson equation. The field sourced by multiple matter densities $\rho = \sum_i \rho_i$ is just the sum of the fields sourced by a single density ρ_i. This important feature allows to solve the two-body problem exactly by decoupling the motion of the center-of-mass and a reduced mass and therefore the two-body problem can be regarded as a solved problem. Newton used it to explain Kepler's laws of planetary motion.

It has been known as early as the mid 19th century that Newton's theory is incomplete. The first example of a post-Newtonian effect is the anomalous motion of Mercury which has been observed in 1859 by Urbain Le Verrier, analyzing historical data on the positioning of the planets from 1697 to 1848. He found that the motion of Mercury deviates from the static elliptical orbit predicted by Kepler's first law. The periastron is found to rotate by 43 arcseconds per century which is importantly much above the measurment error of about 0.1 arcseconds per century (the situation is depicted in Figure 2.2). The resolution of the problem took until the advent of GR in the beginning of the 20th century. Starting from simple assumptions Einstein developed a manifestly coordinate invariant formalism of gravity. His famous field equations are the coordinate invariant generalization of

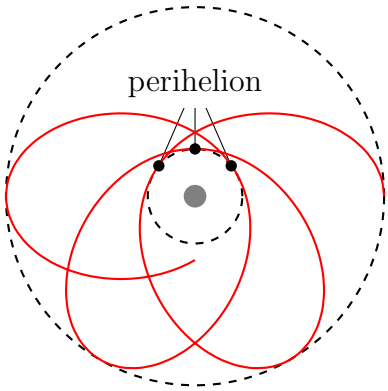

Figure 2.2.: Exaggerated representation of the motion of a light body (mercury) around a heavy central body (sun). The motion is nearly elliptical but the perihelion shifts slightly.

the Poisson equation (2.17) and are given by

$$R_{\mu\nu} - \frac{1}{2}Rg_{\mu\nu} + \Lambda g_{\mu\nu} = 8\pi G T_{\mu\nu} \ . \tag{2.18}$$

In this equation $R_{\mu\nu} = R^{\lambda}{}_{\mu\lambda\nu}$ is the Ricci tensor obtained from a contraction of the Riemann tensor, $R = g^{\mu\nu}R_{\mu\nu}$ is the Ricci scalar $g_{\mu\nu}$ is the metric tensor, Λ is the cosmological constant and $T_{\mu\nu}$ is the energy-momentum tensor describing the matter in the system and which acts as a source of the gravitational field.[2] Einstein's equations (2.18) represent a system of coupled non-linear differential equations, which have to be solved simultaneously which equations of motions for the matter. The coupling of the system leads to a dual view in which (quoting J.A. Weehler) the matter forces the space to curve while space tells matter how to move.

There are a number of predictions of GR of which we list a few here:

Perihelion shift As described before GR predicts a precession of the perihelion of the planetary orbits.

Deflection of light In contrast to Newtonian gravity, in GR gravity couples to energy-momentum distributions. This crucially implies that also massless particles/fields such as electromagnetic waves are attracted by massive objects and heavy objects bend light rays effectively acting as lenses.

Gravitational time dilation and redshift In GR the presence of a graviational field will cause clocks to move slower. This is even of practical relevance for example in satellite-bases positioning systems, such as the Global Positioning System (GPS).

[2] Our conventions are $R^{\lambda}{}_{\mu\rho\nu} = \partial_\rho \Gamma^{\lambda}_{\mu\nu} - \partial_\nu \Gamma^{\lambda}_{\mu\rho} + \Gamma^{\lambda}_{\alpha\rho}\Gamma^{\alpha}_{\mu\nu} - \Gamma^{\lambda}_{\alpha\nu}\Gamma^{\alpha}_{\mu\rho}$. We work in mostly minus signature $\eta_{\mu\nu} = \mathrm{diag}(1,-1,-1,-1)$ and we employ Einstein's summation convention whereby repeated indices are summed over.

Singularities Singularities in the form of Black holes are a robust prediction of GR and can be shown to form under quite general assumptions (see e.g. Ref. [101]). Supermassive black holes are found at the center of most galaxies, for example the Milky Way host the black hole Sagittarius A*. Black holes are strong radio sources and have also been observed through gravitational waves and directly imaged by the event horizon telescope [102].

Cosmology Most of the present cosmic observations are well-described through the Standard Model of cosmology (ΛCDM model) based on GR. For example the observed accelerated expansion of our Universe is described by a cosmological constant term in Einstein's equations. The nature of the cold dark matter in this model (CDM) however remains to be understood.

Gravitational waves Already Einstein himself noted that linearizing the gravitational field equations leads to wave-like solutions. It was unclear for the most part of the 20th century if gravitational waves are physical. The observation of a neuron star binaries by Hulse and Taylor provided an indirect proof, as the systems' loss of energy could is described well through gravitational wave radiation predicted by GR. Gravitational waves from binary mergers have also been directly detected by the LIGO and Virgo observatories [3].

2.1.1. General Relativity as a Classical Field Theory

We can consider GR as a classical field theory of the metric field $g_{\mu\nu}$. The corresponding action functional is the Einstein-Hilbert action

$$S_{\mathrm{EH}}[g_{\mu\nu}] = \int \mathrm{d}^4x \mathcal{L}_{\mathrm{EH}}\,, \quad \mathcal{L}_{\mathrm{EH}} = -\frac{2}{\kappa^2}\sqrt{-g}R\,, \tag{2.19}$$

where as before R is the Ricci scalar $\kappa = \sqrt{32\pi G}$ is the gravitational coupling constant and $\sqrt{-g} = \sqrt{-\det\left(g_{\mu\nu}\right)}$. In order to have a description respecting general coordinate invariance, the coupling of matter is introduced by the minimal substitution of the corresponding flat-space Lagrangian,

$$\eta_{\mu\nu} \to g_{\mu\nu}\,, \quad \partial_\mu \to \nabla_\mu\,, \quad \mathrm{d}^4x \to \sqrt{-g}\,\mathrm{d}^4x\,. \tag{2.20}$$

For example we have for a massive scalar ϕ

$$S_{\mathrm{mat}}[g_{\mu\nu},\phi] = \int \mathrm{d}^4x\sqrt{-g}\left(\frac{1}{2}g^{\mu\nu}\partial_\mu\phi\partial_\nu\phi - \frac{1}{2}m^2\phi^2\right). \tag{2.21}$$

where by a conventional abuse of notation $g^{\mu\nu}$ denotes the inverse of the metric tensor $g_{\mu\nu}$. We did not include a cosmological constant in the action (2.19) as we are interested in phenomena which take place on scales much smaller than the cosmological scales. It is a standard exercise (See e.g. Ref. [103]) to show that the

total action

$$S = S_{\rm EH} + S_{\rm mat}\,, \tag{2.22}$$

reproduces Einstein's equations (2.18) when variations with respect to the metric $g_{\mu\nu}$ are considered. The energy-momentum tensor for the matter is defined by

$$T^{\mu\nu} = -\frac{2}{\sqrt{-g}}\frac{\delta S_{\rm mat}}{\delta g_{\mu\nu}}\,. \tag{2.23}$$

2.1.2. Motion of Point Particles

In order to set the stage for the computations performed in this thesis we find it useful to briefly review the approach based on classical field theory. In this we follow closely Ref. [31].

The traditional approach to solving binary dynamics perturbatively is through the world-line formalism. We assume that the two particles are located at trajectories described by worldlines $x_i^\mu(\lambda_i)$, $i = 1, 2$. The dynamics can then be described by the point-particle action

$$S_{\rm pp} = -\sum_{i=1}^{2} m_i \int {\rm d}\lambda_i \sqrt{g_{\mu\nu}\dot{x}_i^\mu \dot{x}_i^\nu}\,, \quad \dot{x}_i^\mu \coloneqq \frac{{\rm d}x_i^\mu}{{\rm d}\lambda_i}\,. \tag{2.24}$$

Corrections to the point-like nature of the sources can be systematically included by adding non-minimal couplings of the worldline to the metric [28]. However such effects only contribute at high order in the perturbative expansion and we will therefore not discuss them here. The equations of motion derived from the action are the geodesic equations, which can be conveniently formulated in a first-order form

$$\frac{{\rm d}x_i^\mu}{{\rm d}\lambda_i} = g^{\mu\nu}(x_i)v_{i\nu}\,, \quad \frac{{\rm d}v_{i\mu}}{{\rm d}\lambda_i} = \partial_\mu g^{\alpha\beta}(x_i)v_{i\alpha}v_{i\beta}\,. \tag{2.25}$$

The energy momentum tensor for the point-particle action is

$$T^{\mu\nu}(x) = -\frac{2}{\sqrt{-g}}\frac{\delta S_{\rm mat}}{\delta g_{\mu\nu}(x)} = \sum_{i=1}^{2}\int {\rm d}\lambda_i \frac{\delta^{(4)}(x - x_i(\lambda_i))}{\sqrt{-g}}\frac{\dot{x}_i^\mu \dot{x}_i^\nu}{\sqrt{g_{\alpha\beta}\dot{x}_i^\alpha \dot{x}_i^\beta}}\,. \tag{2.26}$$

The equations (2.25) and the Einstein equations (2.18) form a (highly non-trivial) coupled system for the metric $g_{\mu\nu}$, the worldlines x_i^μ and the velocities v_i^μ. Restricting to the weak field limit we can set up perturbation theory around a flat background, writing

$$g^{\mu\nu} = \eta^{\mu\nu} + \sum_{n=1}^{\infty} {}_{(n)}h^{\mu\nu}\,, \quad v_i^\mu = u_i^\mu + \sum_{n=1}^{\infty} {}_{(n)}v_i^\mu\,, \quad x_i^\mu = {}_{(0)}x_i^\mu(0) + u_i^\mu\lambda_i + \sum_{n=1}^{\infty} {}_{(n)}x_i^\mu\,. \tag{2.27}$$

Where the terms denoted by a subscript (n) in this series are of order G^n. A typical observable for scattering paths is the impulse

$$\Delta p_{i\mu} = p_{i\mu}(\infty) - p_{i\mu}(-\infty) = \int_{-\infty}^{\infty} \mathrm{d}\lambda_i \partial_\mu g^{\alpha\beta}(x_i) p_{i\alpha} p_{i\beta} \,, \tag{2.28}$$

where we introduced $p_i = m v_i$. Computations in the world-line formalism up to 2PM order have been performed by Westpfahl in the '80s [84] and the program has only recently been extended to the third and fourth order in the gravitational coupling [93, 104].

2.1.3. Linearized Field Equations and Gravitational Waves

Solving Einstein's equations is a formidable problem and finding analytic solutions is possible only in certain limits. One particularly interesting limit is the weak field limit

$$g_{\mu\nu} = \eta_{\mu\nu} + \kappa h_{\mu\nu} \,, \qquad |\kappa h_{\mu\nu}| \ll 1 \,. \tag{2.29}$$

Here $\eta_{\mu\nu}$ is the fixed flat background Minkowski space metric, where the gravitational field is absent. The fluctuation can be interpreted as a spin-2 field, the graviton, propagating on a the flat background. Expanding Einstein's equations leads to an equation, which is conveniently written in terms of the trace reversed field $\overline{h}_{\mu\nu}$

$$-\frac{1}{2}\Box \overline{h}_{\mu\nu} + \partial_\varrho \partial_{(\mu} \overline{h}_{\nu)}{}^{\varrho} - \frac{1}{2}\eta_{\mu\nu}\partial_\varrho \partial_\sigma \overline{h}^{\varrho\sigma} = \frac{\kappa^2}{4} T_{\mu\nu} \,, \quad \overline{h}_{\mu\nu} \coloneqq h_{\mu\nu} - \frac{1}{2}\eta_{\mu\nu}\eta^{\alpha\beta}h_{\alpha\beta} \,, \tag{2.30}$$

where $\Box = \partial_\mu \partial^\mu$ is the d'Alembertian and $T_{\mu\nu}$ is the energy-momentum tensor containing dependence of the matter field but also higher orders in $h_{\mu\nu}$. The equations (2.30) are still invariant under infinitesimal diffeomorphisms generated by a vector ξ

$$\delta_\xi h_{\mu\nu} = \partial_\mu \xi_\nu + \partial_\nu \xi_\mu \,. \tag{2.31}$$

Therefore, in order to solve the equations it is convenient to fix a gauge. A particular useful gauge is specified by the harmonic (de Donder) gauge condition

$$\partial^\mu \overline{h}_{\mu\nu} = 0 \,. \tag{2.32}$$

In harmonic gauge we find

$$\Box \overline{h}_{\mu\nu} = -\frac{\kappa^2}{2} T_{\mu\nu} \,. \tag{2.33}$$

This is precisely the form of the wave equation as it is known e.g. from Electrodynamics. Einstein's equation therefore predict wave-like perturbations on flat space propagating at the speed of light, sourced by the matter fields and gravitational fields through the energy-momentum tensor $T_{\mu\nu}$.

2.2. Classical Mechanics

In this section we review some basics of classical mechanics, details can be found in most textbooks on the subject, e.g. Landau and Lifshitz [105]. The classical (off-shell) action functional for a path described by a set of generalized coordinates $\underline{q}(t) = \{q_1(t), \ldots, q_n(t)\}$ is

$$S[\underline{q}; t_1, t_0] \coloneqq \int_{t_0}^{t_1} L(\underline{q}(t), \dot{\underline{q}}(t), t)\, \mathrm{d}t\,. \tag{2.34}$$

The motion of the system is determined by the principle of extremal action, that is a path such that the variation vanishes $\delta S = 0$ while the boundary points $\underline{q}(t_1) = \underline{q}_1, \underline{q}(t_0) = \underline{q}_0$ are kept fixed. Equivalently we can describe the system in terms of the Hamiltonian $H(\underline{p}, \underline{q}, t) = \sum_{i=1}^{n} p_i \dot{q}^i - L$

$$S[\underline{q}; t_1, t_0] = \int_{t_0}^{t_1} \sum_{i=1}^{n} p_i \dot{q}^i - H\, \mathrm{d}t\,. \tag{2.35}$$

We can consider S evaluated on a classical path as a function of the endpoint q_1 and t_1, keeping the start-point and the initial time fixed. For simplicity, we write $\underline{q} = \underline{q}_1$ and $t = t_1$. We then have the Hamilton-Jacobi equation

$$\frac{\partial S}{\partial t} = -H(\underline{q}, \underline{p}, t) \quad p_i = \frac{\partial S}{\partial q^i}\,, \tag{2.36}$$

where $\underline{p} = \underline{p}(t_1)$. In what follows we specify to a conservative radial system. The symmetries of the problem allow to restrict the discussion to a plane parameterized by polar coordinates (r, θ). Furthermore the Hamiltonian H and the angular momentum p_θ are conserved along the trajectory and we denote the conserved values by E and J respectively. It is natural to perform a Legendre transformation with respect to the cyclic variables θ, t (and at the same time to subtract a trivial constant) to obtain a new function

$$I_r(r, J, E) \coloneqq S(r, \theta, t) + E(t - t_0) - J(\theta - \theta_0)\,. \tag{2.37}$$

Using the explicit form of the action in Eq. (2.35) we have

$$I_r(r, J, E) = \pi J - \oint p_r(r', J, E)\mathrm{d}r'\,, \tag{2.38}$$

where p_r is determined implicitly through $H(r, p_r(r, J, E), J) = E$ and the integral is evaluated over a trajectory connecting r_0 to r. We will only be interested in the radial action evaluated over a scattering trajectory, which can be obtained using the fact that the motion is symmetric around the point of closest approach $r_{\min}$,

$$I_r(J, E) = \pi J - 2\int_{r_{\min}(J,E)}^{\infty} \mathrm{d}r p_r(J, E, r)\,. \tag{2.39}$$

Here the turning point $r_{\min}$ is determined as the largest positive solution to $p_r(r_{\min}) = 0$. The scattering angle $\chi = \theta - \theta_0$ can be obtained by the inverse Legendre transformation

$$\chi = -\frac{\partial I_r(J,E)}{\partial J}\,. \tag{2.40}$$

If we assume that the Hamiltonian is isotropic, i.e. a function of $\boldsymbol{p}^2 = p_r^2 + J^2/r^2$ we have from the implicit definition of p_r

$$\frac{\partial p_r}{\partial J} = \frac{J}{r^2 p_r}\,. \tag{2.41}$$

and therefore

$$\chi = -\pi + 2J\int_{r_{\min}(J,E)}^{\infty}\frac{\mathrm{d}r}{r^2 p_r}\,. \tag{2.42}$$

2.3. Relativistic Central-Force Problem

Typically, the central-force problem is considered for a velocity-independent potential. However, in the post-Newtonian and in particular in the post-Minkowskian setup the potential will depend on the momentum $\boldsymbol{p}$. The separation between potential and kinetic term is through the power-counting introduced by the coupling constant G. All effects due to special relativity will be treated non-preturbatively. The Hamiltonian for a relativistic two-body system in the COM system

$$H(\boldsymbol{r},\boldsymbol{p}) = \sum_{i=1}^{2}\sqrt{\boldsymbol{p}^2 + m_i^2} + V(\boldsymbol{r},\boldsymbol{p})\,, \tag{2.43}$$

where $\boldsymbol{p}$ is the COM momentum and $\boldsymbol{r}$ the separation of the bodies. We assume that the potential is isotropic and is expanded in a power series of the form

$$V(\boldsymbol{r},\boldsymbol{p}) = \sum_{n=1}^{\infty} c_n(\boldsymbol{p}^2)\frac{G^n}{r^n}\,, \quad r = |\boldsymbol{r}|\,. \tag{2.44}$$

Since the Hamiltonian is isotropic, we can directly make use of the discussion in the previous chapter an find

$$\chi = -\pi + 2J\int_{r_{\min}}^{\infty}\frac{\mathrm{d}r}{r^2|p_r|}\,. \tag{2.45}$$

Since by assumption the interaction mediated by the potential vanishes as $r \to \infty$ we can identify the conserved energy E with the COM momentum at infinity

$$E = \sqrt{p_\infty^2 + m_1^2} + \sqrt{p_\infty^2 + m_2^2}\,. \tag{2.46}$$

The equation $H = E$ can be solved for the radial momentum, leading to the following implicit equation which is convenient because it free of roots

$$\boldsymbol{p}^2 = \frac{\lambda((E - V(\boldsymbol{r}, \boldsymbol{p}))^2, m_1^2, m_2^2)}{4(E - V(\boldsymbol{r}, \boldsymbol{p}))^2}, \quad \boldsymbol{p}^2 = p_r^2 + \frac{J^2}{r^2}. \tag{2.47}$$

Both sides of the equation depend on $\boldsymbol{p}$, but the potential can be treated perturbatively (in G), so we can iteratively solve for p_r as a function of r to any desired order in G,

$$p_r^2(r) = p_\infty^2 - \frac{J^2}{r^2} + \sum_{n=1}^{\infty} P_n \frac{G^n}{r^n}, \tag{2.48}$$

The first few coefficients in this series read [48]

$$P_1 = -2E\xi\bar{c}_1, \tag{2.49}$$

$$P_2 = -2E\xi\bar{c}_2 + (1-3\xi)\bar{c}_1^2 + 4E^2\xi^2\bar{c}_1\bar{c}'_1, \tag{2.50}$$

$$\begin{aligned} P_3 = {} & -2E\xi\bar{c}_3 + 2(1-3\xi)\bar{c}_1\bar{c}_2 - 4E^3\xi^3\bar{c}_1\big(2\bar{c}'^2_1 + \bar{c}_1\bar{c}''_1\big) + 4E^2\xi^2(\bar{c}_2\bar{c}'_1 + \bar{c}_1\bar{c}'_2) \\ & - 6E(1-3\xi)\xi\bar{c}_1^2\bar{c}'_1 + \frac{(1-4\xi)\bar{c}_1^3}{E}, \end{aligned} \tag{2.51}$$

$$\begin{aligned} P_4 = {} & -2E\xi\bar{c}_4 + \frac{8}{3}E^4\xi^4\bar{c}_1\big(6\bar{c}'^3_1 + 9\bar{c}_1\bar{c}''_1\bar{c}'_1 + \bar{c}_1^2\bar{c}'''_1\big) + \frac{5(1-4\xi)\bar{c}_1^4}{4E^2} + \frac{3(1-4\xi)\bar{c}_1^2\bar{c}_2}{E} \\ & - 4E^3\xi^3\big(2\bar{c}_2\big(\bar{c}'^2_1 + \bar{c}_1\bar{c}''_1\big) + \bar{c}_1(4\bar{c}'_1\bar{c}'_2 + \bar{c}_1\bar{c}''_2)\big) + (1-3\xi)\bar{c}_2^2 \\ & + 4E^2\xi^2\big(2(1-3\xi)\bar{c}''_1\bar{c}_1^3 + 6(1-3\xi)\bar{c}'^2_1\bar{c}_1^2 + \bar{c}'_3\bar{c}_1 + \bar{c}_3\bar{c}'_1 + \bar{c}_2\bar{c}'_2\big) \\ & - 6E(1-3\xi)\xi\bar{c}_1(2\bar{c}_2\bar{c}'_1 + \bar{c}_1\bar{c}'_2) + 2\bar{c}_1\big((1-5\xi)^2\bar{c}'_1\bar{c}_1^2 + (1-3\xi)\bar{c}_3\big), \end{aligned} \tag{2.52}$$

with $\bar{c}_n = c_n(p_\infty^2)$. The scattering angle is given by inserting this expansion into Eq. (2.45)

$$\chi = -\pi + 2J\int_{r_{\min}}^{\infty} \frac{\mathrm{d}r}{r^2\sqrt{p_\infty^2 - \frac{J^2}{r^2} + \sum P_i\big(\frac{G}{r}\big)^i}}. \tag{2.53}$$

It is convenient to use a result obtained by Damour and Schäfer [106], whereby integrals of the form (2.53) can be expanded by deforming the root through analytic continuation $1/2 \to 1/2 + \epsilon$, expanding the integrand, performing the integrals that appear by elementary formulas involving beta-functions and finally taking the limit $\epsilon \to 0$. In this process one can neglect the dependence on the endpoint and can set $r_{\min} \to b$. The result for the scattering angle is

$$\begin{aligned} \chi = {} & \frac{P_1}{p_\infty}\left(\frac{G}{J}\right) + \frac{\pi}{2}P_2\left(\frac{G}{J}\right)^2 - \frac{P_1^3 - 12p_\infty^2P_1P_2 - 24p_\infty^4P_3}{12p_\infty^3}\left(\frac{G}{J}\right)^3 \\ & + \frac{3\pi}{8}(P_2^2 + 2P_1P_3 + 2p_\infty^2P_4)\left(\frac{G}{J}\right)^4 + \mathcal{O}\big(G^5\big). \end{aligned} \tag{2.54}$$

2.3.1. Point Particles in a Black Hole Background

The Schwarzschild solution is the unique vacuum solution to Einstein's equations with spherical symmetry. The metric is explicitly given by

$$g_{\mu\nu}\mathrm{d}x^\mu x^\nu = \Big(1-\frac{r_\mathrm{S}}{r}\Big)\mathrm{d}t^2 - \Big(1-\frac{r_\mathrm{S}}{r}\Big)^{-1}\mathrm{d}r^2 - r^2\mathrm{d}\Omega\,, \tag{2.55}$$

where $\mathrm{d}\Omega = (\mathrm{d}\theta^2 + \sin^2\theta\,\mathrm{d}\varphi^2)$ is the volume element on a two-sphere and where the Schwarzschild radius is $r_\mathrm{S} = 2GM$. The parameter M will eventually be identified with the mass of the gravitating object.[3]

The Schwarzschild metric has four Killing vectors. Two of them are associated with the rotation invariance and we can use them to confine the analysis to a plane, choosing say $\theta = \pi/2$. The two remaining Killing vectors are

$$\xi^\mu_{(\varphi)} = \delta^\mu_\varphi\,, \quad \xi^\mu_{(t)} = \delta^\mu_t\,. \tag{2.56}$$

This implies that the following quantities are conserved along a geodesic $x^\mu(\lambda)$:

$$E \coloneqq \xi^\mu_{(\varphi)} g_{\mu\nu}\dot{x}^\nu = \Big(1-\frac{r_\mathrm{S}}{r}\Big)\dot{t}\,, \qquad J \coloneqq \xi^\mu_{(t)} g_{\mu\nu}\dot{x}^\nu = r^2\dot{\varphi}\,, \tag{2.57}$$

where by slightly abusive notation $t = x^t(\lambda)$ etc. The quantities E and L have a natural interpretation as energy and the magnitude of the angular momentum. Also along a geodesic the inner product

$$K = g_{\mu\nu}\dot{x}^\nu\dot{x}^\nu \tag{2.58}$$

is conserved and by reparametrization of the proper time λ can be chosen to equal $K = 0$ for massless particles (lightlike geodesic) and $K = \mu^2$ for massive particles (timelike geodesic) [4]. Writing the parameter K explicitly in terms of the Schwarzschild metric yields

$$\mu^2 = \Big(1-\frac{r_\mathrm{S}}{r}\Big)\dot{t}^2 - \Big(1-\frac{r_\mathrm{S}}{r}\Big)^{-1}\dot{r}^2 - r^2\dot{\varphi}^2\,. \tag{2.59}$$

Using the conserved charges J, E introduced in Eq. (2.57), we can solve for the radius r as a function of the angle φ

$$\begin{aligned}\left(\frac{\mathrm{d}r}{\mathrm{d}\varphi}\right)^2 &= \left(\frac{\mathrm{d}r}{\mathrm{d}\lambda}\right)^2\left(\frac{\mathrm{d}\lambda}{\mathrm{d}\varphi}\right)^2 = \left(\frac{E^2-\mu^2}{J^2}r^4 + \frac{\mu^2}{J^2}r_\mathrm{S}r^3 - r^2 + r_\mathrm{S}r\right)\\ &= \frac{r^4}{J^2}\left(p_\infty^2 - \frac{J^2}{r^2} + \frac{\mu^2 r_\mathrm{S}}{r} + \frac{J^2 r_\mathrm{S}}{r^3}\right),\end{aligned} \tag{2.60}$$

[3] The variable θ is not related to the variable used in the context of the scattering angle in the previous section.

[4] We use the suggestive symbols M and μ for the mass parameter of the Schwarzschild background and the test-particle mass. This parameters are to be interpreted as the total mass and the reduced mass of the binary system respectively.

where p_∞ is the momentum at infinity. For the bound case there are two turning points r_1, r_2, for which $\mathrm{d}r/\mathrm{d}\varphi = 0$ and the periastron advance is equal to twice the integral between the turning points

$$\Delta\Phi = 2J \int_{r_1}^{r_2} \frac{\mathrm{d}r}{r^2\sqrt{p_\infty^2 - \frac{J^2}{r^2} + \frac{\mu^2 r_\mathrm{S}}{r} + \frac{J^2 r_\mathrm{S}}{r^3}}} \,. \tag{2.61}$$

This integral can be solved in terms of a complete elliptic integral of the first kind, which can subsequently be expanded to arbitrary powers of G (see e.g. Ref. [106]). We are interested mostly in the scattering case where the corresponding observable is the scattering angle χ, which is obtained by integrating over the trajectory, using the symmetry around the point of closest approach r_min,

$$\chi = -\pi + 2 \int_{r_\mathrm{min}}^{\infty} \frac{\mathrm{d}r}{r^2\sqrt{p_\infty^2 - \frac{J^2}{r^2} + \frac{\mu^2 r_\mathrm{S}}{r} + \frac{J^2 r_\mathrm{S}}{r^3}}} \,. \tag{2.62}$$

Although there does not exist a simple formula in terms of complete elliptic functions as for the bound case it is straightforward to expand the integral as we did above through the procedure described in Ref. [106]. Expanded in powers of G the angle $\chi^\mathrm{Schw} = \sum_i {}_{(i)}\chi^\mathrm{Schw}$ for the Schwarzschild case is determined by

$${}_{(1)}\chi^\mathrm{Schw} = 2\frac{GM}{J}\frac{2p_\infty^2\mu^2}{p_\infty} \,, \tag{2.63}$$

$${}_{(2)}\chi^\mathrm{Schw} = \frac{3\pi}{4}\left(\frac{GM}{J}\right)^2 (5p_\infty^2 + 4\mu^2) \,, \tag{2.64}$$

$${}_{(3)}\chi^\mathrm{Schw} = 2\left(\frac{GM}{J}\right)^3 \frac{(-\mu^6 + 12\mu^4 p_\infty^2 + 72\mu^2 p_\infty^4 + 64p_\infty^6)}{3p_\infty^3} \,, \tag{2.65}$$

$${}_{(4)}\chi^\mathrm{Schw} = \frac{105}{64}\pi\left(\frac{GM}{J}\right)^4 \left(16\mu^4 + 48\mu^2 p_\infty^2 + 33p_\infty^4\right) . \tag{2.66}$$

Schwarzschild Hamiltonian The motion of a massive point particle of mass μ in a background metric $g_{\mu\nu}$ can be described by a the Lagrangian

$$\mathcal{L}(x^\mu, \dot{x}^\mu) = -\mu\sqrt{g_{\mu\nu}\dot{x}^\mu\dot{x}^\mu} \,. \tag{2.67}$$

We would like to have a Hamiltonian description of the problem. Therefore we first have to assume that we have a timelike Killing field and we can choose a gauge in which $g_{i0} = 0$. It is well-known that due to reparametrization invariance of the Lagrangian, the corresponding Hamiltonian vanishes identically (see e.g. Ref. [107]). Here we break the reparametrization invariance by choosing a gauge. A convenient choice is the static gauge $x^0 = \lambda$, whence the Lagrangian for a point particle reads

$$\mathcal{L}(x^\mu, \dot{x}^\mu) = -\mu\sqrt{g_{00} + g_{ij}\dot{x}^i\dot{x}^j} \,. \tag{2.68}$$

The conjugate momenta are

$$p_i = -\mu \frac{g_{ij}\dot{x}^j}{\sqrt{g_{00} + g_{ij}\dot{x}^i\dot{x}^j}} \,. \tag{2.69}$$

Finally we obtain the Hamiltonian describing the motion of the mass μ in the geometry $g_{\mu\nu}$,

$$H(\boldsymbol{x}, \boldsymbol{p}) = p_i x^i - L = \sqrt{g_{00}}\sqrt{\mu^2 - g^{ij}(\boldsymbol{x})p_i p_j} \,. \tag{2.70}$$

In this thesis we are mainly interested in the motion of a point particle in a Schwarzschild background although more general cases e.g. for a Kerr background are simple to obtain given the general form. The Schwarzschild metric (2.55) in isotropic coordinates $r \mapsto r_{\rm iso}(1 + r_{\rm S}/(4r_{\rm iso}))^2$, (see e.g. Ref. [108]) reads

$$g_{\mu\nu}\mathrm{d}x^\mu x^\nu = \left(\frac{1 - \frac{r_{\rm S}}{4r}}{1 + \frac{r_{\rm S}}{4r}}\right)^2 \mathrm{d}t^2 - \left(1 + \frac{r_{\rm S}}{4r}\right)^4 \mathrm{d}\boldsymbol{r}^2 \,, \tag{2.71}$$

where for notational convenience we dropped the subscript. Inserting in Eq. (2.70), the corresponding *Schwarzschild Hamiltonian* [109] reads

$$H(\boldsymbol{r}, \boldsymbol{p}) = \mu\left[\left(1 - \frac{r_{\rm S}}{4r}\right)\left(1 + \frac{r_{\rm S}}{4r}\right)^{-1}\sqrt{1 + \left(1 - \frac{r_{\rm S}}{4r}\right)^{-4}\frac{\boldsymbol{p}^2}{\mu^2}}\right] . \tag{2.72}$$

In the limit of large distances, $r \gg r_{\rm S} = 2GM$ we recover the usual relativistic Hamiltonian of a free particle with mass μ

$$H(\boldsymbol{r}, \boldsymbol{p}) = \sqrt{\boldsymbol{p}^2 + \mu^2} + \mathcal{O}(r/r_{\rm S}) \,. \tag{2.73}$$

In the Newtonian limit $G \sim \boldsymbol{p}^2 \ll 1$, we find the Hamiltonian of a particle moving in the Newtonian potential

$$H(\boldsymbol{r}, \boldsymbol{p}) = \mu + \frac{\boldsymbol{p}^2}{2\mu} - \mu\frac{GM}{r} + \mathcal{O}(\boldsymbol{p}^2/\mu^2) \,. \tag{2.74}$$

Keeping fixed the total mass M and the COM velocity $\boldsymbol{p}/\mu$, the Hamiltonian is manifestly leading order in the self-force expansion (expansion in powers of ν). This motivates to organize the expressions encountered later in terms of $M, \boldsymbol{p}^2/\mu^2, \nu$ instead of m_1, m_2 and $\sqrt{s}$. The isotropic form of the Hamiltonian allows us to directly use the formula (2.42) together with p_r determined through $H(\boldsymbol{r}, \boldsymbol{p}) = E$,

$$p_r^2 = \frac{\left(1 + \frac{\rm GM}{2r}\right)^6}{\left(1 - \frac{\rm GM}{2r}\right)^2}E^2 - \mu^2\left(1 + \frac{\rm GM}{2r}\right)^4 - \frac{J^2}{r^2} \,. \tag{2.75}$$

The result for the scattering angle agrees with the result found in Eqs. (2.63)–(2.66).

3. Scattering Amplitudes

Setting aside effects associated to the horizons, black holes have no internal structure and are therefore well described by point particles or world lines. The scattering of two black holes is therefore very similar to the scattering of elementary particles such as studied in collider physics experiments. This processes are naturally described in terms of asymptotic data. The scattering process is formally characterized by transition probabilities, encoded in the S-matrix ("scattering matrix") which maps the incoming to the outgoing states $|\text{out}\rangle$,

$$|\text{out}\rangle = S|\text{in}\rangle \,. \tag{3.1}$$

Since for the free theory the evolution is trivial, $S = \mathbb{1}$, we define a "transfer matrix" T, which encodes the non-trivial part of the interaction

$$S = \mathbb{1} + \mathrm{i}T \,. \tag{3.2}$$

Because of translation invariance, the scattering process should conserve four-momentum and therefore it is custom to factor out a delta function to define a scattering amplitude $\mathcal{M}$[1]

$$\langle f|T|i\rangle = (2\pi)^4 \delta^{(4)}(p_i + p_f)\mathcal{M}(i \to f) \,, \tag{3.3}$$

where p_i and p_f are the total initial and final four-momentum respectively. The scattering amplitude contains all information about the scattering process of asymptotic states. An important property of the S-matrix is its unitarity $S^\dagger S = \mathbb{1}$, which implies

$$\mathrm{i}(T^\dagger - T) = T^\dagger T \,. \tag{3.4}$$

By inserting a complete set of states this can be converted into a statement about amplitudes

$$2\,\mathrm{Im}\,\mathcal{M}(i \to f) = \sum_X \mathcal{M}(i \to X)^* \mathcal{M}(X \to f) \,, \tag{3.5}$$

where the sum runs over all possible intermediate states X and also includes an integration over the associated on-shell phase space.

The definition of the scattering amplitude is a-priori non-perturbative, i.e. valid to all orders in the coupling constants of the theory. In practice it is useful to expand the scattering amplitude in powers of the coupling

$$\mathcal{M} = \sum_i \mathcal{M}^{(i)} \,. \tag{3.6}$$

[1]Notice that we us an convention where all momenta are outgoing.

In field theories, the fixed-order amplitudes $\mathcal{M}^{(i)}$ can be computed using for example Feynman rules. Eventually the amplitude will be expressed as a sum of L-loop amplitudes[2]

$$\mathcal{M}^{(L)}(\underline{p},\underline{m}) \quad = \int \mathrm{d}\underline{\ell} \sum_{\Gamma\in\Delta} \frac{N_\Gamma\left(\underline{\ell},\underline{p},\underline{m}\right)}{\prod\limits_{\rho\in\Gamma}\rho\left(\underline{\ell},\underline{p},\underline{m}\right)}\,, \quad \mathrm{d}\underline{\ell} = \prod_{j=1}^{L}\mathrm{d}^D\ell_j\,. \tag{3.7}$$

where the *propagators* ρ are Lorentz-invariant functions of the E independent *external* momenta $\underline{p} = \{p_1,\ldots,p_E\}$ and L *internal* (loop) momenta $\underline{\ell} = \{\ell_1,\ldots,\ell_L\}$ and a set of scalar invariants $\underline{m}$, e.g. particle masses. Typical examples that we will encounter in this thesis are

$$\rho = (\ell - q)^2 - m^2 + \mathrm{i}\varepsilon\,, \quad \rho = v\cdot\ell + \omega + \mathrm{i}\varepsilon\,. \tag{3.8}$$

Propagators of the second type typically arise from expansions in kinematic regions, and are encountered e.g. in heavy quark effective theory (HQET,[110–112]) or the computation of the cusp anomalous dimension [113].

In Eq. (3.7) the *hierarchy* Δ is the set of all inequivalent propagator structures Γ. In some cases, for example for the classical analysis we can already consistently exclude some topologies from the ansatz in the first step. An example for massless two-to-two scattering is shown in Figure. 3.1. Finally, the integrals over the inter-

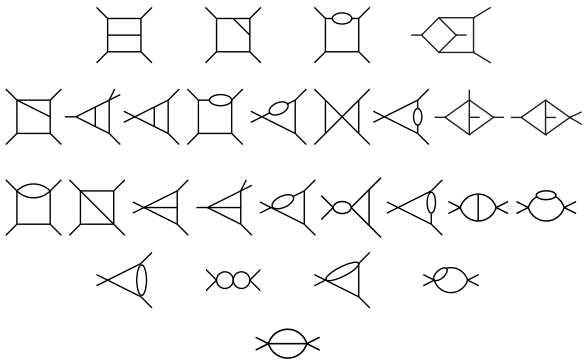

Figure 3.1.: Topologically inequivalent propagator structures for massless two-to-two scattering.

nal degrees of freedom associated with ℓ have to be evaluated. The computation of an amplitude in perturbation theory thereby naturally splits into two separate problems:

- The determination of the integrand, that is finding the form of the numerator N_Γ. While this can be computed using Feynman diagrams, we will present an more effective way using unitarity methods in the following chapter.
- The evaluation of the integrals over the ℓ-variables. This problem will be addressed in chapter 4.

[2]In practice, even when working with Feynman integrals, some of the propagators may enter raised to integer powers.

3.1. Generalized Unitarity

The traditional way to obtain an integrand (3.7) is based on the use of Feynman rules. However, in practice, this comes with several drawbacks, mainly a factorial growth in the number of diagrams that have to be considered and algebraic complexity of intermediate expressions. The main problem in the traditional approach is associated to unphysical degrees of freedom, associated to gauge transformations and field redefinitions [114, 115]. However, the S-matrix and consequently on-shell scattering-amplitudes should be independent of any such ambiguity.

Fortunately, with *generalized unitarity* [33, 34, 116] there is a well established formalism, which allows to compute general loop amplitudes from tree-level amplitudes. The tree-level amplitudes can be computed with different means, but it is in the spirit of the on-shell approach to generate them recursively from on-shell three-point amplitudes, e.g. through the recursion developed by Britto, Cachazo, Feng and Witten (BCFW) [117, 118]. We will only be brief in the description of the method, referring to the literature, e.g. Ref. [119] for more details.

The basic realization of the generalized unitarity method is that the amplitude in general can be constrained by its factorization properties (see e.g. Ref. [120]). A shortcut to the construction of an amplitude is therefore to make an ansatz for the integrand in Eq. (3.7) and then determine the numerators through demanding the correct behavior under factorization.

In practice we make an ansatz for the individual numerators in terms of monomials in Lorentz invariant scalar products involving the loop momenta $\underline{\ell}$ and the external momenta $\underline{p}$ as well as the masses $\underline{m}$ with rational coefficients which are to be determined. For example assume if we were interested in a two-loop topology parameterized through ℓ_1, ℓ_2 with a single external momentum q [3] and by dimensional analysis we have constrained the mass dimension of the numerator to two, then a ansatz is a homogeneous polynomial of degree one

$$N_{\text{⟲}} = a_{\text{⟲},1} q^2 + a_{\text{⟲},2} q \cdot \ell_1 + a_{\text{⟲},3} q \cdot \ell_2 + a_{\text{⟲},4} \ell_1 \cdot \ell_2 + a_{\text{⟲},5} \ell_1^2 + a_{\text{⟲},6} \ell_2^2 \,. \tag{3.9}$$

The maximal powers of the loop momenta can be constrained by power-counting arguments based on Feynman diagrams. For example in the case of pure gravity each vertex is quadratic in the momenta, such that the maximal rank of the tensor in any loop variable cannot be higher than twice the number of graviton vertices. We will discuss this more in the context of practical applications in section 5.

The individual coefficients in the ansatz can be determined by considering certain on-shell configurations of the loop momenta that set some of the propagator to zero. The undetermined coefficients a_Γ are constrained from the factorization properties of the integrand in loop-momenta configurations ℓ_l^Γ where the propagators in P_Γ vanish:

$$\sum_{\text{states}} \prod_{k \in T_\Gamma} \mathcal{M}_k^{\text{tree}}(\ell_l^\Gamma) = \sum_{\Gamma' \geq \Gamma} \frac{N_\Gamma(\ell_l^\Gamma)}{\prod_{\rho \in \Gamma' \setminus \Gamma} \rho(\ell_l^\Gamma)} \,, \tag{3.10}$$

[3] This corresponds to the diagram on the very bottom of Figure. 3.1.

where the right hand side is given as a product of trees, where the cut internal lines are glued together by sums over internal states. In the following we refer to this expression as a *unitary cut*. We give an explicit example of a the graviton state sum in Appendix C.

3.2. The Numerical Unitarity Method

The numerical unitarity method first proposed in Refs. [121, 122] is a particular flavor of the generalized unitary method. The main feature is that all operations discussed in the context of the unitarity method are performed numerically. Initially in floating point or finite-field arithmetic. This provides a very efficient framework for the numeric evaluation of multi-loop amplitudes. In particular its implementation in the `Blackhat` library [123, 124] has been used to compute amplitudes at next-to-leading order for scattering processes with high multiplicity, in particular with up to five jets in the final state in Ref. [125].

The method has subsequently been promoted to the the two-loop level [126–128] and its use was first demonstrated in Ref. [129] for the case of gluonic two-to-two scattering. Since then the implementations have become very mature eventually leading to the public code `Caravel` [130].

We will find the numerical unitarity method particularly useful to deal with multi-loop computations in Einstein gravity, mostly because of the overwhelming algebraic complexity associated with such computations.

3.2.1. Master-Surface Decomposition

When performing the integrand matching there is a large redundancy due to terms that integrate to zero, so-called *surface-terms*. While this pieces do not contribute to the final result for the integrated amplitude, they have to be kept in order to consistently match the integrand.

Instead of using a basis of Lorentz products as in (3.9) it is convenient to organize the integrand in a master-surface decomposition [131], which amounts to the following form of the ansatz for the numerators

$$N_\Gamma = \sum_{i\in M_\Gamma} a_{\Gamma,i} n_i(\underline{\ell}) + \sum_{i\in S_\Gamma} a_{\Gamma,i} n_i(\underline{\ell})\,. \tag{3.11}$$

Here, M_Γ is a set of *master integrands*, and S_Γ a set of surface terms, that is

$$\int \mathrm{d}\underline{\ell}\, \frac{n_i(\underline{\ell})}{\prod_{\rho\in P_\Gamma}\rho(\underline{\ell})} = 0\,, \quad \forall i \in S_\Gamma\,. \tag{3.12}$$

The construction of surface terms is tightly connected to integration-by-parts identities, which will be described in section 4.4. The remainder of the method

proceeds in the same way as in the conventional generalized unitary approach, with the only difference that the solution of the equations is performed numerically, that is we sample a set $\underline{\ell}^{\Gamma}$ of on-shell loop momenta abd solve for the coefficients $a_{\Gamma,i}$. After fitting the ansatz, the surface terms can be immediately dropped and we obtain an expression for the amplitude as a linear combination of master terms

$$\mathcal{M} = \sum_{\Gamma\in\Delta} \sum_{i\in M_\Gamma} a_{\Gamma,i} I_{\Gamma,i} \,, \quad I_{\Gamma,i} = \int \mathrm{d}\underline{\ell} \, \frac{n_i}{\prod_{\rho\in P_\Gamma} \rho} \,. \tag{3.13}$$

Typically in the process we also choose a numerical point for the external kinematics and consequently only obtain a numerical value for the coefficients $a_{\Gamma,i}$. By further sampling of points in external kinematics we can reconstruct the functional form of the $a_{\Gamma,i}$. Together with an efficient numerical evaluation of the tree amplitudes that appear in the system of equations we have therefore obtained an black-box evaluator of the integral coefficients in the amplitude. Starting from this black-box evaluator it is straightforward to reconstruct the full dependence as functions of the external kinematics. This process has become standard practice in high-energy physics, see e.g. Refs. [132–135].

4. Feynman Integrals

The evaluation of scattering amplitudes in perturbation theory generally requires the evaluation of integrals over virtual degrees of freedom. We will discuss this integrals in their avatar most familiar from quantum field theory, namely Feynman integrals. The evaluation of integrals presents one of the main bottlenecks both in the PN and the PM framework (see e.g. Refs. [49, 72, 76, 93]).

It is important to note that this type integrals arise irrespective of the approach and are for example encountered in computations using worldlines [93, 104]. As such the problem of integrals is not directly connected to the amplitude-based approach, but nonetheless the spirit will be similar in that we will try to make maximal use of advanced methods developed in the context of collider phenomenology.

The purpose of this chapter is to introduce some of the important properties associated with Feynman diagrams and explain how to evaluate them. Further details on the computation of Feynman integrals in general can be found in the lecture notes [136–138].

4.1. Notation and Structure of Integrals

An D-dimensional L-loop Feynman integral is an integral of the form

$$I(\underline{p}; D) = \int \mathrm{d}\underline{\ell} \frac{\mathcal{N}(\underline{\ell}, \underline{p})}{\rho_1^{a_1} \cdots \rho_n^{a_n}} \,, \tag{4.1}$$

where the a_i are typically integers and $\underline{p}$ is a set of are external four-vectors in the problem (polarization vectors or momenta of the external states). These are precisely the type of integrals that appear in the evaluation of an amplitude and which are present in Eq. (3.7). In general, the propagators ρ_i depend linearly or quadratically on the loop momenta $\underline{\ell}$, e.g. [1]

$$\rho = (\ell_1 + \ell_2)^2 \,, \quad \rho = (\ell_1 - q)^2 - m^2 \,, \quad \rho = v \cdot \ell_1 + \omega \,. \tag{4.2}$$

[1] If no $\mathrm{i}\varepsilon$ is specified it is always implicitly understood to be $+\mathrm{i}\varepsilon$. Sometimes it is convenient to absorb a sign in the propagators. In this case the prescription is $-\mathrm{i}\varepsilon$, i.e. $-\ell^2 \to -(\ell^2 + \mathrm{i}\varepsilon)$.

Linear propagators (also called eikonal propagators) typically arise from expansions of massive quadratic propagators, e.g. in HQET or the computation of cusp anomalous dimension[2].

We will also see that they naturally arise in the expansion of integrals relevant to classical scattering and they will therefore be the primary type of integrals considered in this thesis, although for the meantime all discussions are general and applicable to a generic form of the propagators, only assuming that they are rational functions of loop momenta and external kinematics.

We can complete the set of propagators present in the integral by a set of so-called *irreducible scalar produces* (ISP), such that every scalar product can be written in terms of these. To uniformize the notation we will denote both propagators and ISP's by ρ_i. The set of propagators plus ISP's will contain $N_\rho = LE + L(L+1)/2$ elements to capture all degrees of freedom of the loop momenta. A general numerator is therefore expressible as a multivariate polynomial in the propagator variables with coefficients depending on scalar products of external momenta. The integration can therefore be broken down to the evaluation of integrals of the form

$$I_{\underline{a}}(\underline{s}; D) = \int \frac{\mathrm{d}\underline{\ell}}{\rho_1^{a_1} \cdots \rho_n^{a_n}}\,, \tag{4.3}$$

where the a_i's can now be either positive or negative, depending on whether they originate from numerators or actual propagators.

An integral *topology* is a list of propagators that are present in a given diagram (i.e. position of the positive indices in the list of indices). Topologies of Feynman integrals can be represented by pictures which contain the information of all propagators by depicting the momentum flow. A *parent* topology is a topology which has additional genuine propagators, while a *daughter* has less propagators (i.e. some of the indices are zero or negative). A *family* of integrals is given by a parent topology and all its daughters.

For concreteness we consider the family of the one-loop massless box integral

$$I^{\square}_{\underline{a}}(s,t;D) = \int \frac{\mathrm{d}^D\ell}{(2\pi)^D} \frac{1}{[(\ell-p_1)^2]^{a_1}[(\ell+p_2)^2]^{a_2}[\ell^2]^{a_3}[(\ell-q)^2]^{a_4}}\,, \tag{4.4}$$

where the massless kinematics is determined by two Mandelstam invariants $s = (p_1+p_2)^2$ and $t = q^2$. The box topology has three types of daughter integrals: triangles with a single index non-positive, bubbles with two non-positive indices and tadpoles with only a single positive index. The nomenclature for these integrals should be evident from the corresponding pictures displayed in Figure 4.1.

In the next chapters, we will show how to deal with divergent Feynman integrals by using dimensional regularization and how to evaluate the resulting regularized integrals.

[2]For some applications using linear propagators in a context different from the present work see e.g. Refs. [97, 99, 139].

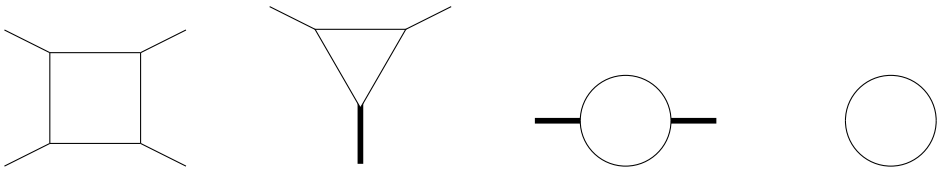

(1) (2) (3) (4)

Figure 4.1.: Sectors in the one-loop box family. Thin lines are on shell, with $p_i^2 = 0$, thick lines are off-shell legs with $p_i^2 \neq 0$.

4.2. Regularization of Divergent Integrals

In intermediate steps of an physical computation one will in general encounter integrals that are individually ill-defined (divergent). This divergences are either of ultraviolet (UV, large $|\ell|$, short-range) or of infrared (IR, small $|\ell|$, long-range) nature.

A first step of dealing with these infinities requires the choice of a *regularization scheme* which allows to systematically track infinities which have to cancel for physical observables, leaving a finite final result. In order to motivate the most common regularization scheme, called *dimensional regularization*, we will consider two prime examples: the bubble integral and the triangle integral. The values of these integrals in dimensional regularization are well-known (see e.g. Ref. [140]) and we will simply use their results here.

4.2.1. Ultraviolet Divergences

The massless bubble integral provides an example for an UV divergence. The integral is formally given by

$$I^{\square}_{0011} = \int \frac{\mathrm{d}^4\ell}{(2\pi)^4} \frac{1}{\ell^2(\ell-q)^2} \,. \tag{4.5}$$

For parametrically large loop momenta $\ell \sim \lambda \gg q$, we have

$$\frac{1}{\ell^2(\ell-q)^2} \sim \frac{1}{(\ell^2)^2} \sim \lambda^{-4} \,, \quad \mathrm{d}^4\ell \sim \lambda^4 \,, \tag{4.6}$$

we therefore expect the integral to be logarithmically divergent. We note that the divergence is dependent on the dimension of the loop-integration and it would be absent in $D < 4$ dimensions. We therefore choose to compute the integral in

$D = 4 - 2\epsilon_{\text{UV}}$ dimensions with $\text{Re}(\epsilon_{\text{UV}}) > 0$, [3]

$$I^{\square}_{0011} \to \mu^{2\epsilon}_{\text{UV}} \int \frac{\mathrm{d}^D \ell}{(2\pi)^D} \frac{1}{\ell^2 (\ell - q)^2} = \frac{\mathrm{i}}{16\pi^2} \left[\frac{1}{\epsilon_{\text{UV}}} - \gamma_{\text{E}} + \log 4\pi + 2 - \log\left(-q^2/\mu^2_{\text{UV}}\right) + \mathcal{O}(\epsilon_{\text{UV}}) \right] . \tag{4.7}$$

Here $\gamma_{\text{E}} = 0.577216\ldots$ is Euler's constant and the dimensionful renormalization scale μ_{UV} is introduced to ensure that the regulated integral has the same integer mass-dimensions as before introducing the regulator.

4.2.2. Infrared Divergences

A simple example for an IR-divergent integral is the triangle integral with two on-shell massless legs $p_1^2 = p_2^2 = 0$ as depicted in Figure. 4.1(2),

$$I^{\square}_{1110} = \int \frac{\mathrm{d}^4 \ell}{(2\pi)^4} \frac{1}{(\ell - p_1)^2 (\ell + p_2)^2 \ell^2} . \tag{4.8}$$

We find that this integral diverges in the region of small $\ell \sim \lambda \ll p_1, p_2$

$$\frac{1}{(\ell - p_1)^2 (\ell + p_2)^2 \ell^2} \sim \frac{1}{(-2p_1 \cdot \ell)(2p_2 \cdot \ell)\ell^2} \sim \lambda^{-4} , \quad \mathrm{d}^4 \ell \sim \lambda^4 . \tag{4.9}$$

Based on the same observation as above we notice that the integral has a definite value when computed in $D = 4 - 2\epsilon_{\text{IR}}$ dimensions, but now we have to require $\text{Re}(\epsilon_{\text{IR}}) < 0$,

$$I^{\square}_{1110} \to \mu^{2\epsilon}_{\text{IR}} \int \frac{\mathrm{d}^D \ell}{(2\pi)^D} \frac{1}{(\ell - p_1)^2 (\ell + p_2)^2 \ell^2} = \frac{\mathrm{i}}{16\pi^2} \frac{1}{s} \left\{ \frac{1}{2\epsilon^2_{\text{IR}}} + \frac{1}{\epsilon_{\text{IR}}} \left[\gamma_{\text{E}} + \log 4\pi - \log\left(-s/\mu^2_{\text{IR}}\right) \right] + \mathcal{O}(\epsilon^0_{\text{IR}}) \right\} , \tag{4.10}$$

where we omitted higher-order terms for brevity. The structure of the divergences will be similar at higher loop orders, with the maximal IR divergence $\epsilon^{-2L}_{\text{IR}}$ and the maximal UV divergence $\epsilon^{-L}_{\text{IR}}$. Finally, we will encounter integrals that are *simultaneously* IR and UV-divergent. A typical example for this is the tadpole integral

$$I^{\square}_{0020} = \int \frac{\mathrm{d}^4 \ell}{(2\pi)^4} \frac{1}{(\ell^2)^2} . \tag{4.11}$$

However, we can still assign values to this integrals in terms of ϵ_{IR} and ϵ_{UV}, by splitting the integration through an arbitrary intermediate scale Λ and by regularizing the UV and the IR divergence separately. The relevant integrals are

[3] The evaluation in dimensions that are not positive integers is to be understood via analytic continuation in D.

straightforwardly computed using D-dimensional polar coordinates[4]

$$I^{\square}_{0020} \to \mu_{\mathrm{IR}}^{2\epsilon} \int_{|\ell|<\Lambda} \frac{\mathrm{d}^{4-2\epsilon_{\mathrm{IR}}}\ell}{(2\pi)^{4-2\epsilon_{\mathrm{IR}}}} \frac{1}{(\ell^2)^2} + \mu_{\mathrm{UV}}^{2\epsilon} \int_{|\ell|>\Lambda} \frac{\mathrm{d}^{4-2\epsilon_{\mathrm{UV}}}\ell}{(2\pi)^{4-2\epsilon_{\mathrm{UV}}}} \frac{1}{(\ell^2)^2} \tag{4.12}$$
$$= \frac{\mathrm{i}}{8\pi^2}\left[-\frac{1}{\epsilon_{\mathrm{IR}}} + \log\big(\Lambda/\mu^2_{\mathrm{IR}}\big) + \mathcal{O}(\epsilon_{\mathrm{IR}})\right] + \frac{\mathrm{i}}{8\pi^2}\left[\frac{1}{\epsilon_{\mathrm{UV}}} - \log\big(\Lambda/\mu^2_{\mathrm{UV}}\big) + \mathcal{O}(\epsilon_{\mathrm{UV}})\right].$$

As both IR and UV divergences have to cancel in the final result, in dimensional regularization we are instructed to forget about the origin of the divergences and set

$$\epsilon_{\mathrm{UV}} = \epsilon_{\mathrm{IR}} = \epsilon, \quad \mu_{\mathrm{UV}} = \mu_{\mathrm{IR}} = \mu\,, \tag{4.13}$$

even though formally there is no choice of ϵ such that all integrals are convergent.

One of the features of dimensional regularization is that scaleless integrals like the massless tadpole $I^{\square}_{0020}$ vanish. This can be understood by dimensional analysis, since the integral should give a dimensionful result, but there is no physical scale it depends on. In practice, the inability to separate IR and UV divergences is a small price to pay compared to the simplicity gained by the fact that dimensionless integrals vanish. Another important property of dimensional regularization is that surface integrals vanish as well (see e.g. Ref. [141]), that is for an arbitrary function F,

$$\int \frac{\mathrm{d}^D\ell}{(2\pi)^D} \frac{\partial}{\partial \ell^\mu} F(\ell) = \text{surface term} = 0\,. \tag{4.14}$$

This property will become important in the context of integration-by-parts identities.

4.2.3. Other Regularization Schemes

There are manifold ways to deform the integrals in Eqs. (4.5) and (4.8) that result in well-defined expressions. The most natural but also practically least convenient is the use of a hard cutoff Λ of the loop integration. While this procedure straightforwardly removes UV and IR divergences it breaks both gauge and Lorentz invariance. Instead of tampering with the dimension we could instead raise the propagators to some powers, where a given choice can regulate either UV or IR divergences. This procedure is called *analytic regularization* it comes with the drawback of breaking gauge invariance, but it is used in situations where integrals are not regularized by dimensional regularization, for example in soft-collinear effective theory (SCET) [142]. Another well-known regularization scheme is the regularization by adding fictitious massive particles, known as *Pauli-Villars regularization*, [143] which however is incompatible with non-abelian gauge theory.

Dimensional regularization on the other hand simultaneously preserves gauge and Lorentz invariance and will therefore be adapted throughout this thesis, with the exception of divergent energy integrals not regulated by dimensional regularization for which we use a custom scheme that will be explained in section 4.7.5.

[4] The cutoff is understood to be applied after Wick rotation $\ell_0 \to \mathrm{i}\ell_0$.

4.2.4. Normalizations

As we have seen the expansions of the integrals (4.7), and (4.10) have a similar structure in the way the constants γ_{E} and $\log 4\pi$ appear. This is no accident, but can be traced to the expansion of the poles times some regular functions. These factors are therefore entirely predicted by the pole coefficient and do not possess any relevance by themselves. As we will see explicitly these factors arise from the expansion of Γ-functions near integer values, which are given by [144]

$$\Gamma(1+\epsilon) = e^{-\gamma_{\mathrm{E}}\epsilon} \exp\left[\sum_{k=2}^{\infty} \frac{(-1)^k \zeta_k}{k} \epsilon^k\right], \quad |\epsilon| < 1\,. \tag{4.15}$$

Feynman integrals also naturally produce factors $\mathrm{i}\pi^{D/2}$ which originate from the evaluation of D-dimensional Gaussian integrals (volumes of spheres in D dimensions), and which together with the measure factor $1/(2\pi)^D$ are the source of the $\log 4\pi$. These terms can be absorbed if one works in the modified minimal subtraction scheme (MS-bar), in which instead of fixing the mass dimension by μ one uses the MS-bar scale

$$\bar{\mu}^2 = \mu^2 \frac{e^{\gamma_{\mathrm{E}}}}{4\pi}\,. \tag{4.16}$$

Since this scales are arbitrary and should drop out of physical quantities, there is no loss of generality. Finally we conventionally separate an overall *loop-factor* of $-\mathrm{i}/(16\pi^2)$ which was also present in the integrals (4.5), (4.8) and (4.12)

$$\bar{\mu}^{2\epsilon} \frac{\mathrm{d}^D\ell}{(2\pi)^D} = -\frac{\mathrm{i}}{16\pi^2} \times \mu^{2\epsilon} \frac{e^{\gamma_{\mathrm{E}}\epsilon}\mathrm{d}^D\ell}{\mathrm{i}\pi^{D/2}}\,. \tag{4.17}$$

In the following integral-computations, we set $\mu = 1$, and recover it in the end by dimensional analysis.

4.3. Methods for Evaluating Integrals

4.3.1. Direct Integration

Simple Feynman integrals can be tackled by directly performing the integrations. Typically one first transforms the integrand to a Gaussian introducing additional parameter integrations, followed by evaluating the momentum integration and then finally computing the remaining parameter integral. To outline this strategy, consider the simplest non-vanishing Feynman integral, is the tadpole with mass m[5],

$$I_a^{\mathrm{tad}}(m^2) = \int \frac{e^{\gamma_{\mathrm{E}}\epsilon}\mathrm{d}^D\ell}{\mathrm{i}\pi^{D/2}} \frac{1}{[-(\ell^2 - m^2 + \mathrm{i}\varepsilon)]^a}\,. \tag{4.18}$$

[5]The use of the additional sign is convenient, in particular in the presence of non-integer a

The idea is to convert this integral to a Gaussian integral and then use the general formula for an D-dimensional Gaussian integral[6]

$$\int \mathrm{d}^D\ell\, e^{\mathrm{i}\alpha\ell^2-2q\cdot\ell} = \mathrm{i}\pi^{D/2}e^{\mathrm{i}\pi D/4}\alpha^{-D/2}e^{-\mathrm{i}q^2/\alpha}\,, \quad \mathrm{Im}\,\alpha > 0\,. \tag{4.19}$$

We achieve our goal by introducing a Schwinger parameter λ

$$\frac{1}{(-A-\mathrm{i}\varepsilon)^a} = \frac{\mathrm{i}^a}{\Gamma(a)}\int_0^\infty \mathrm{d}\lambda\,\lambda^{a-1}e^{\mathrm{i}(A+\mathrm{i}\varepsilon)\lambda}\,. \tag{4.20}$$

Applied to the tadpole integral we find

$$I_a^{\mathrm{tad}} = \frac{\mathrm{i}^a}{\Gamma(a)}\int \frac{e^{\gamma_{\mathrm{E}}\epsilon}\mathrm{d}^D\ell}{\mathrm{i}\pi^{D/2}}\int_0^\infty \mathrm{d}\lambda\,\lambda^{a-1}e^{\mathrm{i}(\ell^2-m^2+\mathrm{i}\varepsilon)\lambda}\,. \tag{4.21}$$

Reversing the order of integration and using the formula for the Gaussian (4.19), we obtain

$$I_a^{\mathrm{tad}} = \frac{\mathrm{i}^a}{\Gamma(a)}e^{\mathrm{i}\pi D/4}\int \mathrm{d}\lambda\,\lambda^{a-1-D/2}e^{-\mathrm{i}\lambda(m^2-\mathrm{i}\varepsilon)} = (m^2+\mathrm{i}\varepsilon)^{-a+D/2}\frac{e^{\gamma_{\mathrm{E}}\epsilon}\Gamma(a-D/2)}{\Gamma(a)}\,. \tag{4.22}$$

This result highlights several general features of loop integrals. First of all this integral is only convergent for $-4+2a < \mathrm{Re}(D) < 2a$ and the value for generic D is understood through analytic continuation. In the following analytic continuation is always understood implicitly. Second, the integral is manifestly real as long as $m^2 > 0$, this is makes perfect sense as the Euclidean version of the integral, obtained by the Wick rotation $\ell^0 \to \mathrm{i}\ell^0_{\mathrm{E}}$ is manifestly real

$$I_a^{\mathrm{tad}} = \int \frac{e^{\gamma_{\mathrm{E}}\epsilon}\mathrm{d}^D\ell_{\mathrm{E}}}{\mathrm{i}\pi^{D/2}}\frac{1}{[\ell^2_{\mathrm{E}}+m^2]^a}\,. \tag{4.23}$$

Furthermore we see that the dependence on the mass parameter m is trivially fixed by dimensional analysis. Finally when Eq. (4.22) is expanded in ϵ, we will find a series that involves transcendental functions (here logarithms) and ζ-values, for example

$$\begin{aligned} I_1^{\mathrm{tad}} = -\frac{1}{m^2}\Big\{&\frac{1}{\epsilon}+[1-\log\big(m^2+\mathrm{i}\varepsilon\big)] \\ &+\epsilon\Big[1+\frac{1}{2}\zeta_2-\log\big(m^2+\mathrm{i}\varepsilon\big)+\frac{1}{2}\log^2(m^2+\mathrm{i}\varepsilon)\Big]+\mathcal{O}(\epsilon)\Big\}\,. \end{aligned} \tag{4.24}$$

More generally integrals will posses *Euclidean regions* where they will be purely real (or imaginary given our normalizations), typically this regions are defined such that all invariants are negative[7]. We will discuss this in the context of massive integrals for two-to-two scattering.

[6] These integrals are usually computed using Wick rotation $\ell_0 \to \mathrm{i}\ell_0$. We choose to stay in Lorentzian signature for simplicity.

[7] The Euclidean regions are defined in terms of graph polynomials. See e.g. Ref. [145].

In order to see how more complicated integrals can be turned into parametric integrals, we turn our attention to another example, the bubble integral

$$I^{\square}_{00ab} = \int \frac{e^{\gamma_{\mathrm{E}}\epsilon}\mathrm{d}^D\ell}{\mathrm{i}\pi^{D/2}} \frac{1}{[-\ell^2 - \mathrm{i}\varepsilon]^a[-(\ell-q)^2 - \mathrm{i}\varepsilon]^b} \,. \tag{4.25}$$

We will use Feynman parametrization to reduce the momentum integration to the tadpole integral that we computed in Eq. (4.22). Feynman parametrization relies on the following elementary identity

$$\frac{1}{AB} = \int_0^1 \frac{\mathrm{d}u}{[uA + (1-u)B]^2} \tag{4.26}$$

and its generalization

$$\frac{1}{A_1^{\alpha_1}\cdots A_n^{\alpha_n}} = \frac{\Gamma(\sum_{k=1}^n \alpha_k)}{\Gamma(\alpha_1)\cdots\Gamma(\alpha_n)} \int_0^1 \prod_i^n \mathrm{d}u_i \frac{\delta(1-\sum_{k=1}^n u_k)\; u_1^{\alpha_1-1}\cdots u_n^{\alpha_n-1}}{(\sum_{k=1}^n u_k A_k)^{\sum_{k=1}^n \alpha_k}} \,. \tag{4.27}$$

Applied to the bubble integral, we find

$$\begin{aligned} I^{\square}_{00ab} &= \frac{\Gamma(a+b)}{\Gamma(a)\Gamma(b)} \int \frac{e^{\gamma_{\mathrm{E}}\epsilon}\mathrm{d}^D\ell}{\mathrm{i}\pi^{D/2}} \int_0^1 \mathrm{d}u \frac{u^{a-1}(1-u)^{b-1}}{[-\ell^2 + 2u\,(\ell\cdot q) - uq^2 - \mathrm{i}\varepsilon]^{a+b}} \\ &= \frac{\Gamma(a+b)}{\Gamma(a)\Gamma(b)} \int \frac{e^{\gamma_{\mathrm{E}}\epsilon}\mathrm{d}^D\ell}{\mathrm{i}\pi^{D/2}} \int_0^1 \mathrm{d}u \frac{u^{a-1}(1-u)^{b-1}}{[-\ell^2 - u(1-u)q^2 - \mathrm{i}\varepsilon]^{a+b}} \,. \end{aligned} \tag{4.28}$$

Now we can reverse the order of integration and perform the momentum integration by making use of Eq. (4.22), which leads to

$$I^{\square}_{00ab} = e^{\gamma_{\mathrm{E}}\epsilon} \frac{\Gamma(a+b-D/2)}{\Gamma(a)\Gamma(b)} \int_0^1 \mathrm{d}u\, u^{a-1}(1-u)^{b-1} \big[u(1-u)(-q^2 - \mathrm{i}\varepsilon)\big]^{-a-b+D/2} \,. \tag{4.29}$$

The parametric integral is an Euler beta function and can therefore be expressed in terms of gamma functions, with the result

$$I^{\square}_{00ab} = (-q^2 - \mathrm{i}\varepsilon)^{-a-b+D/2} e^{\gamma_{\mathrm{E}}\epsilon} \frac{\Gamma(a+b-D/2)}{\Gamma(a)\Gamma(b)} \frac{\Gamma(D/2-a)\Gamma(D/2-b)}{\Gamma(D-a-b)} \,. \tag{4.30}$$

Note that direct integration can also be applied more generally to problems that are more complicated than the simple cases considered here [146, 147].

4.3.2. Sequential Integration

The reader may have noticed that the integrals obtained in Eqs. (4.22) and (4.30) look again like a propagator, including the correct $\mathrm{i}\varepsilon$, raised to an non-integer power multiplied by some function depending on the indices. This can be turned to an advantage through sequential loop integration. For example consider

the sunrise integral

$$I^{\text{Sun}}_{\underline{a}}(q^2;D) = \int \frac{e^{\gamma_{\text{E}}\epsilon}\mathrm{d}^D\ell_1}{\mathrm{i}\pi^{D/2}} \int \frac{e^{\gamma_{\text{E}}\epsilon}\mathrm{d}^D\ell_2}{\mathrm{i}\pi^{D/2}} \frac{1}{[-\ell_1^2]^{a_1}[-\ell_2^2]^{a_2}[-(\ell_1+\ell_2-q)^2]^{a_3}}\,. \tag{4.31}$$

We can choose to first perform the ℓ_2 integration using Eq. (4.30) with the identification $q' = q - \ell_1$, with the result

$$\begin{aligned} I^{\text{Sun}}_{\underline{a}}(q^2;D) = e^{\gamma_{\text{E}}\epsilon}\frac{\Gamma(a_2+a_3-D/2)}{\Gamma(a_2)\Gamma(a_3)}\frac{\Gamma(D/2-a_2)\Gamma(D/2-a_3)}{\Gamma(D-a_2-a_3)} \\ \times \int \frac{e^{\gamma_{\text{E}}\epsilon}\mathrm{d}^D\ell_1}{\mathrm{i}\pi^{D/2}} \frac{1}{[-\ell_1^2]^{a_1}[-(\ell_1-q)^2]^{a_2+a_3-D/2}}\,. \end{aligned} \tag{4.32}$$

The remaining loop integration is readily done once again using Eq. (4.30). The result is

$$\begin{aligned} I^{\text{Sun}}_{\underline{a}}(q^2;D) = e^{2\gamma_{\text{E}}\epsilon}(-q^2)^{D-a_1-a_2-a_3}\frac{\Gamma(a_1+a_2+a_3-D/2)}{\Gamma(a_1)\Gamma(a_2)\Gamma(a_3)} \\ \times \frac{\Gamma(D/2-a_1)\Gamma(D/2-a_2)\Gamma(D/2-a_3)}{\Gamma(3D/2-a_1-a_2-a_3)}\,. \end{aligned} \tag{4.33}$$

Another type of subloop integral that we will frequently encounter are bubbles with a eikonal propagator. This integrals are simple to evaluate using methods similar to the ones described above and are given by Ref. [145]

$$\begin{aligned} \int \frac{e^{\gamma_{\text{E}}\epsilon}\mathrm{d}^D\ell}{\mathrm{i}\pi^{D/2}} \frac{1}{(-\ell^2)^a(2v\cdot\ell+\omega-\mathrm{i}\varepsilon)^b} = e^{\gamma_{\text{E}}\epsilon}\frac{\Gamma(D/2-a)\Gamma(2a+b-D)}{\Gamma(a)\Gamma(b)} \\ \times (v^2)^{a-D/2}(\omega)^{-2a-b+D}\,. \end{aligned} \tag{4.34}$$

Pictorially Eqs. (4.30) and (4.34) translates to the following rules

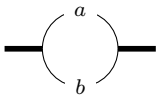

$$= e^{\gamma_{\text{E}}\epsilon}\frac{\Gamma(a+b-D/2)}{\Gamma(a)\Gamma(b)}\frac{\Gamma(D/2-a)\Gamma(D/2-b)}{\Gamma(D-a-b)} \times \; -\,[a+b-D/2]\,- \;, \tag{4.35}$$

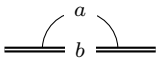

$$= e^{\gamma_{\text{E}}\epsilon}\frac{\Gamma(D/2-a)\Gamma(2a+b-D)}{\Gamma(a)\Gamma(b)}(v^2)^{a-D/2} \times \; =\,[2a+b-D]\,= \;, \tag{4.36}$$

where we use thick lines to represent massive or off-shell lines and doubled lines for eikonal propagators and the numbers decorating the lines are the exponents of the corresponding propagator in a given integral.

4.3.3. Symmetrization Trick

An important method that can be used for the evaluation of integrals with eikonal propagators is the symmetrization trick (see e.g Refs. [148, 149]). We will explain it using the example of the linearized triangle integral depicted in

Figure 4.8(2)

$$I^{\rm II}_{1,0,1,1}(q^2,D) = \int \frac{e^{\gamma_{\rm E}\epsilon}{\rm d}^D\ell}{{\rm i}\pi^{D/2}} \frac{1}{\ell^2(\ell-q)^2(2v\cdot\ell+{\rm i}\varepsilon)}\,, \quad v^2=1\,, \quad v\cdot q = 0\,. \tag{4.37}$$

First it is convenient to choose the rest frame

$$v=(1,0,\dots)\,, \quad q=(0,\boldsymbol{q})\,, \quad \ell_i=(\omega_i,\boldsymbol{\ell}_i)\,. \tag{4.38}$$

As a means to illustrate the general approach, we introduce individual labels ℓ_1,ℓ_2 for the momenta present in the massless propagators. With this we have

$$\begin{aligned} I^{\rm II}_{1,0,1,1}(q^2,D) &= \frac{e^{\gamma_{\rm E}\epsilon}}{{\rm i}\pi^{D/2}} \int {\rm d}^D\ell_1 {\rm d}^D\ell_2 \frac{\delta^{(D)}(\ell_1+\ell_2+q)}{\ell_1^2\ell_2^2(2\omega_1+{\rm i}\varepsilon)} \\ &= \frac{e^{\gamma_{\rm E}\epsilon}}{{\rm i}\pi^{D/2}} \int {\rm d}^D\ell_1 {\rm d}^D\ell_2 \frac{\delta(\omega_1+\omega_2)}{(2\omega_1+{\rm i}\varepsilon)} \frac{\delta^{(D-1)}(\boldsymbol{\ell}_1+\boldsymbol{\ell}_2+\boldsymbol{q})}{\ell_1^2\ell_2^2}\,. \end{aligned} \tag{4.39}$$

We now add over all permutations of the loop-momentum labels, i.e. we symmetrize in ℓ_1 and ℓ_2. This only affects the first term

$$\begin{aligned} \delta(\omega_1+\omega_2)\left[\frac{1}{\omega_1+{\rm i}\varepsilon}+\frac{1}{\omega_2+{\rm i}\varepsilon}\right] &= \delta(\omega_1+\omega_2)\left[\frac{1}{\omega_1+{\rm i}\varepsilon}+\frac{1}{-\omega_1+{\rm i}\varepsilon}\right] \\ &= -2{\rm i}\pi\delta(\omega_1+\omega_2)\delta(\omega_1) \\ &= -2{\rm i}\pi\delta(\omega_1)\delta(\omega_2)\,. \end{aligned} \tag{4.40}$$

Thus, the iterated triangle is proportional to an $D-1$ dimensional Euclidean bubble which is elementary and which we have (up to analytic continuation to Euclidean space) computed in Eq. (4.30),

$$\begin{aligned} I^{\rm II}_{1,0,1,1}(q^2,D) &= -\frac{\sqrt{\pi}}{2}\int \frac{e^{\gamma_{\rm E}\epsilon}{\rm d}^{D-1}\boldsymbol{\ell}}{\pi^{(D-1)/2}} \frac{1}{\boldsymbol{\ell}^2(\boldsymbol{\ell}-\boldsymbol{q})^2} \\ &= -\left(-q^2\right)^{-\frac{1}{2}-\epsilon} e^{\gamma_{\rm E}\epsilon} \frac{\sqrt{\pi}\Gamma\left(\frac{1}{2}-\epsilon\right)^2\Gamma\left(\epsilon+\frac{1}{2}\right)}{2\Gamma(1-2\epsilon)}\,. \end{aligned} \tag{4.41}$$

A suitable multi-loop generalization is [148]

$$\delta\left(\sum_{n=1}^{L+1}\omega_k\right)\prod_{k=1}^{L}\frac{1}{2\sum_{n=1}^{k}\omega_n+{\rm i}\varepsilon} + \text{perm.} = (-{\rm i}\pi)^L\prod_{k=1}^{L+1}\delta(\omega_k)\,. \tag{4.42}$$

We note that the trick is also applicable to more general integrals that are symmetric under the permutation of the massless lines. An example would be the sum of three integrals (two of which being identical)

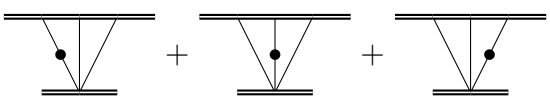

(4.43)

where a dot represents a squared propagator. This integral is consequently proportional to a $D-1$ dimensional Euclidean sunrise integral with a dot.

4.4. Relations Between Integrals

In a typical physical problem the number of individual integrals encountered typically grows rapidly with the number of external momenta and loops. Furthermore Feynman rules typically have momentum dependence, which introduces numerators with high powers of the loop momenta. Similar complicated integrals can be introduced by expanding integrals in kinematic limits. This leads to a large number of different integrals that have to be computed for a multi-loop problem.

However, as it turns out there are many relations among these integrals. The simplest case of such relations are symmetry relations, for example the bubble integral turns into itself (with the exponents of the propagators interchanged) under $\ell \mapsto q - \ell$, which leads to the relation

$$I^{\square}_{00ab} = I^{\square}_{00ba} \,. \tag{4.44}$$

Such relations are also visible as isomorphisms of the associated graphs and can be systematically studied based on the graph polynomials. Important relations are generated by integration-by-parts (IBP) and Lorentz-invariance (LI) identities [150, 151]. Other useful identities include dimensional shifts relating integrals with different dimensions.

4.4.1. Integration-by-Parts Relations

The most important type of relations are integration-by-parts (IBP) relations which were first employed in Refs. [150, 151]. They are derived from the simple fact that surface terms vanish in dimensional regularization. This means that for a given topology we have

$$\int \frac{\mathrm{d}^D \ell}{(2\pi)^D} \frac{\partial}{\partial \ell^\mu} \left[\frac{v^\mu}{\rho_1^{a_1} \cdots \rho_n^{a_n}} \right] = 0 \,. \tag{4.45}$$

where v can be an internal or external Lorentz vector. To make this concrete consider the bubble integral

$$I^{\square}_{00ab} = \int \frac{\mathrm{d}^D \ell}{(2\pi)^D} \frac{1}{[\ell^2]^a [(\ell - q)^2]^b} \,. \tag{4.46}$$

We can set up the following IBP relation by taking a derivative of the simple vector $v^\mu = \ell^\mu$ and subsequently writing the numerator in terms of the propagators

$$0 = \int \frac{\mathrm{d}^D \ell}{(2\pi)^D} \frac{\partial}{\partial \ell^\mu} \frac{\ell^\mu}{[\ell^2]^a [(\ell - q)^2]^b} = (D - 2a - b) I^{\square}_{00ab} - b I^{\square}_{00a-1b+1} + b q^2 I^{\square}_{00ab+1} \,. \tag{4.47}$$

This relation is readily found to be compatible with the explicit result in Eq. (4.30). There are a few things to note about this example which are also true for more general IBP relations. First, the identity does not depend on the $i\varepsilon$ prescrip-

tion. This fact will become important when we will discuss phase-space integrals. Second, IBP relations in general are D-dependent and relate integrals which have different power counting. IBP can therefore turn IR in UV-divergent integrals and vice-versa.[8] This means for example that one needs to subtract all IR divergences from a gravity amplitude before one can study the UV divergences. Third the coefficients in the IBP relation are rational functions of the kinematics (here q^2) and the dimension D.

The IBP relation (4.47) can be used to reduce any integral of the form $I^{\square}_{00ab}$ to the scalar integral $I^{\square}_{0011}$. To see this one can systematically first use the rule to reduce the b index to 1 using that the integral vanishes for $a \leq 0$, after that one can use the symmetry $I^{\square}_{00ab} = I^{\square}_{00ba}$, to do the same for the a index. This means that with $I^{\square}_{0011}$ we have encountered the first case of a *master* integral.

Another important type of identities are Lorentz invariance identities of the form

$$\omega_{\mu\nu} \int \mathrm{d}^D \underline{\ell} \sum_i^L \ell_i^\mu \frac{\partial}{\partial \ell_i^\nu} \left[\frac{1}{\rho_1^{a_1} \cdots \rho_n^{a_n}} \right] = 0 \,, \tag{4.48}$$

where $\omega_{\mu\nu}$ is an anti-symmetric matrix constructed from the external kinematics. In general there are $(L+E)L$ IBP identities and $E(E-1)/2$ LI identities. IBP identities are part of the standard tools widely used in field theory. In the following we will refer to both as simply IBP identities. Generalizing the observation for the bubble integral an important fact is that the number of independent integrals after applying IBP relations is finite [152]. The Laporta algorithm [153, 154] is an systematic way to use IBP and LI relations to reduce a set of integrals to a basis. This algorithm is implemented in mature computer programs like `KIRA` [134], `FIRE` [135] and `Reduze` [155]. In this work we use `FIRE`6.

Master-surface decomposition Each IBP relation generates a function that integrates to zero. These functions can be used as natural ansatz functions for the integrand which will be matched by the numerical unitarity method. In the process we have to take residues of integrands on the zeros of propagators and therefore it is convenient to choose a basis which does not have propagators raised to higher powers. This can be implemented by constructing IBP vectors u_i^ν such that [156, 157]

$$\sum_{i=1}^L u_i^\nu \frac{\partial}{\partial \ell_i^\nu} \rho = f_\rho \rho \,, \qquad \forall \rho \in P_\Gamma \,. \tag{4.49}$$

where f_ρ is some polynomial. Multiplying the vector by a generic polynomial $t(\underline{\ell})$, inserting into the general IBP equation (4.45), specifying $a_i = 1$ we obtain an unitarity-compatible surface term numerator

$$m = -t \sum_{\rho \in P_\Gamma} f_\rho + \sum_{i=1}^L u_i^\nu \frac{\partial t}{\partial \ell_i^\nu} + t \frac{\partial u_i^\nu}{\partial \ell_i^\nu} \,. \tag{4.50}$$

[8] For example the (IR-divergent) massless triangle can be reduced to the (UV-divergent) bubble integral.

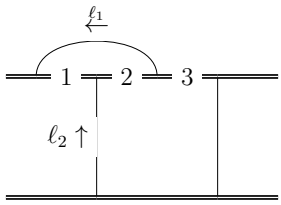

Figure 4.2.: Linear mushroom integral to which partial fraction decomposition can be applied.

4.4.2. Partial Fraction Decomposition

In the computation of Feynman integrals, one can encounter integrals where the propagators are not algebraically independent (that is they satisfy a polynomial relation). The most common case are integrals where two propagators are literally identical, such as for integrals with self-energy insertions. When expanding propagators as dictated by the method of regions, this situation is quite common and one will typically find non-trivial relations between the propagators in the expanded integrals. To give an example, consider the mushroom-type integral, depicted in Figure 4.2. The three marked propagators in this diagram are

$$\rho_1 = 2u_1 \cdot \ell_1 + \mathrm{i}\varepsilon\,, \quad \rho_2 = 2u_1 \cdot (\ell_1 + \ell_2) + \mathrm{i}\varepsilon\,, \quad \rho_3 = 2u_1 \cdot \ell_2 + \mathrm{i}\varepsilon\,, \tag{4.51}$$

which satisfy the trivial relation $\rho_2 = \rho_1 + \rho_3$. Consequently, expressions that contain all three propagators can be simplified, for example we find (up to $\mathrm{i}\varepsilon$ in the numerator)

$$\frac{1}{\rho_1}\frac{1}{\rho_2}\frac{1}{\rho_3} = \frac{1}{\rho_1\rho_3^2} - \frac{1}{\rho_2\rho_3^2}\,. \tag{4.52}$$

For the original mushroom-type integral this leads to the following pictorial identity

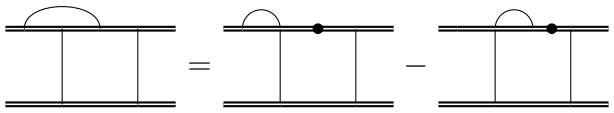

(4.53)

Where now the propagators on the right-hand side of Eq. (4.53) are algebraically independent, i.e. do not satisfy any further relation.

4.5. Differential Equations

The method of differential equations as introduced by Kotikov in Ref. [158] is an powerful method for the evaluation of Feynman integrals. Early applications of the method are performed in Refs. [159–161]. To date it is by far the most common approach used in the computation of complicated integrals relevant for collider phenomenology.[9]

[9]For a selection of state-of-the-art applications see Refs. [96, 98, 162–166].

Differential equations are essentially a direct consequence of IBP identities. We recall that for any given family of integrals there is a finite number of master integrals. By Lorentz invariance, these integrals are functions of the external scalar products $p_i \cdot p_j$ and masses m_i. Setting aside irrelevant mathematical subtleties, we can take derivatives at the integrand level. Taking derivatives with respect to the masses is straightforward, while derivatives with respect to the inner products can be implemented through[10]

$$\frac{\partial}{\partial(p_i \cdot p_j)} = \sum_{k=1}^{E} \left[G^{-1}\right]^{ik} p_k \cdot \frac{\partial}{\partial p_j}\,, \quad i \neq j\,, \qquad \frac{\partial}{\partial(p_i^2)} = \frac{1}{2}\sum_{k=1}^{E} \left[G^{-1}\right]^{ik} p_k \cdot \frac{\partial}{\partial p_i}\,, \tag{4.54}$$

where G is the gram matrix $G_{ij} = p_i \cdot p_j$. Now since the derivatives will preserve the denominator structure of a given integral, only potentially raising indices or canceling denominators, a family of Feynman integrals will be closed under taking derivatives. Together with the fact that the basis of the family is finite we find that by taking derivatives of a basis of Feynman integrals $\vec{g}$, we obtain a differential equation

$$\mathrm{d}\vec{g} = \left[\sum_i A_i(\underline{s}, \epsilon)\mathrm{d}s^i\right]\vec{g}\,, \tag{4.55}$$

where $\underline{s} = \{s_i\}$ is a set of independent invariants parametrizing the external kinematics of the integrals. Because IBP relations only involve rational dependence on ϵ and s_i, the matrix A will have a rational dependence on the kinematics and the dimensional regularization parameter. Together with boundary values, say the values of $\vec{g}$ at a given value of the s_i, this system has an unique solution. In practice, direct solution of the differential equations is only possible in very simple cases. For example some one-loop integrals can be expressed in terms of hypergeometric functions. An example is the family of one-loop integral that we discuss in section 4.9.1. Since eventually we will take the limit $D \to 4$, in practice we do not need to know an exact solution to the differential equation, but only need its behavior near $\epsilon = 0$. The solutions to the differential equations for a set of L-loop integrals will in general be expressible as Laurent expansions in ϵ (see e.g. Ref. [167])

$$\vec{g} = \frac{1}{\epsilon^{2L}}\sum_{k=0}^{\infty} \vec{g}_k \epsilon^k\,. \tag{4.56}$$

Depending on the problem we only need a finite number of coefficients in this expansion. Typically one needs $\vec{g}$ up to $\mathcal{O}(\epsilon^0)$, although the computation of cross sections may necessitate the evaluation of higher orders (see e.g. Ref. [168]). Now although this process can be used to compute integrals, it may in practice be very complicated and for multi-loop multi-scale problems the structure of the matrix A may become arbitrarily complex.

Some of the observed complexity is an artifact introduced by our so far arbitrary choice of basis and parametrization of the external kinematics. In fact the problem

[10] Since the components of the loop momenta form an overcomplete set of variables there are in general many such expressions, which are related through Lorentz invariance. However, Eq. (4.54) is valid in general.

should be equivalently formulated in terms of basis a different basis $\vec{g}' = T(\underline{s}, \epsilon)\vec{g}$ and a different parametrization of the external kinematics $(s')^k = (s')^k(\underline{s})$. The reader may recognize this as the symmetries encoded by a gauge bundle, where the transformation T is called a gauge transformation and $s^k \mapsto (s')^k$ a coordinate transformation (diffeomorphism). In this language A is identified as the connection matrix of the gauge bundle. The transformations are

$$A_k \to T^{-1}A_kT - T^{-1}\partial_{s_k}T\,, \qquad A_k \to A_j\frac{\partial(s')^j}{\partial s^k}\,. \tag{4.57}$$

This transformations have an enormous potential for simplification, which is brought to its logical conclusion in the construction of the so-called canonical form of the differential equation. The canonical basis or ϵ-d log basis of the differential equation is a basis $\vec{f}$ which satisfies

$$\mathrm{d}\vec{f} = \epsilon\sum A_i \mathrm{d}\log(w_i(\underline{s}))\vec{g}\,, \tag{4.58}$$

where now the A_i are *rational* matrices independent of kinematics and the space-time dimension. The canonical form (4.58) has a number of properties which we shall discuss in the following. First, the dependence on kinematics and the dimension is factorized. The differential equation has manifestly at most logarithmic singularities which are located on the surfaces $w_i(\underline{s}) = 0$. The w_i are called letters and the set $\mathbb{A}[\Gamma] = \{w_i\}$ is called the alphabet of the topology Γ. This fact will play an important role when constructing appropriate boundary conditions for the differential equation.

There are some remarks to be made about the existence of a canonical form. First of all it is well-known that the existence is by no means guaranteed and there are relatively simple counterexamples, such two-loop propagator diagrams with massive internal lines [169]. This examples typically feature new functions beyond generalized polylogarithms, with the simplest examples being complete elliptic integrals. Interestingly a slight generalization to the *pre-canonical* form

$$\mathrm{d}\vec{g} = \sum_{w\in\mathbb{A}} A_w(\epsilon)\,\mathrm{d}\log(w)\vec{g}\,, \tag{4.59}$$

covers some of these more complicated cases, while it is known to be insufficient for the most general cases. Alternatively we may loosen the requirement of d log kernels to recover an ϵ-form for the elliptic case [170].

We note that the construction of canonical basis and even more the construction of appropriate bases beyond canonical forms is an art in itself. It is perhaps fair to say that to date there is no fully algorithmic approach to construct a canonical basis given a generic initial basis. There are however many powerful tools available, which can applied in certain situations. In the case of an univariate system which can be fully rationalized, there is an algorithm due to Roman Lee [171], which is implemented in publicly available software [172–174]. Although the two objects are not generally identical [175], there exists a close connection to integrals with manifest logarithmic integrals (so-called dlog integrals), this can be systematically exploited to construct a canonical of master integrals (cf. Ref. [96]).

Although a Feynman integral necessarily satisfies a differential equation. This unfortunately does not drastically constrain the space of functions that arise when expanding the integrals in dimensional regularization. To date a full classification of the most general type of function that can arise in Feynman integrals is lacking, although it is known that for example iterated integrals over Calabi-Yau manifolds may arise in more complicated cases. (See e.g. Ref. [176])

4.6. Phase Space Integrals and Reverse Unitarity

Phase space integrals arise in the computation of observables such as cross sections in collider physics. They are integrals of the form

$$I(\underline{p}) = \int \mathrm{d}\Phi_n(\underline{\ell})\mathcal{I}(\underline{\ell},\underline{p})\,. \tag{4.60}$$

The integration is restricted to positive-energy on-shell momenta, which is encoded in the measure

$$\mathrm{d}\Phi_n(\underline{\ell}) := \widehat{\delta}^{(D)}\left(P + \sum_{i=1}^{n}\ell_i\right)\prod_{j}^{n}\frac{\mathrm{d}^D\ell}{(2\pi)^D}\theta(\ell^0)\delta(\ell_i^2 - m_i^2)\,, \tag{4.61}$$

where n is the number of on-shell legs and P is the total incoming momentum and $\widehat{\delta}^{(D)}(p) = (2\pi)^D\delta^{(D)}(p)$. Apart from the delta functions and step functions this integrals are of the same form as the Feynman integrals encountered in the previous sections. This connection can be made even clearer, by using a trick to represent δ-functions as differences of propagators with different iε prescriptions [177–180]:

$$\frac{2\pi\mathrm{i}}{(-1)^n\,n!}\delta^{(n)}(\rho) = \frac{1}{(\rho - \mathrm{i}\varepsilon)^{n+1}} - \frac{1}{(\rho + \mathrm{i}\varepsilon)^{n+1}}\,. \tag{4.62}$$

As we noted before, IBP relations are agnostic to the iε prescription and thus we can use the same IBP relations for cut integrals as for the uncut ones. For our purposes, the step functions can be ignored as their derivatives are $\delta(\ell^0)$ and the energies of the massive particles are large in the classical limit[11]. In the following they are implicit in all phase-space integrals and affect the final values for the master integrals.

Having made the connection to ordinary Feynman integrals it is evident that we can derive differential equations for cut integrals, which will become important for the evaluation of integrals relevant for classical observables. In fact since the IBP are identical we will find the *same* differential equations for the cut integrals[12], with the only difference being the boundary conditions.

[11] For massless states we get $\delta(\boldsymbol{\ell}^2)$, which does not contribute as it is a integration over a zero-measure set

[12] Cuts can break certain diagram symmetries which may result in symmetry factors with respect to the virtual integral if symmetries have been applied.

As this approach is opposite to the usual unitarity approach which represent loop integrals in terms of cuts, this method is known as *reverse unitarity* [177–180].

4.7. Isolating Classical Contributions

Physical problems in general depend on a large number of scales that quickly make them practically intractable to handle. For example the amplitude for electron-muon scattering depends on the COM energy $E = \sqrt{s}$, the momentum transfer $Q^2 = -t$ as well as the two masses m_e, m_μ of the electron and the muon respectively. On top of this a physical analysis may introduce further scales by imposing cuts on the phase space.

A quick estimate shows that $m_e/m_\mu \sim 1/200$, so it seems perfectly reasonable to compute any given quantity as an expansion in this ratio, keeping in mind that any computation anyway receives larger errors from approximations made elsewhere. We might even go further and focus on say forward scattering $-t/s \ll 1$, because we determined this is the most interesting region for the physics we are interested in. Each of these expansions will remove at least one scale from the problem and subsequently greatly simplify the problem at hand.

The main focus of this work is the *classical limit* which we will discuss in detail later and which can also be interpreted as a kinematic limit. Other common expansions involve soft/collinear limits, Regge (high energy) as well as expansions around threshold (low energy).

Since Feynman integrals in general are complicated transcendental functions, the question is then how to obtain an approximate series of the full result in the limit of a small parameter. This problem is addressed by the *method of regions* introduced by Benecke and Smirnov in Ref. [181] (see also Refs. [145, 182]). In this the integrand gets expanded in several regions defined though the hierarchy of scales of the external kinematics.

It is actually rather miraculous that adding the different regions (with the integrands integrated over the full phases-pace) yields the full answer. We should mention at this point that the method of regions still lacks a general proof and thus may be considered experimental mathematics. There are however compelling arguments as well as a large amount of highly non-trivial examples and the method is generally accepted to be correct[13]. In practice, wherever we made use of the method we used an exhaustive list of cross-checks for our computation.

4.7.1. Long-Range Physics from the Soft Limit

Performing a computation including quantum corrections comes with a large ballast associated with the quantum corrections and short-range physics. This fact

[13] See e.g. Ref. [145] for a discussion on the mathematical status of the expansion by regions.

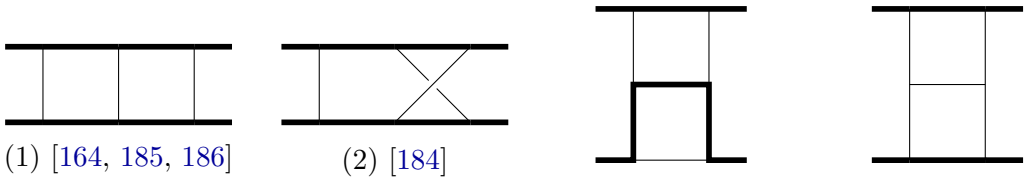

(1) [164, 185, 186] (2) [184] (3) [187] (4) [163, 188]

Figure 4.3.: Top-level integrals that have been studied in the literature. Thick lines and thin lines represent massive and massless propagators respectively. Figures (1)–(3) are relevant for Bhabha scattering.

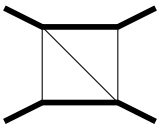

Figure 4.4.: The N-Integral is the simplest integral relevant for Bhabha scattering that contains elliptic integrals at higher order in the ϵ-expansion.

is illustrated vividly by comparing next-to-next-to-leading order (NNLO) results in classical gravity [47] with complete NNLO computations in pure gravity [183].

It should then be obvious that a successful strategy must focus on getting rid of quantum contributions as early and as systematic as possible. In fact the point where the classical limit becomes crucial is the evaluation of integrals. To drive this point home let us quickly comment on the status of integration in Bhabha (ee) scattering, which for all intents and purposes is a simplified version of the scattering of different masses in gravity. The integrals for this case have been studied for some time (cf. Figure 4.3), but to date the complete set of two-loop integrals for this process is missing, for example the non-planar integral depicted in Figure 4.3(2) has only been computed to order ϵ^{-2} in Ref. [184].

Some sub-integrals, e.g. the N-integral depicted in Figure. 4.4 involves functions beyond generalized polyologarithms (GPLs, [189])[14] This places a major obstruction in the computation of scattering amplitudes in gravity at NNLO extremely complicated (one would need a number of integrals unknown to date) and the task of computing N^{3}LO amplitudes with full kinematic dependence is clearly hopeless for the foreseeable future by means of the tools presently used.

Fortunately, we are only interested in the parts of the final results that are classical. The classical limit can be defined as the limit where all conserved charges are large. In practice this means that we have large angular momentum,[15] center of mass energy and particle masses. We therefore have the following hierarchy of scales

$$m_\star^2 \sim s, |u|, m_1^2, m_2^2 \sim J^2|t| \gg |t| = |q|^2 \,. \tag{4.63}$$

[14] At order ϵ^0 the N can be written as a very involved expression in terms of GPLs. [190]

[15] For example a binary system of 10 solar masses each moving at 10% of the speed of light will have an orbital angular momentum of $J \sim 10^{79}$ in natural units.

Where, for convenience we introduced a characteristic large (hard) scale $m_\star$. The corresponding dimensionless expansion parameter λ is the ratio of the Compton wavelength associated to the hard scale $m_\star$ to the impact parameter b, which in natural units reads

$$\lambda = \frac{1}{m_\star b} \sim \frac{|q|}{m_\star} \ll 1 \,. \tag{4.64}$$

In physical units $\lambda \sim \hbar$ and therefore power counting in λ is equivalent to power counting in $\hbar$, with classical terms naturally being of order λ^0. In terms of the hierarchy (4.63), the phase space splits according to

$$\text{phase space} \quad \begin{cases} \text{hard (h):} & \ell \sim m_\star \\ \text{soft (s):} & \ell \lesssim |q| \end{cases} . \tag{4.65}$$

The soft region is sometimes called "small" in the collider physics literature. The hard region encodes the short distance physics. This includes effects related to renormalization and UV divergences, which nicely fits our intuition that such effects should be identified with the quantum theory.[16] The hard region produces a Taylor expansion in q^2, which Fourier transform to local contributions $\sim \partial_r^k \delta(r)$.[17] The soft region on the other hand captures non-analytic effects, which turn into long-range potentials $\sim r^{-n}$ after Fourier transform. Focusing on the classical piece $\mathcal{O}(\lambda^0)$, on dimensional grounds the remaining q-dependence is of the form $(G|q|)^n$ [43]. This directly implies that for each order in G we also need to expand the amplitude to one order higher in q. To be concrete the terms corresponding to the classical potential are, through three loop, $G/|q|^2, G^2/|q|, G^3 \log|q|$ and $G^4|q|$. The counting is modified when one includes spin, tidal effects or quantum corrections (see e.g. Refs. [90, 192, 193]).

In order to make contact with the traditional literature on the subject of perturbation theory in classical gravity, in particular to NRGR [28] it is convenient to further subdivide the soft region. This split is defined by the hierarchy $v \ll 1$, where the power counting parameter can be chosen as a characteristic velocity, e.g. the relative velocity $v = \sqrt{\sigma^2 - 1}$. In the usual language of collider physics, this non-relativistic limit corresponds to a threshold expansion around the production threshold $s \sim (m_1 + m_2)^2$. We have the following possible regions for the momenta $\ell = (\omega, \boldsymbol{\ell})$, which is also depicted in Figure 4.5:

$$\text{soft} \quad \begin{cases} \text{"quantum" soft (qs):} & \omega \sim |q| & \boldsymbol{\ell} \sim |q| \\ \text{potential (p):} & \omega \sim |q| v & \boldsymbol{\ell} \sim |q| \\ \text{radiation (r):} & \omega \sim |q| v & \boldsymbol{\ell} \sim |q| v \end{cases} . \tag{4.66}$$

Note that in the field-theory literature, the quantum soft region is usually just called "soft" and the radiation region "ultra-soft". We use the name quantum soft because this region does not contribute to classical physics because the energy associated to the exchanged quanta should be small.

[16] As mentioned in Ref. [52] at higher order we encounter UV divergences if we consider finite-size effects. Such effects only affect physical observables starting at the 5PN order. Spurious UV divergences also appear in the near-zone far-zone split. (see e.g. Ref. [191])

[17] Such effects can influence the energy levels of the system, similar to the Lamb-shift in QED.

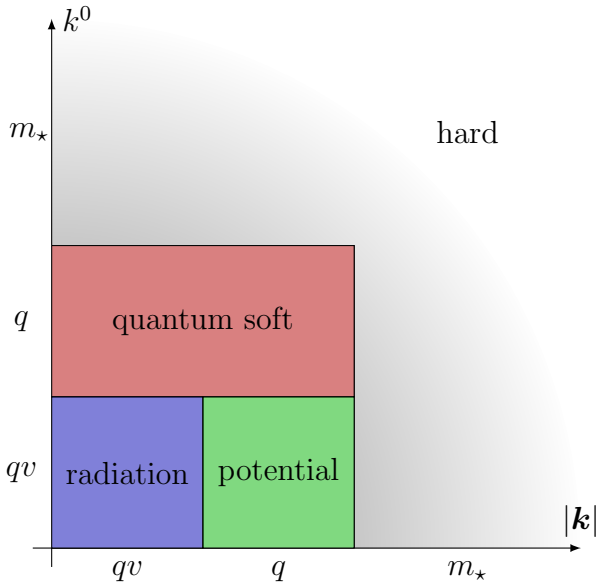

Figure 4.5.: Separation of the phase space for the momentum $k = (k^0, \boldsymbol{k})$ into different regions. Axes have arbitrary scale.

Interactions mediated by potential gravitons are instantaneous[18] and the associated modes are never on-shell and thus do not have to be included as dynamical degrees of freedom in an effective field theory description.

We stress that although the split (4.66) is defined in terms of the power counting variable v, we can perform expansions in the sub-regions to arbitrary order in v. In fact it will be our aim to obtain results formally valid for $v \sim 1$ through the resummation explained in section 4.7.6. This might be surprising, but the purpose of the procedure is to remove the modes of the quantum soft region, which do not correspond to classical dynamics.

4.7.2. Near-static Limit and Classical Regions

As we have seen the classical weak-field approximation enforces a soft expansion in the momentum transfer q. In practice, instead of working in the soft region it may be useful to instead compute in the sum of the potential and the radiation region. While this has the obvious advantage of removing some contributions from the computation, and in particular leading to a more natural interpretation of the terms, this separation of regions comes with some drawbacks. First of all the split breaks the manifest Lorentz invariance. This means that in general the integrals do not need to be analytic functions of the velocity and we cannot use crossing

[18]The potential scalar propagator in position space takes the form

$$G^{(\mathrm{p})}(x, x') = \frac{\delta(t-t')}{|\boldsymbol{x}-\boldsymbol{x}'|} + \frac{1}{2}|\boldsymbol{x}-\boldsymbol{x}'|\partial_t^2\delta(t-t') + \dots \,. \tag{4.67}$$

.

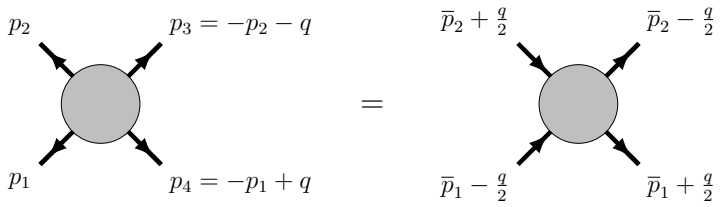

Figure 4.6.: Kinematic setup with Sudakov parametrization.

symmetry to relate integrals in different scattering channels, requiring a larger set of integrals to be computed. Second the computation in the mixed region leads to some combinatorial complexity, with some of the internal momenta in the potential and some in the radiation region. Starting from two-loops this requires an increased amount of bookkeeping.

However, anticipating the application of the method to problems to the three-loop order and beyond it seems the split into regions is warranted as it leads to a reduction of the set of necessary integrals as well as to simpler functions that appear in the expressions.

4.7.3. Sudakov Parametrization

Typically expansion-by-regions is facilitated by an adapted parameterization of the kinematics. A convenient parametrization for massive two-to-two scattering is the Sudakov parametrization [194], as displayed in Figure 4.6 and which is explicitly given by

$$p_1 = -(\bar{p}_1 - q/2)\,, \quad p_2 = -(\bar{p}_2 + q/2)\,, \quad p_3 = \bar{p}_2 - q/2\,, \quad p_4 = \bar{p}_1 + q/2\,. \tag{4.68}$$

By construction the $\bar{p}_i$'s are orthogonal to the momentum transfer q,

$$\bar{p}_1 \cdot q = -\frac{1}{2}\big(p_1^2 - p_4^2\big) = 0\,, \quad \bar{p}_2 \cdot q = \frac{1}{2}\big(p_2^2 - p_3^2\big) = 0\,. \tag{4.69}$$

We further introduce soft masses and four-velocities

$$\bar{m}_i^2 = \bar{p}_i^2 = p_i^2 - q^2/4 = m_i^2 - q^2/4\,, \quad u_i = p_i/\bar{m}_i\,, \tag{4.70}$$

where we do not add a bar to the u_i's for notational simplicity. By virtue of the normalization (4.70) we have

$$u_1^2 = u_2^2 = 1, \quad u_1 \cdot q = u_2 \cdot q = 0. \tag{4.71}$$

Hence, after the soft expansion, the only dimensionful scale of the integrals is q^2 and the dependence on q^2 of each integral can be fixed by dimensional analysis, and the integrals only depend non-trivially on a single dimensionless parameter y,

closely related to the relativistic Lorentz factor σ in Eq. (2.4),

$$y \coloneqq u_1 \cdot u_2 = \sigma + \frac{\sigma(m_1^2 + m_2^2) + 2m_1 m_2}{8 m_1^2 m_2^2}\, q^2 + \mathcal{O}(q^4). \tag{4.72}$$

The computation in full kinematics suffers from the presence of many distinct kinematic roots, which cannot be simultaneously rationalized [195]. However, in the soft expansion, the problem drastically simplifies to a single non-trivial root. For example the four roots relevant for the ladder-box [164] in Figure 4.3(1) are to leading order

$$\begin{aligned} \sqrt{\lambda(s, m_1^2, m_2^2)} \sim \sqrt{\lambda(u, m_1^2, m_2^2)} &\sim 2m_1 m_2 \sqrt{y^2 - 1}\,, \\ \sqrt{-t(4m_i^2 - t)} &\sim 2m_i \sqrt{-t}\,. \end{aligned} \tag{4.73}$$

Therefore, in contrast to the full problem it is possible to find a global rationalization, using the change of variable

$$y = \frac{1 + x^2}{2x}, \quad \sqrt{y^2 - 1} = \operatorname{sign}(x) \frac{1 - x^2}{2x}\,. \tag{4.74}$$

In terms of these variables, the physical region in our scattering processes is given by $1 < y$, i.e. $0 < x < 1$ in the s-channel and $y < -1$, i.e. $-1 < x < 0$ in the u-channel.

As a practical remark, we note that the soft variables can be viewed as a computational scheme. Once we have extracted a classical quantity, e.g. a quantity that is finite as $\hbar \to 0$, we can simply replace $y \to \sigma$, $\bar{m}_i \to m_i$ and u_i by the true four-velocities p_i/m_i as the corrections are higher-order in $\hbar$ and therefore quantum. This is very similar to the situation in collider phenomenology, where individual expressions are scheme dependent but once the divergences (in this case in the dimensional regulator ϵ) have been canceled the final result is scheme independent. This has also been discussed recently in Ref. [196].

4.7.4. Expanding Integrands in the Soft and Near-Static Limit

In order to derive the contribution in the soft region, expansion-by-regions instructs us to perform a small-q expansion at the level of the integrand. Therefore, we need to expand propagators. The graviton loop momenta are always $O(|q|)$ and therefore graviton propagators have homogeneous power counting $|q|^{-2}$. Matter propagator on the other hand have to be expanded. A generic matter propagator is of the form

$$\frac{1}{\left(\ell + \overline{m}_i u_i \pm q/2\right)^2 - m_i^2 + \mathrm{i}\varepsilon} = \frac{1}{\overline{m}_i} \frac{1}{2u_i \cdot \ell + \mathrm{i}\varepsilon} - \frac{1}{\overline{m}_i^2} \frac{\ell^2 \pm \ell \cdot q}{(2u_i \cdot \ell + \mathrm{i}\varepsilon)^2} + \cdots\,, \tag{4.75}$$

where each of the terms is homogeneous in q. The soft expanded integrals can then be treated by IBP reduction. An important fact is that the integrals that scale as even or odd powers in $\sqrt{-q^2}$ cannot be related by IBP since the coefficients in

	soft	potential	radiation
graviton propagator	q^{-2}	$q^{-2}v^{-1}$	$q^{-2}v^{-2}$
matter propagator	q^{-1}	$q^{-1}v^{0}$	$q^{-1}v^{-1}$
measure	q^{D}	$q^{D}v^{1}$	$q^{D}v^{D}$

Table 4.1.: Power counting rules for the subregions of the soft regions.

IBP relations are rational functions of the Mandelstam invariants. [19] The split into even and odd integrals was noted for a similar problem in HQET in Ref. [197].

Expanding in the potential region The potential region can be recognized as a subregion of the soft region, so it can be analyzed after the soft expansion. The expansion is simplified by performing the computation in a frame where u_1 and u_2 are in the (t, z)-plane

$$u_1 = (1, 0, 0, 0)\,, \quad u_2 = (\sqrt{1+v^2}, 0, 0, v\,)\,, \quad q = (0, \boldsymbol{q}, 0)\,. \tag{4.76}$$

By construction of the u_i's, this frame agrees with the rest-frame of particle 1 up to corrections of order q^2 and we have $y = \sqrt{v^2+1}$. We then expand the propagators

$$\frac{1}{\ell^2 + \mathrm{i}\varepsilon} = -\frac{1}{\boldsymbol{\ell}^2} - \frac{\omega^2}{(\boldsymbol{\ell}^2)^2} + \cdots\,, \tag{4.77}$$

$$\frac{1}{u_1 \cdot \ell + \mathrm{i}\varepsilon} = \frac{1}{\omega + \mathrm{i}\varepsilon}\,, \tag{4.78}$$

$$\frac{1}{u_2 \cdot \ell + \mathrm{i}\varepsilon} = \frac{1}{\omega + v\hat{\boldsymbol{z}}\cdot\boldsymbol{\ell} + \mathrm{i}\varepsilon} + v^2 \frac{\omega}{(\omega + v\hat{\boldsymbol{z}}\cdot\boldsymbol{\ell} + \mathrm{i}\varepsilon)^2} + \ldots\,. \tag{4.79}$$

The matter propagators remain structurally unchanged. Since they can still go on-shell (the poles correspond to the positive-energy matter poles of the original integrals), we have to keep track of the $\mathrm{i}\varepsilon$, while for the massless propagators, we can discard it. By considering the leading pieces in the corresponding regions we can derive simple power counting rules, which are very helpful in practice and which are tabulated in Table 4.1. As before IBP relations preserve v-parity, that is integrals even in velocity reduce to integrals even in velocity and the same applies to the odd-ones. Since the expansion of propagators only generates even powers in velocity, this tells us that the series expansion of each integral will have a manifest parity under $v \mapsto -v$ ($\sqrt{y^2-1} \mapsto -\sqrt{y^2-1}$).

The expansion in the soft region also directly sets certain classes of integrals to zero, for example matter contact interactions and on-shell self energy diagrams on-shell vertex diagrams:


$\overset{(s)}{=} 0\,,$

$\overset{(s)}{=} 0\,,$
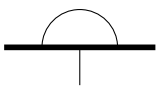
$\overset{(s)}{=} 0\,.$ (4.80)

[19] IBP relations preserve parity under $\sqrt{-q^2} \mapsto -\sqrt{-q^2}$.

The potential region sets mushroom-type integrals and massless subintegrals to zero

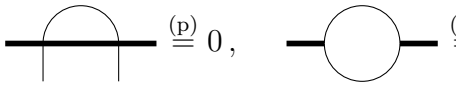

$$\overset{(\mathrm{p})}{=} 0\,, \qquad \overset{(\mathrm{p})}{=} 0\,. \tag{4.81}$$

4.7.5. Regularization of Residual Divergent Integrals

It is well known that the method of regions can introduce additional divergences not regulated by dimensional regularization. This is for example common in soft-collinear effective theory, where these divergences can be handled by analytic regularization [142] or so-called η-regulators [198]. To explain how this problem arises in the context of this work we consider the linearized triangle integral depicted in Figure 4.8(2),

$$I^{\mathrm{II}}_{1,0,1,1} = \int \frac{\mathrm{d}^D \ell e^{\gamma_{\mathrm{E}}\epsilon}}{\mathrm{i}\pi^{D/2}} \frac{1}{\ell^2(\ell-q)^2(2u_1\cdot\ell+\mathrm{i}\varepsilon)}\,. \tag{4.82}$$

Now we expand this integral to leading order[20] in the potential region, choosing the frame (4.76),

$$I^{\mathrm{II},(\mathrm{p})}_{1,0,1,1} = \frac{e^{\gamma_{\mathrm{E}}\epsilon}}{2\mathrm{i}\pi^{D/2}} \int \frac{\mathrm{d}^{D-1}\boldsymbol{\ell}}{\boldsymbol{\ell}^2(\boldsymbol{\ell}-\boldsymbol{q})^2} \times \int \frac{\mathrm{d}\omega}{\omega+\mathrm{i}\varepsilon}\,. \tag{4.83}$$

The first factor is a Euclidean bubble integral in $D-1$ dimensions and regulated by dimensional regularization. The second factor, involving integration over the energy $\ell_0 = \omega$ is ill-defined because of the logarithmic divergence at infinity and we need a prescription of how to compute its value. The integral cannot be regularized by a Lorenz-invariant regularization scheme such as dimensional regularization.

Let us for a moment assume the integral were convergent. A useful prescription should preserve reparametrization invariance of the momentum and so we can symmetrize over ℓ,$-\ell$. This gives

$$\int \frac{\mathrm{d}\omega}{\omega+\mathrm{i}\varepsilon} \overset{!}{=} \frac{1}{2}\int \frac{\mathrm{d}\omega}{\omega+\mathrm{i}\varepsilon} + \frac{1}{2}\int \frac{\mathrm{d}\omega}{-\omega+\mathrm{i}\varepsilon} \overset{!}{=} \frac{1}{2}\int \mathrm{d}\omega\left(\frac{1}{\omega+\mathrm{i}\varepsilon} - \frac{1}{\omega-\mathrm{i}\varepsilon}\right) = -\mathrm{i}\pi\,. \tag{4.84}$$

In other words, in any sensible (additive and parametrization invariant) regularization scheme the triangle integral should be assigned the value [52],

$$\int \frac{\mathrm{d}\omega}{\omega+\mathrm{i}\varepsilon} \equiv -\mathrm{i}\pi\,. \tag{4.85}$$

This prescription is nothing else than the principal value p.v., which in this context might be thought of as a hard cutoff by a scale Λ

$$\text{p.v.}\int_{-\infty}^{\infty} \frac{\mathrm{d}\omega}{\omega+\mathrm{i}\varepsilon} = \lim_{\Lambda\to\infty}\int_{-\Lambda}^{\Lambda} \frac{\mathrm{d}\omega}{\omega+\mathrm{i}\varepsilon} = -\mathrm{i}\pi\,. \tag{4.86}$$

[20] In fact, since the triangle does not depend on y, this expansion is exact.

There are other ways to implement the same prescription, for example by an algebraic regulator. The situation becomes less clear at higher loops however. In order to to see this consider the following integral (which can be obtained from the double-triangle integral depicted in Figure 4.7(1))

$$\int \frac{\mathrm{d}\omega_1 \mathrm{d}\omega_2}{(\omega_1 + \mathrm{i}\varepsilon)(\omega_1 + \omega_2 + \mathrm{i}\varepsilon)} \,. \tag{4.87}$$

We might be inclined to integrate this loop-by-loop using the principal value prescription (4.85). However, if we perform the ω_1 integration first, the integral vanishes as both poles lie on the same side of the real axis. If we integrate over ω_2 first, instead, we get $(-\mathrm{i}\pi)^2 = -\pi^2$. Clearly the prescription is ill-defined. However, we may remember that we were able to asign a value by adding over permutations of energies. The same can be done here and we can assign the value[21]

$$\int \frac{\mathrm{d}\omega_1 \mathrm{d}\omega_2}{(\omega_1+\mathrm{i}\varepsilon)(\omega_1+\omega_2+\mathrm{i}\varepsilon)} \equiv \frac{1}{3!}\sum_{\eta\in S_3}\int \prod_{i=1}^{3}\mathrm{d}\omega_i \frac{\delta(\omega_1+\omega_2+\omega_3)}{(\omega_{\eta(1)}+\mathrm{i}\varepsilon)(\omega_{\eta(1)}+\omega_{\eta(2)}+\mathrm{i}\varepsilon)} \,. \tag{4.88}$$

The integral on the right hand side is well-defined and we find [48, 148, 199]

$$\int \frac{\mathrm{d}\omega_1 \mathrm{d}\omega_2}{(\omega_1 + \mathrm{i}\varepsilon)(\omega_1 + \omega_2 + \mathrm{i}\varepsilon)} = -\frac{2\pi^2}{3} \,. \tag{4.89}$$

In practice, we will evaluate the integrals using the residue method introduced in Ref. [48]. Thereby a generic energy integral gets assigned a definite value as a weighted sum of residues

$$\int \mathrm{d}\omega_1 \cdots \mathrm{d}\omega_n \mathcal{I}(\omega_1, \ldots, \omega_n) = (-\mathrm{i}2\pi)^n \sum_{\underline{r}} c(\underline{r}) \operatorname*{Res}_{\omega_1=r_1,\ldots,\omega_n=r_n} \mathcal{I}(\omega_1, \ldots, \omega_n) \,, \tag{4.90}$$

where the sum runs over all possible multiple residues $\underline{r} = \{r_1, \ldots, r_n\}$ ignoring residues at infinity. And the symmetry factors can then be fixed through demanding values for certain integrals. Let us illustrate how this works. At one-loop we can always take a single residue and we associate the symmetry factor $c\left[\bigtriangledown\right]$ to it. The symmetry factor can for example be fixed by the triangle integral

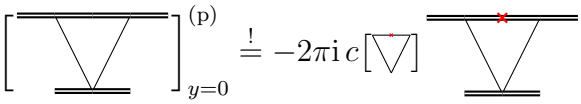

$$\overset{!}{=} -2\pi\mathrm{i}\, c\left[\bigtriangledown\right] \,, \tag{4.91}$$

where the cross on the integral on the right means that we removed the energy integration by taking the residue on the marked propagator. This fixes the symmetry factor to

$$c\left[\bigtriangledown\right] = \frac{1}{2} \,. \tag{4.92}$$

[21] This symmetry is inherited from the permutation symmetry of the original four-dimensional integral.

Similarly at two-loop we have three different symmetry factors which can be fixed through systematization of the associated graphs

$$c\Big[\,\Big] = \frac{1}{6}\,, \quad c\Big[\,\Big] = \frac{1}{3}\,, \quad c\Big[\,\Big] = \frac{1}{6}\,, \quad c\Big[\,\Big] = \big(\,c\big[\,\big]\big)^2 = \frac{1}{4}\,. \tag{4.93}$$




We can check that this prescription is consistent with integrals for which the energy integration is well-defined, for example the ladder-box integral and we find full agreement. We will discuss some two-loop examples in chapter 4.9. An important feature of the residue prescription is that it allows to compute integrals which cannot be computed through symmetrization.

4.7.6. Resummation Through Velocity Differential Equations

The expansion into different regions can be performed to arbitrary order in velocity (the same reasoning applies more generally for expansions defined in terms of a power-counting parameter), for example by IBP reduction of the integrals that arise in the expansion to a basis which can subsequently be computed e.g. using the prescription described in the previous section. This, however, only works to low orders in the expansion parameter, as the complexity of the integrals (measured in terms of the polynomial order of the numerator and propagator powers) increases rapidly.

Alternatively we can reason as follows: the expansion in a given region defines a formal series expansion in v. [22] Assuming that this series converges, this defines a function of v. Now since the IBP reduction for the soft integrals should commute with the expansion this resummed function has to satisfy the same differential equation and the boundary conditions are determined by the first few coefficients of the series expansion.

This approach allows us to derive all-orders-in-v expressions for expansions in regions which are formally only valid for small v. The fact that the resulting expression is Lorentz invariant can be seen from the fact expansion by region is an expansion of the integrand, keeping all orders, the resulting expression transforms identically as the original expression. We can also check this in practice by performing computations in different frames.

The differential-equations-based approach can be viewed as a systematic way of performing the velocity resummation, which in the original work by Bern et. al. [47, 48] and in Ref. [90], was done by an educated guess based on the series expansion.

The dependence on the velocity (e.g. the velocity of particle 2 in the rest-frame of particle 1) is captured by the relativistic y-variable and we find it convenient to derive differential equations in terms of this variable. The differential with respect to y can be expressed in terms of the vectors u_1 and u_2 by using the general

[22] Possibly including some overall factors of the form $v^{a\epsilon}$.

formula (4.54),

$$\frac{\partial}{\partial y} = \frac{\partial}{\partial(u_2 \cdot u_1)} = \frac{y u_1^\mu - u_2^\mu}{y^2 - 1} \frac{\partial}{\partial u_1^\mu} \,. \tag{4.94}$$

As explained before this will produce a differential equation for the master integrals

$$\frac{\partial \vec{g}}{\partial y} = A(y, \epsilon) \vec{g} \,, \tag{4.95}$$

where $A(y, \epsilon)$ depends rationally on y and ϵ. In terms of the x-variable defined in Eq. (4.74), the differential operator takes the form

$$\frac{\partial}{\partial y} = \frac{2x^2}{x^2 - 1} \frac{\partial}{\partial x} \,. \tag{4.96}$$

The differential equation can be brought to (pre-) canonical form

$$\frac{\partial \vec{f}}{\partial x} = \left[\sum_{w \in \mathbb{A}} A_w \frac{\partial}{\partial x} \log w(x) \right] \vec{f} \,, \tag{4.97}$$

where $A_w(\epsilon) = \epsilon A_w$ at one and two-loop level, i.e. the systems in this case are in canonical form. The alphabet through three-loops is

$$\mathbb{A}_{1-\text{loop}} = \{x\} \,, \quad \mathbb{A}_{2-\text{loop}} = \{x, 1 \pm x\} \,, \quad \mathbb{A}_{3-\text{loop}} = \{x, 1 \pm x, 1 \pm \mathrm{i}x\} \,. \tag{4.98}$$

These singular points have a natural interpretation in terms of physical limits in the full problem. The letter x corresponds to the high energy limit $s \to \infty$, while $x \pm 1$ are related to thresholds in the s and u-channel. The letters $1 \pm \mathrm{i}x$, which first appear at three-loops are related to the collinear limit $p_1 \cdot p_2 \to 0$. It will be interesting to assess if the alphabet stabilize with increasing the loop order, that is if $\mathbb{A}_{L-\text{loop}} = \mathbb{A}_{3-\text{loop}}$ for $L \geq 3$.

4.8. Boundary Conditions

4.8.1. Potential Boundary Conditions

Let us again describe the general procedure by an example and consider the following integral

$$\begin{aligned} I^{\text{III}}_{1,1,1,0,1,1,1,0,0} = & \int \frac{\mathrm{d}^D \ell_1 \, e^{\gamma_{\mathbb{E}} \epsilon}}{\mathrm{i}\pi^{D/2}} \int \frac{\mathrm{d}^D \ell_2 \, e^{\gamma_{\mathbb{E}} \epsilon}}{\mathrm{i}\pi^{D/2}} \frac{1}{(2\,\ell_1 \cdot u_1)(-2\,\ell_1 \cdot u_2)(-2\,\ell_2 \cdot u_1)} \\ & \times \frac{1}{\ell_1^2 \ell_2^2 (\ell_1 + \ell_2 - q)^2} \,. \end{aligned} \tag{4.99}$$

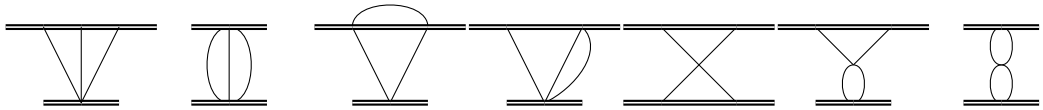

(1) (2) (3) (4) (5) (6) (7)

Figure 4.7.: Single-scale integrals which can be used to fix boundary conditions for two-loop soft integrals.

The leading order in v in the expansion in the potential region is given by

$$I^{\mathrm{III,(p)}}_{1,1,1,0,1,1,1,0,0}\big|_{y=1} = \int \frac{\mathrm{d}^{D-1}\boldsymbol{\ell}_1\, e^{\gamma_{\mathrm{E}}\epsilon}}{\mathrm{i}\pi^{D/2}} \int \frac{\mathrm{d}^{D-1}\boldsymbol{\ell}_2\, e^{\gamma_{\mathrm{E}}\epsilon}}{\mathrm{i}\pi^{D/2}} \frac{1}{\boldsymbol{\ell}_1^2}\frac{1}{\boldsymbol{\ell}_2^2}\frac{1}{(\boldsymbol{\ell}_1+\boldsymbol{\ell}_2-\boldsymbol{q})^2} \times \int \frac{\mathrm{d}\omega_1 \mathrm{d}\omega_2}{(2\omega_1+\mathrm{i}\varepsilon)(-2\omega_2+\mathrm{i}\varepsilon)(-2\omega_1+2v\hat{\boldsymbol{z}}\cdot\boldsymbol{\ell}_1+\mathrm{i}\varepsilon)}\,. \tag{4.100}$$

Performing the energy integration by the symmetrization prescription

$$\int \frac{\mathrm{d}\omega_1 \mathrm{d}\omega_2}{(2\omega_1+\mathrm{i}\varepsilon)(-2\omega_2+\mathrm{i}\varepsilon)(-2\omega_1+2v\hat{\boldsymbol{z}}\cdot\boldsymbol{\ell}_1+\mathrm{i}\varepsilon)} = -\frac{\pi^2}{2v}\frac{1}{2\hat{\boldsymbol{z}}\cdot\boldsymbol{\ell}_1+\mathrm{i}\varepsilon}\,. \tag{4.101}$$

Therefore

$$I^{\mathrm{III,(p)}}_{1,1,1,0,1,1,1,0,0}\big|_{y=1} = \frac{\pi}{2v}\int \frac{\mathrm{d}^{D-1}\boldsymbol{\ell}_1\, e^{\gamma_{\mathrm{E}}\epsilon}}{\pi^{(D-1)/2}} \int \frac{\mathrm{d}^{D-1}\boldsymbol{\ell}_2\, e^{\gamma_{\mathrm{E}}\epsilon}}{\pi^{(D-1)/2}} \frac{1}{\boldsymbol{\ell}_1^2}\frac{1}{\boldsymbol{\ell}_2^2} \frac{1}{(\boldsymbol{\ell}_1+\boldsymbol{\ell}_2-\boldsymbol{q})^2}\frac{1}{(2\hat{\boldsymbol{z}}\cdot\boldsymbol{\ell}_1+\mathrm{i}\varepsilon)}\,. \tag{4.102}$$

For the spatial integral, first integrate the $\boldsymbol{\ell}_2$-subloop and then use the formula for the general triangle integral. The result can be expressed in a closed form in ϵ,

$$\begin{aligned} I^{\mathrm{III,(p)}}_{1,1,1,0,1,1,1,0,0}\big|_{y=1} &= \frac{\mathrm{i}\pi^3}{v}(\boldsymbol{q}^2)^{-2\epsilon-1/2}e^{2\gamma_{\mathrm{E}}\epsilon}2^{2\epsilon-1}\frac{\sec(2\pi\epsilon)\Gamma\left(\frac{1}{2}-\epsilon\right)}{\Gamma\left(\frac{1}{2}-3\epsilon\right)} \\ &= \frac{\mathrm{i}\pi^3}{v}(\boldsymbol{q}^2)^{-2\epsilon-1/2}\left[\frac{1}{4\epsilon}-\frac{1}{2}\log 2+\mathcal{O}(\epsilon)\right]. \end{aligned} \tag{4.103}$$

4.8.2. Soft Boundary Conditions

The soft region is a manifest relativistic region. As such the integrals encountered are of the standard Feynman type regularized by dimensional regularization. Therefore in contrast to the potential region there are many different ways to obtain boundary condition, some of which we will discuss in the following paragraphs.

Direct integration Typically some of the integrals that appear in the DE system are simple enough to compute them directly. In the case at hand this is the case for all integrals that are independent of y. The integrals of this type that appear at the two-loop order are shown in Figures 4.7(1)–4.7(7). This integrals either factorize into one-loop integrals (Figures 4.7(5)–4.7(7)) or can be computed by

a loop-by-loop approach as explained in section 4.3.2. For the double triangle integral in Figure 4.7(1) we can use the symmetrization trick which we discussed in section 4.3.3. We can even go a bit further and apply direct integration to box-type integrals owing to the fact that we have a closed form of the box integral with arbitrary powers of the propagators in Eqs. (A.10) and (A.12). For example

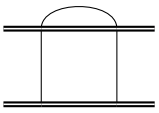

$$= \frac{(\pi^2 4^{2\epsilon-1}\csc(2\pi\epsilon))}{(2\epsilon-1)\Gamma(3/2-2\epsilon)}\left[\sqrt{\pi}\csc(\pi\epsilon)\,{}_2F_1\left[\begin{matrix}1 & 2\epsilon-1\\ \epsilon+1/2\end{matrix};\frac{1-y}{2}\right]\right. \tag{4.104}$$

$$\left. + 2ie^{-i\pi\epsilon}\epsilon\big(y^2-1\big)^{\frac{1}{2}-\epsilon}\Gamma(-\epsilon)\Gamma(\epsilon+1/2)\right].$$

The results can subsequently be expanded to the desired order in ϵ, for example using `HypExp` [200]

$${}_2F_1\left[\begin{matrix}1 & 2\epsilon-1\\ \epsilon+1/2\end{matrix};\frac{1-y}{2}\right] = \frac{x^2+1}{2x} + \frac{1-x^2}{x}\epsilon\log(x) + \mathcal{O}(\epsilon^2)\,. \tag{4.105}$$

(4.106)

Regularity In general, the solution of the DE should satisfy physical constraints. For example a planar integral should not have an u-channel singularity and therefore should be regular at $y = -1$. Up to the two-loop order this only yields constraints for the planar integrals. The three-loop alphabet contains singularities at $y = 0$ which lies inside of the Euclidean region and therefore all integrals should be regular at this point. In practice, regularity in a pre-canonical basis is enforced by choosing the solutions such that they are in the kernel of the associated matrix residue.

Analysis of regions A general approach to the computation of boundary conditions is to compute the functions in a kinematic limit. This brings us back to the method of regions and in the present context it is natural to expand integrals around the threshold $v = 0$. For a concrete example consider the two-loop ladder integral with eikonal propagators. If we use the power counting rules listed in table 4.1, we find that the dominant contribution to this integral comes from the potential region, where this integral scales as $1/v^2$. All other regions are suppressed at least by one power of v. By construction all integrals in a pre-canonical basis have only logarithmic singularities, so the leading order will fix the integral. Therefore we conclude that the integral is identical to the potential contribution, which we have explained how to compute in the previous section. To be concrete, we have the following expansion

$$\epsilon^4(y^2-1)$$ 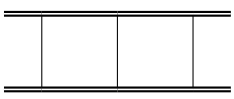 $$= \frac{\pi^2}{2}\epsilon^2 - \frac{\pi^3}{12}\epsilon^3 + \mathcal{O}(\epsilon^4) + \mathcal{O}(v^{1-2\epsilon})\,. \tag{4.107}$$

Numerical evaluation and PSQL fitting Since the integrals in the soft region are well-defined in dimensional regularization, they can be computed with publically

available software designed for the computation of Feynman integrals. Examples are `FIESTA` [201] or `PySecDec` [202] which compute the relevant integrals by Monte-Carlo methods. Let's assume we would like to know the value of the scalar H function at the Euclidean point $y = 0$. Using `PySecDec` it is very easy to get more than 10 digits precision,

$$\left[\epsilon^4\sqrt{y^2-1}\quad \right]_{y=0} = \begin{array}{c} \mathrm{i}(3.875784585037435 \pm 6\cdot 10^{-15})\epsilon^3 \\ +\mathrm{i}(5.37297831514 \pm 2\cdot 10^{-11})\epsilon^4 + \mathcal{O}(\epsilon^5) \end{array} . \tag{4.108}$$

We can make use of PSLQ fitting [203] as implemented in `PolyLogTools` [204], to fit to a set of weight 3 and weight 4 constants $\{\pi^3, \zeta_3, \pi^3\log 2, \pi^4, \pi\zeta_3\}$. The result is

$$\left[\epsilon^4\sqrt{y^2-1}\quad \right]_{y=0} \overset{\text{PSLQ}}{=} \mathrm{i}\frac{\pi^3}{8}\epsilon^3 + \frac{\mathrm{i}}{4}\pi^3\log 2\,\epsilon^4 + \mathcal{O}(\epsilon^5)\,, \tag{4.109}$$

in full agreement with the numerical value (4.108) within 3 times the error given by `PySecDec`. In practice, one needs far less precision than displayed in Eq. (4.108), for example the fit (4.109) can be obtained with only 4 digits precision if one assumes that the coefficient of the ϵ^3, i.e. π^3 is an overall factor. We stress that similar tricks might be applicable at higher loop orders, but the method relies heavily on two facts: first one needs a good set of master integrals, preferably a uniform trancedental (UT) basis in order to limit the number of different transcendental constants that can appear (by definition in an UT basis the coefficients at order ϵ^n have transcendental weight n). Second one needs knowledge of the set of constants that can appear. For example at three-loop order one finds constants beyond zeta-values like Catalan's constant already in the conservative sector for individual integrals.

4.9. Examples

4.9.1. One-loop Integrals With Eikonal Propagators

The linearized box integral which is obtained from its massive counterpart is defined as

$$I^{\text{II}}_{a_1,a_2,a_3,a_4}(q^2, y; D) = \int \frac{\mathrm{d}^D\ell\, e^{\gamma_{\text{E}}\epsilon}}{\mathrm{i}\pi^{D/2}} \frac{1}{(2u_1\cdot\ell)^{a_1}(-2u_2\cdot\ell)^{a_2}(\ell^2)^{a_3}[(\ell-q)^2]^{a_4}}\,. \tag{4.110}$$

The crossed box integral is obtained by replacing $y \mapsto -y$. Using integration-by-parts reduction, all such integrals are rewritten as linear combinations of the

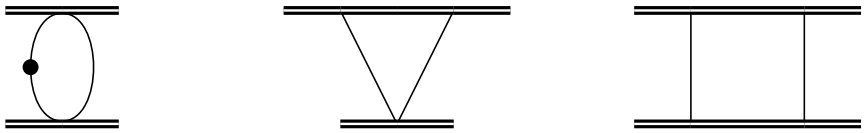

(1) f_1^{II} (2) f_2^{II} (3) f_3^{II}

Figure 4.8.: Master integrals for the box family with eikonal propagators (II).

following three master integrals[23] depicted in Figure 4.8

$$f_1^{\text{II}} = \epsilon(-q^2)\, G^{\text{II}}_{0,0,2,1}\,, \quad f_2^{\text{II}} = \epsilon^2\sqrt{-q^2}\, G^{\text{II}}_{1,0,1,1}\,, \quad f_3^{\text{II}} = \epsilon^2\sqrt{y^2-1}\,(-q^2)\, G^{\text{II}}_{1,1,1,1}\,. \tag{4.111}$$

The normalizations are chosen, such that the system is in canonical form

$$\frac{\mathrm{d}\vec{f}^{\,\text{II}}}{\mathrm{d}x} = \epsilon \begin{pmatrix} 0 & 0 & 0 \\ 0 & 0 & 0 \\ 1 & 0 & 0 \end{pmatrix} \frac{\mathrm{d}}{\mathrm{d}x}\log(x)\vec{f}^{\,\text{II}}\,. \tag{4.112}$$

As we stressed before this differential equation can be applied to either soft, potential or cut integrals, with the following simplifications:

- In the potential region the bubble integral is identical zero.
- When we cut two massive lines, the triangle and bubble vanish.

Potential boundary conditions As commented on before the integral in the potential region is to be understood as a resummation of the integral expanded in the potential region. We recall that the potential region is defined by the scaling

$$\ell^\mu = (\omega, \boldsymbol{\ell}) \sim q(v,1)\,, \quad u_i^\mu = (u_i^0, \boldsymbol{u}_i) \sim (1, v)\,. \tag{4.113}$$

By the velocity powercounting described in section 4.7.4 all integrals are of order $\mathcal{O}(v^0)$, and we therefore only have to expand the integrals to leading order in v. Adapting the rest frame of particle 1, we have

$$I^{\text{II},(\text{p})}_{\underline{a}} = \int \frac{e^{\gamma_{\mathbb{E}}\epsilon}\mathrm{d}^{D-1}\boldsymbol{\ell}\,\mathrm{d}\omega}{\mathrm{i}\pi^{D/2}} \frac{1}{(2\omega+\mathrm{i}\varepsilon)^{a_1}(-2\omega+2v\hat{\boldsymbol{z}}\cdot\boldsymbol{\ell}+\mathrm{i}\varepsilon)^{a_2}\left(-\boldsymbol{\ell}^2\right)^{a_3}\left[-(\boldsymbol{\ell}-\boldsymbol{q})^2\right]^{a_4}}\,. \tag{4.114}$$

where $\hat{\boldsymbol{z}} = (0,0,1)$. The bubble integral $I^{\text{II},(\text{p})}_{1,1,0,0}$ vanishes as the energy integration has no pole. For the triangle and box integrals, we can compute the energy intagration by the prescription in Eq. (4.85) and direct integration respectively. For the triangle we have

$$I^{\text{II},(\text{p})}_{1,0,1,1} = -\frac{\sqrt{\pi}}{2}\int \frac{e^{\gamma_{\mathbb{E}}\epsilon}\mathrm{d}^{D-1}\boldsymbol{\ell}}{\pi^{(D-1)/2}} \frac{1}{\boldsymbol{\ell}^2(\boldsymbol{\ell}-\boldsymbol{q})^2} + \mathcal{O}(v)\,, \tag{4.115}$$

$$I^{\text{II},(\text{p})}_{1,1,1,1} = -\frac{\sqrt{\pi}}{v}\int \frac{e^{\gamma_{\mathbb{E}}\epsilon}\mathrm{d}^{D-1}\boldsymbol{\ell}}{\pi^{(D-1)/2}} \frac{1}{(2\hat{\boldsymbol{z}}\cdot\boldsymbol{\ell}+\mathrm{i}\varepsilon)\boldsymbol{\ell}^2(\boldsymbol{\ell}-\boldsymbol{q})^2} + \mathcal{O}(v^0)\,. \tag{4.116}$$

[23] In contrast the full two-mass box family has 10 master integrals, see e.g. Ref. [48].

The result for the boundary conditions to the pure functions is

$$f_1^{\mathrm{II},(\mathrm{p})}\big|_{y=1} = 0\,, \tag{4.117}$$

$$f_2^{\mathrm{II},(\mathrm{p})}\big|_{y=1} = -\epsilon^2(-q^2)^{-\epsilon}e^{\gamma_{\mathrm{E}}\epsilon}\frac{\sqrt{\pi}\,\Gamma\left(\frac{1}{2}-\epsilon\right)^2\Gamma\left(\epsilon+\frac{1}{2}\right)}{2\Gamma(1-2\epsilon)}\,, \tag{4.118}$$

$$f_3^{\mathrm{II},(\mathrm{p})}\big|_{y=1} = \epsilon^2(-q^2)^{-\epsilon}e^{\gamma_{\mathrm{E}}\epsilon}\frac{\mathrm{i}\pi}{2}\frac{\Gamma(-\epsilon)^2\Gamma(1+\epsilon)}{\Gamma(-2\epsilon)}\,. \tag{4.119}$$

Since the bubble integral is zero all integrals are actually constant and therefore identical to their value at $y = 1$. For the crossed box we cannot use analytic continuation, which is broken by the potential expansion. However, by an explicit computation we find that the boundary condition vanishes as both poles of the energy integral lie on the same side of the real axis and therefore the corresponding integral vanishes. Again the differential equation is the same, with $x \mapsto -x$, so the crossed box vanishes to all orders in the velocity expansion.

Soft boundary conditions Obtaining boundary conditions for the full soft region is arguably simpler than the potential region because all integrals have a well-defined value in dimensional regularization. We can make use of the fact that the box integral should not have an u-channel discontinuity, and thus the integral should be regular at $x = -1$. The triangle and the bubble integral can be computed by elementary means and are special cases of the more general formula (A.2). One finds,

$$= -\left(-q^2\right)^{-1-\epsilon}e^{\gamma_{\mathrm{E}}\epsilon}\frac{\epsilon\Gamma(-\epsilon)^2\Gamma(1+\epsilon)}{2\Gamma(-2\epsilon)}\,, \tag{4.120}$$

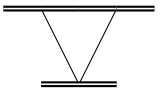

$$= -\left(-q^2\right)^{-\frac{1}{2}-\epsilon}e^{\gamma_{\mathrm{E}}\epsilon}\frac{\sqrt{\pi}\Gamma\left(\frac{1}{2}-\epsilon\right)^2\Gamma\left(\epsilon+\frac{1}{2}\right)}{2\Gamma(1-2\epsilon)}\,. \tag{4.121}$$

The box integral in the Euclidean region $x < 0$ is given by

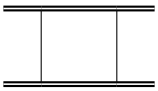

$$= (-q^2)^{-1-\epsilon}e^{\gamma_{\mathrm{E}}\epsilon}\frac{\Gamma(-\epsilon)^2\Gamma(1+\epsilon)}{2\Gamma(-2\epsilon)}\frac{\log(-x)}{\sqrt{y^2-1}}\,, \quad x<0\,. \tag{4.122}$$

By analytic continuation using that $\mathrm{Im}(y) > 0$ and therefore $\mathrm{Im}(x) < 0$, we obtain the box integral in physical kinematics (notice also the change in sign of the square-root)

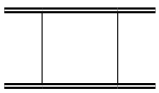

$$= -(-q^2)^{-1-\epsilon}e^{\gamma_{\mathrm{E}}\epsilon}\frac{\Gamma(-\epsilon)^2\Gamma(1+\epsilon)}{2\Gamma(-2\epsilon)}\frac{\log(x)-\mathrm{i}\pi}{\sqrt{y^2-1}}\,, \quad x>0\,. \tag{4.123}$$

In appendix (A.10) and (A.12) we present a closed formula for the box integral with arbitrary indices which is obtained without the use of differential equations, finding full agreement

Two-particle cut For completeness, let us consider the two-particle cut. Again we can use the same differential equation, but now since the bubble and triangle are zero the box integral must be constant. This constant is trivially obtained by direct integration

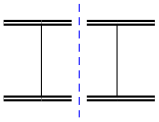

$$\begin{aligned} &= \int \frac{e^{\gamma_{\mathrm{E}}\epsilon}\mathrm{d}^D\ell}{\mathrm{i}\pi^{D/2}} \frac{\hat{\delta}(2u_1\cdot\ell)\,\hat{\delta}(2u_2\cdot\ell)}{\ell^2(\ell-q)^2} \\ &= \frac{-\mathrm{i}\pi}{4\sqrt{y^2-1}} \int \frac{e^{\gamma_{\mathrm{E}}\epsilon}\mathrm{d}^{D-2}\boldsymbol{\ell}_\perp}{\pi^{(D-2)/2}} \frac{1}{\boldsymbol{\ell}_\perp^2(\boldsymbol{\ell}_\perp-\boldsymbol{q}_\perp)^2} \\ &= (-q^2)^{-1-\epsilon} e^{\gamma_{\mathrm{E}}\epsilon} \frac{\mathrm{i}\pi}{4\sqrt{y^2-1}} \frac{\Gamma(-\epsilon)^2\Gamma(1+\epsilon)}{\Gamma(-2\epsilon)}\,. \end{aligned} \tag{4.124}$$

and we can check that the cutting rules are satisfied[24]

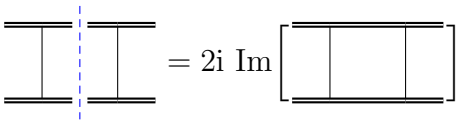

$$= 2\mathrm{i}\ \mathrm{Im}\Big[\quad\Big]\,. \tag{4.125}$$

4.9.2. The Two-Loop Ladder-Box Family

Let us consider the two-loop ladder-box family (III). An integral in this family is explicitly given by

$$\begin{aligned} I^{\mathrm{III}}_{\underline{a}} = &\int \frac{\mathrm{d}^D\ell_1\, e^{\gamma_{\mathrm{E}}\epsilon}}{\mathrm{i}\pi^{D/2}} \int \frac{\mathrm{d}^D\ell_2\, e^{\gamma_{\mathrm{E}}\epsilon}}{\mathrm{i}\pi^{DD/2}} \frac{1}{(2\,\ell_1\cdot u_1)^{a_1}(-2\,\ell_1\cdot u_2)^{a_2}(-2\,\ell_2\cdot u_1)^{a_3}(2\ell_2\cdot u_2)^{a_4}} \\ &\times \frac{[(\ell_1-q)^2]^{-a_8}[(\ell_2-q)^2]^{-a_9}}{(\ell_1^2)^{a_5}(\ell_2^2)^{a_6}[(\ell_1+\ell_2-q)^2]^{a_7}}\,, \end{aligned} \tag{4.126}$$

[24] The additional factor of i is due to our conventions of the integral measure.

where $a_8, a_9 < 0$. The 10 master integrals are depicted in Figure. 4.9. A basis of canonical integrals is given by

$$f_1^{\text{III}} = \epsilon^2(-q^2) I^{\text{III}}_{0,0,0,0,1,2,2,0,0}\,, \tag{4.127}$$
$$f_2^{\text{III}} = \epsilon^4\sqrt{y^2-1}\, I^{\text{III}}_{0,1,1,0,1,1,1,0,0}\,, \tag{4.128}$$
$$f_3^{\text{III}} = \epsilon^3(-q^2)\sqrt{y^2-1}\, I^{\text{III}}_{0,1,1,0,2,1,1,0,0}\,, \tag{4.129}$$
$$f_4^{\text{III}} = -\epsilon^2(-q^2) I^{\text{III}}_{0,2,2,0,1,1,1,0,0} + \epsilon^3 y\,(-q^2) I_{0,1,1,0,2,1,1,0,0}\,, \tag{4.130}$$
$$f_5^{\text{III}} = \epsilon^3\sqrt{y^2-1}\,(-q^2) I^{\text{III}}_{1,1,0,0,1,1,2,0,0}\,, \tag{4.131}$$
$$f_6^{\text{III}} = \epsilon^3(1-6\epsilon)\, I^{\text{III}}_{1,0,1,0,1,1,1,0,0}\,, \tag{4.132}$$
$$f_7^{\text{III}} = \epsilon^4\big(y^2-1\big)(-q^2) I^{\text{III}}_{1,1,1,1,1,1,1,0,0}\,, \tag{4.133}$$
$$f_8^{\text{III}} = \epsilon^3\sqrt{-q^2} I^{\text{III}}_{1,0,0,0,1,1,2,0,0}\,, \tag{4.134}$$
$$f_9^{\text{III}} = \epsilon^3\sqrt{-q^2} I^{\text{III}}_{0,2,1,0,1,1,1,0,0}\,, \tag{4.135}$$
$$f_{10}^{\text{III}} = \epsilon^4\sqrt{y^2-1}\sqrt{-q^2} I^{\text{III}}_{1,1,1,0,1,1,1,0,0}\,. \tag{4.136}$$

The differential equations are obtained by taking derivatives with the operator (4.94) and subsequent IBP reduction and they take the following form

$$\mathrm{d}\vec{f}^{\,\text{III}} = \epsilon\big[A_0^{\text{III}}\,\mathrm{d}\log(x) + A_{+1}^{\text{III}}\,\mathrm{d}\log(x-1) + A_{-1}^{\text{III}}\,\mathrm{d}\log(x+1)\big]\vec{f}^{\,\text{III}}\,. \tag{4.137}$$

Integrals (4.127)–(4.133) have even parity in q. The remaining integrals (4.134)–(4.136) have odd parity. As we have described before the systems decouple, which is manifest in the fact that the connection A has two invariant subspaces

$$A_i^{\text{III}} = \begin{pmatrix} A_i^{\text{III,(e)}} & 0 \\ 0 & A_i^{\text{III,(o)}} \end{pmatrix}, \tag{4.138}$$

where the even matrices are given by

$$A_0^{\text{III,(e)}} = \begin{pmatrix} 0 & 0 & 0 & 0 & 0 & 0 & 0 \\ -\frac{1}{2} & -6 & 0 & -1 & 0 & 0 & 0 \\ -\frac{3}{2} & 0 & 2 & -2 & 0 & 0 & 0 \\ 0 & 12 & 2 & 0 & 0 & 0 & 0 \\ -\frac{3}{4} & 0 & 0 & 0 & 0 & 0 & 0 \\ 0 & 0 & 0 & 0 & 0 & 0 & 0 \\ 0 & 0 & 1 & 0 & -2 & 0 & 0 \end{pmatrix},\quad A_{\pm1}^{\text{III,(e)}} = \begin{pmatrix} 0 & 0 & 0 & 0 & 0 & 0 & 0 \\ 0 & 6 & 0 & 0 & 0 & 0 & 0 \\ 0 & 0 & -2 & 0 & 0 & 0 & 0 \\ 0 & 0 & 0 & 0 & 0 & 0 & 0 \\ 0 & 0 & 0 & 0 & 0 & 0 & 0 \\ 0 & 0 & 0 & 0 & 0 & 0 & 0 \\ 0 & 0 & 0 & 0 & 0 & 0 & 0 \end{pmatrix}, \tag{4.139}$$

and the odd matrices are

$$A_0^{\text{III,(o)}} = \begin{pmatrix} 0 & 0 & 0 \\ 0 & -2 & 0 \\ 0 & 1 & 0 \end{pmatrix},\quad A_{+1}^{\text{III,(o)}} = \begin{pmatrix} 0 & 0 & 0 \\ -3 & -2 & 0 \\ 0 & 0 & 0 \end{pmatrix},\quad A_{-1}^{\text{III,(o)}} = \begin{pmatrix} 0 & 0 & 0 \\ 3 & 6 & 0 \\ 0 & 0 & 0 \end{pmatrix}. \tag{4.140}$$

A curious feature is the fact that the derivatives of all integrals can be written in terms of integrals with at most two matter propagators. In particular the

derivative of the double-box integral does not depend on itself. This means that we only need a suitable boundary value and can then obtain the integral by direct integration.

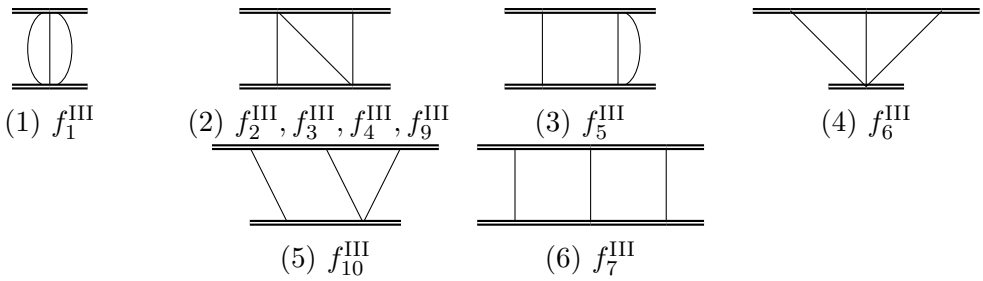

Figure 4.9.: Master integrals in the III family.

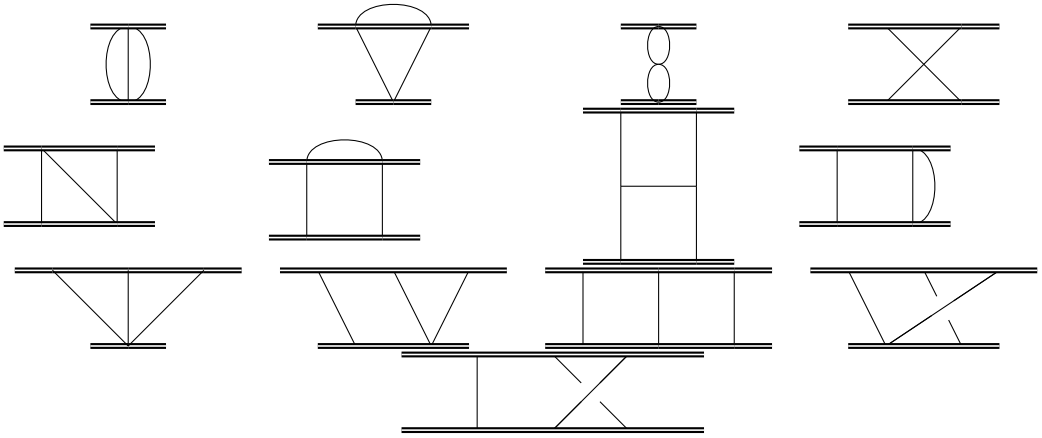

4.9.3. Triple-Cut Integrals

The cut integrals can be straightforwardly obtained from the virtual integrals, using Cutkosky's cutting rules [205]. The cutting rules imply that the sum of cuts in any given channel vanishes. Alternatively it can be rephrased in a way that relates the imaginary part of an integral in terms of cuts.[25] For example we have for the ladder-type integrals

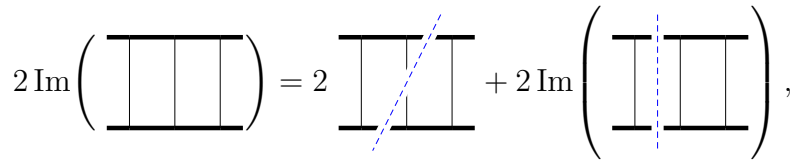

(4.141)

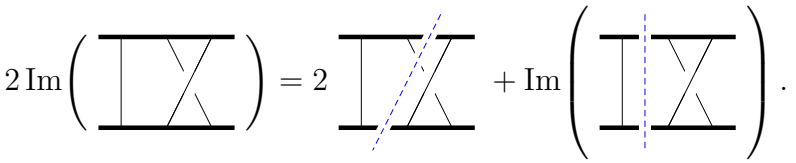

(4.142)

The factors take into account the multiplicity of certain cuts, e.g. the non-planar ladder has only a single s-channel cut. The equations (4.141) and (4.142) are valid

[25] More details are given in Ref. [149].

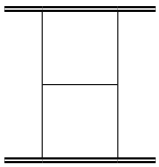

Figure 4.11.: H-topology.

both for the integrals with quadratic and eikonal propagators. As we alluded before cut integrals can be computed in a similar fashion to the virtual (uncut) integrals. The differential equations stay unchanged up to the fact that the introduction of cuts reduces the symmetries of the problem, which can however be taken into account by appropriate symmetry factors.

The only difference in the computation, are once again the boundary conditions. In order to obtain the values we are in principle able to use the same methods as in the previous chapters. First we could in principle attempt direct evaluation of some simple boundary integrals. While this is a viable option for the two-particle cuts, as we have shown explicitly for the one-loop box integral, the direct evaluation of the three-particle cut integrals seems to be infeasible. On the other hand we can use the method of regions. However, we will only employ it in conjunction with power-counting arguments, in order to avoid the explicit evaluation of integrals. Finally, we note that the cutting rules put tight constraints on the integrals which can be exploited. Since the integrals under consideration only have very few cuts in a given channel we can systematically use the cutting rules to determine the values of the integrals.

In particular all integrals in the H-family (the integral depicted in Figure 4.11 and its daughters) only have a single s-channel cut. And therefore we find that the cutting rule for a H-family integral I_{H} is simply

$$I_{\mathrm{H,3pt-cut}} = 2\,\mathrm{Im}\,I_{\mathrm{H}}\,. \tag{4.143}$$

Since we already explained how we can compute the virtual integrals, we get the values of the three-particle cuts of H-type integrals for free. To give an concrete example

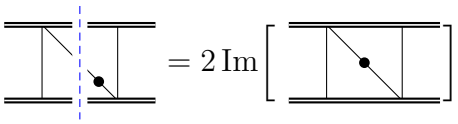

$$= 2\,\mathrm{Im}\Big[$$

$$\Big] \tag{4.144}$$

$$= (-q^2)^{-2\epsilon-1}\frac{\pi}{\epsilon^2\sqrt{y^2-1}}\Big\{1-2\epsilon\Big[\log\big(1-x^2\big)-\log(x)\Big]+\mathcal{O}(\epsilon^2)\Big\}\,.$$

We notice that this reasoning applies to all but four integrals, the III and the IX ladder and the planar and non-planar box triangles. We could apply the same approach, making use of the fact that the cutting rules relate the three-particle cuts to the virtual integral plus two-particle cut which are essentially trivial. However, we find it convenient to use the fact that for all of these integrals the derivatives can be written in terms of integrals with at most two matter lines, which have previously been obtained by the cutting rules. For example the IX ladder is related

only to the N integral

$$\frac{\partial}{\partial x}\left[(y^2-1)\right.$$ 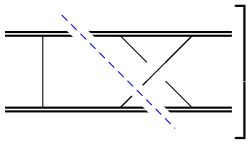 $$\left.\right] = -\frac{1}{x}\left[\sqrt{y^2-1}\right.$$ 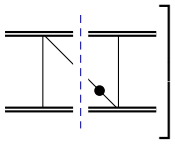 $$\left.\right]. \qquad (4.145)$$

Thereby we obtain the four missing integrals by direct integration. For the boundary conditions we make use of naive power counting. For the triple cut one graviton has to be on-shell and therefore the integrals do not receive contributions from the potential region. The leading behavior instead comes from the potential-radiation region. In all cases we find that the (canonically normalized) integrals scale as at least as $v^{1-2\epsilon}$ and therefore they have to vanish on in the static limit. We proceed by giving an explicit example by integrating Eq. (4.145)

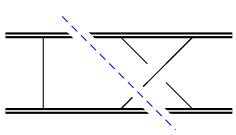 $$= -\frac{1}{y^2-1}\int_1^x \frac{\mathrm{d}x'}{x'}\left[\sqrt{y'^2-1}\right.$$ 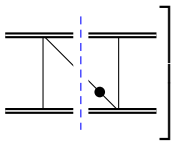 $$\left.\right]$$

$$= -(-q^2)^{-2\epsilon-1}\frac{\pi}{\epsilon^2(y^2-1)}\Big\{\log(x)$$

$$+\epsilon\left[\log(x)^2+\mathrm{Li}_2(x^2)-\frac{\pi^2}{6}\right]+\mathcal{O}(\epsilon^2)\Big\}. \qquad (4.146)$$

4.10. Validation of Two-Loop Integrals

We have performed several checks of the two-loop integrals based on the overcompleteness of the set of boundary conditions. First, we have performed high-precision numerical checks, against `PySecDec` [202, 206] in the Euclidean and to lower precision in the Lorentzian region, finding agreement within the error estimates of the numerical evaluation.

The virtual integrals have also been computed independently in Ref. [207], but using the same methods. We find full agreement to the orders in epsilon provided.

We can also compare to computations of the full integrals. The value of the soft integral can be extracted from the non-analytic-in-q pieces of these results. In the literature the available sources are Ref. [188] (which has also been recently been revisited in Ref. [163]) for the H-type integral and ladder integrals [184–186], to the orders of ϵ available in the literature.

4.11. The Elliptic Sector

One of the major new features of the three loop problem is the appearance of elliptic integrals.[26] There are three lowest-level topologies of this form with two

[26] Some comments on these integrals have also been made in Ref. [93].

of them related by u-channel crossing as shown in Figure 4.12. Each of these topologies has three master integrals. For the potential-region contribution, we can effectively treat the system as if it were on the cut as all daughters vanish in the classical limit, as they either have mushrooms, matter contacts or less than one matter propagator per loop. This sector to which we will be referring to as IK in the following, can not be brought to ϵ-form using Lee's algorithm. Interestingly we find that it can be brought to an $(\epsilon + 1/2)$-form instead (cf. Ref. [208]). We refrain from using the $(\epsilon+1/2)$-form as it introduces additional complexity in the sector mixing the KI with its parents. For the following discussion, we choose the following master integrals:

$$f_1^{\text{KI}} = \epsilon^2$$ 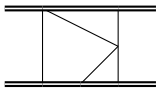 , $$f_2^{\text{KI}} = \epsilon^2$$ 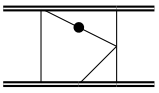 , $$f_3^{\text{KI}} = \frac{\epsilon^3}{1+6\epsilon}$$ 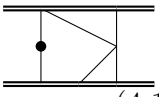 . (4.147)

The differential equation for the KI sub-sector is of the form[27]

$$\begin{aligned} \mathrm{d}\vec{f}^{\,\text{KI}} =& \mathrm{d}\left[\begin{pmatrix} 8\epsilon & 0 & 4\epsilon+2 \\ 0 & -4\epsilon-2 & 8\epsilon+4 \\ 0 & 0 & 0 \end{pmatrix} \log\left(\frac{1-x^2}{2x}\right)\right. \\ &\left. + \begin{pmatrix} -4\epsilon-\frac{1}{2} & \epsilon+\frac{1}{4} & -4\epsilon-2 \\ -8\epsilon-1 & 2\epsilon+\frac{1}{2} & -8\epsilon-4 \\ 2\epsilon+\frac{1}{4} & -\frac{\epsilon}{2}-\frac{1}{8} & 2\epsilon+1 \end{pmatrix} \log\left(\frac{1+x^2}{2x}\right)\right] \vec{f}^{\,\text{KI}} . \end{aligned} \tag{4.148}$$

The conventional approach is to solve the lowest order in ϵ first and then integrate out this solution. For the analysis it is convenient to convert the system to a first-order system for the scalar integral $f_{\text{KI},1}$

$$\begin{aligned} 0 =& f_1^{\text{KI},(3)} + \frac{4(x^2+1)\epsilon - 6x^2}{x(1-x^2)} f_1^{\text{KI},(2)} \\ &+ \frac{x^4(4(\epsilon-3)\epsilon+7) - 4x^2(34\epsilon^2+1) + (1-2\epsilon)^2}{x^2(1-x^2)^2} f_1^{\text{KI},(1)} - \frac{(x^2+1)(1-2\epsilon)^2}{x^3(1-x^2)} f_1^{\text{KI}} . \end{aligned} \tag{4.149}$$

In the following we want to solve Eq. (4.149) to lowest order in the regulator ϵ. This amounts to setting $\epsilon \to 0$,

$$f_1^{\text{KI},(3)}(x) - \frac{6x}{1-x^2} f_1^{\text{KI},(2)}(x) + \frac{(7x^4-4x^2+1)}{x^2(1-x^2)^2} f_1^{\text{KI},(1)}(x) - \frac{x^2+1}{x^3(1-x^2)} f_1^{\text{KI}}(x) = 0 . \tag{4.150}$$

Here and in the following f_1^{KI} denotes the leading-order in ϵ of the corresponding function. Finding solutions of a third-order differential equation is in general a quite formidable problem and there is no general way to find closed-form solutions. Fortunately the differential equation (4.150) takes the form of a "symmetric

[27] Even though the alphabet in this case could be represented in terms of y^2-1 and y we prefer to work with the x-variable here to keep the discussion coherent with the previous chapters.

square"[28]

$$0 = f_1^{\mathrm{KI},(3)} + 3a(x) f_1^{\mathrm{KI},(2)} + \left[2a(x)^2 + a'(x) + 4b(x)\right] f_1^{\mathrm{KI},(1)} + \left[4a(x)b(x) + 2b'(x)\right] f_1^{\mathrm{KI}}\,, \tag{4.151}$$

where

$$a(x) = \frac{2x}{x^2-1}\,, \quad b(x) = \frac{1}{4x^2}\,. \tag{4.152}$$

The third-order differential equation (4.150) is equivalent to the second-order differential equation

$$0 = y^{(2)}(x) + a(x)y'(x) + b(x)y(x) = y''(x) + \frac{2x}{x^2-1}y'(x) + \frac{1}{4x^2}y(x)\,. \tag{4.153}$$

The solutions to the original equation can be written in terms of the two independent solutions y_i of Eq. (4.153)

$$f_1^{\mathrm{KI}} = c_1 y_1^2 + c_2 y_1 y_2 + c_3 y_2^2\,, \tag{4.154}$$

where the c_i's are integration constants. In contrast to the third-order differential equation the solutions to the second-order differential equation (4.153) are readily found and are given by

$$y_1(x) = \sqrt{x}K(x^2)\,, \quad y_2(x) = \sqrt{x}K(1-x^2)\,. \tag{4.155}$$

where K is the complete elliptic function of the first kind,

$$K(k) = \int_0^1 \frac{\mathrm{d}t}{\sqrt{(1-t^2)(1-k^2t^2)}}\,. \tag{4.156}$$

By virtue of the relation between the second-order and third-order solutions (4.154), the solution for the scalar function $f_{\mathrm{KI},1}$ is therefore

$$f_1^{\mathrm{KI}}(x) = x\left[c_1 K(x^2)^2 + c_2 K(x^2)K(1-x^2) + c_3 K(1-x^2)^2\right]. \tag{4.157}$$

By explicitly imposing the boundary condition at $x = 1$, i.e. the static limit, we find

$$f_1^{\mathrm{KI}}(x) = \pi^4 x\epsilon^3 K\left(1-x^2\right)^2. \tag{4.158}$$

The other functions are readily obtained by taking derivatives. We can use identities for elliptic functions to clean this expressions up, also writing them in terms

[28] This method is originally due to Apell and a similar case is discussed in Ref. [209].

(1) (2)

Figure 4.12.: Topologies that contain elliptic integrals. The topologies are related by permutations of the vertices on the bottom. We do not show the u-channel flip of Figure (1) which also contains elliptic integrals.

of the y-variable

$$f_1^{\text{KI}} = \frac{8}{y+1} K^2\left(\tfrac{y-1}{y+1}\right), \tag{4.159}$$

$$f_2^{\text{KI}} = -\frac{2}{y-1}\left[E\left(\tfrac{y-1}{y+1}\right) - K\left(\tfrac{y-1}{y+1}\right)\right]^2, \tag{4.160}$$

$$\begin{aligned} f_3^{\text{KI}} = {} & \frac{(7y^2+6y+3)}{4(y-1)^2(y+1)} K^2\left(\tfrac{y-1}{y+1}\right) - \frac{(y^3+39y^2+15y+9)}{8(y-1)^2(y+1)} K\left(\tfrac{y-1}{y+1}\right) E\left(\tfrac{y-1}{y+1}\right) \\ & + \frac{(y^4+54y^2+9)}{16(y-1)^2(y+1)} E\left(\tfrac{y-1}{y+1}\right)^2. \end{aligned} \tag{4.161}$$

In these expressions E is the elliptic integral of the second kind

$$E(k) = \int_0^1 \mathrm{d}t \frac{\sqrt{1-k^2t^2}}{\sqrt{1-t^2}}. \tag{4.162}$$

The form (4.159)–(4.161) has the added benefit that it is manifestly analytic at $y = 1$, so continuation below threshold (the bound case,$-1 < y < 1$) is straightforward. The higher orders in the expansion can be expressed in terms of elliptic polylogarithms. In practice, we find that only the complete elliptic integrals of first and second kind contribute to the final result. This is in agreement with a naive counting of the maximal transcendental weight of the result. The final result only contains functions up to weight two (multiplied by factors of π). Assigning weight 1 to the elliptic integrals, which is natural because of $K(0) = E(0) = \pi/2$, the leading order already fully saturates this bound. It will be interesting to see if genuine elliptic polylogarithms[29] enter the result at the next order in the PM expansion or once radiative effects are considered.

[29] See Ref. [210] for a definition and discussion of this class of functions.

5. Four-Graviton Amplitudes

The computation of amplitudes in gravity has a long history. It has been known since the seventies that the theory obtained by naive quantization of the Einstein-Hilbert action is not perturbatively renormalizable off-shell [211]. By explicit computations Goroff, Sagnotti and Van de Ven showed that the divergences also persist on-shell if one considers the second order in perturbation theory and thus Einstein gravity is not perturbatively renormalizable [212–214]. Since then, UV properties of amplitudes in Einstein gravity [215, 216] and its supersymmetric extensions [37, 217] have been a frequent object of study. Results for amplitudes have been mostly obtained in supersymmetric theories [218–225]. In pure Einstein gravity on the other hand only the one-loop amplitudes have been computed completely [219, 226]. The polylogarithmic part of the two-loop all-plus amplitude has been computed in Ref. [227].

Our aim is to complete these loop computations in GR by computing the complete set of two-loop four-point amplitudes. Besides the historic significance we find the study of these objects interesting for a variety of reasons.

First, at the time of the computation there was an ongoing debate on the high-energy limit of gravitational amplitudes. In particular the scattering angle in pure GR at $\mathcal{O}(G^3)$ has been computed in a landmark paper by Amati, Ciafaloni and Veneziano [228] has been questioned by Damour who guessed the structure of the angle based on heuristic principles [229].

As another motivation, we can view the computation as a testcase to sharpen our tools used in the numerical unitarity method. By solving a particularly complicated problem we make a strong case for the application of the numerical unitarity framework for the computations of amplitudes in general relativity. This points the way towards more general applications which can be used for the extraction of classical observables. As the study of amplitudes in Einstein gravity fuses many different aspects, starting from the effective field theory setup, to non-planar integrals and high-rank tensor integrals, we will also find that these improvements directly feed back to applications in collider phenomenology, for example to the study of the Higgs effective field theory obtained by integrating out the top-quark contributions.

5.1. General Relativity as a Low-Energy Effective Field Theory

Even tough general relativity is not perturbatively renormalizable [211–214], predictions can be made based on a low-energy effective field theory (EFT) [230]. The Lagrangian $\mathcal{L}$ for the relevant EFT is

$$\mathcal{L} = \mathcal{L}_{\text{EH}} + \mathcal{L}_{\text{GB}} + \mathcal{L}_{\text{R}^3} + \dots, \tag{5.1}$$

In this expression the ellipsis includes higher-order operators which have four more curvature tensors and are at least of order G^4 when expanding around flat space. The three relevant terms are the Einstein-Hilbert Lagrangian (2.19), formulated in D-dimensions as well as the Gauss-Bonnet (GB) and the Goroff-Sagnotti (GS) counter-terms [212, 213, 231, 232],

$$\mathcal{L}_{\text{GB}} = \frac{\mathcal{C}_{\text{GB}}}{(4\pi)^2}\sqrt{-g}(R^2 - R_{\mu\nu}R^{\mu\nu} + R_{\mu\nu\rho\sigma}R^{\mu\nu\rho\sigma}), \tag{5.2}$$

$$\mathcal{L}_{\text{R}^3} = \frac{\mathcal{C}_{\text{R}^3}}{(4\pi)^4}\left(\frac{\kappa}{2}\right)^2\sqrt{-g}R_{\alpha\beta}{}^{\mu\nu}R_{\mu\nu}{}^{\rho\sigma}R_{\rho\sigma}{}^{\alpha\beta}\,. \tag{5.3}$$

All other possible operators with at most six derivatives (third order in curvature) have been removed by partial integration field redefinitions or identities Riemann tensors. The coupling κ is related to Newton's constant G, $\kappa\mu^{-\epsilon} = \sqrt{32\pi G}$. The divergent parts of the Wilson coefficients $\mathcal{C}$ can be fixed by lower-order computations [212, 213, 215] and are explicitly given by

$$\mathcal{C}_{\text{GB}} = \left[\frac{53}{90}\frac{1}{\epsilon} + c_{\text{GB}}(\mu)\right]\bar{\mu}^{-2\epsilon}\,, \quad \mathcal{C}_{\text{R}^3} = \left[\frac{209}{1440}\frac{1}{\epsilon} + c_{\text{R}^3}(\mu)\right]\bar{\mu}^{-4\epsilon}\,, \tag{5.4}$$

where $c_{\text{GB}}(\mu)$ and $c_{\text{R}^3}(\mu)$ represent renormalized couplings.

Perturbation theory is defined in terms of a linear split $g_{\mu\nu} = \eta_{\mu\nu} + \kappa h_{\mu\nu}$ as an expansion in powers of κ or equivalently in terms of Newton's constant. We define the perturbative expansion of the helicity amplitudes through

$$M_{\underline{h}} = \left(\frac{\kappa}{2}\right)^2\mathcal{N}_{\underline{h}}\sum_{j=0}^{\infty}\left(\frac{\bar{\kappa}}{2}\right)^{2j}\mathcal{M}_{\underline{h}}^{(j)}\,, \tag{5.5}$$

with $\bar{\kappa} = \kappa\mu^{-\epsilon}/(4\pi)$. The set $\underline{h}$ specifies the helicities of the external gravitons. It is sufficient to compute the amplitudes with $\underline{h} = \{\pm,+,+,+\}$ and $\{-,-,+,+\}$ since all others configurations are related by bosonic symmetry or parity conjugation which is obtained through complex conjugation. The normalizations $\mathcal{N}$ are pure phases absorbing the phases of the amplitudes, such that the $\mathcal{M}_{\underline{h}}^{(j)}$'s are Lorentz-invariant functions. They are explicitly given by the following expressions

in terms of spinor-helicity notation (see e.g. Ref. [233])

$$\mathcal{N}_{++++} = \mathrm{i}\left(\frac{[12][34]}{\langle 12\rangle\langle 34\rangle}\right)^2 = \mathrm{i}\left(\frac{st}{\langle 12\rangle\langle 23\rangle\langle 34\rangle\langle 41\rangle}\right)^2, \tag{5.6}$$

$$\mathcal{N}_{-+++} = \mathrm{i}\left(\frac{\langle 12\rangle}{[12]}\frac{[23]}{\langle 23\rangle}\frac{[24]}{\langle 24\rangle}\right)^2 = \mathrm{i}\left(\frac{st}{u}\frac{[24]^2}{[12]\langle 23\rangle\langle 34\rangle[41]}\right)^2, \tag{5.7}$$

$$\mathcal{N}_{--++} = \mathrm{i}\left(\frac{\langle 12\rangle}{[12]}\frac{[34]}{\langle 34\rangle}\right)^2. \tag{5.8}$$

Although not manifest, all weights have the corresponding symmetry of the amplitudes that are required by bose symmetry, e.g. $\mathcal{N}_{-+++}$ is invariant under permutations of $2, 3, 4$. This entails that the normalized amplitudes $\mathcal{M}_{\underline{h}}^{(j)}$ retain the symmetry of the amplitudes. Since the different Lagrangians have different orders in the coupling a fixed-order computation involves the computation of lower-order diagrams with counter-term insertions. Schematically the amplitudes up to NNLO in the gravitational coupling receive contributions of the form

$\mathcal{M}_{\underline{h}}^{(0)} \sim$  $+\ldots$, $\mathcal{M}_{\underline{h}}^{(1)} \sim$  $+\ldots$,

$\mathcal{M}_{\underline{h}}^{(2)} \sim$ 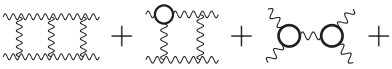 $+\ldots$. (5.9)

In this expression, the white ovals correspond to insertion of a vertex computed from $\mathcal{L}_{\mathrm{GB}}$, while gray ovals represent insertions of a $\mathcal{L}_{\mathrm{R}^3}$ vertex. All other vertices and propagators are computed using the Einstein-Hilbert action. Since the Gauss-bonnet operator vanishes in $D = 4$ dimensions the contribution from a single insertion in a tree is absent and the counter-terms first contribute at order κ^6. The counter-terms by construction remove the UV divergences from the theory, but the resulting expressions still contain IR divergences. The IR structure of graviton amplitudes are well understood [234–237], and the divergences do exponentiate, leading to the definition of a finite function $\mathcal{F}_{\underline{h}}^{(j)}(\epsilon)$ through

$$M_{\underline{h}} = \left(\frac{\kappa}{2}\right)^2 \mathcal{N}_{\underline{h}} \exp\left[\left(\frac{\bar{\kappa}}{2}\right)^2 \mathcal{S}\right] \sum_{j=0}^{\infty}\left(\frac{\bar{\kappa}}{2}\right)^{2j} \mathcal{F}_{\underline{h}}^{(j)}(\epsilon)\,,\,, \quad \mathcal{S} = \sum_{i<j}^{4} \frac{\mu^{2\epsilon}}{\epsilon^2}[-(p_i+p_j)^2]^{1-\epsilon}\,. \tag{5.10}$$

These functions then define remainder functions $\mathcal{R}_{\underline{h}}^{(i)} := \mathcal{F}_{\underline{h}}^{(i)}(0)$, which capture the new four-dimensional information at a given loop order. To be concrete, the two-loop remainder is

$$\mathcal{R}_{\underline{h}}^{(2)} = \mathcal{F}_{\underline{h}}^{(2)}(0) = \lim_{\epsilon\to 0}\left(\mathcal{M}_{\underline{h}}^{(2)} - \mathcal{S}\mathcal{M}_{\underline{h}}^{(1)} + \frac{\mathcal{S}^2}{2}\mathcal{M}_{\underline{h}}^{(0)}\right). \tag{5.11}$$

5.2. Tree-Level Recursion and Cubic Reformulation

The computation of tree-level amplitudes which are the fundamental building blocks for the unitarity method is obstructed by the presence of an infinite number of Feynman rules derived from the non-polynomial nature of the Einstein-Hilbert action (2.19). While for a fixed-order computation one could go ahead and implement the necessary rules up to the required order in the coupling this quickly becomes infeasible due to to the complexity of these terms [35]. In order to overcome this obstruction, we will follow the suggestion by Cheung and Remmen [238] and instead make use of a cubic reformulation of the theory[1]. This makes use of field redefinitions such that it is crucial that we are working in an on-shell setup in which does not depend on the choice of field variables.

We start by considering the Einstein-Hilbert Lagrangian, but with the connection as a dynamical field and using the "Gothic metric"

$$\mathfrak{g}^{\mu\nu} = \sqrt{-g}g^{\mu\nu} \tag{5.12}$$

instead of the usual metric. The resulting Palatini action [240] is given by

$$S_{\mathrm{P}}[\Gamma^{\lambda}_{\mu\nu}, \mathfrak{g}^{\mu\nu}] = \int \mathrm{d}^4x \mathcal{L}_{\mathrm{P}}\,, \quad \mathcal{L}_{\mathrm{P}} = -\frac{2}{\kappa^2}\mathfrak{g}^{\mu\nu}\left[\partial_\beta\Gamma^{\beta}_{\mu\nu} - \partial_\nu\Gamma^{\beta}_{\mu\beta} + \Gamma^{\beta}_{\alpha\beta}\Gamma^{\alpha}_{\mu\nu} - \Gamma^{\beta}_{\alpha\nu}\Gamma^{\alpha}_{\mu\beta}\right]. \tag{5.13}$$

The Palatini action has an additional 40 components associated to the dynamical connection $\Gamma^{\lambda}_{\mu\nu}$. However, it is well-known that the equation of motion enforces the Christoffel connection

$$\frac{\delta S_{\mathrm{P}}}{\delta\Gamma^{\lambda}_{\mu\nu}} = 0 \implies \Gamma^{\lambda}_{\mu\nu} = \frac{1}{2}g^{\lambda\alpha}\left[\partial_{(\mu}g_{\nu)\alpha} - \partial_\alpha g_{\mu\nu}\right], \tag{5.14}$$

where $(\mu\nu)$ denotes symmetrization with unit weight. The action in Eq. (5.13) is manifestly cubic in the fields, although it has a somewhat unusual kinetic term. We can diagonalize it by a field redefinition

$$\mathfrak{g}^{\mu\nu} \mapsto \eta^{\mu\nu} - h^{\mu\nu}\,, \tag{5.15}$$

$$\begin{aligned}\Gamma^{\lambda}_{\mu\nu} \mapsto A^{\lambda}_{\mu\nu} &+ \frac{1}{2}\eta^{\lambda\alpha}\left[\partial_{(\mu}h_{\nu)\alpha} - \partial_\alpha h_{\mu\nu} + \frac{1}{D-2}\eta_{\mu\nu}\partial_\alpha h\right] \\ &+ \left[\frac{1}{1-D}\delta^{\lambda}_{(\mu}A^{\alpha}_{\nu)\alpha} - \frac{1}{2(D-2)}\delta^{\lambda}_{(\mu}\partial_{\nu)}h\right],\end{aligned} \tag{5.16}$$

where $h = \eta^{\mu\nu}h_{\mu\nu}$ is the trace. For the remainder of this section we will raise and lower indices with the flat metric $\eta_{\mu\nu}$. In addition we supplement a harmonic gauge fixing term, which in terms of the new variables takes the form

$$\mathcal{L}_{\mathrm{GF}} = -\frac{1}{2}(\partial_\lambda h^{\lambda}_{\mu})(\partial_\rho h^{\rho\mu})\,. \tag{5.17}$$

[1] comments in that direction have also been made by Deser [239]

The total gauge fixed action is then given by [238]

$$\mathcal{L}_{\rm CR} = \mathcal{L}_{AA} + \mathcal{L}_{hh} + \mathcal{L}_{hhh} + \mathcal{L}_{hhA} + \mathcal{L}_{hAA}\,. \tag{5.18}$$

The terms quadratic in the fields are

$$\mathcal{L}_{hh} = \frac{1}{4}\left(h_{\mu\nu}\Box h^{\mu\nu} - \frac{1}{D-2}h\Box h\right), \tag{5.19}$$

$$\mathcal{L}_{AA} = -\eta^{\mu\nu}\left(A^{\alpha}_{\beta\mu}A^{\beta}_{\alpha\nu} - \frac{1}{D-1}A^{\alpha}_{\alpha\mu}A^{\beta}_{\beta\nu}\right). \tag{5.20}$$

Notice that $\mathcal{L}_{AA}$ is free of derivatives, and therefore the A field is not propagating, in agreement with the fact that the field is auxiliary. The interactions between the two fields are purely cubic and given by

$$\mathcal{L}_{hhh} = \frac{1}{4}h^{\alpha\beta}\left[\partial_\alpha h_{\mu\nu}\partial_\beta h^{\mu\nu} + 2\partial_{[\mu}h_{\nu]\beta}\partial^\nu h_\alpha{}^\mu + \frac{1}{D-2}(2\partial_\mu h_{\alpha\beta}\partial^\mu h - \partial_\alpha h\partial_\beta h)\right], \tag{5.21}$$

$$\mathcal{L}_{hhA} = h^{\alpha\beta}\left[A^{\mu}_{\alpha\nu}(\partial^\nu h_{\beta\mu} - \partial_{(\beta}h_{\mu)}{}^{\nu}) - \frac{1}{D-2}(\eta_{\alpha\nu}A^{\nu}_{\beta\mu}\partial^\mu h - A^{\mu}_{\mu\alpha}\partial_\beta h)\right], \tag{5.22}$$

$$\mathcal{L}_{hAA} = h^{\alpha\beta}\left(A^{\mu}_{\alpha\nu}A^{\nu}_{\beta\mu} - \frac{1}{D-1}A^{\mu}_{\mu\alpha}A^{\nu}_{\nu\beta}\right), \tag{5.23}$$

where $[\mu\nu]$ denotes antisymmetrization with unit weight. Given the cubic nature, the reformulated theory (5.18) is well-suited for the computation of tree-level amplitudes using Berends-Giele (BG) recursion [241]. We have implemented this recursion into the `Caravel` framework [130] allowing for the extraction of arbitrary-multiplicity tree-level graviton amplitudes in D-dimensions[2].

As a check of the implementation, we have numerically computed tree-amplitudes up to six points and compared against analytic results obtained from gauge theory amplitudes [243] through Kawai-Lewellen-Tye (KLT) relations [244].

Since at the linearized level the field redefinition for the graviton field only amounts to a shift of the trace, the polarization states can be chosen identically to the original theory.

While it seems feasible to modify the cubic reformulation to include counter-terms, we refrain from doing so as the problem is simpler than the two-loop computation and therefore a optimization is not pressing. Instead, we use the original form of the Lagrangian and the Feynman rules extracted using the program `xAct` [245–247]. They are very complicated and we do not find it illuminating to print them here.

[2]Our choice of the BG recursion over on-shell recursions like the Britto-Cachazo-Feng-Witten (BCFW) recursion [117, 118] is mostly rooted in the fact that we want to stay as close as possible to previous computations using the `Caravel` framework. It should be noted that even analytic results might be outperformed by a BG recursion [242], although the situation might be significantly different in the context of gravity and would require a further study.

5.3. Master-Surface Decomposition

For the amplitude we use a decomposition into master and surface terms as described in section 3.1. The relevant topologies are depicted in Figure 5.1. A main challenge here is the high power counting which requires large ansatze for the numerator of the individual typologies. For the top-level diagrams we assume that the total power of the loop momentum is bound by twice the number of graviton vertices and the same bound is also applied loop-by-loop. For the lower-levels we have to take into account that they receive contributions from diagrams higher in the hierarchy, since $2\ell \cdot p = \ell^2 - (\ell + p)^2 - p^2$ we find that in the worst case the power counting is only reduced by one per level, where one would naively expect a decrease by two. For amplitudes with counter-terms this power counting is even higher: a GB insertion increases the naive power counting bound by two and a R^3 insertion increases it by four powers of the loop momentum.

In practice this means that we have to solve relatively large linear systems of up to the order of 3000 by 3000 for the lowest topologies in the hierarchy. In terms of computation time, we find solving the linear systems to be comparable to the evaluation of the trees by BG recursion.

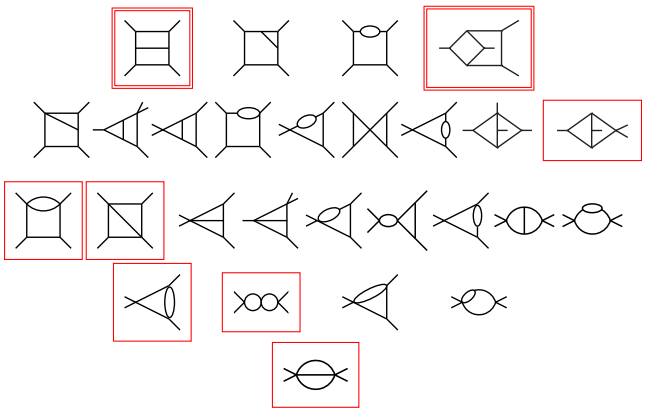

Figure 5.1.: Topologically inequivalent propagator structures for massless 2-to-2 scattering. Topologies with master integrals are framed red, a double frame means that the corresponding topology has two master integrals.

5.4. Function Space and Analytic Reconstruction

From `Caravel` we can efficiently obtain numerical results for the amplitudes' coefficients of the individual master integrals in the massless process for given values of the external kinematics parametrized by s, t, as well as the dimension parameters D and D_s. Since the dependence on those parameters is rational we can find the analytic form of these coefficients by multivariate rational reconstruction [132]. For the internal state dimension D_s we can use that since the Lagrangian has no explicit D-dependence, poles can only be produced by the graviton propagator.

This also implies that there will be at most a single pole in $(D_s - 2)$ per loop which we can use to simplify the reconstruction.

In order to avoid issues due to numerical instability, which are particularly pressing for the case at hand because of the large linear systems we choose to perform the computation in a prime field of cardinality of order 2^{31}. This approach has been pioneered in the context of collider phenomenology in Refs. [132, 248] and has since then become a standard tool.

Since we are interested mainly in the amplitudes in $D = 4-2\epsilon$ it is advantageous to directly consider the remainder function in the 't Hooft-Veltman (HV) scheme, setting $D_s = D$. Since the master integrals are known [249–252] the explicit knowledge of the function space allows us to write

$$\mathcal{R}^{(2)}_{\underline{h}}(s,t) = \sum_{r\in B} d_r(s,t)\, r(s,t)\,. \tag{5.24}$$

Where, to be concrete the set B contains products of functions from the set (assuming s-channel kinematics)

$$\begin{aligned}\{&1, \mathrm{i}\pi, \zeta_3, \log(s), \log(-t), \log(-u), \mathrm{Li}_2(-t/s),\\ &\mathrm{Li}_3(-t/s), \mathrm{Li}_3(-u/s), \mathrm{Li}_4(-t/s), \mathrm{Li}_4(-t/u), \mathrm{Li}_4(-u/s)\}\end{aligned} \tag{5.25}$$

such that the transcendental weight is lower than four. The functions in the set are chosen such that they satisfy no functional relations among them. It is then much more efficient to reconstruct the coefficients d_r instead of the coefficients of the master integrals [253–256].

The analysis can be simplified by noting that the amplitude is a homogeneous function of the invariants. Therefore the remainder can be written as a function of a single dimensionless ratio $x = t/s$,

$$\mathcal{R}^{(2)}_{\underline{h}}(s,t) = s^3 \mathcal{R}^{(2)}_{\underline{h}}(1,x)\,. \tag{5.26}$$

This means that we can perform a univariate Thiele reconstruction [257] to determine the coefficient functions d_i. We find that this process requires around 20 numerical samples for each helicity configuration.

Finally we have to lift the result from the finite field. For this we use the Chinese remainder theorem and rational reconstruction techniques [258]. We find that the computation in two finite fields is enough to lift the result to the rational numbers. A third finite-field evaluation is used as a check.

5.5. One-Loop Amplitudes

The complete set of one-loop amplitudes have been first computed in Ref. [219]. We have recomputed these amplitudes using the numerical unitarity setup also

including terms up to $\mathcal{O}(\epsilon)$, which are needed for the IR subtraction of the two-loop amplitudes.

The all-plus amplitudes up to 6-point have first been computed in Ref. [220], the single-minus case has been computed in Ref. [226] and the maximally helicity violating (MHV) amplitudes in Ref. [219]. The four-point one-loop amplitudes are

$$\mathcal{R}^{(1)}_{++++} = -\frac{2\pi^2}{15}(s^2+t^2+u^2)\,, \tag{5.27}$$

$$\mathcal{R}^{(1)}_{-+++} = \frac{2\pi^2}{45}(s^2+t^2+u^2)\,, \tag{5.28}$$

$$\begin{aligned}\mathcal{R}^{(1)}_{--++} = \frac{s^2}{z}\Bigg\{&\left(-z^4+8z^3-10z^2+4z-\frac{3}{4}\right)[\log^2(t/u)+\pi^2]+\frac{1}{4}\log^2 z\\ &+\left(-z^3+\frac{47z^2}{6}-\frac{87z}{10}-\frac{1}{2}\log z\right)\frac{u-t}{s}\log(t/u)\\ &+\frac{3\pi^2}{4}+z^3-\frac{95z^2}{12}+\frac{841z}{90}\Bigg\}\,,\end{aligned} \tag{5.29}$$

where $z = tu/s^2$. These expressions are written assuming that $s,t,u<0$, which is of course inconsistent with the constraint $s+t+u=0$. However, in this fictitious region all imaginary parts are conveniently absorbed into the logarithms (which is due to the fact that each individual integral has an Euclidean region). The analytic continuation to any channel is performed by setting e.g. $\log(-s)\to\log(s)-\mathrm{i}\pi$. In all cases we find agreement with the available literature [219, 220, 226] and agree with an independent unpublished computation [259]. It has to be mentioned that the result in Ref. [219] contains an incorrect sign for the $\mathcal{N}=1$ contribution in the supersymmetric decomposition, which is simple to account for.

5.6. Counter-Term Amplitudes

For the counter-term contributions we need to evaluate tree and one-loop amplitudes with one or two vertices derived from the GB or GS counter-term. These terms come with couplings with two and four additional powers of the coupling, such that for the $\mathcal{O}(\kappa^6)$ we need to evaluate a tree amplitude with as single GS insertion and two GB insertions, while we only need the one-loop amplitude with a single GB insertion. The tree-level amplitudes are essentially trivial with the only complexity being the involved Feynman rules. We derived these rules form the Lagrangians in Eqs. (5.2) and (5.3) using Feynman rules derived using `xAct` and implemented into `Caravel`. The results for the counter-term insertions into

tree amplitudes are simple even though the Feynman rules are very involved,

$$\mathcal{M}^{\text{tree,GB}^2}_{++++} = 24stu\epsilon(1+\epsilon)\mathcal{C}_{\text{GB}} \tag{5.30}$$

$$\mathcal{M}^{\text{tree,GB}^2}_{-+++} = 0\,, \tag{5.31}$$

$$\mathcal{M}^{\text{tree,GB}^2}_{--++} = 8s^3\epsilon(1+\epsilon)\mathcal{C}_{\text{GB}}\,, \tag{5.32}$$

$$\mathcal{M}^{\text{tree,R}^3}_{++++} = -60stu\mathcal{C}_{\text{R}^3} \tag{5.33}$$

$$\mathcal{M}^{\text{tree,R}^3}_{-+++} = -6stu\mathcal{C}_{\text{R}^3}\,, \tag{5.34}$$

$$\mathcal{M}^{\text{tree,R}^3}_{--++} = 0\,. \tag{5.35}$$

For the loop amplitude with a GB insertion we have

$$\mathcal{M}^{1-\text{loop,GB}}_{++++} = -\frac{2(56\epsilon+65)}{225}\mathcal{C}_{\text{GB}}\big[(-s)^{3-\epsilon}+(-t)^{3-\epsilon}+(-u)^{3-\epsilon}\big]\,, \tag{5.36}$$

$$\begin{aligned}\mathcal{M}^{1-\text{loop,GB}}_{-+++} = \frac{3stu}{15}\mathcal{C}_{\text{GB}}\Bigg[5+\epsilon\Bigg\{&\frac{24z^3+73z^2+72z-24}{6z^2}\\ &+\frac{-15z^3+94z^2-108z+24}{z^3}\log(-s)\\ &+\frac{45z^3-115z^2+72z-12}{z^4}\big(\log^2(-s)+\pi^2\big)\\ &-2z(7-12z)\left(\log(-t)\log(-u)+\frac{\pi^2}{2}\right)\Bigg\}\Bigg)+\text{cyclic }(s,t,u)\Bigg]\,,\end{aligned} \tag{5.37}$$

$$\begin{aligned}\mathcal{M}^{1-\text{loop,GB}}_{--++} = \frac{2s^3}{15z^3}\mathcal{C}_{\text{GB}}(-s)^{-\epsilon}\Bigg[&-\frac{212}{3}z^3+\epsilon\big\{4z^3\big(9z^2-20z+15\big)\big[\log^2(t/u)+\pi^2\big]\\ &-(6+19z)\log(z)+(15z^2-5z-3)\big(\log^2(t/s)+\log^2(u/s)+2\pi^2\big)\\ &-z^2\left(36z^2+\frac{3953}{30}z+6\right)+\big[z\big(36z^3-74z^2-31z-6\big)\\ &-\big(13z^2+11z+3\big)\log(z)\big]\frac{u-t}{s}\log(t/u)\Big\}\Bigg]\,.\end{aligned} \tag{5.38}$$

Where cyclic (s,t,u) instructs to sum over all cyclic permutations of s,t,u. All amplitudes are manifestly symmetric (totally symmetric for $\{+,+,+,+\}$ and $\{-,+,+,+\}$ t-u symmetric for $\{-,-,+,+\}$).

The values of the counter-term amplitudes have in part been computed previously. The GB tree-level and one-loop amplitudes for the $\{+,+,+,+\}$ and $\{-,-,+,+\}$ configuration have been computed in Ref. [259] and are in agreement with the results presented here. Tree amplitudes with a single R^3 insertion have been presented in Refs. [215, 227] and here as well we find full agreement.

5.7. Two-Loop Amplitudes

Finally we turn our attention to the two-loop amplitudes. Combining the one-loop amplitudes with the counter-term amplitudes in Eqs. (5.30)–(5.38) we can

extract the remainder function at two-loop order. The single-minus and MHV amplitudes are to long to present here, but are available as an ancillary file to Ref. [260]. The all-plus remainder however neatly fits in a few lines:

$$\begin{aligned}\mathcal{R}^{(2)}_{++++} = stu\left[\frac{117617}{21600} + 30(c_{\mathrm{GB}} - 2c_{\mathrm{R}^3})\right] \\ + \frac{7}{60}(s^2+t^2+u^2)[s\log\left(-s/\bar{\mu}^2\right) + t\log\left(-t/\bar{\mu}^2\right) + u\log\left(-u/\bar{\mu}^2\right)] \\ + \frac{1}{36}(s^3+t^3+u^3)[\log\left(-s/\bar{\mu}^2\right) + \log\left(-t/\bar{\mu}^2\right) + \log\left(-u/\bar{\mu}^2\right)]\,. \quad (5.39)\end{aligned}$$

We note that the constant $\frac{117617}{21600}$ does not have a physical meaning and depends on the regularization scheme. The $\{+,+,+,+\}$ amplitude matches the results of Ref. [259] and is also consistent with Ref. [227]

6. From Amplitudes to Classical Observables

The S-matrix and consequently on-shell scattering amplitudes contain all the information of the classical scattering process. Unfortunately the translation from a quantum scattering amplitude to a classical observable presents a non-trivial task. The main reason for this is that the amplitude, as opposed to a cross section, is not an observable and therefore does not need to posses a well-defined classical limit. Instead we find that an amplitude will in general be singular as $\hbar \to 0$. A second problem is that the quantum amplitudes describe processes with an fixed and small number of exchanged quanta, while the classical physics is described by a large number of such quanta.

The first problem is addressed by targeting classical quantities (these are IR-save quantities in the language of collider physics), while the second is dealt with through a form of exponentiation, which we will discuss later. The approaches taken so far roughly split into three groups.

First, we can match the problem to an effective field theory and extract the effective two-body potential. This approach was pioneered by Neill and Rothstein [43] and subsequently expanded to a relativistic framework by Cheung, Rothstein and Solon [52]. We will discuss the matching to an EFT in section 6.1.

Second we can use the fact that the IR singularities in the $\hbar \to 0$ limit of the amplitudes are an artifact of the perturbative expansion. This divergences are cured by a suitable exponentiation of the amplitude to a phase. Through its avatars in form of partial-wave unitarity and the eikonal exponentiation this approach has a long tradition and was for example used by Amati, Ciafaloni and Veneziano to derive the deflection angle for scattering of massless states in GR up to order G^3 in Ref. [228]. A similar approach which also has many features of the EFT approach is the amplitude action relation we have found in Ref. [49]. We will discuss the strategy of exponentiation in section 6.2.

Finally a direct approach based on the S-matrix has been proposed by Kosower Maybee and O'Connell [46]. We will briefly review some details of this approach in section 6.4.

6.1. Matching With an Non-Relativistic Effective Field Theory

Effective field theories (EFT) are an useful tool to disentangle the relevant dynamical degrees of freedom (see e.g. Ref. [261]). The non-relativistic EFT[1] we consider here was first introduced by Cheung, Rothstein and Solon [52] as a generalization of the non-relativistic EFT in Ref. [43]. It can be considered as a top-down EFT obtained from the full theory of two massive scalars minimally coupled to Einstein gravity by integrating out the potential modes of the graviton and the negative-energy modes of the scalars. The resulting theory is conveniently formulated in the COM frame, where it takes the form

$$\begin{aligned}\mathcal{L} = &\sum_{i=1}^{2}\int_{\boldsymbol{k}}\phi_i^\dagger(-\boldsymbol{k})\left(\mathrm{i}\partial_t - \sqrt{\boldsymbol{k}^2+m_1^2}\right)\phi_i(\boldsymbol{k})\\ &-\int_{\boldsymbol{k},\boldsymbol{k}'}\phi_1^\dagger(\boldsymbol{k}')\phi_1(\boldsymbol{k})V(\boldsymbol{k},\boldsymbol{k}')\phi_2^\dagger(-\boldsymbol{k}')\phi_2(-\boldsymbol{k})\,,\end{aligned} \tag{6.1}$$

where we introduced the short-hand $\int_{\boldsymbol{k}_1\cdots\boldsymbol{k}_n} \coloneqq \int\prod_{i=1}^{n}\frac{\mathrm{d}^{D-1}\boldsymbol{k}_i}{(2\pi)^{D-1}}$. The form of the kinetic term manifests the absence of anti-particles but still includes an infinite number of relativistic corrections. The fact that the interaction is non-local is a direct consequence of the masslessness of the force carriers that have been integrated out. The interactions are however local in time (in fact they are instantaneous). The main motivation for using the EFT is that it provides a direct way to compute the two-body Hamiltonian, which is a quantity directly usable for phenomenological purposes (see e.g. Ref. [262]).

We make the following ansatz for the potential in position space motivated by the form of the Newtonian potential in $3-2\epsilon$ spatial dimensions:[2]

$$V(\boldsymbol{p},\boldsymbol{r}) = \int_{\boldsymbol{q}} e^{\mathrm{i}\boldsymbol{q}\cdot\boldsymbol{r}}V(\boldsymbol{p},\boldsymbol{p}-\boldsymbol{q}) = \sum_{n=1}^{\infty}c_n(\boldsymbol{p}^2)\frac{G^n(r^2\bar{\mu}^2e^{2\gamma_{\mathrm{E}}})^{n\epsilon}}{r^n}\,. \tag{6.2}$$

In momentum space the potential takes the form

$$V(\boldsymbol{p},\boldsymbol{p}-\boldsymbol{q}) = \frac{(4\pi)^{(D-1)/2}}{|\boldsymbol{q}|^{D-1}}\sum_{n=1}^{\infty}\left(\frac{G|\boldsymbol{q}|}{2}\right)^{n(1-2\epsilon)}\frac{\Gamma[(D-1-n(1-2\epsilon))/2]}{\Gamma(n(1-2\epsilon)/2)}(\bar{\mu}^2)^{n\epsilon}\,c_n\big(\boldsymbol{p}^2\big)\,. \tag{6.3}$$

[1] Notice that this EFT is not related to the various other EFT's relevant in the present context, for example the low-energy EFT discussed in section 5 and EFT's describing finite-size effects [28].

[2] In this form the potential we can match classical contributions $\mathcal{O}(\hbar^0)$, in order to match quantum corrections we would need additional terms with the same powers of G but higher powers of $1/r$.

If the coefficients are finite in dimensional regularization we can simply expand in $D = 4 - 2\epsilon$, dropping terms local in q^2:

$$V(\boldsymbol{p}, \boldsymbol{p} - \boldsymbol{q}) = \frac{4\pi G}{\boldsymbol{q}^2} c_1(\boldsymbol{p}^2) + \frac{2\pi^2 G^2}{|\boldsymbol{q}|} c_2(\boldsymbol{p}^2) - 2\pi G^3 \log \boldsymbol{q}^2 \, c_3(\boldsymbol{p}^2) + \dots \,.$$

However we will find divergent coefficients starting at three-loop order, so it will be important to consistently keep higher orders in the expansion in ϵ.

Since the degrees of freedom associated with the force carrier are integrated out this theory can (under exchange of G for an appropriate coupling) be used to match other theories like scalar quantum electrodynamics (SQED) or scalar-QCD. In the context of this thesis we will be interested exclusively in gravity. The EFT (6.1) has very simple Feynman rules

$$\underset{(k_0, \boldsymbol{k})}{\text{———}} = \frac{\mathrm{i}}{k_0 - \sqrt{\boldsymbol{k}^2 + m_i^2} + \mathrm{i}\varepsilon} \,, \qquad \underset{\begin{matrix} \boldsymbol{k} & \boldsymbol{k}' \\ -\boldsymbol{k} & -\boldsymbol{k}' \end{matrix}}{\times} = -\mathrm{i} V(\boldsymbol{k}, \boldsymbol{k}') \,. \tag{6.4}$$

For practical computations it is convenient to integrate bubble integrals, which yields an effective one-body propagator

$$\begin{aligned} \Delta(\boldsymbol{k}) &= \mathrm{i} \int \frac{\mathrm{d}k^0}{2\pi} \frac{1}{k_0 - \sqrt{\boldsymbol{k}^2 + m_1^2} + \mathrm{i}\varepsilon} \frac{1}{E - k_0 - \sqrt{\boldsymbol{k}^2 + m_2^2} + \mathrm{i}\varepsilon} \\ &= \frac{1}{E - \sqrt{\boldsymbol{k}^2 + m_1^2} - \sqrt{\boldsymbol{k}^2 + m_2^2} + \mathrm{i}\varepsilon} \,. \end{aligned} \tag{6.5}$$

The EFT (6.1) captures the complete potential dynamics. Radiative effects can be taken into account by including the degrees of freedom for the radiative gravitons. It is not to hard to convince oneself that the EFT approach is equivalent to the use of the Lippmann-Schwinger equation (see e.g. Refs. [263, 264])

$$\mathcal{M} = V + \int \frac{\mathrm{d}^3 \boldsymbol{k}}{(2\pi)^3} \frac{V(\boldsymbol{k}, \boldsymbol{p}) \mathcal{M}(\boldsymbol{k}, \boldsymbol{p}')}{E_{\boldsymbol{p}} - E_{\boldsymbol{k}} + \mathrm{i}\varepsilon} \,, \tag{6.6}$$

which upon repeated insertion can be seen to produce exactly the EFT amplitude.

To perform matching with the full theory we have to align the normalization by dividing the relativistic amplitude by the factor $4E_1E_2$ originating from the two-particle phase-space. The matching condition is therefore

$$\mathcal{M}^{\text{full}} = 4E_1E_2 \mathcal{M}^{\text{EFT}} \,. \tag{6.7}$$

Both the full theory and the EFT will produce IR-divergent contributions (amplitudes themselves are not observables and therefore do not need to be IR safe). We can expose the IR structure by expanding the EFT integrand around the poles[3]

$$Y = \boldsymbol{\ell}^2 + 2\boldsymbol{\ell} \cdot \boldsymbol{p} + \mathrm{i}\varepsilon \quad \text{or} \quad Z = 2\hat{\boldsymbol{z}} \cdot \boldsymbol{\ell} + \mathrm{i}\varepsilon \,. \tag{6.8}$$

[3]This is just an expansion-by-regions of the EFT amplitudes.

The two-body propagator has the following expansions

$$\Delta(\boldsymbol{p}+\boldsymbol{\ell}) = -\frac{2E\xi}{Y} - \frac{(1-3\xi)}{2E\xi} + \dots\,, \tag{6.9}$$

$$\Delta(\boldsymbol{p}+\boldsymbol{\ell}) = -\frac{2E\xi}{|\boldsymbol{p}|}\left(1+\frac{\boldsymbol{q}^2}{8\boldsymbol{p}^2}\right)\frac{1}{Z} - \frac{(1-3\xi)}{2E\xi} + \frac{2E\xi}{\boldsymbol{p}^2}\frac{1}{Z^2}(\boldsymbol{\ell}^2+\boldsymbol{\ell}\cdot\boldsymbol{q}) + \dots\,. \tag{6.10}$$

The first choice has been adopted in Refs. [48, 52], while the latter is more natural in the context of the relativistic integration method and therefore was used in Ref. [49].[4] The expansion in terms of Z poles has the disadvantage that the expansion produces higher orders in the pole, which can be treated by IBP reduction on the EFT side. In both cases we could in principle match in four-dimensions, since the IR divergences cancel exactly in the EFT and the full theory. This is what was done in Ref. [48]. For the Z poles it is more natural to formulate the EFT in D dimensions. This allows us to use IBP relations for the Z integrals reducing the integrals to a small number of scalar masters.

6.1.1. Effective Field Theory Amplitudes

In order to perform matching, we have to compute the amplitudes in the EFT. Given the simple Feynman rules it is straightforward to derive the following amplitudes up to order G^3 [48],

$$\mathcal{M}_1^{\text{EFT}} = -\frac{4\pi G c_1}{\boldsymbol{q}^2}\,, \tag{6.11}$$

$$\mathcal{M}_2^{\text{EFT}} = -\frac{2\pi^2 G^2 c_2}{|\boldsymbol{q}|} + \frac{\pi^2 G^2}{E\xi|\boldsymbol{q}|}\left[(1-3\xi)c_1^2 + 4\xi^2 E^2 c_1 c_1'\right] + \int_\ell \frac{32E\xi\pi^2 G^2 c_1^2}{\boldsymbol{\ell}^2(\boldsymbol{\ell}+\boldsymbol{q})^2(\boldsymbol{\ell}^2+2\boldsymbol{p}\cdot\boldsymbol{\ell})}\,, \tag{6.12}$$

$$\begin{aligned}\mathcal{M}_3^{\text{EFT}} = {}& 2\pi G^3 \log \boldsymbol{q}^2 c_3 - \frac{\pi G^3 \log \boldsymbol{q}^2}{E^2\xi}\Big[(1-4\xi)c_1^3 - 8\xi^3 E^4 c_1 {c_1'}^2 - 4\xi^3 E^4 c_1^2 c_1'' \\ & + 4\xi^2 E^3 c_2 c_1' + 4\xi^2 E^3 c_1 c_2' - 2(3-9\xi)\xi E^2 c_1^2 c_1' + 2E(1-3\xi)c_1 c_2\Big] \\ & + \int_\ell \frac{16\pi^3 G^3 c_1[2E\xi c_2 - (1-3\xi)c_1^2 - 4\xi^2 E^2 c_1 c_1']}{\boldsymbol{\ell}^2|\boldsymbol{\ell}+\boldsymbol{q}|(\boldsymbol{\ell}^2+2\boldsymbol{p}\cdot\boldsymbol{\ell})} \\ & - \int_{\ell_1,\ell_2} \frac{256E^2\xi^2\pi^3 G^3 c_1^3}{\boldsymbol{\ell}_1^2(\boldsymbol{\ell}_1+\boldsymbol{\ell}_2)^2(\boldsymbol{\ell}_2+\boldsymbol{q})^2(\boldsymbol{\ell}_1^2+2\boldsymbol{p}\cdot\boldsymbol{\ell}_1)(\boldsymbol{\ell}_2^2+2\boldsymbol{p}\cdot\boldsymbol{\ell}_2)}\,.\end{aligned} \tag{6.13}$$

The Feynman integrals in the EFT amplitudes (6.11)–(6.13) are IR-divergent. They are straightforward to evaluate in dimensional regularization. However, a more efficient procedure is to match them with the identical divergences in the full-theory amplitudes. As such we do not need to evaluate them and do not need to introduce a regularization scheme.

[4] Note that the Z poles already appeared in the boundary conditions of the potential master integrals, e.g. for the box integral in Eq. (4.119).

6.2. Exponentiation

The amplitudes with massless intermediate states will generally diverge for small momentum transfer. To give an example, the amplitude for scattering of two same-helicity gravitons is

$$\mathcal{M}^{(0)}_{--++} = \frac{s^3}{tu} \simeq \frac{s^2}{-t}\,, \tag{6.14}$$

which explicitly features a pole for small momentum transfer t. This means that when the amplitudes are considered perturbatively, i.e. at a fixed order in G, unitary is violated for small angles. This is an artifact of the expansion and in order to restore unitarity, this contributions have to exponentiate.[5]

Since its purpose is to restore unitary, exponentiation must be a direct consequence of unitarity relation (3.5), which adapted to the case at hand reads

$$\begin{aligned} 2\,\mathrm{Im}\,\mathcal{M}(p_1,p_2,p_3,p_4) &= \int \mathrm{d}\Phi_2(\ell_1,\ell_2)\mathcal{M}(p_1,p_2,\ell_1,\ell_2)\mathcal{M}(\ell_1,\ell_2,p_3,p_4) \\ &+ \sum_X \int \mathrm{d}\Phi_{2+|X|}(\ell_1,\ell_2,\ell_X)\mathcal{M}(p_1,p_2,\ell_1,\ell_2,\ell_X)\mathcal{M}(\ell_1,\ell_2,p_3,p_4,\ell_X)\,. \end{aligned} \tag{6.15}$$

The sum includes all intermediate multi-particle massless states X and an appropriate phase-space integration.[6]

The right-hand side involves a phase space integral, and it is natural to perform a transformation to impact-parameter space or partial-wave space, where this convolution is trivialized. The first approach leads to the so-called eikonal approximation, while the latter is simply referred to as partial-wave exponentiation. On the other hand exponentiation in momentum space is less convenient and the corresponding exponential is the exponentiation of an operator which leads to iterated convolutions, instead of multiplications. We have performed this exercise in Ref. [149], but will not repeat it here.

Exponentiation is conceptually important as it can explain why an amplitude that is valid for small $q \sim \hbar$ can express classical physics with a macroscopic momentum transfer Δp^μ. The interaction is mediated by large numbers of soft exchanges, which in turn are fixed by the exponentiation. In principle the EFT discussed in the previous section can be considered along the same lines, as after matching the theory predicts processes with an arbitrary amount of potential interactions.

[5] This is the usual problem of limits that one encounters when expanding say $e^{-\alpha/x}$ in α.

[6] In principle we also need to add massive intermediate states. However, this corresponds to black hole pair creation which is not relevant in the context of this thesis.

6.2.1. Exponentiation in Partial-Wave Space

Instead of working in impact parameter space we can expand the amplitude in terms of partial waves[7]

$$\mathcal{M}(s,t) = \left(\frac{\boldsymbol{p}^2}{4\pi\mu^2}\right)^{\epsilon} \frac{\sqrt{s}}{2|\boldsymbol{p}|} 16\pi\Gamma(1-\epsilon) \sum_{J=0}^{\infty} \frac{1}{N_J^{(\epsilon)}} a_J P_J^{(\epsilon)}(x)\,, \quad x = 1 + \frac{t}{2\boldsymbol{p}^2}\,. \tag{6.16}$$

The polynomials $P_J^{(\epsilon)}(x)$ are D-dimensional generalizations of the Legendre polynomials and $N_J^{(\epsilon)} = 2/(2J+1) + \mathcal{O}(\epsilon)$ is an normalization factor. Further details are given in appendix B.2. The expansion coefficients are given by

$$a_J(\boldsymbol{p}^2) = \frac{(4\pi/\boldsymbol{p}^2)^{\epsilon}}{\Gamma(1-\epsilon)} \frac{2|\boldsymbol{p}|}{\sqrt{s}} \int_{-1}^{1} \mathrm{d}x\, (1-x^2)^{-\epsilon} P_J^{(\epsilon)}(x) \frac{\mathcal{M}(s,t(x))}{16\pi}\,, \quad t(x) = 4\boldsymbol{p}^2\left(\frac{x-1}{2}\right). \tag{6.17}$$

The partial-wave transformation has the useful property that it trivializes phase space-integrals which applied to the unitarity relation for a system with no internal degrees of freedom, gives

$$2\,\mathrm{Im}\, a_J(\boldsymbol{p}^2) = \left|a_J(\boldsymbol{p}^2)\right|^2 + \mathcal{P}[n > 2\text{-particle cuts}]\,. \tag{6.18}$$

The cuts are irrelevant to the conservative problem and therefore in that case we find

$$a_J(\boldsymbol{p}^2) = -\mathrm{i}(e^{2\mathrm{i}\delta_J(\boldsymbol{p}^2)} - 1) \tag{6.19}$$

for some real δ_J. In other words, the S-matrix is a pure phase, which makes sense for a conservative process. We note that, in contrast to the eikonal exponentiation this statement needs no proof but is actually equivalent to elastic unitary. We can also try to match this including radiative effects, however, in this case the exponentiation is not guaranteed. Radiative effects can be incorporated by allowing for an imaginary part of δ_J or equivalently the introduction of an absoptive coefficients. Since the n-particle cuts give a positive contribution, unitary implies that

$$\mathrm{Im}\,\delta_J \geq 0\,. \tag{6.20}$$

The phase shifts can be directly obtained from the partial-wave amplitude a_J

$$\delta_J(\boldsymbol{p}^2) = -\frac{\mathrm{i}}{2}\ln\left[1 + \mathrm{i}\, a_J(\boldsymbol{p}^2)\right]. \tag{6.21}$$

Expanding the right hand side gives for the first few orders

$$\delta_J^{(0)}(\boldsymbol{p}^2) = \frac{1}{2} a_J^{(0)}(\boldsymbol{p}^2)\,, \tag{6.22}$$

$$\delta_J^{(1)}(\boldsymbol{p}^2) = \frac{1}{2} a_J^{(1)}(\boldsymbol{p}^2) - \frac{\mathrm{i}}{4}\left[a_J^{(0)}(\boldsymbol{p}^2)\right]^2, \tag{6.23}$$

$$\delta_J^{(2)}(\boldsymbol{p}^2) = \frac{1}{2} a_J^{(2)}(\boldsymbol{p}^2) - \frac{\mathrm{i}}{2} a_J^{(0)}(\boldsymbol{p}) a_J^{(1)}(\boldsymbol{p}) - \frac{1}{6}\left[a_J^{(0)}(\boldsymbol{p}^2)\right]^3. \tag{6.24}$$

[7] For a textbook treatment see Ref. [265]. For a discussion of the massless case in dimensional regularization see Ref. [266]. We give further details in appendix B.3.

Going back to momentum space, we have

$$\mathrm{i}\mathcal{M}(s,t) = \left(\frac{\boldsymbol{p}^2}{4\pi\mu^2}\right)^{\epsilon} \frac{\sqrt{s}}{2|\boldsymbol{p}|} 16\pi\Gamma(1-\epsilon) \sum_{J=0}^{\infty} \frac{1}{N_J^{(\epsilon)}} (e^{2\mathrm{i}\delta_J(\boldsymbol{p}^2)} - 1) P_J^{(\epsilon)}(x)\,, \quad x = 1 + \frac{t}{2\boldsymbol{p}^2}\,. \tag{6.25}$$

A simple stationary phase argument, the details of which are detailed in appendix B.4 leads to

$$\chi = -2\frac{\partial \operatorname{Re}\delta_J}{\partial J}\,. \tag{6.26}$$

6.3. The Amplitude-Action Relation

The phase shifts and the radial action can be viewed as thermodynamic potentials. At fixed energy E they give the angle by taking derivatives with respect to J. It is therefore natural to conjecture that the phase-shift and the radial action are the same object $2\delta_J(E) = I_r(J,E)$ at least to leading order in the classical expansion. A proof through WKB methods has been presented in Ref. [267]; further details will also be given elsewhere [268]. The amplitude-action relation found in Ref. [49] reads

$$\mathrm{i}\mathcal{M}(\boldsymbol{q}) = 4E|\boldsymbol{p}|\mu^{-2\epsilon} \int \mathrm{d}^{D-2}\boldsymbol{b}\, e^{\mathrm{i}\boldsymbol{b}\cdot\boldsymbol{q}} \left(e^{\mathrm{i}I_r(J)} - 1\right), \quad J = |\boldsymbol{p}||\boldsymbol{b}|\,. \tag{6.27}$$

Expanding the integrals we find Fourier transforms of powers, which can be turned into iterated convolutions, by the Fourier convolution theorem

$$\int \mathrm{d}^{D-2}\boldsymbol{b}\, e^{\mathrm{i}\boldsymbol{b}\cdot\boldsymbol{q}} \left[I_r(J)\right]^n = \int \prod_{i=1}^{n} \frac{\mathrm{d}^{D-2}\boldsymbol{\ell}_i}{(2\pi)^{D-2}} \widetilde{I}_r(\boldsymbol{\ell}_1)\cdots\widetilde{I}_r(\boldsymbol{\ell}_n) \widehat{\delta}^{(D-2)}\Big(\textstyle\sum_{j=1}^{n}\boldsymbol{\ell}_j - \boldsymbol{q}\Big) \tag{6.28}$$

We can use the Euclidean version of the symmetrization trick in Eq. (4.42) to lift the integral to a $D-1$ dimensional integral, with the additional dimension spanned by the unit vector $\hat{\boldsymbol{z}}$

$$\int \mathrm{d}^{D-2}\boldsymbol{b}\, e^{\mathrm{i}\boldsymbol{b}\cdot\boldsymbol{q}} \frac{[\mathrm{i}I_r(J)]^n}{n!} = \mathrm{i}\int_{\boldsymbol{\ell}} \frac{\tilde{I}_r(\boldsymbol{\ell}_1)\ldots\tilde{I}_r(\boldsymbol{\ell}_n)}{Z_1\ldots Z_{n-1}}\,, \tag{6.29}$$

where radial action depends only on the transversal part of $\boldsymbol{q}$ and the Z poles are

$$Z_j = -4E|\boldsymbol{p}|\left[(\boldsymbol{\ell}_1 + \boldsymbol{\ell}_2 + \cdots + \boldsymbol{\ell}_j)\cdot\hat{\boldsymbol{z}} + \mathrm{i}\varepsilon\right]. \tag{6.30}$$

Thereby the relation in Eq. (6.27) takes the following equivalent form

$$\mathcal{M}(\boldsymbol{q}) = 4E|\boldsymbol{p}|\mu^{-2\epsilon} \sum_{n=1}^{\infty} \frac{(-\mathrm{i})^n}{n!} \int_{\boldsymbol{\ell}} \frac{\tilde{I}_r(\boldsymbol{\ell}_1)\ldots\tilde{I}_r(\boldsymbol{\ell}_n)}{Z_1\ldots Z_{n-1}}\,. \tag{6.31}$$

The reason why we pressed the expression in this form is that the poles are identical to the one that appear when the amplitude is expanded in the potential region. As such we do not actually need to compute the integrals with Z poles, but

we can subtract them at the integrand level similar in spirit to the approach presented in Refs. [47, 48]. The amplitude-action relation is conveniently expanded in perturbation theory and matched order-by-order. For illustrative purposes, we list the first few relations arising from this

$$\mathcal{M}_1(\boldsymbol{q}) = \tilde{I}_{r,1}(\boldsymbol{q})\,, \tag{6.32}$$

$$\mathcal{M}_2(\boldsymbol{q}) = \tilde{I}_{r,2}(\boldsymbol{q}) + \int_{\boldsymbol{\ell}} \frac{\tilde{I}_{r,1}\tilde{I}_{r,1}}{Z_1}\,, \tag{6.33}$$

$$\mathcal{M}_3(\boldsymbol{q}) = \tilde{I}_{r,3}(\boldsymbol{q}) + \int_{\boldsymbol{\ell}} \frac{\tilde{I}^3_{r,1}}{Z_1 Z_2} + \int_{\boldsymbol{\ell}} \frac{\tilde{I}_{r,1}\tilde{I}_{r,2}}{Z_1}\,, \tag{6.34}$$

$$\mathcal{M}_4(\boldsymbol{q}) = \tilde{I}_{r,4}(\boldsymbol{q}) + \int_{\boldsymbol{\ell}} \frac{\tilde{I}^4_{r,1}}{Z_1 Z_2 Z_3} + \int_{\boldsymbol{\ell}} \frac{\tilde{I}^2_{r,1}\tilde{I}_{r,2}}{Z_1 Z_2} + \int_{\boldsymbol{\ell}} \frac{\tilde{I}_{r,1}\tilde{I}_{r,3}}{Z_1} + \int_{\boldsymbol{\ell}} \frac{\tilde{I}^2_{r,2}}{Z_1}\,. \tag{6.35}$$

In all above expressions the sum over permutations of distinct $\tilde{I}_{r,n}$ is implicit, for instance, $\tilde{I}_{r,1}\tilde{I}_{r,2} \equiv \tilde{I}_{r,1}(\boldsymbol{\ell}_1)\tilde{I}_{r,2}(\boldsymbol{\ell}_2) + \tilde{I}_{r,2}(\boldsymbol{\ell}_1)\tilde{I}_{r,1}(\boldsymbol{\ell}_2)$ while $\tilde{I}^3_{r,1} \equiv \tilde{I}_{r,1}(\boldsymbol{\ell}_1)\tilde{I}_{r,1}(\boldsymbol{\ell}_2)\tilde{I}_{r,1}(\boldsymbol{\ell}_3)$. In the expressions above we explicitly see that all integrals that have Z-poles are due to lower-loop iterations and can thus can be dropped freely when we are matching the $\tilde{I}_{r,i}$. The method described here fuses the advantages of relativistic approaches based on exponentiation with the benefits of the EFT approach as initially used by Refs. [47, 48, 52].

On the one hand it allows for cancellation of divergences at the integrand level, i.e. without the evaluation of the corresponding loop integrals. This also allows to discard contributions to the relativistic integrals. Since all super-classical contributions have been canceled we only need integrals with classical q scaling. In practice, this means that e.g. at three loops we do not need to compute any q-odd integral. On the other hand we are directly aligned with the method of differential equations adapted to the classical problem [149] and the amplitude computed in that way will be written in terms of the same IR poles and thus directly be amendable for the matching.

6.4. Direct Approach Through Observables

The problem with the scattering amplitude is that it by itself is not physical. By itself, the amplitude does not posses a well-defined classical limit and we have to use the schemes detailed in the previous chapters to extract the information about classical physics. In contrast, suitably defined physical observables need to have a well-defined classical limit.

Defining observables in gravity is typically a hard problem, but here we are interested in perturbation theory, i.e. on a flat background and the interaction vanishes at infinity. As such we can define observables through asymptotic data encoded in S-matrix elements. An observable O for a state ψ in a Hilbert-space is described by the expectation value of an Hermitian operator $\mathbb{O}$

$$O(\psi) = \langle\psi|\mathbb{O}|\psi\rangle\,. \tag{6.36}$$

For scattering processes which are defined in terms of asymptotic data it is natural to consider the change of an observable between the infinite past and future

$$\Delta O = O(\text{out}) - O(\text{in}) = \langle \text{out}|\mathbb{O}|\text{out}\rangle - \langle \text{in}|\mathbb{O}|\text{in}\rangle \,. \tag{6.37}$$

For the problem at hand the initial state $\langle$in is constructed from two-particle momentum eigenstates $|p_1, p_2\rangle$ with wavefunctions $\phi_i(p_i)$, which are well separated by an impact parameter b

$$|\text{in}\rangle = \int \mathrm{d}\Phi_2(p_1,p_2)\, \phi_1(p_1)\phi_2(p_2) e^{\mathrm{i}b\cdot p_1}\, |p_1,p_2\rangle \,. \tag{6.38}$$

The out state is determined by the S-matrix via $|\text{out}\rangle = S|\text{in}\rangle$. Inserting into the definition (6.37) and reorganizing terms into commutators, we find

$$\Delta O = \int \mathrm{d}\Phi_4(p_1,\cdots,p_4)\, \phi_1(p_1)\phi_2(p_2)\phi_2(p_3)^*\phi_1(p_4)^* e^{\mathrm{i}\,b\cdot q} \langle p_4,p_3|S^\dagger[\mathbb{O},S]|p_1,p_2\rangle \,, \tag{6.39}$$

where $q = p_1 + p_4$. In analogy to the amplitudes, it is natural separate a momentum-conservation delta function and to define a stripped kernel $\mathcal{I}_O$,

$$\widehat{\delta}^{(D)}\big(\textstyle\sum_{i=1}^4 p_i\big)\, \mathcal{I}_O \coloneqq -\mathrm{i}\, \langle p_4,p_3|S^\dagger[\mathbb{O},S]|p_1,p_2\rangle \,. \tag{6.40}$$

In order to make contact with amplitudes, we expand the S-matrix in terms of the transfer matrix $S = 1 + \mathrm{i}T$ and find

$$\mathcal{I}_O = \mathcal{I}_{O,\mathrm{v}} + \mathcal{I}_{O,\mathrm{r}} \,, \tag{6.41}$$

where, borrowing language from collider physics we have introduced a *virtual* kernel $\mathcal{I}_{O,\mathrm{v}}$ and a *real* kernel $\mathcal{I}_{O,\mathrm{r}}$,

$$\widehat{\delta}^{(D)}\big(\textstyle\sum_{i=1}^4 p_i\big)\mathcal{I}_{O,\mathrm{v}} \coloneqq \langle p_4,p_3|[\mathbb{O},T]|p_1,p_2\rangle \,, \tag{6.42}$$

$$\widehat{\delta}^{(D)}\big(\textstyle\sum_{i=1}^4 p_i\big)\mathcal{I}_{O,\mathrm{r}} \coloneqq -\mathrm{i}\, \langle p_4,p_3|T^\dagger[\mathbb{O},T]|p_1,p_2\rangle \,. \tag{6.43}$$

The virtual part can be directly related to measurement function $\Delta\mathbb{O}$ acting on the scattering amplitude $\mathcal{M}$,

$$\mathcal{I}_{O,\mathrm{v}} = \Delta\mathbb{O}\big[\mathcal{M}(p_1,p_2,p_3,p_4)\big] = \Delta\mathbb{O}\Bigg[$$

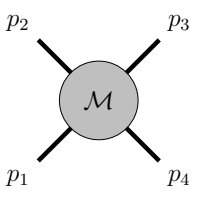

$$\Bigg] \,. \tag{6.44}$$

The real contribution can be related to amplitudes by inserting a complete stet of states

$$\langle p_4,p_3|T^\dagger[\mathbb{O},T]|p_1,p_2\rangle = \sum_X \int \mathrm{d}\Phi_{2+|X|}(r_1,r_2,X)\, \langle p_4,p_3|T^\dagger|r_1,r_2,X\rangle\langle r_1,r_2,X|[\mathbb{O},T]|p_1,p_2\rangle \,, \tag{6.45}$$

where the sum again runs over all massless intermediate (messenger) particles. Thereby the real kernel obtains the following pictorial representation

$$\begin{aligned}\mathcal{I}_{O,\mathrm{r}} = -\mathrm{i}\sum_X \int \mathrm{d}\Phi_{2+|X|}(r_1, r_2, \ell_X)\, \hat{\delta}^{(D)}(p_1+p_2+r_1+r_2+\ell_X) \\ \times \Delta\mathbb{O}\big[\mathcal{M}(p_1,p_2,r_2,r_1,\ell_X)\big]\, \mathcal{M}^*(-\ell_X,-r_1,-r_2,p_3,p_4)\end{aligned}$$

$$= -\mathrm{i}\sum_X \int \mathrm{d}\widetilde{\Phi}_{2+|X|}\ \Delta\mathbb{O}$$

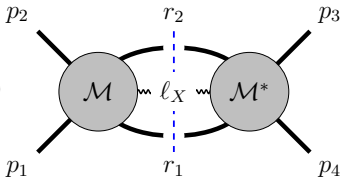

, (6.46)

in this, the measuring function acts on the amplitude to the left of the unitarity cut. The observable includes a dependence on the shape of the wave functions in momentum space. As argued in Ref. [46], in the classical limit the dependence on the form of the wave functions is insubstantial and the wave packets peak around their classical value. In the classical limit the observable takes a simple form [8]

$$\Delta O = \mathrm{i}\int \frac{\mathrm{d}^D q}{(2\pi)^D}\, \hat{\delta}(-2p_1\cdot q)\, \hat{\delta}(2p_2\cdot q) e^{\mathrm{i}b\cdot q}\, (\mathcal{I}_{O,\mathrm{v}} + \mathcal{I}_{O,\mathrm{r}})\,. \tag{6.47}$$

We can obtain two key observables, the impulse Δp_i^μ and the radiated momentum ΔR^μ, by considering the expectation values of the momentum $\mathbb{P}_i^\mu$ or the total messenger momentum $\mathbb{R}^\mu$

$$\Delta p_i^\mu = \langle \mathbb{P}_i^\mu \rangle \qquad \Delta R^\mu = \langle \mathbb{R}^\mu \rangle = -\sum_{i=1}^{2} \Delta p_i^\mu\,. \tag{6.48}$$

The radiated energy is given by

$$\Delta E = \Delta R^0 = -\Delta E_1 - \Delta E_2\,. \tag{6.49}$$

In the conservative case there is a single scattering angle

$$2\sin\chi/2 = \frac{\sqrt{-(\Delta p_1)^2}}{p_\infty} = \frac{\sqrt{-(\Delta p_2)^2}}{p_\infty}\,. \tag{6.50}$$

The definition of the scattering angle is less clear in the presence of radiation. The reason for this is that the radiative process should be thought of as a two-to-three process, which is parameterized by three energies $s_1, s_2, s_3 > 0$ and two t-channel invariants $t_1, t_2 < 0$ or alternatively three energies and two angles. These variables can be chosen as the initial COM energy $\sqrt{s}$, the two radiated energies ΔE_i and the two angles χ_i. To the leading order in G, which we are working here we can neglect recoil effects and therefore the single angle is still directly related to the

[8] In this expression we have expanded the argument of the delta function and dropped theta functions ensuring positive energy, which are trivial in the classical limit as the energies of the external particles are much larger than those of the virtual particles.

transversal impulse [9]

$$\sin\chi/2 = \frac{\sqrt{-(\Delta p_{1,\perp})^2}}{2|\boldsymbol{p}|}\,. \tag{6.51}$$

It will be convenient to decompose the impulse into transverse $\Delta p^\mu_\perp$ and longitudinal component $\Delta p^\mu_\parallel$

$$\Delta p^\mu = \Delta p^\mu_\perp + \Delta p^\mu_\parallel\,, \qquad u_i\cdot\Delta p_\perp = q\cdot\Delta p_\parallel = 0\,. \tag{6.52}$$

We define a basis of dual vectors by

$$\check{u}^\mu_1 = \frac{y u^\mu_2 - u^\mu_1}{y^2-1}, \quad \check{u}^\mu_2 = \frac{y u^\mu_1 - u^\mu_2}{y^2-1}, \qquad u_i\cdot\check{u}_j = \delta_{ij}\,, \quad \check{u}\cdot q = 0\,. \tag{6.53}$$

This allows the decomposition of a generic loop momentum[10]

$$\ell^\mu = \frac{\ell\cdot q}{q^2}q^\mu + (\ell\cdot u_1)\,\check{u}^\mu_1 + (\ell\cdot u_2)\,\check{u}^\mu_2\,. \tag{6.54}$$

Consequently the impulse kernel takes the form

$$\mathcal{I}^\mu_{\Delta p_1} = \mathcal{I}_\perp\, q^\mu + \sum_{i=1}^{2}\mathcal{I}_{u_i}\,\check{u}^\mu_i\,, \qquad \mathcal{I}_\perp \coloneqq \frac{1}{q^2}q\cdot\mathcal{I}_{\Delta p_1}\,, \quad \mathcal{I}_{u_i}\coloneqq u_i\cdot\mathcal{I}_{\Delta p_1}\,. \tag{6.55}$$

[9] Alternatively we can define the angle though the projection onto b, both definitions are equivalent at the order considered here.

[10] In principle, the loop momentum also has components orthogonal to the scattering plane, e.g. $\varepsilon(\cdot, q, u_1, u_2)$. For observables linear in the loop momentum such contributions integrate to zero. Alternatively one can argue based on the parity of the observables.

7. Classical Observables

In this chapter we describe the application of amplitude-based methods for the computation of classical observables. In the section 7.1 we will derive the phase-shift and eventually the scattering angle for scattering processes of massless objects. This results have also been discussed in Ref. [269]. In the section we will discuss the computation of the potential contribution at the fourth order in perturbation theory which we presented in Ref. [49]. Finally in section 7.3, we will discuss observables including radiative effects. The results of that section have been published in Refs. [88, 89].

7.1. Scattering Angles in Massless Theories

Having the scatting amplitude for four gravitons in the low-energy EFT of quantum gravity at hand we can study the implication for the corresponding classical process of scattering of fixed-polarization gravitational waves. Only the spin-conserving amplitudes for graviton scattering $--\to--$, $+-\to+-$, $++\to++$ and $-+\to-+$ are non-trivial in the classical limit. These amplitudes are all described by the s-channel amplitude with helicities $\{-,-,+,+\}$.[1]

As for the massive case the classical limit is defined by the limit $-t \ll s$, which due to the lack of scales is identical with the high-energy (Regge) limit. In contrast to the massive case we have obtained the amplitudes the generic kinematics and the classical limit is obtained by subsequent expansion in the Regge limit.

[1] Remember that we are using an all incoming convention and helicity flips sign under exchanging an incoming with an outgoing particle.

In order to extract the scattering angles from the massless amplitudes, it is first convenient to rearrange the expressions to a remainder form[2]

$$M^{(0)}(s,-\boldsymbol{q}^2) = \quad = 8\pi\mathcal{N}Gs\frac{s}{\boldsymbol{q}^2}\,, \tag{7.2}$$

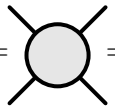

$$M^{(1)}(s,-\boldsymbol{q}^2) = \quad = 4r_\Gamma\mathcal{N}\,G^2s^2\left(\frac{\bar{\mu}^2}{\boldsymbol{q}^2}\right)^\epsilon\left[-\frac{2\pi\mathrm{i}}{\epsilon}\frac{s}{\boldsymbol{q}^2}+\frac{1}{\epsilon}(2L+2-2\pi\mathrm{i})+F^{(1)}\right], \tag{7.3}$$

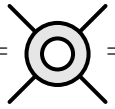

$$M^{(2)}(s,-\boldsymbol{q}^2) = \quad = 2\frac{r_\Gamma^2}{\pi}\mathcal{N}\,G^3s^3\left(\frac{\bar{\mu}^2}{\boldsymbol{q}^2}\right)^{2\epsilon}\left[\pi^2\left(-\frac{2}{\epsilon^2}+12\zeta_3\epsilon\right)\frac{s}{\boldsymbol{q}^2}\right. \tag{7.4}$$
$$\left.-\frac{2\pi\mathrm{i}}{\epsilon^2}(2L+2-\mathrm{i}\pi)-\frac{2\pi\mathrm{i}}{\epsilon}F^{(1)}+F^{(2)}\right],$$

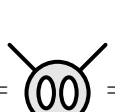

where $r_\Gamma \coloneqq e^{\epsilon\gamma_{\mathrm{E}}}\Gamma(1+\epsilon)\Gamma(1-\epsilon)^2/\Gamma(1-2\epsilon)$, $L \coloneqq \log(s/\boldsymbol{q}^2)$ and $\mathcal{N} = \mathcal{N}_{--++}$ is the phase weight in Eq. (5.6). The term proportional to ζ_3, has not been computed in here, but is instead dictated by the leading-order eikonal exponentiation (see e.g. Ref [270]). The remainders for pure gravity are obtained from the full one and two-loop four-graviton amplitudes that we have computed in chapter 5

$$\begin{aligned}F^{(1)}_{\mathrm{GR}} &= 2L^2+2\mathrm{i}\pi L+24\zeta_2-\frac{87}{10}L+\frac{841}{90}\\ &\quad+\epsilon\left[-\frac{2}{3}L^3-6\zeta_2L+6\zeta_3+\frac{47}{20}L^2-18\zeta_2-\frac{6913}{225}L+\frac{35597}{1200}\right.\\ &\quad\left.+\mathrm{i}\pi\left(-L^2+2\zeta_2+10L+\frac{1957}{360}\right)\right]+\mathcal{O}(\epsilon^2)\,,\end{aligned} \tag{7.5}$$

$$\begin{aligned}F^{(2)}_{\mathrm{GR}} &= -2\pi^2L^2+4\pi^2L-\frac{\pi^4}{90}+\frac{13403\pi^2}{675}-\frac{13049}{2160}\\ &\quad+\mathrm{i}\pi\left[\frac{4}{3}L^3-\frac{47}{10}L^2+\frac{5893}{150}L-20\zeta_3+\frac{2621\pi^2}{210}-\frac{106289}{3375}\right]+\mathcal{O}(\epsilon)\,.\end{aligned} \tag{7.6}$$

We do not display the remainders for the supersymmetric theories, but they are straightforward to extract from the amplitudes given in Ref. [271]. The first two orders of the phase-shift are purely real, as they have to be because the three-particle cut is of order $\mathcal{O}(G^3)$ and the therefore the process is purely conservative

[2]The prefactor $(\bar{\mu}^2/\boldsymbol{q}^2)^\epsilon$ is used for convenience and resums an infinite series of terms of the form $\log^k(\boldsymbol{q}^2/\bar{\mu}^2)$, which otherwise would lead to contributions with arbitrary negative exponents of the dimensional regularization parameter ϵ after the partial-wave transform

$$\mathcal{P}\left[\frac{1}{\boldsymbol{q}^2}\log^k(\boldsymbol{q}^2/\bar{\mu}^2)\right] = \mathcal{O}(\epsilon^{-k-1})\,. \tag{7.1}$$

Also note that this subtraction is different from the IR subtraction in Eq. (5.11).

up to order $\mathcal{O}(G^2)$. The explicit expressions are

$$\delta_J^{(0)} = \frac{Gs}{2}\left(\frac{\bar{\mu}^2\tilde{\mathcal{J}}^2}{s}\right)^{\epsilon}\left[-\frac{1}{\epsilon}-\frac{1}{3J^2}+\mathcal{O}(\epsilon,J^{-4})\right], \tag{7.7}$$

$$\delta_J^{(1)} = \frac{G^2s^2}{2\pi J^2}\left(\frac{\bar{\mu}^2\tilde{\mathcal{J}}^2}{s}\right)^{2\epsilon}\left[\frac{1}{\epsilon}-\frac{(\mathcal{N}-6)}{2}\log\tilde{\mathcal{J}}^2+C(\mathcal{N})+\mathcal{O}(\epsilon,J^{-2})\right], \tag{7.8}$$

where $\mathcal{N}$ is the number of supercharges ($\mathcal{N}=0$ for pure gravity) and $C(\mathcal{N})$ is a theory dependent constant equal to 1 for $\mathcal{N}>4$, equal to $1/2$ for $\mathcal{N}=4$ and equal to $-67/20$ for pure gravity respectively, while $\tilde{\mathcal{J}}^2 = J(J+1-2\epsilon)e^{2\gamma_{\mathbb{E}}\epsilon}$. The one-loop phase is purely quantum as manifest by the absence of a term with classical scaling $\sim J^{-1}$. The real part of the NNLO phase-shift is given by

$$\operatorname{Re}\delta_J^{(2)}(s) = \frac{G^3s^3}{3J^2}\left(\frac{\bar{\mu}^2\tilde{\mathcal{J}}^2}{s}\right)^{3\epsilon}\left[1+\mathcal{O}(\epsilon,J^{-4})\right]. \tag{7.9}$$

We now have all ingredients to compute the scattering angle. Before we do so let us briefly comment on the imaginary part of the phase-shift that first arises at $\mathcal{O}(G^3)$ and which is closely related to the three-particle cut and signals the presence of dissipative effects (radiation reaction). The imaginary part is theory-dependent and for Einstein gravity given by

$$\operatorname{Im}\delta_J^{(2)} = \frac{G^3s^3}{2\pi J^2}\left(\frac{\bar{\mu}^2\tilde{\mathcal{J}}}{s}\right)^{3\epsilon}\left[-\frac{1}{\epsilon}\Big(1+\log\tilde{\mathcal{J}}^2\Big)+2\log\tilde{\mathcal{J}}^2-\frac{13\pi^2}{6}+\frac{17749}{1800}+\mathcal{O}(\epsilon,J^{-4})\right]. \tag{7.10}$$

We can understand the non-universality of this quantity because radiation is sensitive to the number of messengers, which is different in the various supersymmetric theories. Finally we can compute the classical scattering angle

$$\frac{1}{2}\chi(s,J) = -\frac{\partial}{\partial J}\operatorname{Re}\delta_J = \frac{Gs}{J}+\frac{2}{3}\frac{G^3s^3}{J^3}+\mathcal{O}(J^{-5}), \tag{7.11}$$

which is finite as is should be as it is a physical observable. Equivalently, using the relation (2.10) to express the angular momentum through the eikonal impact parameter:

$$\sin\frac{1}{2}\chi(s,b_{\mathrm{e}}) = \frac{R}{b_{\mathrm{e}}}+\left(\frac{R}{b_{\mathrm{e}}}\right)^3+\mathcal{O}\left[\left(\frac{R}{b_{\mathrm{e}}}\right)^5\right], \quad R=G\sqrt{s}, \tag{7.12}$$

which is precisely the result found by Amati, Ciafaloni and Veneziano in Ref. [228]. The fact that even corrections are absent is related to the fact that massless scattering amplitudes cannot produce non-analytic behavior in s in the Regge limit [228]. Therefore in order to obtain the next non-vanishing order G^5 in the scattering angle, we have to consider scattering amplitude at four-loop order.

7.2. The Gravitational Potential at Order $\mathcal{O}(G^4)$

As we have explained before the potential contribution is a specific piece of the full dynamics that is precisely defined in terms of the method of regions. In contrast to the computation at lower PM orders, at 4PM order the definition of the potential region does no longer coincide with the conservative dynamics. At this order we have to take into account the effect of radiation that is back-scattered of the potential and does not leave the system (so-called conservative radiation). This missing piece that we are not computing here is intimately tied to spurious IR-divergences.

In the following, we briefly explain the construction of the integrand. Then we discuss the integration, which is one of the main complications at this order because of the appearance of a new class of elliptic integrals. Finally we derive physical quantities, in particular the radial action, the angle and the correction to the potential in isotropic gauge.

7.2.1. Integrand Construction

The integrand is constructed by the method of maximal unitarity following closely the two-loop computation described in Ref. [48]. The main difference is the increased complexity due to the additional loop.

As described in section 3.1 the integrand can be characterized by the possible singularities, which can be represented by cubic graphs. Up to relabeling of the external momenta there are 51 such graphs at the three-loop order. In this we excluded from the start diagrams that will not contribute in the potential region, for example mushroom-type integrals (three-loop generalizations of the diagram on the right-hand side of Eq. (4.104)) and topologies with less than three matter propagators (remember that otherwise the energy integration will be scaleless). For each of these diagrams, we then make an ansatz which will be fixed through unitarity cuts.

Some of the cubic diagrams have dangling trees which do not affect the singularities of the integrand (the momentum flowing to the corresponding lines is purely fixed by the external kinematics). This diagrams can be embedded into other cubic diagrams and in this way we arrive at a set of 40 cubic graphs relevant for the potential region which are displayed in Figure 7.1. Once again we also include the graphs obtained by permutations of the external momenta.

For the fit of the ansatz we consider the eight spanning cuts depicted in Figure 7.2. The required tree-level amplitudes entering the cuts are constructed from the Bern-Carrasco-Johansson (BCJ) double copy [36, 37, 272–274], that is from field theory tree amplitudes. The most complicated tree amplitude is the two-scalar-four-graviton amplitude and the five-graviton amplitude, which enter the first and the last cut in Figure 7.2 respectively. The physical-state projectors, that have to be inserted for the cut lines are conveniently simplified by organizing the

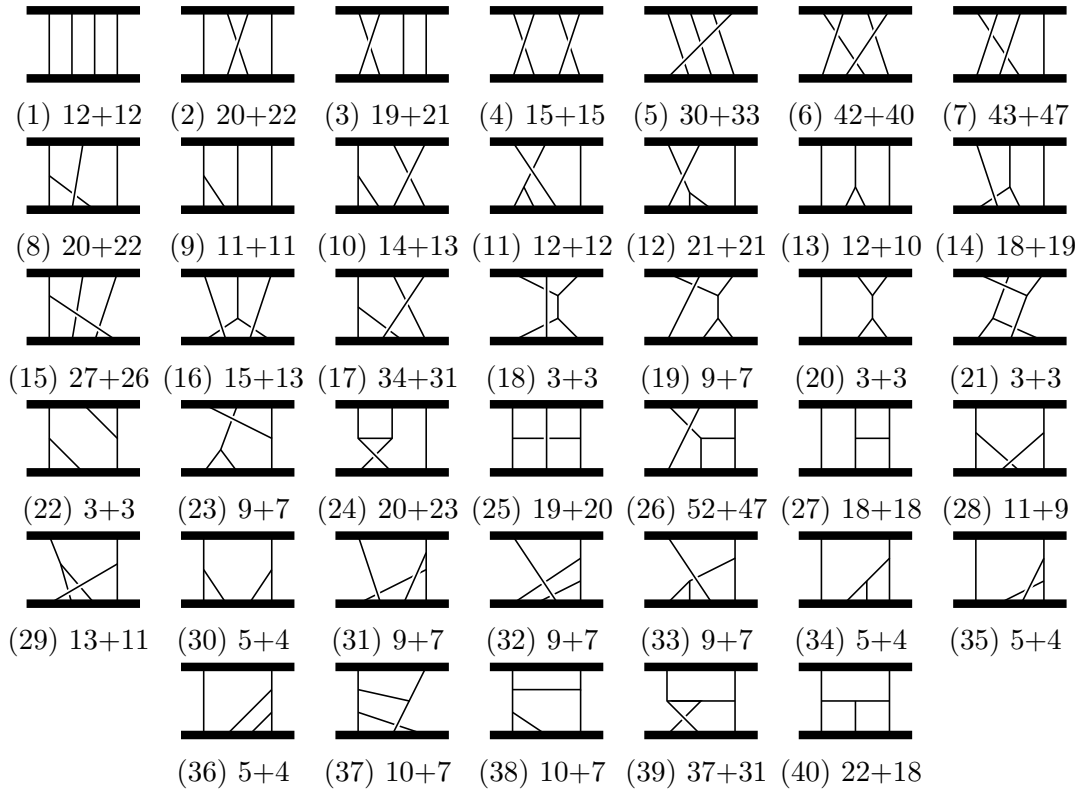

Figure 7.1.: The 40 integral families contributing to the potential region at three-loop order. The numbers indicate the odd and even master integrals in the respective topology.

tree amplitudes such that they obey generalized Ward identities. A systematic way of constructing such amplitudes is described in Ref. [275].

Since at 4PM order IR divergences are known to remain in the final result [276–281], we need to carefully track the dimensional dependence of different pieces entering the integrand. In particular we compute the integrand in D_s internal dimensions. It was found for the 3PM case in Refs. [47, 48] that the classical limit can be obtained from a four-dimensional integrand and it will be interesting to know if the same is true for the 4PM case once all divergences have been subtracted. We leave this for future work.

By the unitary method we determine the numerators of all cubic diagrams. In the next step we perform the expansion in the soft region as explained in section 4.7.4. The classical order is $|q|$ and the leading divergence of the amplitude is of order $|q|^{-2}$. Therefore all integrals have to be expanded to at most three orders in the q-expansion. After the expansion we use `FIRE6` to reduce the soft integrals to a set of master integrals. The integrals are then organized in families defied by the cubic diagrams in Figure 7.1, but with the quadratic propagators replaced by their linearized counterparts.

As we have described before, the system actually splits into systems of integrals with definite q-parity. If we take into account that daughter integrals are shared between the topologies, we find a total of 159 parity-even and 137 party-odd

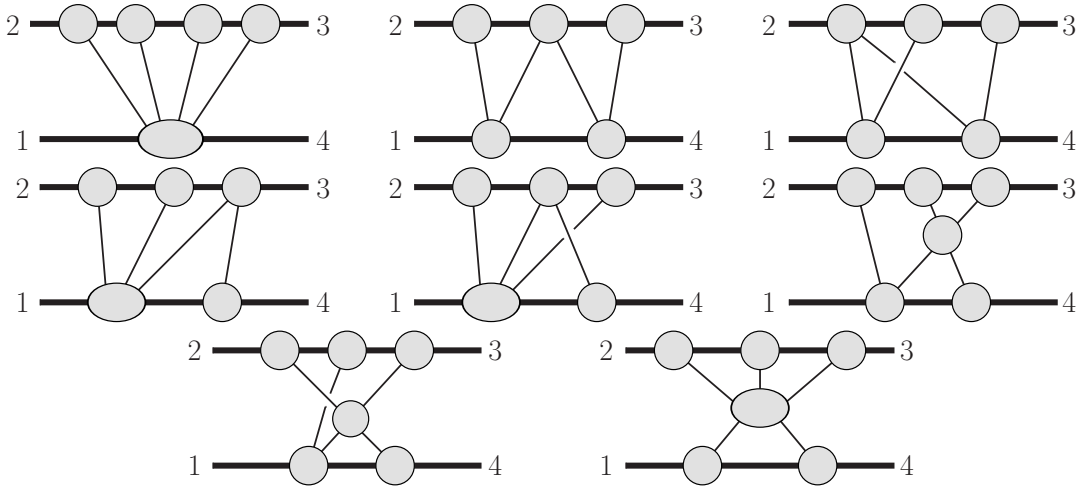

Figure 7.2.: Generalized unitarity cuts necessary to determine the conservative part of the amplitude at 4PM order. Gray ovals represent tree amplitudes, thin lines represent on-shell gravitons and thick lines on-shell massive scalars.

integrals. Instead of direct evaluation of the integrals as we have done at two-loop order in Ref. [149] we find it conveniently to first disentangle some of the contributions.

7.2.2. Organizing Results in Terms of Three-Dimensional Integrals

As we have seen explicitly in the cases of one and two-loop integrals in section 4.9, when we expand an integral in the potential region, after performing the energy integration the result will be expressed in terms of three-dimensional Euclidean integrals. At three loops we find that three of the required integrals are massless propagator-type integrals

$$I^{(1)}_{\text{3D}} = \quad , \qquad I^{(2)}_{\text{3D}} = \quad , \qquad I^{(3)}_{\text{3D}} = \quad . \tag{7.13}$$

The remaining six master integrals have up to three linearized matter propagators

$$I^{(4)}_{\text{3D}} = \quad , \quad I^{(4)}_{\text{3D}} = \quad , \quad I^{(5)}_{\text{3D}} = \quad ,$$
$$I^{(6)}_{\text{3D}} = \quad , \quad I^{(7)}_{\text{3D}} = \quad , \quad I^{(8)}_{\text{3D}} = \quad . \tag{7.14}$$

This means that any integral when expanded in the potential region takes the form

$$I = \sum_{j=1}^{8} f^{(j)}(y,\epsilon) I_{\text{3D}}^{(j)} \,. \tag{7.15}$$

Since the integrals in Eqs. (7.13) and (7.14) form a basis and do not depend on y, the differential equations for the initial integral can be separated into eight different differential equations for the contribution proportional to each of the three-dimensional integrals. Integrals $I_{\text{3D}}^{(4)}$–$I_{\text{3D}}^{(5)}$ have a Z-pole and are thus purely iteration. This means that we do not need the value of the corresponding coefficients. Only the three coefficients of the integrals with $j = 1, 2, 3$ are needed. As can be readily seen from their topology, the elliptic integrals discussed in section 4.11 only have contributions from $j = 1$. On the other hand we find that the contributions with $j = 2, 3$ can be solved in terms of polylogarithms in all cases. The integration for these cases is straightforward as the alphabet is linear in x once we use $1 + x^2 = (x + \mathrm{i})(x - \mathrm{i})$ and it is straightforward to integrate to any order in terms of generalized polylogarithms. The resulting functions can be expressed in terms of classical polylogarithms with complex arguments.

Remarkably we find that all such complex functions cancel in the end and we can express the amplitude in terms of polylogarithms with real arguments, although we require non-trivial relations like

$$\begin{aligned}
&\mathrm{Li}_2(1-y) + \mathrm{Li}_2(-y) \\
&= -2\,\mathrm{Li}_2(-x) + 2\,\mathrm{Li}_2(x) - 2\,\mathrm{Li}_2\left[\frac{1+\mathrm{i}}{2}(-\mathrm{i}+x)\right] + 2\,\mathrm{Li}_2\left[\frac{-1+\mathrm{i}}{2}(-\mathrm{i}+x)\right] \\
&\quad - 2\,\mathrm{Li}_2\left[\frac{1-\mathrm{i}}{2}(\mathrm{i}+x)\right] + 2\,\mathrm{Li}_2\left[\frac{-1-\mathrm{i}}{2}(\mathrm{i}+x)\right] + \text{logarithms}\,.
\end{aligned} \tag{7.16}$$

This relations can for example be constructed by making an ansatz, taking derivatives and then integrating up again. Once found a relation can be checked numerically with `Mathematica` [282] or `GiNaC` [283–285].

Finally we can express the amplitude in the form

$$\mathcal{M}_4 = G^4 M^7 \nu^2 \pi^2 |\boldsymbol{q}| 2^{2\epsilon} \left(\frac{\boldsymbol{q}^2}{\bar{\mu}^2}\right)^{-3\epsilon} \sum_{j=1}^{8} \mathcal{M}_{\text{3D}}^{(j)}(y,\epsilon) I_{\text{3D}}^{(j)} \,. \tag{7.17}$$

As we have associated them with iterations, we can then drop all contributions coming from $I_{\text{3D}}^{(4)}$–$I_{\text{3D}}^{(5)}$. For $I_{\text{3D}}^{(2)}$–$I_{\text{3D}}^{(3)}$ we can explicitly insert the values for the master integrals obtained by solving the differential equations. For the remaining piece proportional to $I_{\text{3D}}^{(1)}$ we find that it is finite in ϵ, so we only need to find a single function $\mathcal{M}_{\text{3D}}^{(1)}(y) = \mathcal{M}_{\text{3D}}^{(1)}(y,0)$. Instead of solving the differential equation, we use it to produce series expansion to in principle arbitrary orders in velocity. Based on the knowledge of the simplest elliptic integrals, and anticipating that the transcendental weight of the final expression will be bound by two, we make

the following ansatz, in terms of unknown polynomials $p_i(y)$[3]

$$\mathcal{M}_{3\mathrm{D}}^{(1)} = \sum_{i=0}^{2} p_i \frac{\mathrm{d}^i}{\mathrm{d}y^i} \frac{K^2\left(\frac{y-1}{y+1}\right)}{y+1} + p_3\pi^2 \,. \tag{7.18}$$

Expansion up to order $(y-1)^{43}$ completely fixes the coefficients in the polynomials (that is after that all coefficients are found to be zero). The result is

$$\begin{aligned}\mathcal{M}_{3\mathrm{D}}^{(1)} = {} & \frac{1200y^2+2095y+834}{16(y^2-1)} K^2\left(\frac{y-1}{y+1}\right) + \frac{7(380y^2+169)}{32(y-1)} E^2\left(\frac{y-1}{y+1}\right) \\ & - \frac{1200y^3+2660y^2+2929y+1183}{16(y^2-1)} K\left(\frac{y-1}{y+1}\right) E\left(\frac{y-1}{y+1}\right) \\ & - \frac{\pi^2}{16}(y-1)\left(25y^5+25y^4-5y^3-65y^2+64y-12\right) . \end{aligned} \tag{7.19}$$

Further expansion confirms that the ansatz is valid up to order $(y-1)^{200}$. We note that this piece is completely free of polylogarithms. As such the split induced by the $I_{3\mathrm{D}}^{(i)}$'s seems to be efficient in separating different classes of functions. It will be interesting to study if a similar organization continues to hold at higher orders in perturbation theory, where we expect more complicated functions to arise.

7.2.3. Potential Amplitude

Finally we are in a position to write down the full potential amplitude at 4PM order, which constitutes one of the main results of the present thesis

$$\begin{aligned}\mathcal{M}_4(\boldsymbol{q}) = {} & G^4M^7\nu^2\pi^2|\boldsymbol{q}|2^{2\epsilon}\left(\frac{\boldsymbol{q}^2}{\bar{\mu}^2}\right)^{-3\epsilon}\left\{f_4^{\mathrm{pp}}(\sigma) + \nu\left[\frac{1}{\epsilon}f^{\mathrm{tail}}(\sigma) + f^{\mathrm{fin}}(\sigma)\right]\right\} \\ & + \int_{\boldsymbol{\ell}} \frac{\tilde{I}_{r,1}^4}{Z_1Z_2Z_3} + \int_{\boldsymbol{\ell}} \frac{\tilde{I}_{r,1}^2\tilde{I}_{r,2}}{Z_1Z_2} + \int_{\boldsymbol{\ell}} \frac{\tilde{I}_{r,1}\tilde{I}_{r,3}}{Z_1} + \int_{\boldsymbol{\ell}} \frac{\tilde{I}_{r,2}^2}{Z_1} \,. \end{aligned} \tag{7.20}$$

In the expression we have separated a point-particle piece f_4^{pp}, an IR-divergent (tail) piece f^{tail} and a finite piece f^{fin}. The point-particle and tail contributions are

$$f_4^{\mathrm{pp}} = -\frac{35(1-18\sigma^2+33\sigma^4)}{8(\sigma^2-1)} \,, \quad f^{\mathrm{tail}} = h_1 + h_2\log\left(\tfrac{\sigma+1}{2}\right) + h_3\frac{\operatorname{arccosh}(\sigma)}{\sqrt{\sigma^2-1}} \,. \tag{7.21}$$

[3] In Ref. [49] the ansatz was made in terms of the x variable and a different basis. This however does not affect the argument made here.

The finite piece is

$$
\begin{aligned}
f^{\text{fin}} = {} & h_4 + h_5 \log\left(\tfrac{\sigma+1}{2}\right) + h_6 \frac{\operatorname{arccosh}(\sigma)}{\sqrt{\sigma^2-1}} + h_7 \log(\sigma) - h_2 \frac{2\pi^2}{3} + h_8 \frac{\operatorname{arccosh}^2(\sigma)}{\sigma^2-1} \\
& + h_9 \left[\operatorname{Li}_2\left(\tfrac{1-\sigma}{2}\right) + \frac{1}{2}\log^2\left(\tfrac{\sigma+1}{2}\right)\right] + h_2 \frac{2\sigma(2\sigma^2-3)}{(\sigma^2-1)^{3/2}} \left[\operatorname{Li}_2\left(\sqrt{\tfrac{\sigma-1}{\sigma+1}}\right) - \operatorname{Li}_2\left(-\sqrt{\tfrac{\sigma-1}{\sigma+1}}\right)\right] \\
& + h_{11}\left[\operatorname{Li}_2\left(\tfrac{1-\sigma}{1+\sigma}\right) - \operatorname{Li}_2\left(\tfrac{\sigma-1}{\sigma+1}\right) + \frac{\pi^2}{3}\right] + h_{10}\left[\operatorname{Li}_2\left(\tfrac{1-\sigma}{2}\right) - \frac{\pi^2}{6}\right] \\
& + \frac{2h_3}{\sqrt{\sigma^2-1}}\left[\operatorname{Li}_2\left(1-\sigma-\sqrt{\sigma^2-1}\right) - \operatorname{Li}_2\left(1-\sigma+\sqrt{\sigma^2-1}\right)\right. \\
& \qquad \left. + 5\operatorname{Li}_2\left(\sqrt{\tfrac{\sigma-1}{\sigma+1}}\right) - 5\operatorname{Li}_2\left(-\sqrt{\tfrac{\sigma-1}{\sigma+1}}\right) + 2\log\left(\tfrac{\sigma+1}{2}\right)\operatorname{arccosh}(\sigma)\right] \\
& + h_{12} K^2\left(\tfrac{\sigma-1}{\sigma+1}\right) + h_{13} K\left(\tfrac{\sigma-1}{\sigma+1}\right) E\left(\tfrac{\sigma-1}{\sigma+1}\right) + h_{14} E^2\left(\tfrac{\sigma-1}{\sigma+1}\right). \qquad (7.22)
\end{aligned}
$$

The h_i are rational coefficient functions and are explicitly listed in Appendix D. If we are only interested in the new contribution at 4PM order we can drop all iterations tagged by Z poles in Eq. (7.20). However, we can use the IR structure as a non-trivial check and use the poles to extract the lower-order radial actions. We find the following expressions up to $\mathcal{O}(G^3)$

$$
\tilde{I}_{r,1}(\boldsymbol{q}) = 16\pi G M^4 \nu^2 \frac{1}{\boldsymbol{q}^2}(2\sigma^2-1)\,, \qquad (7.23)
$$

$$
\tilde{I}_{r,2}(\boldsymbol{q}) = 6\pi^2 M^5 \nu^2 \frac{1}{|\boldsymbol{q}|}(5\sigma^2-1)\,, \qquad (7.24)
$$

$$
\begin{aligned}
\tilde{I}_{r,3}(\boldsymbol{q}) = {} & 2\pi G^3 M^6 \nu^2 \log \boldsymbol{q}^2 \left\{ -\frac{2(64\sigma^6 - 120\sigma^4 + 60\sigma^2 - 5)}{3(\sigma^2-1)^2} \right. \\
& + \nu\left[\frac{4}{3}\frac{-36\sigma^6 + 28\sigma^5 + 142\sigma^4 + 22\sigma^3 - 110\sigma^2 - 50\sigma + 5}{(\sigma+1)(\sigma^2-1)}\right. \\
& \left.\left. + \frac{8(4\sigma^4 - 12\sigma^2 - 3)\operatorname{arccosh}(\sigma)}{\sqrt{\sigma^2-1}}\right]\right\}. \qquad (7.25)
\end{aligned}
$$

This is in agreement with known results [53, 54] which provides a very strong check of our computation. Finally the new information is contained in the 4PM radial action which can be directly extracted from Eq. (7.20),

$$
\tilde{I}_{r,4}(\boldsymbol{q}) = G^4 M^7 \nu^2 \pi^2 |\boldsymbol{q}| 2^{2\epsilon} \left(\frac{\boldsymbol{q}^2}{\bar{\mu}^2}\right)^{-3\epsilon} \left\{ f_4^{\text{pp}}(\sigma) + \nu\left[\frac{1}{\epsilon} f^{\text{tail}}(\sigma) + f^{\text{fin}}(\sigma)\right]\right\}. \qquad (7.26)
$$

We note that the mass dependence of this expression is very simple and the terms are naturally organized in a self-force expansion [75, 229]. Through Fourier transformation (B.4) or the partial-wave transform (B.24), we obtain the radial action

in angular momentum space

$$I_{r,4}(J) = -\frac{G^4M^7\nu^2\pi\boldsymbol{p}^2}{8EJ^3}\left(\frac{4\bar{\mu}^2e^{2\gamma_{\rm E}}J^2}{\boldsymbol{p}^2}\right)^{4\epsilon} \times\left\{f_4^{\rm pp}(\sigma)+\nu\left[\frac{1}{\epsilon}f^{\rm tail}(\sigma)+f^{\rm fin}(\sigma)-14f^{\rm tail}(\sigma)\right]\right\}. \tag{7.27}$$

The scattering angle is obtained by taking a derivative with respect to the angular momentum J

$$\chi_4 = -\frac{\partial I_{r,4}}{\partial J} = -\frac{3G^4M^7\nu^2\pi\boldsymbol{p}^2}{8EJ^4}\left(\frac{4\bar{\mu}^2e^{2\gamma_{\rm E}}J^2}{\boldsymbol{p}^2}\right)^{4\epsilon} \times\left\{f_4^{\rm pp}(\sigma)+\nu\left[\frac{1}{\epsilon}f^{\rm tail}(\sigma)+f^{\rm fin}(\sigma)-\frac{50}{3}f^{\rm tail}(\sigma)\right]\right\}. \tag{7.28}$$

We can also employ the EFT approach, adapted to the Z poles, to obtain the c_4 coefficient in the PM potential [4]

$$\begin{aligned} c_4 =& \frac{M^7\nu^2}{4\xi E^2}\left[f_4^{\rm pp}+\nu\left(\frac{1}{\epsilon}f^{\rm tail}+f^{\rm fin}-10f_4^{\rm tail}\right)\right]+\frac{\mathrm{d}^3}{\mathrm{d}^3\boldsymbol{p}^2}\left[\frac{E^3\xi^3}{3}c_1^4\right] \\ &+\frac{\mathrm{d}^2}{\mathrm{d}^2\boldsymbol{p}^2}\left[\left(\frac{E^3\xi^3}{\boldsymbol{p}^2}+\frac{E\xi(3\xi-1)}{2}\right)c_1^4-2E^2\xi^2c_1^2c_2\right] \\ &+\left(\frac{\mathrm{d}}{\mathrm{d}\boldsymbol{p}^2}+\frac{1}{\boldsymbol{p}^2}\right)\left[E\xi(2c_1c_3+c_2^2)+\left(\frac{4\xi-1}{4E}+\frac{2E^3\xi^3}{\boldsymbol{p}^4}+\frac{E\xi(3\xi-1)}{\boldsymbol{p}^2}\right)c_1^4\right. \\ &\left.+\left((1-3\xi)-\frac{4E^2\xi^2}{\boldsymbol{p}^2}\right)c_1^2c_2\right]. \end{aligned} \tag{7.29}$$

The lower-order coefficients c_1 to c_3 can be found Eq. (10) of Ref. [47]. We note that all quantities suffer from an IR divergence which manifests in terms of a $1/\epsilon$ pole. This pole is an artifact caused by the fact that the computation was split between the near and the far zone. The potential region we have considered here only includes effects from the near zone. The near-zone IR pole will cancel against an UV divergence from the far zone [276–281].

We have performed extensive checks on our results. First of all we have checked that wherever available we match the PN literature. Explicitly we compared the scattering angle in Eq. (7.28) to the angle obtained by the potential contributions to the Hamiltonian up to 5PN order which have been computed by Blümlein et al. and presented in Eqs. (21)–(26) of Ref. [286] and Eq. (5) of Ref. [76]. Following the publication of our work the result was also confirmed to the 6PN order [77]. We have also checked that our result reproduces the correct dynamics in the point-particle limit. For example the scattering angle in Eq. (7.28) reduces to the point-particle result presented in Eq. (2.66).

Some of the pieces of our result are not affected by the missing pieces due to conservative radiation. These are in particular the pieces that contains the

[4] Alternatively it can be extracted directly from the scattering angle (See e.g. Ref. [54]).

elliptic functions. We have therefore compared the π^3 terms with the 6PN result in Eq. (8.4) of Ref. [287], finding full agreement.

Further comparisons can be made once radiation effects are included, for example to the full 4PN Hamiltonian [61–63, 66, 288–290] and the scattering angle to 6PN order [75, 100, 287].

Another strong check is provided by the fact that the IR divergence is closely related to the energy loss due to radiation [100, 291, 292], which applied to the case at hand yields,

$$\Delta E = \frac{G^3 M^7 \nu^3 \pi \boldsymbol{p}^2}{4E^2 J^3} f^{\text{tail}}(\sigma)\,. \tag{7.30}$$

In the next chapter we will rederive this result using a independent method finding full agreement. We will describe further checks of this piece in that section.

Finally since the original announcement of our result in Ref. [49] it has also been confirmed independently by a computation based on a purely classical approach using the worldline formalism, but using the same integration technique in Ref. [93].

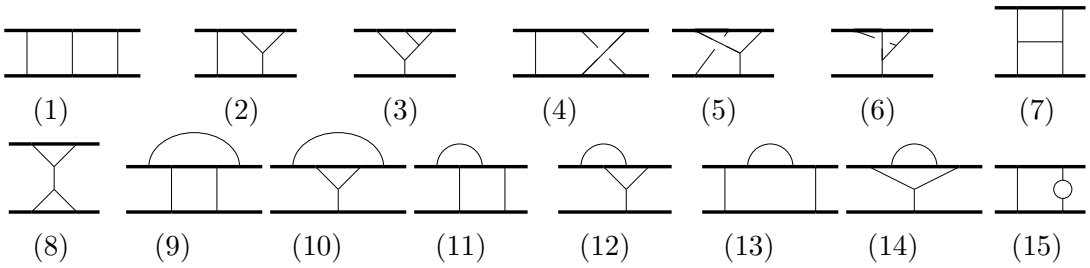

Figure 7.3.: Cubic diagrams required for the classical part of the amplitude at $\mathcal{O}(G^3)$. The graphs (1)–(8) are already required for the conservative sector [47, 48].

7.3. Radiation

In this section we present results for radiative contributions to observables at NNLO order in the gravitational coupling. The content is mostly based on Refs. [88] and [89]. Throughout we are using the KMOC formalism described in section 6.4, as it can account for radiative effects.

We will focus on two scalar observables, the radiated energy and the scattering angle which are both derived from the impulse. Radiative effects to these quantities first arise at third order in the gravitational coupling. Computations at tree and one-loop level are therefore identical to the conservative setup and in the interest of brevity we skip the computations of these low-order quantities. [5]

As we are interested in the radiative effects, we cannot restrict to the potential region, but need to include additional regions as well. Although it would be most prudent to add only the relevant regions, which are mixed potential-radiation regions, we will instead compute in the full soft region, which up to the order considered here does not lead to a drastic increase in complexity.

7.3.1. Integrands

For the integrands we use the unitarity method described in section 3.1. We first identify the 15 cubic graphs relevant for the problem, which are displayed in Figure 7.3. Thereby we have already excluded diagrams which cannot contribute to classical physics, a sample of which are depicted in Figures 7.4(1)-7.4(3). In the next step, we make an ansatz for the numerators of the cubic diagrams in terms of the eleven independent Lorentz products build from the momenta $p_1, p_2, p_3, \ell_1, \ell_2$. The mass dimension of the numerators is simple to determine by naive dimensional analysis of the vertices and we find that in all cases the mass dimension is 12. This means that the most general ansatz is a homogeneous multivariate polynomial of degree 6 in the invariants. Naively therefore the ansatz has $15 \times \binom{16}{10} = 120120$ undetermined constants. We can do better by noting a few constraints:

[5] The computation based on the KMOC formalism is described in Ref. [89] and in full agreement with known results from the PM literature (see e.g. Ref. [47]).

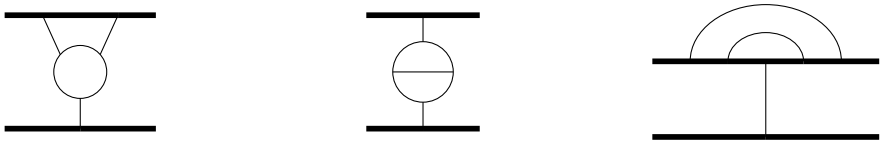

Figure 7.4.: Examples of diagrams that do not contribute to classical physics. Diagrams (1) and (1) are of order q and q^2 respectively and therefore beyond classical power-counting. Diagram (3) has classical power-counting but is scaleless after soft expansion.

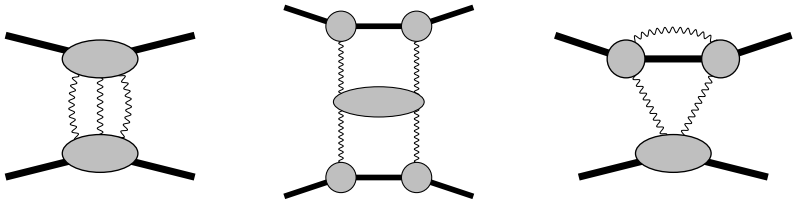

Figure 7.5.: Spanning set of unitarity cuts relevant for the soft region at $\mathcal{O}(G^3)$.

1. We enforce on-shell condition whenever a collapse would lead to an non-classical diagram. For example in graph 7.3(9) none of the graviton propagators nor the top-center propagator can be pinched, effectively removing three degrees of freedom from the ansatz.

2. We demand that the numerator has the symmetries associated with the graph (for example $N_{(1)}$ for graph 7.3(1) should be symmetric under $\{p_1, p_4\} \leftrightarrow \{p_2, p_3\}$).

3. For each all graviton vertex we require the numerator to scale at least as q^2 in the classical counting. For example the numerator $N_{(2)}$ cannot include terms like $(p_1 \cdot p_2)^6$.

4. The numerator of a diagram with an n s-channel two-particle cuts is assumed to be proportional to $n-1$ copies of the tree amplitude. For example $N_{(4)}$ has an overall factor of $(s - m_1^2 - m_2^2)^2 - 4m_1^2 m_2^2$.

This severely constrains the ansatz and for example completely fixed the numerator of the diagram (1) in Figure 7.3 up to a overall prefactor

$$N_{(1)} = a_1[(s - m_1^2 - m_2^2)^2 - 4m_1^2 m_2^2]^3 \,. \tag{7.31}$$

Incorporating the constraints, the ansatz contains a total of 3731 parameters across all 15 topologies. We then proceed to determine the unknowns through matching against the spanning cuts in Figure 7.5. As an alternative way, which is still feasible at this order, we can compute the integrand in a traditional fashion using Feynman diagrams. We note that due to the relative simplicity of the scalar-graviton vertices as compared to the pure graviton vertices as well as the scalar external states, this computation is drastically less complicated than the four-graviton computation described in chapter 5. For this computation we use simplified Feynman rules [238, 293] following closely a setup that is used in the context of PM

corrections in the worldline formalism [294, 295]. In this computation we neglect the contributions from ghosts, which only contribute in closed graviton loops and therefore only to diagrams similar to Figure 7.3(15). It is straightforward to include this contributions, but they will cancel from any classical observable. For example the contribution to graph 7.3(15) will cancel against a iteration of the quantum contribution to the one-loop potential (see e.g. Ref. [296]). The resulting Feynman diagram integrand has been checked to agree on the set of spanning cuts in Figure 7.5.

We simultanously perform the analysis for $\mathcal{N} = 8$ supergravity, using as a starting point the simple integrand in terms of scalar integrals given in Ref. [149].

Having an integrand at hand we can proceed to extract classical observables through the KMOC formalism. For this we have to insert additional numerators of the form $u \cdot \ell_i$ and $q \cdot \ell_i$ into our integrand as dictated by the reduction in (6.55).

In a final step we expand the integrands in the soft limit as explained in section 4.7, including terms up to order q^0. By IBP relations and applying partial fraction decomposition we map these integrals to a set of master integrals depicted in Figure 4.9. The cut contributions can be obtained by either cutting before or after IBP reduction. After inserting the values for these integrals we obtain the impulse kernel. In the next section we will present the result restricting to the potential region, which will mainly serve as a cross check against the available literature. In the section right after that we will present the full result in the soft region thereby including for the first time radiative effects.

7.3.2. Conservative Sector

We start by computing the conservative contributions at two-loop order. This serves both as a check of our method and as a means to separate the radiative effects. In the following we will split the impulse

$$\Delta p_1^\mu = \Delta p_{1\,,\text{cons}}^\mu + \Delta p_{1\,,\text{rad}}^\mu \,. \tag{7.32}$$

Up to order G^3, which is the order we consider here, the conservative piece is identical to the contribution from the potential region. For $\mathcal{N} = 8$ supergravity we find

$$\begin{aligned}
\mathcal{I}_{\perp,\text{cons}}^{(2),\mathcal{N}=8} &= -\frac{(-q^2)^{-2\epsilon}}{\epsilon} \frac{16\,\pi\, G^3\, m_1^2 m_2^2\, (\sigma - \cos\phi)^4}{\sqrt{\sigma^2-1}} \left[\frac{(\sigma-\cos\phi)^2\, s}{(\sigma^2-1)^{3/2}} + 2 m_1 m_2\, \operatorname{arccosh}\sigma \right] \\
\mathcal{I}_{u_1,\text{cons}}^{(2),\mathcal{N}=8} &= \mathcal{I}_{u_2,\text{cons}}^{(2),\mathcal{N}=8} = 0\,.
\end{aligned} \tag{7.33}$$

For Einstein gravity

$$\mathcal{I}^{(2),\mathrm{GR}}_{\perp,\mathrm{cons}} = (-q^2)^{-2\epsilon}\frac{2\pi G^3 m_1^2 m_2^2}{\epsilon}\left[s\left(16\sigma^2 - \frac{1}{(\sigma^2-1)^2}\right) - \frac{4}{3}m_1 m_2\,\sigma\big(14\sigma^2+25\big)\right.$$
$$\left. + 4m_1 m_2\big(-4\sigma^4+12\sigma^2+3\big)\frac{\operatorname{arccosh}\sigma}{\sqrt{\sigma^2-1}}\right], \quad (7.34)$$

$$\mathcal{I}^{(2),\mathrm{GR}}_{u_1,\mathrm{cons}} = -\mathcal{I}^{(2),\mathrm{GR}}_{u_2,\mathrm{cons}} = \mathrm{i}(-q^2)^{\frac{1}{2}-2\epsilon}\frac{12\pi^2\,G^3\,m_1^2 m_2^3(m_1+m_2)(2\sigma^2-1)(5\sigma^2-1)}{\sqrt{\sigma^2-1}}\,. \quad (7.35)$$

After Fourier transform to impact parameter space, we find

$$\Delta p^{\mu,(2),\mathcal{N}=8}_{1,\mathrm{cons}} = -\frac{G^3M^4\nu}{|b|^3}\frac{16\,(\sigma-\cos\phi)^4}{(\sigma^2-1)}\frac{b^\mu}{|b|}\left[\frac{(\sigma-\cos\phi)^2\,h^2(\sigma,\nu)}{(\sigma^2-1)^{3/2}} + 4\nu\,\operatorname{arccosh}\sigma\right], \quad (7.36)$$

$$\Delta p^{\mu,(2),\mathrm{GR}}_{1,\perp,\mathrm{cons}} = \frac{G^3M^4\nu}{|b|^3}\frac{2}{\sqrt{\sigma^2-1}}\frac{b^\mu}{|b|}\left[h^2(\sigma,\nu)\left(16\sigma^2-\frac{1}{(\sigma^2-1)^2}\right)\right. \quad (7.37)$$
$$\left. - \frac{4}{3}\nu\,\sigma\big(14\sigma^2+25\big) - 4\nu\big(4\sigma^4-12\sigma^2-3\big)\frac{\operatorname{arccosh}\sigma}{\sqrt{\sigma^2-1}}\right],$$

$$\Delta p^{\mu,(2),\mathrm{GR}}_{1,u,\mathrm{cons}} = \frac{G^3M^5\nu^2}{|b|^3}\frac{3\pi(2\sigma^2-1)(5\sigma^2-1)}{2\,(\sigma^2-1)}\left(\frac{1}{m_1}\,\check{u}_1^\mu - \frac{1}{m_2}\,\check{u}_2^\mu\right). \quad (7.38)$$

We note that in the conservative case the longitudinal impulse is fixed completely by the on-shell constraint

$$0 = (p_1+\Delta p_1)^2 - m_1^2\,, \quad (7.39)$$

and thus does not contain any new information. Computing it and checking that the on-shell constraint is satisfied provides a convenient cross-check. The conservative impulse has a logarithmic divergence at high energies, corresponding to that in the scattering angle of Refs. [47, 48].

7.3.3. Dissipative Sector

The radiative part of the two-loop impulse kernel for both GR and $\mathcal{N}=8$ supergravity can be parameterized in terms of a few rational functions r_i,

$$\mathcal{I}^{(2)}_{\perp,\text{rad}} = 4\pi\frac{(-q^2)^{-2\epsilon}}{\epsilon}G^3m_1^3m_2^3\left[r_1(\sigma)+\sigma r_2(\sigma)\frac{1}{2}\frac{\operatorname{arccosh}\sigma}{\sqrt{\sigma^2-1}}\right], \tag{7.40}$$

$$\mathcal{I}^{(2)}_{u_1,\text{rad}} = 0\,, \tag{7.41}$$

$$\begin{aligned}\mathcal{I}^{(2)}_{u_2,\text{rad}} &= \mathrm{i}(-q^2)^{\frac{1}{2}-2\epsilon}8\pi^2G^3m_1^3m_2^3\sqrt{\sigma^2-1}\\ &\quad\times\left[r_3(\sigma)+r_4(\sigma)\log\left(\frac{\sigma+1}{2}\right)+\sigma r_5(\sigma)\frac{1}{2}\frac{\operatorname{arccosh}\sigma}{\sqrt{\sigma^2-1}}\right].\end{aligned} \tag{7.42}$$

For $\mathcal{N}=8$ supergravity only three of the functions are independent and we have

$$r_1(\sigma) = r_3(\sigma) = \frac{8(\sigma-\cos\phi)^6}{(\sigma^2-1)^{3/2}}\,, \tag{7.43}$$

$$r_2(\sigma) = r_5(\sigma) = \frac{16(\sigma-\cos\phi)^5(\sigma^2+\sigma\cos\phi-2)}{\sigma(\sigma^2-1)^{3/2}}\,, \tag{7.44}$$

$$r_4(\sigma) = -\frac{8(\sigma-\cos\phi)^4}{\sqrt{\sigma^2-1}}\,. \tag{7.45}$$

In the case of pure gravity all rational functions are independent and slightly more complicated

$$r_1(\sigma) = -\frac{(2\sigma^2-1)^2(5\sigma^2-8)}{3(\sigma^2-1)^{3/2}}\,, \tag{7.46}$$

$$r_2(\sigma) = \frac{2(2\sigma^2-1)^2(2\sigma^2-3)}{(\sigma^2-1)^{3/2}}\,, \tag{7.47}$$

$$r_3(\sigma) = \frac{210\sigma^6-552\sigma^5+339\sigma^4-912\sigma^3+3148\sigma^2-3336\sigma+1151}{48(\sigma^2-1)^{3/2}}\,, \tag{7.48}$$

$$r_4(\sigma) = -\frac{35\sigma^4+60\sigma^3-150\sigma^2+76\sigma-5}{8\sqrt{\sigma^2-1}}\,, \tag{7.49}$$

$$r_5(\sigma) = \frac{(2\sigma^2-3)(35\sigma^4-30\sigma^2+11)}{8(\sigma^2-1)^{3/2}}\,. \tag{7.50}$$

After performing the Fourier transformation to impact parameter space, the radiative part of the impulse is expressed as

$$\begin{aligned}\Delta p^{\mu,(2)}_{1,\text{rad}} = \frac{G^3M^4\nu^2}{|b|^3}\Bigg\{&\frac{4}{\sqrt{\sigma^2-1}}\frac{b^\mu}{|b|}\left[r_1(\sigma)+\sigma r_2(\sigma)\frac{1}{2}\frac{\operatorname{arccosh}\sigma}{\sqrt{\sigma^2-1}}\right]\\ &+\pi\,\breve{u}_2^\mu\left[r_3(\sigma)+r_4(\sigma)\log\left(\frac{\sigma+1}{2}\right)+\sigma r_5(\sigma)\frac{1}{2}\frac{\operatorname{arccosh}\sigma}{\sqrt{\sigma^2-1}}\right]\Bigg\}.\end{aligned} \tag{7.51}$$

Scattering angle The conservative part of the scattering angle is given by

$$\chi_{\text{cons}}^{(2),\text{GR}} = \frac{G^3M^3}{|b|^3}\frac{2h}{\sigma^2-1}\left[h^2\left(16\sigma^2 - \frac{1}{(\sigma^2-1)^2}\right)\right. \tag{7.52}$$
$$\left. - \frac{4}{3}\nu\,\sigma\big(14\sigma^2+25\big) - 4\nu\big(4\sigma^4-12\sigma^2-3\big)\frac{\operatorname{arccosh}\sigma}{\sqrt{\sigma^2-1}}\right],$$
$$\chi_{\text{cons}}^{(2),\mathcal{N}=8} = -\frac{G^3M^3h}{|b|^3}\frac{16\ (\sigma-\cos\phi)^4}{\sigma^2-1}\left[\frac{(\sigma-\cos\phi)^2\,h^2(\sigma,\nu)}{(\sigma^2-1)^2} + 4\nu\,\frac{\operatorname{arccosh}\sigma}{\sqrt{\sigma^2-1}}\right]. \tag{7.53}$$

The radiative contribution to the angle is directly given in terms of the longitudinal part of the radiative contribution to the impulse

$$\chi_{\text{rad}}^{(2)} = \chi^{(2)} - \chi_{\text{cons}}^{(2)} = \frac{1}{|\boldsymbol{p}|}\frac{b}{|b|}\cdot\Delta p_{1,\text{rad}}^{(2)} = \frac{G^3M^3\nu}{|b|^3}\frac{4h}{\sigma^2-1}\left[r_1(\sigma)+\sigma r_2(\sigma)\frac{1}{2}\frac{\operatorname{arccosh}\sigma}{\sqrt{\sigma^2-1}}\right]. \tag{7.54}$$

For the case of $\mathcal{N}=8$ supergravity we can compare to the result for $\phi=\pi/2$, presented in Refs. [297, 298]. The scattering angle in GR has been computed in Ref. [299] via a linear response formula derived in Ref. [300]. In both cases we find full agreement with the result presented here.

Radiated energy The radiated energy can be directly extracted from the radiated four momentum ΔR^μ. We can compute this directly using the formulae presented in section 6.4. We find that the total radiated energy takes the simple form

$$\Delta R^\mu = \frac{G^3m_1^2m_2^2}{|b|^3}\frac{u_1^\mu+u_2^\mu}{\sigma+1}\mathcal{E}(\sigma)+\mathcal{O}(G^4)\,, \tag{7.55}$$

where we define

$$\mathcal{E}(\sigma) \coloneqq \pi\left[r_3(\sigma)+r_4(\sigma)\log\left(\frac{\sigma+1}{2}\right)+\sigma r_5(\sigma)\frac{1}{2}\frac{\operatorname{arccosh}\sigma}{\sqrt{\sigma^2-1}}\right], \tag{7.56}$$

where the coefficients the r-functions are given in Eqs. (7.43)–(7.45) and (7.46)–(7.50). As a check we assert that momentum conservation is satisfied

$$0 = \Delta R^\mu + \Delta p_1^\mu + \Delta p_2^\mu\,, \tag{7.57}$$

where the impulse of particle 2 is obtained by trivial relabeling $1\leftrightarrow 2$. The total COM energy loss during a scattering event is given by

$$\Delta E^{\text{hyp}} = \frac{(p_1+p_2)\cdot\Delta R}{|p_1+p_2|} = \frac{G^3M^4\nu^2}{|b|^3\,h(\nu,\sigma)}\,\mathcal{E}(\sigma)+\mathcal{O}(G^4)$$
$$= \frac{G^3M^7\nu^5(1-\sigma^2)^{\frac{3}{2}}}{J^3\,h(\nu,\sigma)^4}\,\mathcal{E}(\sigma)+\mathcal{O}(G^4)\,. \tag{7.58}$$

In order to make contact with the PN-literature for the elliptic case, we can use analytic continuation from the physical scattering kinematics $\sigma>1$ to the bound

case $\sigma < 1$. As described in Ref. [53, 54, 100] the relation between the hyperbolic and the elliptic result is simple

$$\Delta E^{\text{ell}}(\sigma, J) = \Delta E^{\text{hyp}}(\sigma, J) - \Delta E^{\text{hyp}}(\sigma, -J)\,. \tag{7.59}$$

The energy loss is an odd function in J, so in the case at hand the result for the elliptic case is twice the hyperbolic result

$$\Delta E^{\text{ell}}(\sigma, J) = -\mathrm{i}\frac{G^3 M^7 \nu^5 (1-\sigma^2)^{\frac{3}{2}}}{J^3\, h(\nu,\sigma)^4}\, 2\mathcal{E}(\sigma) + \mathcal{O}(G^4)\,, \tag{7.60}$$

where the analytic continuation is given by

$$\operatorname{arccosh}(\sigma) = \mathrm{i}\arccos(\sigma)\,, \quad (\sigma^2-1)^\alpha = e^{\mathrm{i}\alpha\pi}(1-\sigma^2)^\alpha\,, \quad \sigma < 1\,. \tag{7.61}$$

Let us proceed by describing some checks that we have performed on our result. First of all as we have described in the previous section the energy loss is consistent with the IR divergence computed in the previous section. In order to compare our result with PN data we can now proceed and expand the elliptic energy loss in small relative velocity $v = \sqrt{\sigma^2-1}/\sigma$, with the result

$$\frac{\mathcal{E}(\sigma)}{\pi} = \frac{37}{15}v + \frac{2393}{840}v^3 + \frac{61703}{10080}v^5 + \frac{3131839}{354816}v^7 + \mathcal{O}(v^9)\,. \tag{7.62}$$

The function controlling the energy loss is actually analytic at $\sigma = 1$ and therefore the corresponding series for the bound case is twice Eq. (7.62). There is only sparse literature for the hyperbolic case, but we can compare up to fifth order in velocity to Refs. [100, 301, 302]. After the initial posting of our work it was reproduced to fifth order in Ref. [303] using a quantized worldline approach, by classical methods to order v^7 in Ref. [304] and to order v^{15} in Ref. [305].

For the hyperbolic case there is another interesting limit, namely the high-energy limit $\sigma \gg 1$ which is closely related to the massless process studied in chapter 5. We find that the logarithmic divergence in Eq. (7.58) cancels in this limit, in agreement to similar findings for the scattering angle which has been discussed in Refs. [297–299]. The leading order is

$$\mathcal{E} = \frac{35}{8}\pi(1+2\log 2)\sigma^3 + \mathcal{O}\big(\sigma^2\big)\,. \tag{7.63}$$

This result structurally agrees with an prediction made by Kovacs and Thorne long ago [301], but disagrees in the numerical coefficient.[6] Finally the complete result was also confirmed by similar methods to the ones employed here in Ref. [207].

[6] The results from Ref. [301] are used in Ref. [306]. From Figure 4 in Ref. [306] one can deduce the asymptotic $\mathcal{E} \approx 20\sigma^3 + \mathcal{O}(\sigma^2)$ while we have $\mathcal{E} \sim 32.79\sigma^3 + \mathcal{O}(\sigma^2)$. The result for the high-energy asymptotic was later confirmed numerically in Ref. [305], where the authors find $\mathcal{E} \sim 32.78(2)\sigma^3 + \mathcal{O}(\sigma^2)$.

8. Discussion and Outlook

In this thesis, we have demonstrated the power of an approach centered around on-shell scattering amplitudes to problems in gravity both in the context of classical and quantum physics.

One of our main results is the potential contribution to the scattering process at fourth order in perturbation theory. This result can be stated in a variety of equivalent ways, perhaps most pointedly, we have computed the effective correction to the Newtonian potential to order G^4, including an infinite number of velocity corrections. In order to make our result useful for phenomenological applications, the most pressing task is to complete the conservative sector at G^4. For this we have to include effects due to conservative radiation and in particular the effects of hereditary tails [276–281].

With an eye towards next-generation gravitational-wave experiments [17–19], one of the main points in favor of the amplitudes-based approach is scalability. While in the long term results are desired to the seventh order in the gravitational coupling [307], which translates to a computation involving six loops, the rapid progress in the field in the last years is encouraging. Gravitational amplitudes are known up to order G^6 [37] and we are confident that the corrections at least to order G^5 are within reach in the near future.

Realistically, the main bottleneck for higher-order computations will be associated to the evaluation of loop integrals. The methods described in this thesis have been crucial to obtain the results at the present state of the art [49, 93]. We have shown that the method of differential equations, in conjunction with the method of regions is a very efficient tool to compute the integrals necessary in the post-Minkowskian approximation. Already at the three-loop order required for G^4, we have encountered simple elliptic integrals. At higher orders and in the dissipative sector we might find even more complicated functions. This might make it necessary to divert our path towards series expansions or even fully numerical integral evaluation. Similar approaches have been taken recently in the collider-physics literature [165, 308, 309].

Another important result of this thesis are expressions for observables including dissipative effects. Making use of the observable-based approach by Kosower, Maybee and O'Connel [46] we have computed corrections to the scattering angle and the integrated energy loss due to gravitational bremsstrahlung, both at order G^3. A natural direction for the future is to compute more general observables. Very interesting in that regard are the extension to spin [310] and the possibility to extract waveforms directly [311]. In the spirit of collider physics and motivated by experimental demand it is also natural to consider more differential observables.

Most straightforward, we can consider the spectrum and the angular distribution of the radiated energy. Once again, work in this direction has already been performed in the context of collider phenomenology [179, 312]. For the moment the only major complication seems to be the introduction of additional scales which vastly increases the complexity of the associated integral functions. It will also be important to push the computations presented in this thesis to the next order in perturbation theory in order to complete the description of binary dynamics at the fourth order in the gravitational coupling.

In a different but related project we have used the method of multi-loop numerical unitarity to compute the two-loop four-graviton scattering amplitudes. This completes a long standing cycle of computations in perturbative quantum gravity, starting with the seminal works by 't Hooft and Veltman [211], Goroff and Sagnotti [212, 213] and van de Ven [313]. One of the main motivations for this work was to clear up a persisting controversy around the high-energy limit of gravitational scattering. Through the direct computation of the scattering angle in Einstein gravity at order G^3, we explicitly confirmed the result by Amati, Ciafaloni and Veneziano [228] which was questioned by Damour [229] recently.

As a byproduct of our computation we have demonstrated that the numerical unitarity method can be applied to intricate problems in quantum field theory that are characterized by high power counting and which include corrections beyond the planar limit. This opens up two major routes to pursuit: on the one hand we should continue focusing on problems in gravity, perhaps to obtain the three-loop corrections to the four-graviton amplitudes which are interesting in the context of studying the exponentiation structure of this amplitudes [270] or in the context of classical gravity for example through the inclusion of spin or finite-size effects (cf. Refs. [90, 91, 192]). On the other hand, we have made major progress towards addressing more complicated problems important for collider-physics phenomenology, most importantly the computation of amplitudes for processes describing the production of a Higgs boson in association with many jets which are important for collider-physics phenomenology (See e.g. Ref. [314]). We have already computed one and two-loop amplitudes for this class of processes and hope to report on progress soon.

A major point of the methods discussed in this thesis is the uniformization of the language with collider physics. To date, the dialogue between the collider physics and gravitational physics communities has been very fruitful, but in many ways we have reached the state of the art in collider physics. Pushing the methods further will require a combined effort from both communities.

A. Integrals

A.1. List of Feynman Integrals

In this appendix we list some useful formulas for Feynman integrals

Bubble integral with an off-shell eikonal propagator The bubble integral with an off-shell eikonal propagator is given by [145],

$$\int \frac{\mathrm{d}^D\ell}{\mathrm{i}\pi^{D/2}} \frac{1}{(-\ell^2)^{a_1}(2v\cdot\ell+\omega-\mathrm{i}\varepsilon)^{a_2}} = (v^2)^{a_1-D/2}\omega^{-2a_1-a_2+D} \times \frac{\Gamma(D/2-a_1)\Gamma(2a_1+a_2-D)}{\Gamma(a_1)\Gamma(a_2)}\,. \tag{A.1}$$

Triangle integral with eikonal propagators The on-shell triangle integral ($v\cdot q=0$) with an eikonal propagator is given by [145],

$$\int \frac{\mathrm{d}^D\ell}{\mathrm{i}\pi^{D/2}} \frac{1}{[-\ell^2]^{a_1}[-(\ell-q)^2]^{a_2}[-2v\cdot\ell-\mathrm{i}\varepsilon]^{a_3}} = (-q^2)^{D/2-a_1-a_2-1/2a_3}(v^2)^{-a_3} \times \frac{\Gamma(a_3/2)\Gamma(D/2-a_1-a_3/2)\Gamma(D/2-a_2-a_3/2)\Gamma(a_1+a_2+a_3/2-D/2)}{2\Gamma(a_1)\Gamma(a_2)\Gamma(a_3)\Gamma(D-a_1-a_2-a_3)}\,. \tag{A.2}$$

In the limit $a_3\to 0$ we recover the bubble integral, which was also derived explicitly in the main text

$$\int \frac{\mathrm{d}^D\ell}{\mathrm{i}\pi^{D/2}} \frac{1}{[-\ell^2]^{a_1}[-(\ell-q)^2]^{a_2}} = (-q^2)^{D/2-a_1-a_2} \times \frac{\Gamma(D/2-a_1-a_3/2)\Gamma(D/2-a_2-a_3/2)\Gamma(a_1+a_2+a_3/2-D/2)}{\Gamma(a_1)\Gamma(a_2)\Gamma(D-a_1-a_2-a_3)}\,. \tag{A.3}$$

Box integral with eikonal propagators We are interested in the evaluation of the integral

$$I^{\mathrm{II}}_{a_1,a_2,a_3,a_4} \coloneqq \int \frac{\mathrm{d}^D\ell}{\mathrm{i}\pi^{D/2}} \frac{1}{[2u_1\cdot\ell+\mathrm{i}\varepsilon]^{a_1}[-2u_2\cdot\ell+\mathrm{i}\varepsilon]^{a_2}[\ell^2]^{a_3}[(\ell-q)^2]^{a_4}}\,. \tag{A.4}$$

We start by introducing a Feynman parameterization

$$\begin{aligned} I^{\text{II}}_{a_1,a_2,a_3,a_4} &= \int \frac{\mathrm{d}^D\ell}{\mathrm{i}\pi^{D/2}} \frac{1}{[2u_1\cdot\ell+\mathrm{i}\varepsilon]^{a_1}[-2u_2\cdot\ell+\mathrm{i}\varepsilon]^{a_2}[\ell^2]^{a_3}[(\ell-q)^2]^{a_4}} \\ &= \frac{\Gamma(a_1+a_2)}{\Gamma(a_1)\Gamma(a_2)} \int \frac{\mathrm{d}^D\ell}{\mathrm{i}\pi^{D/2}} \int_0^1 \frac{\mathrm{d}u\, u^{a_1-1}(1-u)^{a_2-1}[\ell^2]^{-a_3}[(\ell-q)^2]^{-a_4}}{[(2uu_2-2(1-u)u_1)\cdot\ell+\mathrm{i}\varepsilon]^{a_1+a_2}} \,. \end{aligned} \tag{A.5}$$

We recognize that this expression is again of the form of the triangle integral in Eq. (A.2), with the identification

$$v^\mu = uu_2^\mu - (1-u)u_1^\mu \,, \quad v\cdot q = 0, \quad v^2 = u^2+(1-u)^2-2yu(1-u)\,. \tag{A.6}$$

Thereby the integral is reduced to a parametric integral

$$I^{\text{II}}_{a_1,a_2,a_3,a_4} = I^{\text{II}}_{a_1+a_2,0,a_3,a_4} \frac{\Gamma(a_1+a_2)}{\Gamma(a_1)\Gamma(a_2)} \int_0^1 \frac{\mathrm{d}u\, u^{a_1-1}(1-u)^{a_2-1}}{[u^2+(1-u)^2-2yu(1-u)]^{(a_1+a_2)/2}} \,. \tag{A.7}$$

We can use the parameterization by the x-variable introduced in Eq. (4.74), which allows us to factor the quadratic

$$u^2+(1-u)^2-2yu(1-u) = [1-(1+x)u][1-(1+x)/xu]\,. \tag{A.8}$$

The remaining u-integral is of the form of the Appel hypergeometric function F_1 [315], but is actually a special case that can be reduced to the Gauss hypergeometric function ${}_2F_1$ [316],

$$\begin{aligned} &\frac{\Gamma(a_1+a_2)}{\Gamma(a_1)\Gamma(a_2)} \int_0^1 \frac{\mathrm{d}u\, u^{a_1-1}(1-u)^{a_2-1}}{[u^2+(1-u)^2-2yu(1-u)]^{(a_1+a_2)/2}} \\ &= \frac{\Gamma(a_1+a_2)}{\Gamma(a_1)\Gamma(a_2)} \int_0^1 \frac{\mathrm{d}u\, u^{a_1-1}(1-u)^{a_2-1}}{\{[1-(1+x)u][1-(1+x)/xu]\}^{(a_1+a_2)/2}} \\ &= F_1\left[a_1; (a_1+a_2)/2, (a_1+a_2)/2; a_1+a_2; 1+x, \frac{1+x}{x}\right] \\ &= (-1)^{a_1}x^{a1}{}_2F_1\left[\begin{matrix} a_1 & (a_1+a_2)/2 \\ & a_1+a_2 \end{matrix}; 1-x^2\right]. \end{aligned} \tag{A.9}$$

Using identities for hypergeometric functions we obtain the following expression for the box integral with generic indices:

$$I^{\text{II}}_{a_1,a_2,a_3,a_4} = I^{\text{II}}_{a_1+a_2,0,a_3,a_4} {}_2F_1\left[\begin{matrix} a_1 & a_2 \\ (a_1+a_2+1)/2 \end{matrix}; \frac{1+y}{2}\right]. \tag{A.10}$$

In this form we can continue to scattering kinematics $y > 1$ using the following analytic continuation of the hypergeometric function [317]

$$
\begin{aligned}
{}_2F_1\left[\begin{matrix}\alpha & \beta\\ & \gamma\end{matrix};z\right] &= \frac{\Gamma(\gamma)\Gamma(\gamma-\alpha-\beta)}{\Gamma(\gamma-\alpha)\Gamma(\gamma-\beta)}{}_2F_1\left[\begin{matrix}\alpha & \beta\\ \alpha+\beta-\gamma+1\end{matrix};1-z\right] \\
&\quad + (1-z)^{-\alpha-\beta+\gamma}\frac{\Gamma(\gamma)\Gamma(\alpha+\beta-\gamma)}{\Gamma(\alpha)\Gamma(\beta)}{}_2F_1\left[\begin{matrix}\gamma-\alpha & \gamma-\beta\\ 1+\gamma-\alpha-\beta\end{matrix};1-z\right].
\end{aligned}
\tag{A.11}
$$

Using this relation in conjunction to additional identities for hypergeometric functions, we find the following formula valid for $y > 1$

$$
\begin{aligned}
I^{\text{II}}_{a_1,a_2,a_3,a_4} &= I^{\text{II}}_{a_1+a_2,0,a_3,a_4}\Gamma[(1-a_1-a_2)/2]\Gamma[(1+a_1+a_2)/2] \\
&\quad\times\left\{\frac{1}{\Gamma[(1+a_1-a_2)/2]\Gamma[(1-a_1+a_2)/2]}{}_2F_1\left[\begin{matrix}a_1 & a_2\\ (a_1+a_2+1)/2\end{matrix};\frac{1-y}{2}\right]\right. \\
&\quad\left.+\frac{e^{\mathrm{i}\pi\frac{1-a_1-a_2}{2}}}{\Gamma(a_1)\Gamma(a_2)}\left(\frac{y^2-1}{4}\right)^{\frac{1-a_1-a_2}{2}}{}_2F_1\left[\begin{matrix}1-a_1 & 1-a_2\\ (3-a_1-a_2)/2\end{matrix};\frac{1-y}{2}\right]\right\}.
\end{aligned}
\tag{A.12}
$$

This form is particularly useful as it fully exposes the terms with potential non-analytic scaling as $y \to 1$ which are related to the radiation region as well as the imaginary part of the expression. Formula (A.12) may also be used if a_2 is a negative integer, which allows to evaluate a general class of triangle tensor integrals. We also note that due to an identity by Euler, the hypergeometric function at argument $1/2$ can be expressed in terms of Gamma functions

$$
{}_2F_1\left[\begin{matrix}a_1 & a_2\\ (a_1+a_2+1)/2\end{matrix};\frac{1}{2}\right] = \frac{\sqrt{\pi}\Gamma[(a_1+a_2+1)/2]}{\Gamma[(a_1+1)/2]\Gamma[(a_2+1)/2]}
\tag{A.13}
$$

and thus the boundary conditions at $y = 0$, when expanded in ϵ are expressible in terms of zeta values.

Euclidean triangle integral with eikonal propagator For the boundary conditions in the potential region, we need the Euclidean version of the triangle integral, which is obtained by analytic continuation of Eq. (A.2)

$$
\begin{aligned}
&\int\frac{\mathrm{d}^{D-1}\boldsymbol{\ell}}{\pi^{(D-1)/2}}\frac{1}{(\boldsymbol{\ell}^2)^a[(\boldsymbol{\ell}-\boldsymbol{q})^2]^b(2\hat{\boldsymbol{z}}\cdot\boldsymbol{\ell}-\mathrm{i}\varepsilon)^c} \\
&= e^{\frac{\mathrm{i}\pi c}{2}}(\boldsymbol{q}^2)^{\frac{3}{2}-a-b-\frac{c}{2}-\epsilon}\frac{\Gamma\left(\frac{c}{2}\right)\Gamma\left(\frac{3}{2}-a-\frac{c}{2}-\epsilon\right)\Gamma\left(\frac{3}{2}-b-\frac{c}{2}-\epsilon\right)\Gamma\left(a+b+\frac{c}{2}+\epsilon-\frac{3}{2}\right)}{2\Gamma(a)\Gamma(b)\Gamma(c)\Gamma(3-a-b-c-2\epsilon)}.
\end{aligned}
\tag{A.14}
$$

Taking the limit $c \to 0$, we find the bubble integral

$$
\begin{aligned}
&\int\frac{\mathrm{d}^{D-1}\boldsymbol{\ell}}{\pi^{(D-1)/2}}\frac{1}{(\boldsymbol{\ell}^2)^a[(\boldsymbol{\ell}-\boldsymbol{q})^2]^b} \\
&= (\boldsymbol{q}^2)^{\frac{3}{2}-a-b-\epsilon}\frac{\Gamma\left(\frac{3}{2}-a-\epsilon\right)\Gamma\left(\frac{3}{2}-b-\epsilon\right)\Gamma\left(a+b+\epsilon-\frac{3}{2}\right)}{\Gamma(a)\Gamma(b)\Gamma(3-a-b-2\epsilon)}.
\end{aligned}
\tag{A.15}
$$

In the main text we have used the following special cases

$$\int \frac{\mathrm{d}^{D-1}\boldsymbol{\ell}}{\pi^{(D-1)/2}} \frac{1}{\boldsymbol{\ell}^2(\boldsymbol{\ell}-\boldsymbol{q})^2(2\hat{\boldsymbol{z}}\cdot\boldsymbol{\ell}-\mathrm{i}\varepsilon)} = \left(\boldsymbol{q}^2\right)^{-\epsilon-1} \frac{\mathrm{i}\sqrt{\pi}\,\Gamma(-\epsilon)^2\Gamma(1+\epsilon)}{2\Gamma(-2\epsilon)}\,, \tag{A.16}$$

$$\int \frac{\mathrm{d}^{D-1}\boldsymbol{\ell}}{\pi^{(D-1)/2}} \frac{1}{\boldsymbol{\ell}^2(\boldsymbol{\ell}-\boldsymbol{q})^2} = \left(\boldsymbol{q}^2\right)^{-\epsilon-1/2} \frac{\Gamma\left(\frac{1}{2}-\epsilon\right)^2\Gamma\left(\frac{1}{2}+\epsilon\right)}{\Gamma(1-2\epsilon)}\,. \tag{A.17}$$

B. Transformations

B.1. Fourier Transform

In the main text we are interested in the transversal, i.e. $D-2$ dimensional Fourier transform and its inverse

$$(\mathcal{F}f)(\boldsymbol{b}) \coloneqq \frac{\mu^{2\epsilon}}{4E|\boldsymbol{p}|}\int \frac{\mathrm{d}^{D-2}\boldsymbol{q}}{(2\pi)^{D-2}}\, e^{\mathrm{i}\boldsymbol{q}\cdot\boldsymbol{b}}\, f(\boldsymbol{q})\,, \tag{B.1}$$

$$(\mathcal{F}^{-1}f)(\boldsymbol{q}) = 4E|\boldsymbol{p}|\mu^{-2\epsilon}\int \mathrm{d}^{D-2}\boldsymbol{b}\, e^{-\mathrm{i}\boldsymbol{q}\cdot\boldsymbol{b}}\, f(\boldsymbol{b})\,. \tag{B.2}$$

The Fourier transformation has the useful property that it trivializes convolutions:

$$\mathcal{F}(f_1\otimes f_2) = \mathcal{F}(f_1)\mathcal{F}(f_2)\,, \qquad (f_1\otimes f_2)(\boldsymbol{q}) \coloneqq \frac{\mu^{2\epsilon}}{4E|\boldsymbol{p}|}\int \frac{\mathrm{d}^{D-2}\boldsymbol{\ell}}{(2\pi)^{D-2}}\, f_1(\boldsymbol{\ell})\, f_2(\boldsymbol{q}-\boldsymbol{\ell})\,. \tag{B.3}$$

All Fourier integrals in the main text can be derived from the well-known formula

$$\mathcal{F}\big[(\boldsymbol{q}^2)^\alpha\big] = \frac{\mu^{2\epsilon}}{E|\boldsymbol{p}|}\frac{2^{2\alpha-2}}{\pi^{1-\epsilon}}\frac{\Gamma(1+\alpha-\epsilon)}{\Gamma(-\alpha)}\frac{1}{(\boldsymbol{b}^2)^{\alpha+1-\epsilon}}\,. \tag{B.4}$$

We also need the convolution of a vector, which is obtained though taking a derivative:

$$\mathcal{F}[\boldsymbol{q}(\boldsymbol{q}^2)^\alpha] = -\mathrm{i}\frac{\partial}{\partial\boldsymbol{b}}\mathcal{F}\big[(\boldsymbol{q}^2)^\alpha\big] = \mathrm{i}\frac{\mu^{2\epsilon}}{E|\boldsymbol{p}|}\frac{2^{2\alpha-1}}{\pi^{1-\epsilon}}\frac{\Gamma(2+\alpha-\epsilon)}{\Gamma(-\alpha)}\frac{\boldsymbol{b}}{(\boldsymbol{b}^2)^{\alpha+2-\epsilon}}\,. \tag{B.5}$$

B.2. Regularized Legendre Polynomials

We define generalizations of the Legendre polynomials in $D=4-2\epsilon$ dimensions, explicitly through normalized Jacobi polynomial

$$P_J^{(\epsilon)}(x) \coloneqq P_J^{(-\epsilon,-\epsilon)}(x)/P_J^{(-\epsilon,-\epsilon)}(1) = {}_2F_1\left[\begin{matrix}-J & J+1-2\epsilon \\ & 1-\epsilon\end{matrix}; \frac{1-x}{2}\right]. \tag{B.6}$$

These polynomials are also closely related to the Gegenbauer polynomials $C_n^{(\nu)}(x)$

$$P_J^{(\epsilon)}(x) = \frac{\Gamma(J+1)\Gamma(1-2\epsilon)}{\Gamma(J+1-2\epsilon)}C_J^{(1/2-\epsilon)}(x)\,. \tag{B.7}$$

For the convenience of the reader we collect some properties of the dimensional-regularized Legendre polynomials $P_J^{(\epsilon)}$, which are direct consequences of the properties of the Gegenbauer polynomials and Jacobi polynomials (see e.g. Refs. [317, 318]).

Explicit representation The explicit series representation of the regularized Legendre polynomials is

$$P_J^{(\epsilon)}(x) = \frac{\Gamma(1-\epsilon)}{\sqrt{\pi}} 2^{-2\epsilon} \sum_{m=0}^{\lfloor J/2 \rfloor} (-1)^m \frac{J!}{m!(J-2m)!} \frac{\Gamma\left(J-m-\epsilon+\frac{1}{2}\right)}{\Gamma(J-2\epsilon+1)} (2x)^{J-2m} . \tag{B.8}$$

Normalization This functions are normalized at $x = 1$ and reduce to the familiar Legendre polynomials in the limit $\epsilon \to 0$

$$P_J^{(0)}(x) = P_J(x) , \quad P_J^{(\epsilon)}(1) = 1 . \tag{B.9}$$

Rodrigues' formula The regularized Legendre polynomials are generated by the following Rodrigues' formula

$$P_J^{(\epsilon)}(x) = \left(\frac{-1}{2}\right)^J \frac{\Gamma(1-\epsilon)}{\Gamma(J+1-\epsilon)} \left(1-x^2\right)^{\epsilon} \frac{\mathrm{d}^J}{\mathrm{d}x^J} \left[\left(1-x^2\right)^{J-\epsilon}\right] . \tag{B.10}$$

Completeness and orthogonality The functions form an complete orthogonal system with

$$\int_{-1}^{1} \mathrm{d}x \, (1-x^2)^{-\epsilon} P_J^{(\epsilon)}(x) P_{J'}^{(\epsilon)}(x) = N_J^{(\epsilon)} \delta_{JJ'} , \tag{B.11}$$

$$\sum_{J=0}^{\infty} \frac{1}{N_J^{(\epsilon)}} P_J^{(\epsilon)}(x) P_J^{(\epsilon)}(y) = (1-x^2)^{\epsilon} \delta(x-y) , \; x, y \in [-1, 1] . \tag{B.12}$$

The normalization constant $N_J^{(\epsilon)}$ is given by

$$N_J^{(\epsilon)} = \frac{\mathrm{Vol}(\mathbb{S}^{D-1})}{\mathrm{Vol}(\mathbb{S}^{D-2}) \dim(H_J^{D-1})} = \frac{2^{1-2\epsilon}}{2J+1-2\epsilon} \frac{\Gamma(J+1)\Gamma(1-\epsilon)^2}{\Gamma(J+1-2\epsilon)} , \tag{B.13}$$

where H_J^{D-1} is the space of harmonic polynomials and $\mathbb{S}^n$ is an n-Sphere.

Large-J asymptotic In the limit of large J, the regularized Legendre polynomials have the following asymptotic expansion

$$P_J^{(\epsilon)}(\cos\theta) \sim \frac{2^{\frac{1}{2}-\epsilon} \Gamma(1-\epsilon) (J \sin\theta)^{\epsilon-\frac{1}{2}} \cos\left(J\theta + \left(\epsilon - \frac{1}{2}\right)\left(\frac{\pi}{2} - \theta\right)\right)}{\sqrt{\pi}} . \tag{B.14}$$

The normalization factor has the following asymptotic

$$\frac{1}{N_J^{(\epsilon)}} \sim \frac{2^{2\epsilon} J^{1-2\epsilon}}{\Gamma(1-\epsilon)^2} \,. \tag{B.15}$$

Angular momentum eigenfunctions The angular momentum operator can be expressed as

$$\widehat{J}^2 f \coloneqq \Delta_{\mathbb{S}^n} f = \frac{1}{\sin^{n-1}\theta} \frac{\partial}{\partial\theta} \left(\sin\theta^{n-1} \frac{\partial f}{\partial\theta} \right) + \frac{1}{\sin^2\theta} \Delta_{\mathbb{S}^{n-1}} f \,. \tag{B.16}$$

The conservative process is confined to a plane, so solutions should be invariant on the sphere $\mathbb{S}^{n-2}$. Therefore

$$\Delta_{\mathbb{S}^n} f(\theta) = \frac{1}{\sin^{n-1}\theta} \frac{\partial}{\partial\theta} \left(\sin\theta^{n-1} \frac{\partial f}{\partial\theta} \right) . \tag{B.17}$$

Now in the case at hand $n = D - 2 = 2 - 2\epsilon$ such that

$$\widehat{J}^2 P_J^{(\epsilon)}(\cos\theta) = J(J+1-2\epsilon) P_J^{(\epsilon)}(\cos\theta) \,. \tag{B.18}$$

The eigenvalue $C_J = J(J+1-2\epsilon)$ is the Casimir of the rotation group.

B.3. Partial-Wave Analysis in Dimensional Regularization

As the amplitudes encountered in the main text are divergent as for small angles, their partial-wave transform is in general ill-defined. A simple example of this is the partial-wave transform of the tree amplitude, which involves the divergent integral

$$\int_{-1}^{1} \frac{\mathrm{d}x}{(1-x)} P_J(x) \,. \tag{B.19}$$

In order to overcome this issue, we work in $3 - 2\epsilon$ spatial dimension, with $\epsilon < 0$. We define the following *partial-wave transformation*[1]

$$(\mathcal{P}f)(J) \coloneqq \frac{(\boldsymbol{p}^2/(4\pi\mu^2))^{-\epsilon}}{16\pi\Gamma(1-\epsilon)} \frac{2|\boldsymbol{p}|}{\sqrt{s}} \int_{-1}^{1} \mathrm{d}x \, (1-x^2)^{-\epsilon} \, P_J^{(\epsilon)}(x) f(x) \,. \tag{B.20}$$

The inverse transformation is

$$(\mathcal{P}^{-1}g)(x) = \left(\frac{\boldsymbol{p}^2}{4\pi\mu^2} \right)^{\epsilon} \frac{\sqrt{s}}{2|\boldsymbol{p}|} 16\pi\Gamma(1-\epsilon) \sum_{J=0}^{\infty} \frac{1}{N_J^{(\epsilon)}} g_J P_J^{(\epsilon)}(x) \tag{B.21}$$

[1] The reason for the prefactors will become evident later.

In the limit $\epsilon \to 0$ we recover the familiar form of the partial-wave transform in three spatial dimensions

$$(\mathcal{P}f)(J) \to \frac{|\boldsymbol{p}|}{8\pi\sqrt{s}} \int_{-1}^{1} \mathrm{d}x\, P_J(x) f(x)\,, \quad (\mathcal{P}^{-1}g)(x) \to \frac{4\pi\sqrt{s}}{|\boldsymbol{p}|} \sum_{J=0}^{\infty} (2J+1) g_J P_J(x)\,. \tag{B.22}$$

The partial-wave amplitudes $a_J(\boldsymbol{p}^2)$ are defined as

$$a_J(\boldsymbol{p}^2) \coloneqq \mathcal{P}\mathcal{M} = \frac{(\boldsymbol{p}^2/(4\pi\mu^2))^{-\epsilon}}{16\pi\Gamma(1-\epsilon)} \frac{2|\boldsymbol{p}|}{\sqrt{s}} \int_{-1}^{1} \mathrm{d}x\, (1-x^2)^{-\epsilon}\, P_J^{(\epsilon)}(x) \mathcal{M}(\boldsymbol{p}^2, x) \tag{B.23}$$

For the analysis in the main text we are interested mainly in the small angle limit $\theta \ll 1, x \sim 1$, which corresponds to the large angular momentum limit. For this we need the following master formula assuming a is not a positive integer

$$\mathcal{P}\left[\left(\frac{1-x}{2}\right)^a\right] = \frac{(\boldsymbol{p}^2/(\pi\mu^2))^{-\epsilon}}{8\pi} \frac{2|\boldsymbol{p}|}{\sqrt{s}} \frac{\Gamma(J-a)\Gamma(1+a-\epsilon)}{\Gamma(-a)\Gamma(a+J+2-2\epsilon)} \tag{B.24}$$

We can see that for large J this terms scale as

$$\mathcal{P}\left[\left(\frac{1-x}{2}\right)^a\right] \sim \frac{(\boldsymbol{p}^2/(\pi\mu^2))^{-\epsilon}}{8\pi} \frac{2|\boldsymbol{p}|}{\sqrt{s}} \frac{\Gamma(1+a-\epsilon)}{\Gamma(-a)} J^{-2-2a+2\epsilon} \tag{B.25}$$

We see that higher powers of $\boldsymbol{q}^2$ are suppressed in the classical limit as expected.

In case a is a positive integer we can decompose $(1-x)^a$ as a finite sum of Gegenbauer polynomials, each of which would transform to a Kronecker delta, i.e. a finite, fixed J. Therefore we can see that analytic-in-q^2 parts do not contribute to the large $J \to \infty$ limit. In the case $a = -1$ which is encountered at leading order, we find

$$\mathcal{P}\left[\frac{1}{1-x}\right] = -\frac{|\boldsymbol{p}|}{2\pi\sqrt{s}} \frac{1}{\epsilon} + \mathcal{O}(\epsilon^0)\,, \tag{B.26}$$

which explicitly shows that the integral is divergent in three spatial dimensions.

It is rather straightforward to prove the master formula (B.24) by using the Rodrigues' formula (B.10) and repeated partial integration using that for appropriate

$\epsilon < 0$ all boundary terms vanish. Explicitly we have

$$\begin{aligned}
&\int_{-1}^{1} \mathrm{d}x\,(1-x^2)^{-\epsilon}\,P_J^{(\epsilon)}(x)(1-x)^{\alpha} \\
&= \left(\frac{-1}{2}\right)^J \frac{\Gamma(1-\epsilon)}{\Gamma(J+1-\epsilon)} \int_{-1}^{1} \mathrm{d}x\,(1-x)^{\alpha} \frac{\mathrm{d}^J}{\mathrm{d}x^J}\left[(1-x^2)^{J-\epsilon}\right] \\
&= 2^{-J} \frac{\Gamma(1+\alpha)}{\Gamma(1-J+\alpha)} \frac{\Gamma(1-\epsilon)}{\Gamma(J+1-\epsilon)} \int_{-1}^{1} \mathrm{d}x\,(1-x)^{\alpha-J}(1-x^2)^{J-\epsilon} \\
&= 2^{-J} \frac{\Gamma(1+\alpha)}{\Gamma(1-J+\alpha)} \frac{\Gamma(1-\epsilon)}{\Gamma(J+1-\epsilon)} \frac{2^{\alpha+J-2\epsilon+1}\Gamma(\alpha+1-\epsilon)\Gamma(J+1-\epsilon)}{\Gamma(J+\alpha+2-2\epsilon)} \\
&= \frac{2^{\alpha-2\epsilon+1}\Gamma(1-\epsilon)\Gamma(\alpha-\epsilon+1)\Gamma(J-\alpha)}{\Gamma(-\alpha)\Gamma(J+\alpha-2\epsilon+2)}\,.
\end{aligned} \tag{B.27}$$

In this derivation we also made use of the elementary integral

$$\int_{-1}^{1} (1-x^2)^{\alpha}(1-x)^{\beta} = \frac{2^{2\alpha+\beta+1}\Gamma(\alpha+1)\Gamma(\alpha+\beta+1)}{\Gamma(2\alpha+\beta+2)}\,. \tag{B.28}$$

Partial-wave convolution theorem We define the following angular convolution

$$\begin{aligned}
&[f \star g](x) \\
&:= \frac{(\mu^2)^{\epsilon}|\boldsymbol{p}|^{D-3}}{E\sqrt{1-x^2}} \frac{(4\pi)^{(1-D)/2}}{\Gamma[(D-3)/2]} \int_{-1}^{1} \mathrm{d}y \int_{-1}^{1} \mathrm{d}z \left(\frac{1-x^2-y^2-z^2+2xyz}{1-x^2}\right)^{\frac{D-5}{2}} f(y)g(z)\,.
\end{aligned} \tag{B.29}$$

As a special case of the convolution theorem for the Jacobi transform (see e.g. Ref. [319]), we have

$$\mathcal{P}(f \star g) = \mathcal{P}(f)\mathcal{P}(g)\,. \tag{B.30}$$

We can relate the above integral to a two-particle phase space integral. First we have

$$\mathrm{d}\Phi_2 = \frac{(\mu^2)^{\epsilon}|\boldsymbol{p}|^{D-3}}{4E} \frac{\mathrm{d}^{D-2}\Omega}{(2\pi)^{D-2}}\,. \tag{B.31}$$

We define three angular variables

$$x = \frac{\boldsymbol{p}\cdot\boldsymbol{p}'}{\boldsymbol{p}^2}\,, \quad y = \frac{\boldsymbol{\ell}\cdot\boldsymbol{p}}{\boldsymbol{p}^2}\,, \quad z = \frac{\boldsymbol{\ell}\cdot\boldsymbol{p}'}{\boldsymbol{p}^2}\,, \tag{B.32}$$

The angular integration can be split into a part in the plane spanned by $\boldsymbol{p}$ and $\boldsymbol{p}'$ and a part perpendicular to it

$$\boldsymbol{\ell}_{\perp}^2 = \mathrm{Gram}(\boldsymbol{p},\boldsymbol{p}',\boldsymbol{\ell})/\,\mathrm{Gram}(\boldsymbol{p},\boldsymbol{p}') = \boldsymbol{p}^2 \frac{1-x^2-y^2-z^2+2xyz}{1-x^2}\,. \tag{B.33}$$

The integration measure splits

$$\mathrm{d}^{D-2}\Omega = \frac{\mathrm{d}y\mathrm{d}z}{\sqrt{1-x^2}} \mathrm{d}^{D-4}\Omega \left(\frac{1-x^2-y^2-z^2+2xyz}{1-x^2}\right)^{\frac{D-5}{2}}\,, \tag{B.34}$$

such that we have

$$\mathrm{d}\Phi_2 = \frac{(\mu^2)^\epsilon |\boldsymbol{p}|^{D-3}}{4E} \frac{1}{(2\pi)^{D-2}} \frac{\mathrm{d}y\mathrm{d}z}{\sqrt{1-x^2}} \mathrm{d}^{D-4}\Omega \left(\frac{1-x^2-y^2-z^2+2xyz}{1-x^2} \right)^{\frac{D-5}{2}} . \tag{B.35}$$

If the functions only depend on the perpendicular component of the loop momentum, the angular integration can be trivially performed

$$\int \mathrm{d}^{D-4}\Omega = \frac{2\pi^{(D-3)/2}}{\Gamma[(D-3)/2]} . \tag{B.36}$$

Assembling the pieces, we find

$$f \star g = \int \mathrm{d}\Phi_2 f(y) g(z) . \tag{B.37}$$

B.4. Relation Between Phase Shift and Scattering Angle

Recall that the amplitude expressed in terms of partial waves is

$$\mathcal{M}(s,t) = \left(\frac{\boldsymbol{p}^2}{4\pi\mu^2} \right)^\epsilon \frac{\sqrt{s}}{2|\boldsymbol{p}|} 16\pi\Gamma(1-\epsilon) \sum_{J=0}^{\infty} \frac{1}{N_J^{(\varepsilon)}} (e^{2\mathrm{i}\delta_J(\boldsymbol{p}^2)} - 1) P_J^{(\epsilon)}(\cos\theta) . \tag{B.38}$$

We will ignore the identity-piece in the as it corresponds to free propagation (which is exactly forward with $\theta = \pi$) in the following, explicitly we have

$$\sum_{J=0}^{\infty} \frac{1}{N_J^{(\epsilon)}} P_J^{(\epsilon)}(\cos\theta) = (\sin\theta)^{2\epsilon} \, \delta(\cos\theta - 1) . \tag{B.39}$$

Furthermore the dominant contribution will come from $J \gg 0$, so we can approximate the summand using the expansions (B.14) and (B.15),

$$\mathcal{M}(s,t) \sim -\frac{2\mathrm{i}}{\sqrt{\pi}\Gamma(1-\epsilon)} \sum_{J=0}^{\infty} e^{2\mathrm{i}\delta_J} \left(\frac{J}{2} \sin\theta \right)^{1/2-\epsilon} \cos\Big[(1/2-\epsilon)\Big(\theta - \frac{\pi}{2}\Big) + J\theta \Big] \tag{B.40}$$

The expressing the cosine in terms of exponentials, the integrand can be written in terms of two phase factors which depending on J

$$\Phi_\pm = 2\,\mathrm{Re}\,\delta_J \pm J\theta . \tag{B.41}$$

The phase Φ_- is related to an outgoing wave and can be neglected. The classical scattering angle χ can be identified angle at which the phase is stationary

$$\left. \frac{\partial \Phi_+}{\partial J} \right|_{\theta=\chi} = 0 , \tag{B.42}$$

which directly leads to the condition, relating the conservative angle to the phase

$$\chi = -2\frac{\partial \operatorname{Re} \delta_J}{\partial J} \,. \tag{B.43}$$

Although the phase δ_J is in general divergent as $\epsilon \to 0$ the scattering angle is finite.

C. Graviton States in $D_{\rm S}$ Dimensions

The polarization of spin-two fields are represented by symmetric transverse traceless (STT) tensors $\epsilon^{\lambda}_{\mu\nu}$

$$\eta^{\mu\nu}\epsilon^{\lambda}_{\mu\nu} = 0\,, \quad p^{\mu}\epsilon^{\lambda}_{\mu\nu} = 0\,, \quad \epsilon^{\lambda}_{[\mu\nu]} = 0\,. \tag{C.1}$$

In $D_{\rm s}$ dimensions, there are $(D_{\rm s}-2+1)(D_{\rm s}-2)-1$ independent STT tensors. In four dimensions we can construct the two polarizations of the graviton from vector polarizations $\epsilon^{\pm}$ [320]

$$\epsilon^{\pm\pm}_{\mu\nu} = \epsilon^{\pm}_{\mu}\epsilon^{\pm}_{\nu}\,. \tag{C.2}$$

For dimensions beyond four, we can use a dimensional reduction approach. A basis in $D_{\rm s}$ dimensions is constructed in Ref. [321]. However, the basis given in that reference is not orthonormal and thus does not satisfy a simple completeness relation, but this is readily fixed by using the Gram–Schmidt process. The resulting basis is the following

$$\epsilon^{ii}_{\mu\nu} = \sqrt{\frac{i+1}{i+2}}\left(\frac{1}{i+1}\sum_{j\in\{\pm,1,\ldots,i-1\}}\epsilon^{j}_{\mu}\epsilon^{*j}_{\nu} + \epsilon^{i}_{\mu}\epsilon^{i}_{\nu}\right), \tag{C.3}$$

$$\epsilon^{\pm i}_{\mu\nu} = \frac{1}{\sqrt{2}}\left(\epsilon^{\pm}_{\mu}\epsilon^{i}_{\nu} + \epsilon^{i}_{\mu}\epsilon^{\pm}_{\nu}\right), \tag{C.4}$$

$$\epsilon^{ij}_{\mu\nu} = \frac{1}{\sqrt{2}}\left(\epsilon^{i}_{\mu}\epsilon^{j}_{\nu} + \epsilon^{j}_{\mu}\epsilon^{i}_{\nu}\right), i<j\,, \tag{C.5}$$

where $i,j \in \{1,\ldots,D_{\rm s}-4\}$ and the vector polarizations beyond four dimensions ϵ^{i} satisfy

$$\epsilon^{\pm}\cdot\epsilon^{i} = 0\,, \quad p\cdot\epsilon^{i} = 0\,, \quad \epsilon^{i}\cdot\epsilon^{j} = -\delta^{ij}\,. \tag{C.6}$$

It is straightforward to to check that this vectors are orthonormal and complete

$$\epsilon^{\lambda}_{\mu\nu}\epsilon^{\lambda'\,\mu\nu} = \delta^{\lambda\lambda'}\,, \tag{C.7}$$

$$\sum_{\lambda}\epsilon^{\lambda}_{\mu\nu}\epsilon^{*\lambda\,\rho\sigma} = \Pi^{(2)\rho\sigma}_{\mu\nu}\,, \tag{C.8}$$

where $\Pi^{(2)}_{\mu\nu\rho\sigma}$ is the projector onto the space of STT-tensors and $\Pi^{(1)}_{\mu\nu}$, which has the following representation in terms of transversal vector projectors $\Pi^{(1)\nu}_{\mu}$

$$\Pi^{(2)\rho\sigma}_{\mu\nu} = \frac{1}{2}\left(\Pi^{(1)\rho}_{\mu}\Pi^{(1)\sigma}_{\nu} + \Pi^{(1)\sigma}_{\mu}\Pi^{(1)\rho}_{\nu}\right) - \frac{1}{D_{\rm s}-2}\Pi^{(1)}_{\mu\nu}\Pi^{(1)\rho\sigma}\,. \tag{C.9}$$

D. Functions in the 4PM Amplitude

The coefficient functions appearing in the amplitude in Eq. (7.21) are explicitly

$$h_1 = \frac{1151 - 3336\sigma + 3148\sigma^2 - 912\sigma^3 + 339\sigma^4 - 552\sigma^5 + 210\sigma^6}{12(\sigma^2-1)}\,, \tag{D.1}$$

$$h_2 = \frac{1}{2}\big(5 - 76\sigma + 150\sigma^2 - 60\sigma^3 - 35\sigma^4\big)\,, \tag{D.2}$$

$$h_3 = \sigma\frac{(-3+2\sigma^2)}{4(\sigma^2-1)}\big(11 - 30\sigma^2 + 35\sigma^4\big)\,, \tag{D.3}$$

$$\begin{aligned} h_4 = \frac{1}{144\big(\sigma^2-1\big)^2\sigma^7}(&-45 + 207\sigma^2 - 1471\sigma^4 + 13349\sigma^6 \\ &- 37566\sigma^7 + 104753\sigma^8 - 12312\sigma^9 - 102759\sigma^{10} - 105498\sigma^{11} \\ &+ 134745\sigma^{12} + 83844\sigma^{13} - 101979\sigma^{14} + 13644\sigma^{15} + 10800\sigma^{16}\big)\,, \end{aligned} \tag{D.4}$$

$$\begin{aligned} h_5 = \frac{1}{4(\sigma^2-1)}\big(&1759 - 4768\sigma + 3407\sigma^2 - 1316\sigma^3 + 957\sigma^4 \\ &- 672\sigma^5 + 341\sigma^6 + 100\sigma^7\big)\,, \end{aligned} \tag{D.5}$$

$$\begin{aligned} h_6 = \frac{1}{24(\sigma^2-1)^2}\big(&1237 + 7959\sigma - 25183\sigma^2 + 12915\sigma^3 + 18102\sigma^4 \\ &- 12105\sigma^5 - 9572\sigma^6 + 2973\sigma^7 + 5816\sigma^8 - 2046\sigma^9\big)\,, \end{aligned} \tag{D.6}$$

$$h_7 = 2\sigma\frac{(-852 - 283\sigma^2 - 140\sigma^4 + 75\sigma^6)}{3(\sigma^2-1)}\,, \tag{D.7}$$

$$\begin{aligned} h_8 = \frac{\sigma}{8(\sigma^2-1)^2}\big(&-304 - 99\sigma + 672\sigma^2 + 402\sigma^3 - 192\sigma^4 - 719\sigma^5 \\ &- 416\sigma^6 + 540\sigma^7 + 240\sigma^8 - 140\sigma^9\big)\,, \end{aligned} \tag{D.8}$$

$$h_9 = \frac{1}{2}\big(52 - 532\sigma + 351\sigma^2 - 420\sigma^3 + 30\sigma^4 - 25\sigma^6\big)\,, \tag{D.9}$$

$$h_{10} = 2\big(27 + 90\sigma^2 + 35\sigma^4\big)\,, \tag{D.10}$$

$$h_{11} = 20 + 111\sigma^2 + 30\sigma^4 - 25\sigma^6\,, \tag{D.11}$$

$$h_{12} = \frac{834 + 2095\sigma + 1200\sigma^2}{2(\sigma^2-1)}\,, \tag{D.12}$$

$$h_{13} = -\frac{1183 + 2929\sigma + 2660\sigma^2 + 1200\sigma^3}{2(\sigma^2-1)}\,, \tag{D.13}$$

$$h_{14} = \frac{7(169 + 380\sigma^2)}{4(\sigma-1)}\,. \tag{D.14}$$

List of Tables

List of Figures

German Abstract

Wir wenden on-shell Methoden die im Kontext der Beschleunigerphysik eingeführt wurden auf Probleme in der klassischen und der quantisierten Gravitation an. Die Hauptergebnisse sind präzise Berechnungen verschiedener Größen die zur theoretischen Beschreibung des gravitationellen Zweikörperproblems benötigt werden.

Ein zentrales Ergebnis ist die Bestimmung des Zweikörperpotentials zur vierten Ordnung in der Störungstheorie. Daneben bestimmen wir den Effekt von Strahlungskorrekturen induziert durch Abstrahlung von Gravitationswellen auf den Steuwinkel zweier massiver Objekte. Wir bestimmen zudem die totale abgestrahlte Energie während des Streuprozess sowie eines Umlaufs in einem gebundenen Zweikörpersystem.

Wir beschreiben das Wörterbuch das zum Übertrag von quantemechanischen Streuprozessen zu klassischen Observablen verwendet werden kann. Wir führen zudem neue Methoden ein die diese Rechnungen signifikant vereinfachen. Wir legen besonderen Fokus auf die Auswertung komplizierter Integrale und beschreiben im Detail wie diese effizient berechnet werden können

Ein weiteres Resultat ist die Streuamplitude vierer Gravitonen zur dritten Ordnung in der Störungstheorie unter Einbezug von Quanteneffekten. Ausgehend von dieser Berechnung verifizieren wir ein Ergebnis für den Hochenergielimes des Streuwinkels gravitationeller Streuprozesse. Damit liefern wir einen wichtigen Beitrag zu einer anhaltenden Kontroverse über den Zusammenhang zwischen Streuprozessen von masselosen und massiven Objekten in der klassischen Gravitation.

Bibliography

[1] R. A. Hulse and J. H. Taylor, Astrophys. J. Lett. **195**, L51 (1975).

[2] B. Abbott *et al.* (LIGO Scientific, Virgo), Phys. Rev. Lett. **116**, 061102 (2016), arXiv:1602.03837 [gr-qc] .

[3] B. P. Abbott *et al.* (LIGO Scientific, Virgo), Phys. Rev. Lett. **119**, 161101 (2017), arXiv:1710.05832 [gr-qc] .

[4] R. Abbott *et al.* (LIGO Scientific, KAGRA, VIRGO), Astrophys. J. Lett. **915**, L5 (2021), arXiv:2106.15163 [astro-ph.HE] .

[5] C. M. Will, Living Rev. Rel. **17**, 4 (2014), arXiv:1403.7377 [gr-qc] .

[6] N. Yunes, K. Yagi, and F. Pretorius, Phys. Rev. D **94**, 084002 (2016), arXiv:1603.08955 [gr-qc] .

[7] B. P. Abbott *et al.* (LIGO Scientific, Virgo), Phys. Rev. Lett. **116**, 241102 (2016), arXiv:1602.03840 [gr-qc] .

[8] R. Abbott *et al.* (LIGO Scientific, Virgo), Phys. Rev. X **11**, 021053 (2021), arXiv:2010.14527 [gr-qc] .

[9] E. E. Flanagan and T. Hinderer, Phys. Rev. D **77**, 021502 (2008), arXiv:0709.1915 [astro-ph] .

[10] B. P. Abbott *et al.* (LIGO Scientific, Virgo), Phys. Rev. Lett. **121**, 161101 (2018), arXiv:1805.11581 [gr-qc] .

[11] T. Dietrich, T. Hinderer, and A. Samajdar, Gen. Rel. Grav. **53**, 27 (2021), arXiv:2004.02527 [gr-qc] .

[12] B. P. Abbott *et al.* (LIGO Scientific, Virgo, Fermi GBM, INTEGRAL, IceCube, AstroSat Cadmium Zinc Telluride Imager Team, IPN, Insight-Hxmt, ANTARES, Swift, AGILE Team, 1M2H Team, Dark Energy Camera GW-EM, DES, DLT40, GRAWITA, Fermi-LAT, ATCA, ASKAP, Las Cumbres Observatory Group, OzGrav, DWF (Deeper Wider Faster Program), AST3, CAASTRO, VINROUGE, MASTER, J-GEM, GROWTH, JAGWAR, CaltechNRAO, TTU-NRAO, NuSTAR, Pan-STARRS, MAXI Team, TZAC Consortium, KU, Nordic Optical Telescope, ePESSTO, GROND, Texas Tech University, SALT Group, TOROS, BOOTES, MWA, CALET, IKI-GW Follow-up, H.E.S.S., LOFAR, LWA, HAWC, Pierre Auger, ALMA, Euro VLBI Team, Pi of Sky, Chandra Team at McGill University, DFN, ATLAS Telescopes, High Time Resolution Universe Survey, RIMAS,

RATIR, SKA South Africa/MeerKAT), Astrophys. J. Lett. **848**, L12 (2017), arXiv:1710.05833 [astro-ph.HE] .

[13] C. M. Will, Phys. Rev. D **57**, 2061 (1998), arXiv:gr-qc/9709011 .

[14] J. Ellis, N. E. Mavromatos, and D. V. Nanopoulos, Mod. Phys. Lett. A **31**, 1675001 (2016), arXiv:1602.04764 [gr-qc] .

[15] B. P. Abbott *et al.* (LIGO Scientific, Virgo), Phys. Rev. Lett. **116**, 221101 (2016), [Erratum: Phys.Rev.Lett. 121, 129902 (2018)], arXiv:1602.03841 [gr-qc] .

[16] B. P. Abbott *et al.*, Phys. Rev. D **93**, 112004 (2016), [Addendum: Phys.Rev.D 97, 059901 (2018)], arXiv:1604.00439 [astro-ph.IM] .

[17] M. Punturo *et al.*, Classical and Quantum Gravity **27**, 194002 (2010).

[18] D. Reitze *et al.*, Bull. Am. Astron. Soc. **51**, 035 (2019), arXiv:1907.04833 [astro-ph.IM] .

[19] P. Amaro-Seoane *et al.*, Class. Quant. Grav. **29**, 124016 (2012), arXiv:1202.0839 [gr-qc] .

[20] S. Hild, S. Chelkowski, and A. Freise, (2008), arXiv:0810.0604 [gr-qc] .

[21] S. Hild *et al.*, Class. Quant. Grav. **28**, 094013 (2011), arXiv:1012.0908 [gr-qc] .

[22] M. Pürrer and C.-J. Haster, Phys. Rev. Res. **2**, 023151 (2020), arXiv:1912.10055 [gr-qc] .

[23] F. Pretorius, Phys. Rev. Lett. **95**, 121101 (2005), arXiv:gr-qc/0507014 .

[24] M. Campanelli, C. O. Lousto, P. Marronetti, and Y. Zlochower, Phys. Rev. Lett. **96**, 111101 (2006), arXiv:gr-qc/0511048 .

[25] J. G. Baker, J. Centrella, D.-I. Choi, M. Koppitz, and J. van Meter, Phys. Rev. Lett. **96**, 111102 (2006), arXiv:gr-qc/0511103 .

[26] A. Buonanno and T. Damour, Physical Review D **59** (1999), 10.1103/physrevd.59.084006.

[27] J. D. E. Creighton, Phys. Rev. D **60**, 022001 (1999), arXiv:gr-qc/9901084 .

[28] W. D. Goldberger and I. Z. Rothstein, Phys. Rev. D **73**, 104029 (2006), arXiv:hep-th/0409156 .

[29] W. D. Goldberger, in *Les Houches Summer School - Session 86: Particle Physics and Cosmology: The Fabric of Spacetime* (2007) arXiv:hep-ph/0701129 .

[30] J. B. Gilmore and A. Ross, Phys. Rev. D **78**, 124021 (2008), arXiv:0810.1328 [gr-qc] .

[31] T. Damour, Phys. Rev. D **97**, 044038 (2018), arXiv:1710.10599 [gr-qc] .

[32] S. J. Parke and T. R. Taylor, Phys. Rev. Lett. **56**, 2459 (1986).

[33] Z. Bern, L. J. Dixon, D. C. Dunbar, and D. A. Kosower, Nucl. Phys. B **435**, 59 (1995), arXiv:hep-ph/9409265 [hep-ph] .

[34] R. Britto, F. Cachazo, and B. Feng, Nucl. Phys. B **725**, 275 (2005), arXiv:hep-th/0412103 [hep-th] .

[35] B. S. DeWitt, Phys. Rev. **162**, 1239 (1967).

[36] Z. Bern, J. J. Carrasco, M. Chiodaroli, H. Johansson, and R. Roiban, (2019), arXiv:1909.01358 [hep-th] .

[37] Z. Bern, J. J. Carrasco, W.-M. Chen, A. Edison, H. Johansson, J. Parra-Martinez, R. Roiban, and M. Zeng, Phys. Rev. D **98**, 086021 (2018), arXiv:1804.09311 [hep-th] .

[38] Y. Iwasaki, Prog. Theor. Phys. **46**, 1587 (1971).

[39] Y. Iwasaki, Lett. Nuovo Cim. **1S2**, 783 (1971).

[40] S. N. Gupta and S. F. Radford, Phys. Rev. D **19**, 1065 (1979).

[41] B. R. Holstein and J. F. Donoghue, Phys. Rev. Lett. **93**, 201602 (2004), arXiv:hep-th/0405239 .

[42] B. R. Holstein and A. Ross, (2008), arXiv:0802.0716 [hep-ph] .

[43] D. Neill and I. Z. Rothstein, Nucl. Phys. B **877**, 177 (2013), arXiv:1304.7263 [hep-th] .

[44] N. E. J. Bjerrum-Bohr, J. F. Donoghue, and P. Vanhove, JHEP **02**, 111 (2014), arXiv:1309.0804 [hep-th] .

[45] V. Vaidya, Phys. Rev. D **91**, 024017 (2015), arXiv:1410.5348 [hep-th] .

[46] D. A. Kosower, B. Maybee, and D. O'Connell, JHEP **02**, 137 (2019), arXiv:1811.10950 [hep-th] .

[47] Z. Bern, C. Cheung, R. Roiban, C.-H. Shen, M. P. Solon, and M. Zeng, Phys. Rev. Lett. **122**, 201603 (2019), arXiv:1901.04424 [hep-th] .

[48] Z. Bern, C. Cheung, R. Roiban, C.-H. Shen, M. P. Solon, and M. Zeng, J. High Energy Phys. **10**, 206 (2019), arXiv:1908.01493 [hep-th] .

[49] Z. Bern, J. Parra-Martinez, R. Roiban, M. S. Ruf, C.-H. Shen, M. P. Solon, and M. Zeng, Phys. Rev. Lett. **126**, 171601 (2021), arXiv:2101.07254 [hep-th] .

[50] B. Kocsis, M. E. Gaspar, and S. Marka, Astrophys. J. **648**, 411 (2006), arXiv:astro-ph/0603441 .

[51] S. Mukherjee, S. Mitra, and S. Chatterjee, (2020), arXiv:2010.00916 [gr-qc] .

[52] C. Cheung, I. Z. Rothstein, and M. P. Solon, Phys. Rev. Lett. **121**, 251101 (2018), arXiv:1808.02489 [hep-th] .

[53] G. Kälin and R. A. Porto, JHEP **01**, 072 (2020), arXiv:1910.03008 [hep-th] .

[54] G. Kälin and R. A. Porto, JHEP **02**, 120 (2020), arXiv:1911.09130 [hep-th] .

[55] T. Ohta, H. Okamura, T. Kimura, and K. Hiida, Prog. Theor. Phys. **50**, 492 (1973).

[56] P. Jaranowski and G. Schaefer, Phys. Rev. D **57**, 7274 (1998), [Erratum: Phys.Rev.D 63, 029902 (2001)], arXiv:gr-qc/9712075 .

[57] T. Damour, P. Jaranowski, and G. Schaefer, Phys. Rev. D **62**, 044024 (2000), arXiv:gr-qc/9912092 .

[58] L. Blanchet and G. Faye, Phys. Lett. A **271**, 58 (2000), arXiv:gr-qc/0004009 .

[59] T. Damour, P. Jaranowski, and G. Schaefer, Phys. Lett. B **513**, 147 (2001), arXiv:gr-qc/0105038 .

[60] S. Foffa and R. Sturani, Phys. Rev. D **87**, 064011 (2013), arXiv:1206.7087 [gr-qc] .

[61] T. Damour, P. Jaranowski, and G. Schäfer, Phys. Rev. D **89**, 064058 (2014), arXiv:1401.4548 [gr-qc] .

[62] P. Jaranowski and G. Schäfer, Phys. Rev. D **92**, 124043 (2015), arXiv:1508.01016 [gr-qc] .

[63] L. Bernard, L. Blanchet, A. Bohé, G. Faye, and S. Marsat, Phys. Rev. D **93**, 084037 (2016), arXiv:1512.02876 [gr-qc] .

[64] S. Foffa, P. Mastrolia, R. Sturani, and C. Sturm, Phys. Rev. D **95**, 104009 (2017), arXiv:1612.00482 [gr-qc] .

[65] R. A. Porto and I. Z. Rothstein, Phys. Rev. D **96**, 024062 (2017), arXiv:1703.06433 [gr-qc] .

[66] T. Marchand, L. Bernard, L. Blanchet, and G. Faye, Phys. Rev. D **97**, 044023 (2018), arXiv:1707.09289 [gr-qc] .

[67] S. Foffa and R. Sturani, Phys. Rev. D **100**, 024047 (2019), arXiv:1903.05113 [gr-qc] .

[68] S. Foffa, R. A. Porto, I. Rothstein, and R. Sturani, Phys. Rev. D **100**, 024048 (2019), arXiv:1903.05118 [gr-qc] .

[69] A. Lorentz and J. Droste, Versl. K. Akad. Wet. Amsterdam **26**, 293,649 (1917).

[70] A. Einstein, L. Infeld, and B. Hoffmann, Annals Math. **39**, 65 (1938).

[71] A. Eddington and C. G.L., Proc. Roy. Soc. **A166**.

[72] S. Foffa, P. Mastrolia, R. Sturani, C. Sturm, and W. J. Torres Bobadilla, Phys. Rev. Lett. **122**, 241605 (2019), arXiv:1902.10571 [gr-qc] .

[73] J. Blümlein, A. Maier, and P. Marquard, Phys. Lett. B **800**, 135100 (2020), arXiv:1902.11180 [gr-qc] .

[74] D. Bini, T. Damour, and A. Geralico, Phys. Rev. Lett. **123**, 231104 (2019), arXiv:1909.02375 [gr-qc] .

[75] D. Bini, T. Damour, and A. Geralico, Phys. Rev. D **102**, 024062 (2020), arXiv:2003.11891 [gr-qc] .

[76] J. Blümlein, A. Maier, P. Marquard, and G. Schäfer, Nucl. Phys. B **965**, 115352 (2021), arXiv:2010.13672 [gr-qc] .

[77] J. Blümlein, A. Maier, P. Marquard, and G. Schäfer, Phys. Lett. B **816**, 136260 (2021), arXiv:2101.08630 [gr-qc] .

[78] B. Bertotti, Nuovo Cim. **4**, 898 (1956).

[79] R. P. Kerr, Nuovo Cim. **13**, 469 (1959).

[80] M. Portilla, J. Phys. A **12**, 1075 (1979).

[81] K. Westpfahl and M. Goller, Lett. Nuovo Cim. **26**, 573 (1979).

[82] M. Portilla, J. Phys. A **13**, 3677 (1980).

[83] L. Bel, T. Damour, N. Deruelle, J. Ibanez, and J. Martin, Gen. Rel. Grav. **13**, 963 (1981).

[84] K. Westpfahl, Fortsch. Phys. **33**, 417 (1985).

[85] T. Damour, Phys. Rev. D **94**, 104015 (2016), arXiv:1609.00354 [gr-qc] .

[86] M. E. Lower, E. Thrane, P. D. Lasky, and R. Smith, Phys. Rev. D **98**, 083028 (2018), arXiv:1806.05350 [astro-ph.HE] .

[87] D. Kosmopoulos and A. Luna, JHEP **07**, 037 (2021), arXiv:2102.10137 [hep-th] .

[88] E. Herrmann, J. Parra-Martinez, M. S. Ruf, and M. Zeng, Phys. Rev. Lett. **126**, 201602 (2021), arXiv:2101.07255 [hep-th] .

[89] E. Herrmann, J. Parra-Martinez, M. S. Ruf, and M. Zeng, (2021), arXiv:2104.03957 [hep-th] .

[90] C. Cheung and M. P. Solon, Phys. Rev. Lett. **125**, 191601 (2020), arXiv:2006.06665 [hep-th] .

[91] Z. Bern, J. Parra-Martinez, R. Roiban, E. Sawyer, and C.-H. Shen, JHEP **05**, 188 (2021), arXiv:2010.08559 [hep-th] .

[92] P. A. Baikov, K. G. Chetyrkin, and J. H. Kühn, Phys. Rev. Lett. **118**, 082002 (2017), arXiv:1606.08659 [hep-ph] .

[93] C. Dlapa, G. Kälin, Z. Liu, and R. A. Porto, (2021), arXiv:2106.08276 [hep-th] .

[94] J. M. Henn, A. V. Smirnov, and V. A. Smirnov, JHEP **07**, 128 (2013), arXiv:1306.2799 [hep-th] .

[95] J. M. Henn, A. V. Smirnov, and V. A. Smirnov, JHEP **03**, 088 (2014), arXiv:1312.2588 [hep-th] .

[96] J. Henn, B. Mistlberger, V. A. Smirnov, and P. Wasser, JHEP **04**, 167 (2020), arXiv:2002.09492 [hep-ph] .

[97] J. M. Henn, G. P. Korchemsky, and B. Mistlberger, JHEP **04**, 018 (2020), arXiv:1911.10174 [hep-th] .

[98] R. Brüser, C. Dlapa, J. M. Henn, and K. Yan, Phys. Rev. Lett. **126**, 021601 (2021), arXiv:2007.04851 [hep-th] .

[99] Z. L. Liu and M. Stahlhofen, JHEP **02**, 128 (2021), arXiv:2010.05861 [hep-ph] .

[100] D. Bini, T. Damour, and A. Geralico, Phys. Rev. D **102**, 084047 (2020), arXiv:2007.11239 [gr-qc] .

[101] R. Penrose, Phys. Rev. Lett. **14**, 57 (1965).

[102] K. Akiyama *et al.* (Event Horizon Telescope), Astrophys. J. Lett. **875**, L1 (2019), arXiv:1906.11238 [astro-ph.GA] .

[103] S. M. Carroll, *Spacetime and Geometry* (Cambridge University Press, 2019).

[104] G. Kälin, Z. Liu, and R. A. Porto, Phys. Rev. Lett. **125**, 261103 (2020), arXiv:2007.04977 [hep-th] .

[105] L. Landau and E. Lifshitz, *Mechanics*, 3rd ed., Course of theoretical physics, Vol. 1 (Butterworth-Heinemann, 1976).

[106] T. Damour and G. Schaefer, Nuovo Cim. B **101**, 127 (1988).

[107] C. Lanczos, *The Variational Principles of Mechanics*, 4th ed. (Dover Publications, inc., New York, US, 1970).

[108] C. W. Misner, K. Thorne, and J. Wheeler, *Gravitation* (W. H. Freeman, San Francisco, 1973).

[109] N. Wex and G. Schafer, Classical and Quantum Gravity **10**, 2729 (1993).

[110] W. E. Caswell and G. P. Lepage, Phys. Lett. B **167**, 437 (1986).

[111] M. Neubert, Phys. Rept. **245**, 259 (1994), arXiv:hep-ph/9306320 .

[112] A. V. Manohar and M. B. Wise, *Heavy quark physics*, Vol. 10 (Cambridge university press, 2000).

[113] A. M. Polyakov, Nucl. Phys. B **164**, 171 (1980).

[114] J. S. R. Chisholm, Nucl. Phys. **26**, 469 (1961).

[115] S. Kamefuchi, L. O'Raifeartaigh, and A. Salam, Nucl. Phys. **28**, 529 (1961).

[116] Z. Bern, L. J. Dixon, D. C. Dunbar, and D. A. Kosower, Nucl. Phys. **B425**, 217 (1994), arXiv:hep-ph/9403226 [hep-ph] .

[117] R. Britto, F. Cachazo, and B. Feng, Nucl. Phys. B **715**, 499 (2005), arXiv:hep-th/0412308 .

[118] R. Britto, F. Cachazo, B. Feng, and E. Witten, Phys. Rev. Lett. **94**, 181602 (2005), arXiv:hep-th/0501052 .

[119] Z. Bern and Y.-t. Huang, J. Phys. A **44**, 454003 (2011), arXiv:1103.1869 [hep-th] .

[120] S. Weinberg, *The Quantum theory of fields. Vol. 1: Foundations* (Cambridge University Press, 2005).

[121] R. K. Ellis, W. T. Giele, and Z. Kunszt, J. High Energy Phys. **03**, 003 (2008), arXiv:0708.2398 [hep-ph] .

[122] W. T. Giele, Z. Kunszt, and K. Melnikov, J. High Energy Phys. **04**, 049 (2008), arXiv:0801.2237 [hep-ph] .

[123] C. F. Berger, Z. Bern, L. J. Dixon, F. Febres Cordero, D. Forde, H. Ita, D. A. Kosower, and D. Maitre, Phys. Rev. D **78**, 036003 (2008), arXiv:0803.4180 [hep-ph] .

[124] C. F. Berger, Z. Bern, L. J. Dixon, F. Febres Cordero, D. Forde, H. Ita, D. A. Kosower, and D. Maitre, *Proceedings, 9th DESY Workshop on Elementary Particle Theory: Loops and Legs in Quantum Field Theory: Sondershausen, Germany, 20-25 April 2008*, Nucl. Phys. Proc. Suppl. **183**, 313 (2008), arXiv:0807.3705 [hep-ph] .

[125] Z. Bern, L. J. Dixon, F. Febres Cordero, S. Höche, H. Ita, D. A. Kosower, D. Maître, and K. J. Ozeren, Phys. Rev. D **88**, 014025 (2013), arXiv:1304.1253 [hep-ph] .

[126] H. Ita, Phys. Rev. D **94**, 116015 (2016), arXiv:1510.05626 [hep-th] .

[127] S. Abreu, F. Febres Cordero, H. Ita, M. Jaquier, B. Page, and M. Zeng, Phys. Rev. Lett. **119**, 142001 (2017), arXiv:1703.05273 [hep-ph] .

[128] S. Abreu, F. Febres Cordero, H. Ita, M. Jaquier, and B. Page, Phys. Rev. D **95**, 096011 (2017), arXiv:1703.05255 [hep-ph] .

[129] S. Abreu, F. Febres Cordero, H. Ita, B. Page, and M. Zeng, Phys. Rev. D **97**, 116014 (2018), arXiv:1712.03946 [hep-ph] .

[130] S. Abreu, J. Dormans, F. Febres Cordero, H. Ita, M. Kraus, B. Page, E. Pascual, M. S. Ruf, and V. Sotnikov, Comput. Phys. Commun. **267**, 108069 (2021), arXiv:2009.11957 [hep-ph] .

[131] H. Ita, *Proceedings, 13th DESY Workshop on Elementary Particle Physics: Loops and Legs in Quantum Field Theory (LL2016): Leipzig, Germany, April 24-29, 2016*, PoS **LL2016**, 080 (2016), arXiv:1607.00705 [hep-ph] .

[132] T. Peraro, J. High Energy Phys. **12**, 030 (2016), arXiv:1608.01902 [hep-ph] .

[133] J. Klappert and F. Lange, Comput. Phys. Commun. **247**, 106951 (2020), arXiv:1904.00009 [cs.SC] .

[134] J. Klappert, F. Lange, P. Maierhöfer, and J. Usovitsch, Comput. Phys. Commun. **266**, 108024 (2021), arXiv:2008.06494 [hep-ph] .

[135] A. V. Smirnov and F. S. Chuharev, Comput. Phys. Commun. **247**, 106877 (2020), arXiv:1901.07808 [hep-ph] .

[136] A. G. Grozin, Int. J. Mod. Phys. A **19**, 473 (2004), arXiv:hep-ph/0307297 .

[137] J. M. Henn, J. Phys. **A48**, 153001 (2015), arXiv:1412.2296 [hep-ph] .

[138] C. Duhr, in *Theoretical Advanced Study Institute in Elementary Particle Physics: Journeys Through the Precision Frontier: Amplitudes for Colliders* (2014) arXiv:1411.7538 [hep-ph] .

[139] A. Grozin, J. M. Henn, G. P. Korchemsky, and P. Marquard, JHEP **01**, 140 (2016), arXiv:1510.07803 [hep-ph] .

[140] R. K. Ellis and G. Zanderighi, JHEP **02**, 002 (2008), arXiv:0712.1851 [hep-ph] .

[141] J. C. Collins, *Renormalization*, Cambridge Monographs on Mathematical Physics, Vol. 26 (Cambridge University Press, Cambridge, 1986).

[142] T. Becher and G. Bell, Phys. Lett. B **713**, 41 (2012), arXiv:1112.3907 [hep-ph] .

[143] W. Pauli and F. Villars, Rev. Mod. Phys. **21**, 434 (1949).

[144] The Wolfram functions site, "Logarithm of the gamma function," (2001), accessed: 31.3.2021.

[145] V. A. Smirnov, *Analytic tools for Feynman integrals*, Vol. 250 (Springer, 2012).

[146] E. Panzer, *Feynman integrals and hyperlogarithms*, Ph.D. thesis, Humboldt U. (2015), arXiv:1506.07243 [math-ph] .

[147] F. Brown, arXiv preprint arXiv:0910.0114 (2009).

[148] R. Akhoury, R. Saotome, and G. Sterman, Phys. Rev. D **103**, 064036 (2021), arXiv:1308.5204 [hep-th] .

[149] J. Parra-Martinez, M. S. Ruf, and M. Zeng, JHEP **11**, 023 (2020), arXiv:2005.04236 [hep-th] .

[150] F. V. Tkachov, Phys. Lett. **100B**, 65 (1981).

[151] K. G. Chetyrkin and F. V. Tkachov, Nucl. Phys. B **192**, 159 (1981).

[152] A. V. Smirnov and A. V. Petukhov, Lett. Math. Phys. **97**, 37 (2011), arXiv:1004.4199 [hep-th] .

[153] S. Laporta, Int. J. Mod. Phys. **A15**, 5087 (2000), arXiv:hep-ph/0102033 [hep-ph] .

[154] S. Laporta and E. Remiddi, Phys. Lett. B **379**, 283 (1996), arXiv:hep-ph/9602417 [hep-ph] .

[155] C. Studerus, Comput. Phys. Commun. **181**, 1293 (2010), arXiv:0912.2546 [physics.comp-ph] .

[156] J. Gluza, K. Kajda, and D. A. Kosower, Phys. Rev. D **83**, 045012 (2011), arXiv:1009.0472 [hep-th] .

[157] R. M. Schabinger, J. High Energy Phys. **01**, 077 (2012), arXiv:1111.4220 [hep-ph] .

[158] A. V. Kotikov, Phys. Lett. **B254**, 158 (1991).

[159] Z. Bern, L. J. Dixon, and D. A. Kosower, Phys. Lett. B **302**, 299 (1993), [Erratum: Phys.Lett.B 318, 649 (1993)], arXiv:hep-ph/9212308 .

[160] E. Remiddi, Nuovo Cim. **A110**, 1435 (1997), arXiv:hep-th/9711188 [hep-th] .

[161] T. Gehrmann and E. Remiddi, Nucl. Phys. **B580**, 485 (2000), arXiv:hep-ph/9912329 [hep-ph] .

[162] D. D. Canko, C. G. Papadopoulos, and N. Syrrakos, JHEP **01**, 199 (2021), arXiv:2009.13917 [hep-ph] .

[163] P. A. Kreer and S. Weinzierl, Phys. Lett. B **819**, 136405 (2021), arXiv:2104.07488 [hep-ph] .

[164] M. Heller, (2021), arXiv:2105.08046 [hep-ph] .

[165] S. Abreu, H. Ita, F. Moriello, B. Page, W. Tschernow, and M. Zeng, JHEP **11**, 117 (2020), arXiv:2005.04195 [hep-ph] .

[166] S. Abreu, H. Ita, B. Page, and W. Tschernow, (2021), arXiv:2107.14180 [hep-ph] .

[167] C. Bogner and S. Weinzierl, J. Math. Phys. **50**, 042302 (2009), arXiv:0711.4863 [hep-th] .

[168] S. Weinzierl, Phys. Rev. D **84**, 074007 (2011), arXiv:1107.5131 [hep-ph] .

[169] S. Bloch and P. Vanhove, J. Number Theor. **148**, 328 (2015), arXiv:1309.5865 [hep-th] .

[170] L. Adams and S. Weinzierl, Phys. Lett. B **781**, 270 (2018), arXiv:1802.05020 [hep-ph] .

[171] R. N. Lee, JHEP **04**, 108 (2015), arXiv:1411.0911 [hep-ph] .

[172] M. Prausa, Comput. Phys. Commun. **219**, 361 (2017), arXiv:1701.00725 [hep-ph] .

[173] O. Gituliar and V. Magerya, Comput. Phys. Commun. **219**, 329 (2017), arXiv:1701.04269 [hep-ph] .

[174] R. N. Lee, Comput. Phys. Commun. **267**, 108058 (2021), arXiv:2012.00279 [hep-ph] .

[175] F. Brown and C. Duhr (2020) arXiv:2006.09413 [hep-th] .

[176] F. Brown and O. Schnetz, Duke Math. J. **161**, 1817 (2012), arXiv:1006.4064 [math.AG] .

[177] C. Anastasiou and K. Melnikov, Nucl. Phys. B **646**, 220 (2002), arXiv:hep-ph/0207004 .

[178] C. Anastasiou, L. J. Dixon, and K. Melnikov, Nucl. Phys. B Proc. Suppl. **116**, 193 (2003), arXiv:hep-ph/0211141 .

[179] C. Anastasiou, L. J. Dixon, K. Melnikov, and F. Petriello, Phys. Rev. Lett. **91**, 182002 (2003), arXiv:hep-ph/0306192 .

[180] C. Anastasiou, C. Duhr, F. Dulat, E. Furlan, F. Herzog, and B. Mistlberger, JHEP **08**, 051 (2015), arXiv:1505.04110 [hep-ph] .

[181] M. Beneke and V. A. Smirnov, Nucl. Phys. B **522**, 321 (1998), arXiv:hep-ph/9711391 .

[182] V. A. Smirnov, *Applied asymptotic expansions in momenta and masses* (Springer).

[183] S. Abreu, F. Febres Cordero, H. Ita, M. Jaquier, B. Page, and M. Zeng, Phys. Rev. Lett. **119**, 142001 (2017), arXiv:1703.05273 [hep-ph] .

[184] G. Heinrich and V. A. Smirnov, Phys. Lett. B **598**, 55 (2004), arXiv:hep-ph/0406053 .

[185] V. A. Smirnov, Phys. Lett. B **524**, 129 (2002), arXiv:hep-ph/0111160 .

[186] J. M. Henn and V. A. Smirnov, JHEP **11**, 041 (2013), arXiv:1307.4083 [hep-th] .

[187] C. Duhr, V. A. Smirnov, and L. Tancredi, (2021), arXiv:2108.03828 [hep-ph] .

[188] M. S. Bianchi and M. Leoni, Phys. Lett. B **777**, 394 (2018), arXiv:1612.05609 [hep-ph] .

[189] A. B. Goncharov, Math. Res. Lett. **5**, 497 (1998), arXiv:1105.2076 [math.AG] .

[190] M. Heller, A. von Manteuffel, and R. M. Schabinger, Phys. Rev. D **102**, 016025 (2020), arXiv:1907.00491 [hep-th] .

[191] S. Foffa and R. Sturani, Phys. Rev. D **104**, 024069 (2021), arXiv:2103.03190 [gr-qc] .

[192] Z. Bern, A. Luna, R. Roiban, C.-H. Shen, and M. Zeng, (2020), arXiv:2005.03071 [hep-th] .

[193] N. E. J. Bjerrum-Bohr, J. F. Donoghue, and B. R. Holstein, Phys. Rev. D **67**, 084033 (2003), [Erratum: Phys.Rev.D 71, 069903 (2005)], arXiv:hep-th/0211072 .

[194] P. V. Landshoff and J. C. Polkinghorne, Phys. Rev. **181**, 1989 (1969).

[195] D. Festi and D. van Straten, Comm. Number Theor. Phys. **13**, 463 (2019), arXiv:1809.04970 [math.AG] .

[196] A. Brandhuber, G. Chen, G. Travaglini, and C. Wen, (2021), arXiv:2108.04216 [hep-th] .

[197] A. G. Grozin, A. V. Smirnov, and V. A. Smirnov, JHEP **11**, 022 (2006), arXiv:hep-ph/0609280 .

[198] M. A. Ebert, I. Moult, I. W. Stewart, F. J. Tackmann, G. Vita, and H. X. Zhu, JHEP **04**, 123 (2019), arXiv:1812.08189 [hep-ph] .

[199] N. E. J. Bjerrum-Bohr, P. H. Damgaard, G. Festuccia, L. Planté, and P. Vanhove, Phys. Rev. Lett. **121**, 171601 (2018), arXiv:1806.04920 [hep-th] .

[200] T. Huber and D. Maitre, Comput. Phys. Commun. **178**, 755 (2008), arXiv:0708.2443 [hep-ph] .

[201] A. V. Smirnov, Comput. Phys. Commun. **204**, 189 (2016), arXiv:1511.03614 [hep-ph] .

[202] S. Borowka, G. Heinrich, S. Jahn, S. P. Jones, M. Kerner, and J. Schlenk, Comput. Phys. Commun. **240**, 120 (2019), arXiv:1811.11720 [physics.comp-ph] .

[203] H. R. P. Ferguson, D. H. Bailey, and S. Arno, Math. Comp. **68**, 351 (1999).

[204] C. Duhr and F. Dulat, J. High Energy Phys. **08**, 135 (2019), arXiv:1904.07279 [hep-th] .

[205] R. E. Cutkosky, J. Math. Phys. **1**, 429 (1960).

[206] S. Borowka, G. Heinrich, S. Jahn, S. Jones, M. Kerner, J. Schlenk, and T. Zirke, Comput. Phys. Commun. **222**, 313 (2018), arXiv:1703.09692 [hep-ph] .

[207] P. Di Vecchia, C. Heissenberg, R. Russo, and G. Veneziano, JHEP **07**, 169 (2021), arXiv:2104.03256 [hep-th] .

[208] R. N. Lee, JHEP **10**, 176 (2018), arXiv:1806.04846 [hep-ph] .

[209] G. S. Joyce, Philos. Trans. R. Soc. Lond.. Series A **273**, 583 (1997).

[210] J. Broedel, C. Duhr, F. Dulat, and L. Tancredi, JHEP **05**, 093 (2018), arXiv:1712.07089 [hep-th] .

[211] G. 't Hooft and M. J. G. Veltman, Annales Henri Poincaré **20**, 69 (1974).

[212] M. H. Goroff and A. Sagnotti, Phys. Lett. B **160**, 81 (1985).

[213] M. H. Goroff and A. Sagnotti, Nucl. Phys. B **266**, 709 (1986).

[214] A. E. M. van de Ven, *Conference on Strings and Symmetries Stony Brook, New York, May 20-25, 1991*, Nucl. Phys. B **378**, 309 (1992).

[215] Z. Bern, C. Cheung, H.-H. Chi, S. Davies, L. Dixon, and J. Nohle, Phys. Rev. Lett. **115**, 211301 (2015), arXiv:1507.06118 [hep-th] .

[216] Z. Bern, H.-H. Chi, L. Dixon, and A. Edison, Phys. Rev. D **95**, 046013 (2017), arXiv:1701.02422 [hep-th] .

[217] Z. Bern, J. J. Carrasco, L. J. Dixon, H. Johansson, and R. Roiban, Phys. Rev. Lett. **103**, 081301 (2009), arXiv:0905.2326 [hep-th] .

[218] M. B. Green, J. H. Schwarz, and L. Brink, Nucl. Phys. B **198**, 474 (1982).

[219] D. C. Dunbar and P. S. Norridge, Nucl. Phys. B **433**, 181 (1995), hep-th/9408014 .

[220] Z. Bern, L. J. Dixon, M. Perelstein, and J. S. Rozowsky, Nucl. Phys. B **546**, 423 (1999), arXiv:hep-th/9811140 .

[221] S. G. Naculich, H. Nastase, and H. J. Schnitzer, Nucl. Phys. B **805**, 40 (2008), arXiv:0805.2347 [hep-th] .

[222] C. Boucher-Veronneau and L. J. Dixon, J. High Energy Phys. **12**, 046 (2011), arXiv:1110.1132 [hep-th] .

[223] S. Abreu, L. J. Dixon, E. Herrmann, B. Page, and M. Zeng, J. High Energy Phys. **03**, 123 (2019), arXiv:1901.08563 [hep-th] .

[224] D. Chicherin, T. Gehrmann, J. M. Henn, P. Wasser, Y. Zhang, and S. Zoia, J. High Energy Phys. **03**, 115 (2019), arXiv:1901.05932 [hep-th] .

[225] J. M. Henn and B. Mistlberger, J. High Energy Phys. **05**, 023 (2019), arXiv:1902.07221 [hep-th] .

[226] Z. Bern, D. C. Dunbar, and T. Shimada, Phys. Lett. B **312**, 277 (1993), arXiv:hep-th/9307001 .

[227] D. C. Dunbar, G. R. Jehu, and W. B. Perkins, Phys. Rev. **D95**, 046012 (2017), arXiv:1701.02934 [hep-th] .

[228] D. Amati, M. Ciafaloni, and G. Veneziano, Nucl. Phys. B **347**, 550 (1990).

[229] T. Damour, Phys. Rev. D **102**, 024060 (2020), arXiv:1912.02139 [gr-qc] .

[230] J. F. Donoghue, Phys. Rev. D **50**, 3874 (1994), arXiv:gr-qc/9405057 .

[231] G. W. Gibbons, S. W. Hawking, and M. J. Perry, Nucl. Phys. B **138**, 141 (1978).

[232] S. W. Hawking and W. Israel, *General Relativity: An Einstein Centenary Survey* (Cambridge University Press, Cambridge, UK, 1979).

[233] D. Maitre and P. Mastrolia, Comput. Phys. Commun. **179**, 501 (2008), arXiv:0710.5559 [hep-ph] .

[234] S. Weinberg, Phys. Rev. **140**, B516 (1965).

[235] S. G. Naculich and H. J. Schnitzer, J. High Energy Phys. **05**, 087 (2011), arXiv:1101.1524 [hep-th] .

[236] S. G. Naculich, H. Nastase, and H. J. Schnitzer, J. High Energy Phys. **04**, 114 (2013), arXiv:1301.2234 [hep-th] .

[237] R. Akhoury, R. Saotome, and G. Sterman, Phys. Rev. D **84**, 104040 (2011), arXiv:1109.0270 [hep-th] .

[238] C. Cheung and G. N. Remmen, JHEP **09**, 002 (2017), arXiv:1705.00626 [hep-th] .

[239] S. Deser, Gen. Rel. Grav. **1**, 9 (1970), arXiv:gr-qc/0411023 .

[240] M. Ferraris, F. M., and R. C., General Relativity and Gravitation **14**, 243–254 (1982).

[241] F. A. Berends and W. T. Giele, Nucl. Phys. B **306**, 759 (1988).

[242] S. Badger, B. Biedermann, L. Hackl, J. Plefka, T. Schuster, and P. Uwer, Phys. Rev. **D87**, 034011 (2013), arXiv:1206.2381 [hep-ph] .

[243] M. L. Mangano, S. J. Parke, and Z. Xu, Nucl. Phys. B **298**, 653 (1988).

[244] H. Kawai, D. C. Lewellen, and S. H. H. Tye, Nucl. Phys. B **269**, 1 (1986).

[245] J. M. Martín-García, "xAct: Efficient tensor computer algebra for the Wolfram Language," `http://www.xact.es`, accessed: 13.9.2019.

[246] D. Brizuela, J. M. Martín-García, and G. A. Mena Marugan, Gen. Rel. Grav. **41**, 2415 (2009), arXiv:0807.0824 [gr-qc] .

[247] T. Nutma, Comput. Phys. Commun. **185**, 1719 (2014), arXiv:1308.3493 [cs.SC] .

[248] A. von Manteuffel and R. M. Schabinger, Phys. Lett. B **744**, 101 (2015), arXiv:1406.4513 [hep-ph] .

[249] V. A. Smirnov, Phys. Lett. B **460**, 397 (1999), arXiv:hep-ph/9905323 [hep-ph] .

[250] J. B. Tausk, Phys. Lett. B **469**, 225 (1999), arXiv:hep-ph/9909506 [hep-ph] .

[251] V. A. Smirnov and O. L. Veretin, Nucl. Phys. B **566**, 469 (2000), arXiv:hep-ph/9907385 [hep-ph] .

[252] C. Anastasiou, J. B. Tausk, and M. E. Tejeda-Yeomans, *Zeuthen Workshop on Elementary Particle Theory: Loops and Legs in Quantum Field Theory Koenigstein-Weissig, Germany, April 9-14, 2000*, Nucl. Phys. Proc. Suppl. **89**, 262 (2000), arXiv:hep-ph/0005328 [hep-ph] .

[253] S. Abreu, J. Dormans, F. Febres Cordero, H. Ita, and B. Page, Phys. Rev. Lett. **122**, 082002 (2019), arXiv:1812.04586 [hep-ph] .

[254] S. Badger, C. Brønnum-Hansen, H. B. Hartanto, and T. Peraro, J. High Energy Phys. **01**, 186 (2019), arXiv:1811.11699 [hep-ph] .

[255] S. Abreu, J. Dormans, F. Febres Cordero, H. Ita, B. Page, and V. Sotnikov, J. High Energy Phys. **05**, 084 (2019), arXiv:1904.00945 [hep-ph] .

[256] S. Badger, D. Chicherin, T. Gehrmann, G. Heinrich, J. M. Henn, T. Peraro, P. Wasser, Y. Zhang, and S. Zoia, Phys. Rev. Lett. **123**, 071601 (2019), arXiv:1905.03733 [hep-ph] .

[257] M. Abramowitz and I. A. Stegun, *Handbook of mathematical functions: with formulas, graphs, and mathematical tables*, Vol. 55 (Courier Corporation, 1964).

[258] P. S. Wang, in *Proceedings of the Fourth ACM Symposium on Symbolic and Algebraic Computation*, SYMSAC '81 (ACM, New York, NY, USA, 1981) pp. 212–217.

[259] Z. Bern, C. Cheung, H.-H. Chi, S. Davies, L. Dixon, and J. Nohle, (n.d.), unpublished.

[260] S. Abreu, F. Febres Cordero, H. Ita, M. Jaquier, B. Page, M. S. Ruf, and V. Sotnikov, Phys. Rev. Lett. **124**, 211601 (2020), arXiv:2002.12374 [hep-th] .

[261] C. P. Burgess, Ann. Rev. Nucl. Part. Sci. **57**, 329 (2007), arXiv:hep-th/0701053 .

[262] A. Antonelli, A. Buonanno, J. Steinhoff, M. van de Meent, and J. Vines, Phys. Rev. D **99**, 104004 (2019), arXiv:1901.07102 [gr-qc] .

[263] A. Cristofoli, N. Bjerrum-Bohr, P. H. Damgaard, and P. Vanhove, Phys. Rev. D **100**, 084040 (2019), arXiv:1906.01579 [hep-th] .

[264] N. E. J. Bjerrum-Bohr, A. Cristofoli, and P. H. Damgaard, JHEP **08**, 038 (2020), arXiv:1910.09366 [hep-th] .

[265] C. Itzykson and J. B. Zuber, *Quantum Field Theory*, International Series In Pure and Applied Physics (McGraw-Hill, New York, 1980).

[266] M. Soldate, Phys. Lett. B **186**, 321 (1987).

[267] P. H. Damgaard, L. Plante, and P. Vanhove, (2021), arXiv:2107.12891 [hep-th] .

[268] Z. Bern, J. Parra-Martinez, R. Roiban, M. S. Ruf, C.-H. Shen, M. P. Solon, and M. Zeng, In preparation.

[269] Z. Bern, H. Ita, J. Parra-Martinez, and M. S. Ruf, Phys. Rev. Lett. **125**, 031601 (2020), arXiv:2002.02459 [hep-th] .

[270] P. Di Vecchia, S. G. Naculich, R. Russo, G. Veneziano, and C. D. White, JHEP **03**, 173 (2020), arXiv:1911.11716 [hep-th] .

[271] C. Boucher-Veronneau and L. J. Dixon, J. High Energy Phys. **12**, 046 (2011), arXiv:1110.1132 [hep-th] .

[272] Z. Bern, J. Carrasco, and H. Johansson, Phys. Rev. D **78**, 085011 (2008), arXiv:0805.3993 [hep-ph] .

[273] Z. Bern, J. J. M. Carrasco, and H. Johansson, Phys. Rev. Lett. **105**, 061602 (2010), arXiv:1004.0476 [hep-th] .

[274] Z. Bern, J. J. M. Carrasco, W.-M. Chen, H. Johansson, R. Roiban, and M. Zeng, Phys. Rev. D **96**, 126012 (2017), arXiv:1708.06807 [hep-th] .

[275] D. Kosmopoulos, (2020), arXiv:2009.00141 [hep-th] .

[276] W. Bonnor, Philos. Trans. R. Soc. Lond. A **251**, 233 (1959).

[277] B. W. B. and R. M. A., Philos. Trans. R. Soc. Lond. A **289**, 247–274 (1966).

[278] K. S. Thorne, Rev. Mod. Phys. **52**, 299 (1980).

[279] L. Blanchet and T. Damour, Phys. Rev. D **37**, 1410 (1988).

[280] L. Blanchet and T. Damour, Phys. Rev. D **46**, 4304 (1992).

[281] L. Blanchet and G. Schaefer, Class. Quant. Grav. **10**, 2699 (1993).

[282] Wolfram Research, Inc., "Mathematica, Version 12.3.1," Champaign, IL, 2021.

[283] C. W. Bauer and B. O. Lange, (2009), arXiv:0905.4739 [hep-ph] .

[284] J. Vollinga and S. Weinzierl, Comput. Phys. Commun. **167**, 177 (2005), arXiv:hep-ph/0410259 [hep-ph] .

[285] J. Vollinga, Nucl. Instrum. Meth. A **559**, 282 (2006), arXiv:hep-ph/0510057 .

[286] J. Blümlein, A. Maier, P. Marquard, and G. Schäfer, Nucl. Phys. B **955**, 115041 (2020), arXiv:2003.01692 [gr-qc] .

[287] D. Bini, T. Damour, and A. Geralico, Phys. Rev. D **102**, 024061 (2020), arXiv:2004.05407 [gr-qc] .

[288] L. Bernard, L. Blanchet, A. Bohé, G. Faye, and S. Marsat, Phys. Rev. D **95**, 044026 (2017), arXiv:1610.07934 [gr-qc] .

[289] L. Bernard, L. Blanchet, A. Bohé, G. Faye, and S. Marsat, Phys. Rev. D **96**, 104043 (2017), arXiv:1706.08480 [gr-qc] .

[290] L. Bernard, L. Blanchet, G. Faye, and T. Marchand, Phys. Rev. D **97**, 044037 (2018), arXiv:1711.00283 [gr-qc] .

[291] D. Bini and T. Damour, Phys. Rev. D **96**, 064021 (2017), arXiv:1706.06877 [gr-qc] .

[292] L. Blanchet, S. Foffa, F. Larrouturou, and R. Sturani, Phys. Rev. D **101**, 084045 (2020), arXiv:1912.12359 [gr-qc] .

[293] C. Cheung and G. N. Remmen, JHEP **01**, 104 (2017), arXiv:1612.03927 [hep-th] .

[294] S. Rafie-Zinedine, *Simplifying Quantum Gravity Calculations*, Master's thesis, Lund U. (2018), arXiv:1808.06086 [hep-th] .

[295] G. Kälin and R. A. Porto, JHEP **11**, 106 (2020), arXiv:2006.01184 [hep-th] .

[296] J. F. Donoghue, Phys. Rev. Lett. **72**, 2996 (1994), arXiv:gr-qc/9310024 .

[297] P. Di Vecchia, C. Heissenberg, R. Russo, and G. Veneziano, Phys. Lett. B **811**, 135924 (2020), arXiv:2008.12743 [hep-th] .

[298] P. Di Vecchia, C. Heissenberg, R. Russo, and G. Veneziano, Phys. Lett. B **818**, 136379 (2021), arXiv:2101.05772 [hep-th] .

[299] T. Damour, Phys. Rev. D **102**, 124008 (2020), arXiv:2010.01641 [gr-qc] .

[300] D. Bini and T. Damour, Phys. Rev. D **86**, 124012 (2012), arXiv:1210.2834 [gr-qc] .

[301] S. Kovacs and K. Thorne, Astrophys. J. **224**, 62 (1978).

[302] L. Blanchet and G. Schaefer, Mon. Not. Roy. Astron. Soc. **239**, 845 (1989), [Erratum: Mon.Not.Roy.Astron.Soc. 242, 704 (1990)].

[303] G. U. Jakobsen, G. Mogull, J. Plefka, and J. Steinhoff, Phys. Rev. Lett. **126**, 201103 (2021), arXiv:2101.12688 [gr-qc] .

[304] S. Mougiakakos, M. M. Riva, and F. Vernizzi, Phys. Rev. D **104**, 024041 (2021), arXiv:2102.08339 [gr-qc] .

[305] D. Bini, T. Damour, and A. Geralico, (2021), arXiv:2107.08896 [gr-qc] .

[306] P. Peters, Phys. Rev. D **1**, 1559 (1970).

[307] A. Buonanno, "Status and challenges of theoretical and experimental gravitational-wave physics," (2021), talk given at GGI Conference "Gravitational scattering, inspiral, and radiation".

[308] M. Hidding, Comput. Phys. Commun. , 108125 (2021), arXiv:2006.05510 [hep-ph] .

[309] F. Moriello, JHEP **01**, 150 (2020), arXiv:1907.13234 [hep-ph] .

[310] B. Maybee, D. O'Connell, and J. Vines, JHEP **12**, 156 (2019), arXiv:1906.09260 [hep-th] .

[311] A. Cristofoli, R. Gonzo, D. A. Kosower, and D. O'Connell, (2021), arXiv:2107.10193 [hep-th] .

[312] C. Anastasiou, L. J. Dixon, K. Melnikov, and F. Petriello, Phys. Rev. D **69**, 094008 (2004), arXiv:hep-ph/0312266 .

[313] A. E. M. van de Ven, *Conference on Strings and Symmetries Stony Brook, New York, May 20-25, 1991*, Nucl. Phys. B **378**, 309 (1992).

[314] S. Amoroso *et al.*, in *11th Les Houches Workshop on Physics at TeV Colliders: PhysTeV Les Houches* (2020) arXiv:2003.01700 [hep-ph] .

[315] The Wolfram functions site, "Appell hypergeometric function F_1, integral representations," (2001), accessed: 1.4.2021.

[316] The Wolfram functions site, "Appell hypergeometric function F_1, special values," (2001), accessed: 14.8.2021.

[317] DLMF, "NIST Digital Library of Mathematical Functions," F. W. J. Olver, A. B. Olde Daalhuis, D. W. Lozier, B. I. Schneider, R. F. Boisvert, C. W. Clark, B. R. Miller, B. V. Saunders, H. S. Cohl, and M. A. McClain, eds., accessed: 14.8.2021.

[318] W. Magnus, F. Oberhettinger, and F. Tricomi, *Higher transcendental functions*, edited by A. Erdélyi (McGraw-Hill, 1953).

[319] G. Gasper, Annals of Mathematics **93**, 112 (1971).

[320] F. A. Berends, W. T. Giele, and H. Kuijf, Phys. Lett. B **211**, 91 (1988).

[321] D. C. Dunbar and N. W. P. Turner, Class. Quant. Grav. **20**, 2293 (2003), arXiv:hep-th/0212160 .

Acknowledgments

I would like to thank my supervisor Harald Ita for his support and encouragement. In particular for believing in me and giving me the freedom I needed for pursuing my own research interests, while still giving important advice when it was needed.

I am grateful to my second supervisor Fernando Febres Coderro, whose door was virtually always open and whose joyful presence took away much of the stress that comes with dealing with complicated problems.

I am fortunate to have met Christian Steinwachs, who closely mentored me and to whom I owe much of my success in physics.

I would like to thank the spokespersons and my fellow researchers in the RTG 2044 for an lively atmosphere, interesting talks and discussion on topics beyond the topics of this thesis.

I would like to thank my collaborators on various projects, for their shared enthusiasm and knowledge.

I would like to thank Fabian Bär, Harald Ita, Maximilan Klinkert and Christian Steinwachs for carefully reading this thesis.

I am grateful to my friends and family for their continuous support, in particular my parents for always encouraging to continue on my path.